

The copyright of this thesis vests in the author. No quotation from it or information derived from it is to be published without full acknowledgement of the source. The thesis is to be used for private study or non-commercial research purposes only.

Published by the University of Cape Town (UCT) in terms of the non-exclusive license granted to UCT by the author.

*A Lagrangian Moisture Source Attribution Model and Analysis of  
Southern Africa*

*Christopher David Jack*

*Thesis Presented for the Degree of*

*DOCTOR OF PHILOSOPHY*

*in the*

*Department of Environmental and Geographical Science,  
Faculty of Science*

*UNIVERSITY OF CAPE TOWN*

*December 2012*

## *Acknowledgements*

I would like to acknowledge the support and direction provided by my supervisor, Prof. Bruce Hewitson as well as the periodic input of Dr Daithí Stone, Prof William Gutowski and many others.

I would also like to acknowledge the critical role of my wife, Angela, who has tirelessly supported and encouraged me through the many challenging stages of this work.

## Thesis Abstract

*A Lagrangian moisture source attribution model is developed in order to explore the regional moisture source dynamics of southern Africa. In particular, the model was developed in order to explore the role of the regional land surface as a source of moisture for regional precipitation. This work was prompted by previous studies suggesting that the land surface may play an important role in the regional climate system and particularly in the regional hydrological cycle.*

*Existing moisture transport and source methodologies have a number of limitations. Correlation analysis, which is often used to identify linkages between moisture sources and precipitation, is limited by the inability to deduce causation or physical processes. Moisture flux analyses are constrained by certain assumptions regarding vertical structure as well as time averaging of the moisture fields. Likewise, bulk recycling methods rely on significant assumptions around mixing and time averaging.*

*The model developed is based on Lagrangian principles and is driven by a Regional Climate Model (RCM) which provides the 3 dimensional wind and moisture fields required. The model operates in reversed time and as such traces moisture from the end point (precipitation event) backwards towards the moisture sources. The model converts the RCM moisture flux fields into Lagrangian moisture parcels at the boundaries of a precipitation target analysis domain. A precipitation diagnosis component determines the contribution of each parcel to precipitation events, both within the target analysis domain as well as along the remainder of the parcels path. Likewise, an evaporation contribution component determines the amount of moisture contributed to a parcel by the underlying land surface.*

*A critical component of the model is the attribution coefficient. This coefficient captures the effects of along path precipitation events on the final absolute contributions of upstream moisture sources. The principle is that while an upstream moisture source may contribute a large amount of moisture to an overpassing air parcel, if the air parcel subsequently loses that moisture to a precipitation event then the total contribution of the original source is reduced. Further downstream evaporative sources, even if of smaller magnitude, can contribute a greater amount of moisture to the final precipitation event. The attribution coefficient captures this effect by reducing the moisture gain of further upstream evaporative events when the parcel loses moisture to a precipitation event along its path.*

*A two summer season analysis of moisture sources for four target domains in South Africa was performed and the results analysed through a number of methods. Two interesting results can be highlighted. Firstly, the land surface is identified as being a very important source of moisture for precipitation with as much as 50% of moisture being sourced from the regional land surface. This is considerably higher than previous estimates placing this fraction at around 20%. Likewise, the regional ocean surface plays a secondary role as a moisture source. The traditionally understood eastern moisture sources are not nearly as strongly attributed as would be expected given the literature.*

*A high altitude, western boundary source at 35°S is also identified contrary to previous work which identifies such an air stream with dry conditions. However further analysis reveals that while there are some uncertainties, this source deserves further investigation.*

*Uncertainties in the model and forcing fields are discussed at length along with their implications for analysis and interpretation of the results. Conclusions drawn are that the model is robust at a qualitative level and provides new potential insights into the moisture dynamics of the region. Further possible developments are highlighted along with some interesting areas for exploration including the moisture leap frog process whereby moisture is transported across the continent through a series of evaporation-precipitation cycles.*

# Contents

<b>1</b>	<b>Introduction</b>	<b>13</b>
1.1	The Southern African Context . . . . .	14
1.1.1	Climate Variability . . . . .	15
1.1.2	Climate Change . . . . .	16
1.1.3	The observation record problem . . . . .	17
1.1.4	Moisture Transport Analysis . . . . .	19
1.2	Southern African Regional Climate System . . . . .	22
1.2.1	General regional circulation . . . . .	23
1.2.2	Absolutely stable layers . . . . .	26
1.2.3	Superposition of systems and sequencing . . . . .	26
1.2.4	Tropical Temperate Troughs . . . . .	27
1.2.5	Convective precipitation . . . . .	28
1.2.6	Frontal precipitation . . . . .	28
1.2.7	Seasonal variability . . . . .	29
1.2.8	El-Nino Southern Oscillation . . . . .	29
1.2.9	Land Surface . . . . .	30
1.3	Conclusion . . . . .	31
<b>2</b>	<b>Lagrangian Model Development</b>	<b>33</b>
2.1	Introduction . . . . .	33
2.2	The precipitation process . . . . .	35
2.3	Data Sources for moisture source analysis . . . . .	36

2.3.1	Global Climate Models . . . . .	36
2.3.2	Regional Climate Models . . . . .	38
2.4	Moisture Transport Methodologies . . . . .	39
2.4.1	Direct techniques . . . . .	42
2.4.2	Eulerian techniques . . . . .	42
2.4.3	Lagrangian techniques . . . . .	43
2.4.3.1	Gridded wind field accuracy . . . . .	43
2.4.3.2	Interpolation errors . . . . .	44
2.4.3.3	Integration errors . . . . .	44
2.4.3.4	Unresolved processes . . . . .	44
2.4.3.5	Monte Carlo trajectory modeling . . . . .	45
2.4.3.6	Time reversed Lagrangian trajectories . . . . .	45
2.4.3.7	Trajectory vertical velocity . . . . .	46
2.5	Methodology . . . . .	46
2.5.1	Trajectory generation . . . . .	47
2.5.2	Precipitation diagnosis . . . . .	48
2.5.3	Trajectory Integration . . . . .	51
2.5.4	Evaporation and source attribution . . . . .	52
2.5.5	Trajectory endpoints . . . . .	54
2.6	Test integration . . . . .	56
2.6.1	Model configuration . . . . .	56
2.6.2	Land surface model . . . . .	57
2.6.3	Model output . . . . .	57
2.6.4	RCM and Lagrangian model validation . . . . .	58
2.6.5	Case Study Results . . . . .	60
2.7	Discussion and conclusions . . . . .	68

<b>3 Land and Ocean Results</b>	<b>69</b>
3.1 Description of experiment . . . . .	69
3.2 Presentation of results . . . . .	70
3.3 Seasonal Synoptic Anomalies . . . . .	71
3.4 Results . . . . .	73
3.4.1 Land Surface . . . . .	77
3.4.2 Ocean Surface . . . . .	95
3.5 Conclusions . . . . .	102
<b>4 Boundary Results</b>	<b>105</b>
4.1 Monthly Results . . . . .	105
4.1.1 Domain SA1 . . . . .	105
4.1.2 Domain SA2 . . . . .	106
4.1.3 Domain SA3 . . . . .	108
4.1.4 Domain SA4 . . . . .	112
4.2 Clustering Results . . . . .	112
4.2.1 Domain SA1 . . . . .	114
4.2.2 Domain SA2 . . . . .	118
4.2.3 Domain SA3 . . . . .	118
4.2.4 Domain SA4 . . . . .	118
4.3 Discussion . . . . .	125
4.4 Conclusions . . . . .	129
<b>5 Discussion</b>	<b>131</b>
5.1 The Lagrangian Attributed Source Model . . . . .	132
5.1.1 Regional Climate Model . . . . .	133
5.1.2 Lagrangian model skill . . . . .	133
5.1.3 Unresolved convective motion . . . . .	134
5.1.4 Impacts on attribution coefficient . . . . .	135

5.1.5	Evaporation diagnosis . . . . .	136
5.1.6	Future Developments . . . . .	137
5.1.7	Lagrangian Model Conclusions . . . . .	137
5.2	Discussion of the results . . . . .	138
5.2.1	Land surface moisture sources . . . . .	138
5.2.2	Western boundary source . . . . .	140
5.2.3	Circulation Linkages . . . . .	143
5.2.4	The Precipitation Process . . . . .	145
5.2.5	Climate Change Implications . . . . .	145
5.3	Conclusions . . . . .	146
<b>A</b>	<b>Lagrangian Model Code Details</b>	<b>149</b>
A.1	Introduction . . . . .	149
A.2	Pre-existing code and rationale for development . . . . .	149
A.3	Code details . . . . .	149
A.3.1	Treatment of input data and configuration . . . . .	150
A.3.2	Output data and archiving . . . . .	150
	<b>Bibliography</b>	<b>151</b>

# List of Figures

1.1	Map of weather station locations for which publicly available rainfall and temperature data is available for a least a 10 year period (Sources: GHCN, South African Weather Service, Agricultural Research Center) . . . . .	18
1.2	Austral summer general regional circulation. High pressure anti-cyclones are represented by H, the Inter Tropical Convergence Zone (ITCZ) and the Zaire Air Boundary (ZAB) are indicated by the yellow line. Blue arrows indicate the general lower level atmospheric circulation. . . . .	23
1.3	Austral winter general regional circulation. High pressure anti-cyclones are represented by H, blue arrows indicate the general lower level atmospheric circulation. . . . .	24
1.4	Mean heights of absolutely stable layers during summer and winter over Bethlehem (BETH), Bloemfontein (BLM), Pretoria (PTA), Port Elizabeth (PE) and Durban (DBN). Standard deviations for the base heights of the layers are illustrated by vertical lines. (Freiman and Tyson [2000]) . . . . .	27
2.1	December–February (DJF) 1988=89 seasonal rainfall (mm): a) CRU, b) CMAP. DJF inter-annual (1988=89–1991=92) rainfall anomaly (mm=season): c) CRU, d) CMAP ( Tadross et al. [2006]) . . . . .	40
2.2	DJF MM5 rainfall anomaly (mm=season) with respect to CRU observations (MM5-CRU) for the 1988=89 season. a) KF/MRF, b) BM/MRF, c) KF/ETA and d) BM/ETA ( Tadross et al. [2006]) . . . . .	41
2.3	Moisture trajectory generation: Model level integration mass flux ( $qU$ ) is calculated at each level. This mass flux is converted into trajectory parcels (green circles). The trajectory parcels are then traced through the target domain. Parcels that are involved in precipitation within the domain are retained and their trajectories are continued into the remainder of the domain. Parcels not involved in precipitation within the domain are terminated (red circles). . . . .	49
2.4	Idealised trajectory pathway with evaporative source and precipitation event. Initial parcel moisture is source from source A (50mm). 25mm is lost to the precipitation event. The evaporative source contributes 25mm to the parcel moisture. The resultant mixture of sources arriving at the target domain is 50% for source A and 50% for source B even though source B contributed twice as much moisture in absolute terms. . . . .	53
2.5	Idealised trajectory parameters varying through 66 hours of trajectory integration. The x axis represents time in hours prior to the event. Evap is the diagnosed evaporative uptake of the trajectory parcel which shows a regular idealised diurnal cycle. Precip is the diagnosed precipitation from the trajectory parcel and shows an initial event around $t=0$ and an upstream event peaking at $t=-38h$ . Attribution is the attribution coefficient as described in the text. Attributed evaporation is the product of the trajectory evaporative uptake and the attribution coefficient illustrating the reduced attribution of evaporation as a result of upstream precipitation events. . . . .	55

2.6 RCM geographical domain and surface altitude (meters) with analysis target regions SA2 and SA3 identified by the black rectangles . . . . .	57
2.7 Hourly time series of RCM precipitation averaged over domain SA2 (top) and Lagrangian diagnosed precipitation (bottom) for December 1988 illustrating the ability of the Lagrangian model to reproduce the RCM precipitation field. . . . .	59
2.8 Time mean (DJF 1988/9) vertical (height in Pa) profile of Lagrangian model moisture ( $kg/m^2$ ) source arriving at boundaries of target domain SA2 . . . . .	60
2.9 Time series of area averaged precipitation for region SA2 for the event of the 15th February 1989. (a) RCM simulated precipitation (mm/hour) and (b) Lagrangian attributed source moisture (mm/hour). The Lagrangian model captures the event but underestimates the magnitude. . . . .	61
2.10 Sequence of synoptic states: (a) 0600 14 Feb, (b) 1800 14 Feb, (c) 0600 15 Feb, (d) 1800 15 Feb. Contours are 500hPa geopotential height (m). The synoptic sequence is described in detail in the text. . . . .	62
2.11 Sequence of synoptic states: (a) 0600 14 Feb, (b) 1800 14 Feb, (c) 0600 15 Feb, (d) 1800 15 Feb. Contours are Sea Level Pressure (SLP) (hPa), solid lines are sea level pressure in Pa. The synoptic sequence is described in detail in the text. . . . .	63
2.12 Total attributed source moisture ( $kg/m^2$ ) across the RCM western boundary (altitude in Pa) during the period of 13-16 Feb 1989 for domain SA2. This field identifies the western boundary source as a being at high altitude (500hPa) and at latitude 32°S . . . . .	64
2.13 Time mean cross section (altitude in Pa) (35°S - 30°S) of Lagrangian parcel moisture field ( $kg/m^2$ ) for the period 11 - 15 Feb 1989 for domain SA2. The field illustrates the progression of moisture from the western boundary source at 500hPa altitude down to lower levels nearer the target domain SA2. . . . .	65
2.14 Mean Lagrangian parcel moisture field ( $kg/m^2$ ) between 600 hPa and 400 hPa altitude for the period 11-15 Feb 1989 for domain SA2. This field shows the progression of moisture from the high level western boundary source directly eastward towards the target domain. . . . .	66
2.15 Lagrangian land surface attributed source moisture ( $kg/m^2$ ) for the period 14 - 16 Feb 1989 for domain SA2 showing significant land source regions spread both north and south west of the target domain. . . . .	67
3.1 RCM domain map showing topography contours (meters) and the four analysis target domain, SA1, SA2, SA3 and SA4 . . . . .	71
3.2 RCM simulated monthly total rainfall (mm) for each Lagrangian target domain for each season (1988/9 and 1991/2) . . . . .	72
3.3 Dec, Jan and Feb SLP (Pa) and 700 hPa geopotential height (m) anomaly fields for 1988/9 season. Anomalies calculated from Dec-Feb 1988/9 seasonal mean. . . . .	74
3.4 Dec, Jan and Feb SLP (Pa) and 700 hPa geopotential height (m) anomaly fields for 1991/2 season. Anomalies calculated from Dec-Feb 1991/2 seasonal mean. . . . .	75
3.5 Total land surface attributed moisture source for Dec, Jan, Feb and total DJF periods for 1988/9 season, for target domains SA1, SA2, SA3 and SA4. Values are attributed moisture contribution in 10th's of a mm. . . . .	77

3.6	Total land surface attributed moisture source for Dec, Jan, Feb and total DJF periods for 1991/2 season, for target domains SA1, SA2, SA3 and SA4. Values are attributed moisture contribution in 10th's of a mm. . . . .	78
3.7	Seasonal mean attribution coefficient for all domains for 1998/9 season. Magnitudes are unitless ranging between 0 and 1. . . . .	80
3.8	RCM Precipitation field, 28th Dec through to 2nd Jan 1988/9, (mm/day) . . . . .	83
3.9	Land based source moisture (mm) for 31st Dec 1988 (a) and 1st Jan1989 (b) feeding target domain SA3 . . . . .	84
3.10	Vertical cross sections of Lagrangian parcel moisture (kg). (a) Latitudinal averaged between 25°S and 22°S, (b) Longitudinal averaged between 24°E and 26°E. . . . .	85
3.11	Target domain SA1 clustering results (column 1) and composite 850hPa sequences (-36 hour, -24 hours, -12 hours, 0 hours), clusters are ordered from 1 on the bottom row through to 5 on the top row. . . . .	89
3.12	Target domain SA2 clustering results (column 1) and composite 850hPa synoptic sequences (-36 hour, -24 hours, -12 hours, 0 hours), clusters are ordered from 1 on the bottom row through to 5 on the top row. . . . .	90
3.13	Target domain SA3 clustering results (column 1) and composite 850hPa sequences (-36 hour, -24 hours, -12 hours, 0 hours), clusters are ordered from 1 on the bottom row through to 5 on the top row. . . . .	91
3.14	Target domain SA4 clustering results (column 1) and composite 850hPa sequences (-36 hour, -24 hours, -12 hours, 0 hours), clusters are ordered from 1 on the bottom row through to 5 on the top row. . . . .	92
3.15	Total ocean surface attributed moisture source for Dec, Jan, Feb and total DJF periods for 1988/9 season, for target domains SA1, SA2, SA3 and SA4. Values are attributed moisture contribution in 10th's of a mm. . . . .	96
3.16	Total ocean surface attributed moisture source for Dec, Jan, Feb and total DJF periods for 1991/2 season, for target domains SA1, SA2, SA3 and SA4. Values are attributed moisture contribution in 10th's of a mm. . . . .	97
3.17	Target domain SA1 ocean source clustering results (column 1) and composite SLP sequences (-36 hour, -24 hours, -12 hours, 0 hours), clusters are ordered from 1 on the bottom row through to 5 on the top row. . . . .	98
3.18	Target domain SA2 ocean source clustering results (column 1) and composite SLP sequences (-36 hour, -24 hours, -12 hours, 0 hours), clusters are ordered from 1 on the bottom row through to 5 on the top row. . . . .	99
3.19	Target domain SA3 ocean source clustering results (column 1) and composite SLP sequences (-36 hour, -24 hours, -12 hours, 0 hours), clusters are ordered from 1 on the bottom row through to 5 on the top row. . . . .	100
3.20	Target domain SA4 ocean source clustering results (column 1) and composite 850hPa sequences (-36 hour, -24 hours, -12 hours, 0 hours), clusters are ordered from 1 on the bottom row through to 5 on the top row. . . . .	101

4.1 Domain SA1, Eastern boundary Dec, Jan, Feb and DJF total attributed moisture for 1988/9 and 1991/2 season. . . . .	106
4.2 Domain SA1, Western boundary Dec, Jan, Feb and DJF total attributed moisture for 1988/9 and 1991/2 season. . . . .	107
4.3 Domain SA1, Southern boundary Dec, Jan, Feb and DJF total attributed moisture for 1988/9 and 1991/2 season. . . . .	107
4.4 Domain SA1, Northern boundary Dec, Jan, Feb and DJF total attributed moisture for 1988/9 and 1991/2 season. . . . .	108
4.5 Domain SA2, eastern boundary Dec, Jan, Feb and DJF total attributed moisture for 1988/9 and 1991/2 season. . . . .	109
4.6 Domain SA2, western boundary Dec, Jan, Feb and DJF total attributed moisture for 1988/9 and 1991/2 season. . . . .	109
4.7 Domain SA2, southern boundary Dec, Jan, Feb and DJF total attributed moisture for 1988/9 and 1991/2 season. . . . .	110
4.8 Domain SA2, northern boundary Dec, Jan, Feb and DJF total attributed moisture for 1988/9 and 1991/2 season. . . . .	110
4.9 Domain SA3, eastern boundary Dec, Jan, Feb and DJF total attributed moisture for 1988/9 and 1991/2 season. . . . .	111
4.10 Domain SA3, western boundary Dec, Jan, Feb and DJF total attributed moisture for 1988/9 and 1991/2 season. . . . .	111
4.11 Domain SA3, southern boundary Dec, Jan, Feb and DJF total attributed moisture for 1988/9 and 1991/2 season. . . . .	112
4.12 Domain SA4, eastern boundary Dec, Jan, Feb and DJF total attributed moisture for 1988/9 and 1991/2 season. . . . .	113
4.13 Domain SA4, western boundary Dec, Jan, Feb and DJF total attributed moisture for 1988/9 and 1991/2 season. . . . .	113
4.14 Domain SA4, northern boundary Dec, Jan, Feb and DJF total attributed moisture for 1988/9 and 1991/2 season. . . . .	114
4.15 Domain SA1 eastern boundary cluster composite boundary moisture sources (column 1) and 850 hPa height synoptic sequences. Cluster 1 is on the bottom row and cluster 2 is on the top row. . . . .	115
4.16 Domain SA1 western boundary cluster composite boundary moisture sources and 500 hPa height synoptic sequence. Cluster 1 is on the bottom row and cluster 2 is on the top row. . . . .	116
4.17 Domain SA1 southern boundary cluster composite boundary moisture sources and SLP synoptic sequence. Cluster 1 is on the bottom row and cluster 2 is on the top row. . . . .	117
4.18 Domain SA2 eastern boundary cluster composite boundary moisture sources and 850 hPa synoptic sequence. Cluster 1 is on the bottom row and cluster 2 is on the top row. . . . .	119

4.19 Domain SA2 western boundary cluster composite boundary moisture sources and 500 hPa synoptic sequence. Cluster 1 is on the bottom row and cluster 2 is on the top row. . . . .	120
4.20 Domain SA2 southern boundary cluster composite boundary moisture sources and SLP synoptic sequence. Cluster 1 is on the bottom row and cluster 2 is on the top row. . . . .	121
4.21 Domain SA3 eastern boundary cluster composite boundary moisture sources and 850 hPa synoptic sequence. Cluster 1 is on the bottom row and cluster 2 is on the top row. . . . .	122
4.22 Domain SA3 western boundary cluster composite boundary moisture sources and 500 hPa synoptic sequence. Cluster 1 is on the bottom row and cluster 2 is on the top row. . . . .	123
4.23 Domain SA3 southern boundary cluster composite boundary moisture sources and SLP synoptic sequence. Cluster 1 is on the bottom row and cluster 2 is on the top row. . . . .	124
4.24 Domain SA4 eastern boundary cluster composite boundary moisture sources and 850 hPa synoptic sequence. Cluster 1 is on the bottom row and cluster 2 is on the top row. . . . .	125
4.25 Domain SA4 western boundary cluster composite boundary moisture sources and 500 hPa synoptic sequence. Cluster 1 is on the bottom row and cluster 2 is on the top row. . . . .	126
4.26 Domain SA4 southern boundary cluster composite boundary moisture sources and SLP synoptic sequence. Cluster 1 is on the bottom row and cluster 2 is on the top row. . . . .	127
4.27 Latitudinal cross section (height (m) versus longitude) of Lagrangian parcel trajectories originating at the western boundary and arriving at target domain SA2 for event of the 16 Feb 1988 . . . . .	128
5.1 Annual mean precipitation recycling ratio (%) at 1000km spatial scale. Trenberth [1999a] . . . . .	139
5.2 January mean backward trajectories for north west South Africa for dry days over the north eastern parts of South Africa. Contours represent percentage occurrence of trajectories. Thick lines represent the maximum frequency pathways. Large numbers indicate time of trajectory travel in days and small numbers indicate the average trajectory specific humidity ( $\text{g}\cdot\text{kg}^{-1}$ ) (D'Abreton and Tyson [1996]) . . . . .	141
5.3 Schematic diagram showing the main (solid) and secondary (dashed) pathways of ten-day backward trajectory clusters from a point centered over the northern interior (23 S, 30 E). The trajectories were initiated at 12:00 UTC on 14 February 1996 at the 750hPa level, which is the time of a significant precipitation event. The numbers indicate the approximate starting and ending altitudes in hPa (Crimp 1996) . . . . .	141
5.4 January trajectory fields for rain days for the north west of South Africa. Contours represent frequency of occurrence of trajectories. The thick line represents the highest frequency trajectory. Large numbers represent travel time in days and small numbers indicate specific humidity ( $\text{g}\cdot\text{kg}^{-1}$ ) (D'Abreton and Tyson [1996]) . . . . .	142



# List of Tables

2.1	Total and fractional Lagrangian attributed moisture sources ( $kg/m^2$ ) for domain SA2 during the event of 14 - 16 Feb 1989 for Land, Ocean and RCM boundary. Land surface and ocean surface are diagnosed as the two most important moisture sources for this event. . . . .	62
3.1	Attributed source moisture (mm) for 1988/9 DJF season for each target domain. Percentage values are the fraction of total source moisture. RCM precipitation totals (mm) are included for comparison. . . . .	76
3.2	Attributed source moisture (mm) for 1991/2 DJF season for each target domain. Percentage values are the fraction of total source moisture. RCM precipitation totals (mm) are included for comparison. . . . .	76
3.3	Relative moisture source amounts (mm) and percentages for 31st Dec through 1st Jan 1988/9 . . . . .	82
3.4	NCEP Re-analysis variables used in synoptic sequence compositing . . . . .	88

University of Cape Town



# Chapter 1

## Introduction

The thesis explores the role of atmospheric moisture sources, sinks and transport as one way to understand the regional climate processes over South Africa. The work builds on earlier studies (New et al. [2003], MacKellar et al. [2007, 2009]) suggesting that the regional land surface is an important component in the moisture cycle of the South African regional climate. In particular, the thesis recognizes that the land surface plays an important role as a source of moisture for local precipitation, and remains a poorly understood element of the regional climate dynamics. To address this issue the thesis develops a methodology to better explore this moisture component of the climate system. The methodology is based on Lagrangian trajectory modeling, a Regional Climate Model (RCM), and a moisture source attribution model.

**This aim of this thesis to enhance our understanding of the regional moisture processes over southern Africa, and so provide insights into the role of the regional land and ocean surfaces as important components of the regional climate system.**

The intention is to advance our knowledge of the regional system to inform the wider body of work that addresses climate vulnerability, impacts and adaptation.

To achieve this aim the thesis is structured around two broad elements; the development of a methodology that enhances our investigation of moisture, and the use of this methodology to explore selected questions of regional moisture. Within this overall focus three specific objectives are addressed:

- Develop a new Lagrangian based moisture source attribution model to overcome limitations and challenges of other moisture analysis methodologies.
- Evaluate the models ability to identify regional moisture sources.
- Apply the model to the southern African domain and explore the dynamics of the moisture sources under two contrasting seasonal modes, paying particular attention to the role of the regional land surface.

The focus domain of the study is southern Africa with a special attention to the summer rainfall area of South Africa due to its importance as a food production area as well as an area of rapid population growth and urbanization. The area is also of interest as it lies in an region impacted by both sub-tropical and mid-latitude weather systems. However, the methodological issues as well the moisture processes discussed are certainly generally applicable to a large number of domains globally.

Exploration of inter-annual variability of regional moisture sources and the impact of global scale tele-connection drivers are not within the scope of this study but would certainly constitute a priority follow on activity. Likewise, while

seasonal forecasting skill is discussed as an important part of the larger context, an analysis of the role of regional moisture sources in seasonal variability or seasonal forecast skill is also outside of the scope of this study but could readily form the basis for further work.

The climate system is a remarkably complex system. This is a result of the large number of component systems, substantial scale interactions, and a multitude of feed-backs, thresholds and oscillations. Component sub-systems include the atmosphere itself, the ocean, the land surface, and the physical processes within these including the chemistry and hydrological systems. Spatial scales and scale interactions range from the global scale in the form of the integrated radiative balances through to the molecular such as cloud micro-physics. Time scales and interactions range from millennial, that include plate tectonics and orbital shifts, through to seconds such as in boundary layer mixing and turbulent flows. The large scale, both temporal and spatial, is a composite reflection of and a driver of the small scale.

Regional scale climate systems are arguably uniquely complex in their positioning with the spectrum of scales and systems. While partly driven by the larger hemispheric or global scale systems, they are also driven by local and even micro-scale processes and systems. Many analysis methods, theoretical frameworks, and modeling systems, fail to adequately capture these factors. This poses a problem to climate forecasting at the seasonal time scale as well as projecting future climate states. It is essential that our understanding of the complexities of the regional climate system is improved in order that our ability to understand, forecast and project regional climates can be enhanced.

The intent of this thesis is to explore one aspect of this complex system, that of the regional land surface as a source of moisture for precipitation. This component of the system is arguably one of the least well understood both due to observational limitations as well as analysis limitations that will be discussed in this chapter (Koster et al. [2002]).

As the thesis is focused on both a methodological question as well as questions of regional moisture dynamics in southern Africa, this chapter serves as an introduction to the existing methodologies used to study moisture dynamics as well as the current understanding of regional moisture dynamics in the region. Chapter 2 will provide a more detailed description of methodological issues to investigate moisture transport and source as well as details of the development of the Lagrangian moisture source attribution model. Chapters 3 and 4 will describe the results using a two season integration of the Lagrangian model for the southern African domain, using two seasons that represent examples of two opposing modal states of the regional climate. Chapter 5 will conclude with a discussion of the results and further research questions that emerge.

The remainder of this chapter sets the scene for the subsequent chapters and discussion. As already mentioned, the issues and features identified with this region are not unique and similar issues and challenges can be identified in many other regions.

## 1.1 The Southern African Context

The southern African region is characterized by diversity, both of climate, land surface, regional ocean currents, and human development. The climate varies from dune deserts in Namibia, with annual precipitation of less than 20 mm, to a Mediterranean temperate climate in the south, to sub-tropical and tropical regions with annual precipitation as high as 2000 mm as we move north and east. Some of the climate gradients are fairly gradual while others are sharply defined. These sharp climate gradients are largely tied to topographic features such as the eastern escarpment which extends from the Drakensberg mountains in Lesotho northwards through Mozambique and Zimbabwe.

The region is characterized by large areas of dry climate zone, and water forms a critical element for the region, with significant dependency on the regional river systems (many of which are trans-boundary). This includes several

large rivers cross the region. The most significant of these for South Africa is the Orange River which drains the Lesotho highlands and large areas of South Africa before entering the Atlantic Ocean. The Orange river also borders Namibia for a significant section and is critical to dry land agriculture along its length. Further north the Limpopo river originates in Botswana and flows through Zimbabwe, South Africa and Mozambique. It forms a border between South Africa and Botswana and South Africa and Zimbabwe. Even further to the north lies the Zambezi, Africa's fourth largest river system, which originates in north western Zambia, crosses into Angola then back into Zambia, Zimbabwe and Mozambique. The Zambezi flows through a number of dams including the Kariba hydro-electric dam which is an important source of electrical power for both Zambia and Zimbabwe. Downstream lies the Cahora Bassa dam in Mozambique which provides power for Mozambique and South Africa. The cross boundary nature of these rivers raises many questions around rights of access and has been identified as a potential source of conflict in the future (Ashton [2002]). As important as these rivers are for the region, much of the agriculture is rain fed which does not draw on adjacent rivers but relies on seasonal rainfall. Rain fed agriculture provides the staple food supply for the region and hence dependence on timely seasonal rains is critical for effective food security in the region.

The region is therefore one of great complexity, geographically, climatologically and socially. However, a great deal of the prosperity, livelihood, health and well being of people in the region is tied to the climate and particularly water, whether directly or indirectly (Vogel [2005]) While people are certainly able to adapt to climates in different areas and have proved extremely resourceful in obtaining water, there is still great vulnerability to changes in the climate from year to year as well from decade to decade. Such variability in climate is a core characteristic of the region.

### 1.1.1 Climate Variability

Climate variability in the region, on a range of time and space scales, shows marked extremes with extensive and severe droughts occurring throughout recorded history, along with equally destructive floods in areas (such as occurred in Mozambique in 2000). Variability spans a range of time scales, but of societal relevance the most critical include intra-seasonal variability of dry and wet spells, extreme events, and seasonal timing of rainfall onset and cessation. These factors vary additionally on interannual time scales with frequent anonymously wet or dry years. Moisture (or lack of) is a key element of this variability, and extending our understanding of moisture processes can help understand the regional responses to the large scale variability.

Historical records show that the region experiences large climate variability on an inter-annual basis as well as over longer periods (Rouault and Richard [2005], Giannini et al. [2008]). Clearly the ability to deal with and adapt to this variability has formed an important part of development in the region ranging from the local scale to the national and regional scale. However, as populations grow and urbanization accelerates, strain is placed on existing natural and artificial systems that provide water and food in the region (Handmer et al. [1999], Hendrix and Glaser [2007]).

A classic example of this is the Highlands water scheme that involves pumping large amounts of water from dams in the Lesotho highlands through large tunnels into the Vaal river and Vaal dam in order to supply water to the growing industrial/economic region of Gauteng. In addition it provides nearly 100% of Lesotho's power requirements through hydro-electric power. However, this scheme has been controversial as there has been some dispute regarding the compensation of people displaced by the dams as well as the ecological consequences of changing river flows. Such large transfer schemes could increasingly become necessary in the future given population growths and the ongoing rural-urban migrations to cities that do not have adequate water supplies. Population and industrial growth pressures additionally create a changing water demand environment that needs to be dealt with regardless of any consideration of future climate change in the region.

Thus climate variability plays a very important part in this landscape as the design and management of water supply systems must be able to deal not only with the mean climate state but with a strongly varying climate.

Seasonal forecasting is an important tool for planning and management of water resource infrastructure as well agriculture. Current forecast skill in the region is dependent on the phase of ENSO as well as other factors. In particular, skill is good during predominantly wet conditions (La Nina) and moderate during predominantly dry conditions (El Nino), but remains weak during neutral ENSO years as documented in Landman and Beraki [2012]. Johnston et al. [2004] concluded that at more local scales current forecast skill is problematic with respect to user needs.

A number of modeling studies have suggested that improved initialization of regional soil moistures can contribute to improved seasonal forecast skill ( Fennessy and Shukla [1999], Ferranti and Viterbo [2006], Koster et al. [2004a] While these studies do not disaggregate the role of soil moisture on latent heat versus evaporative sources, it remains likely that an improved understanding of the internal drivers of the regional climate system, including soil moisture, could contribute towards improving seasonal forecasting skills and hence assist in effective water resource management in the region. It must be noted that this thesis is not focused on seasonal forecasting or seasonal forecast skill as such and will not attempt to show a linkage between regional moisture sources and seasonal forecast skill. This thesis aims to provide insights into the role of the regional land and ocean surfaces as important components of the regional climate system and so add to the understanding of this system.

### 1.1.2 Climate Change

The influence of climate change in the southern African region is an area of much ongoing study (Reason et al. [2006]). Africa as a whole has been identified as an area highly vulnerable to global warming driven climate change (Boko et al. [2007]). This is partly due to the magnitude of the temperature changes projected for the continent (Christensen et al. [2007]) and partly due to the marginal economic and infrastructural state of much of the continent. This leaves large fractions of the population highly vulnerable to long term climate change. However, regional projections of climate change are uncertain. While Global Climate Model (GCM) based projections for the area show strong agreement for temperature, precipitation projections are more varied across between models (Christensen et al. [2007]). For South Africa there does seem to be some consensus that the eastern side of the sub-continent could experience wetter mean conditions in the future while the western parts will remain the same or experience slightly drier conditions (Hewitson and Crane [2006], Christensen et al. [2007]). However, it is possible that the strongest influence of climate change in the region, as indeed globally, will be experienced not through a change in the mean but rather through a change in the distribution of events, and especially in the extremes (Field et al. [2012]). For the southern African region some of the main concerns are extreme dry and hot conditions, heavy rainfall events causing flooding, and increased variability

Changes in the mean temperature are likely to be as high as 3°C by 2050 (Christensen et al. [2007]). Such an increase in the mean temperature will have significant consequences for agriculture and natural systems as well as human water supply infrastructure and management.

As already noted, climate model projections for the region do not paint a cohesive picture of future change for all regions, especially the interior summer rainfall region of South Africa. However, there is some agreement around the changes in the large scale circulation dynamics that might be experienced. Global warming generally results in a more intense hydrological cycle (Huntington [2006], Trenberth [1999b]). Strong global warming is projected to produce an expansion of the Hadley circulation towards the poles (Lu et al. [2007], Hu et al. [2007]) which leads to larger subtropical high pressure systems. These high pressure systems dominate the continental dynamics producing greater subsidence and stability which generally suppresses rainfall. However, the same intensified circulation systems and a moister atmosphere could result in a greater flux of moisture from the Indian Ocean into the subcontinent which could help explain the projections of wetter conditions along the eastern part of the sub-continent. Enhanced surface warming and strong topographic forcing in the region could also contribute to these projected precipitation increases.

The increased high pressure systems also result in a southerly shift in the mid-latitude systems possibly resulting in less frequent or less intense rainfall events in the south of the continent in winter. However, a moister atmosphere interacting with high topography in the area could result in increase orographic rainfall in mountainous regions of the south west continent.

It is therefore clear that a better understanding of the regional moisture dynamics is of great value in understanding and improving future projections of climate in the region. Global climate models are not capable of capturing the complex regional dynamics that are so critical in the regional climate. It is therefore necessary that these model results are interpreted with an understanding of the regional dynamics. It is also important that an understanding of local scale influences such as topography, soil moisture, vegetation and regional Sea Surface Temperatures (SST) are incorporated.

Once again, an improved understanding of the regional climate system will potentially improve our ability to interpret, understand, and integrate climate projections into regional planning and development and hence reduce the regional exposure to climate change risks.

### 1.1.3 The observation record problem

As so much of our understanding of the global and regional climate is fundamentally based on observations of climate over long periods it is worth briefly noting the challenges involved with observational data. These observations, whether from weather stations at the surface, from radiosondes ascending periodically to high altitudes or from satellite systems, are the critical foundation of any climate study. Many climate related studies in the southern African region have been hindered by the scarcity and poor quality of the observational data. While some countries such as South Africa and Namibia have maintained relatively good climate records at a large number of locations, other countries have recorded very little and often records are lost or of such poor quality that they cannot be used with confidence (Figure 1.1). Other institutional issues such as data access policies restrict the availability of such data. This is an unfortunate constraint on research in the region and an improvement of the observational network needs to take high priority at the national and regional level with support from the international community.

It is therefore always important to remember that the climate in the region is not well observed and hence many methodologies, models, and analysis, are limited by the inherent observational uncertainties. Such limitations also extend to atmospheric re-analysis datasets. While more recently satellite derived datasets have been able to provide information to fill in gaps where station and vertical profile observations are lacking (Rouault et al. [2001]), the absence of surface and profile observations is still an important concern in such datasets. Certainly any re-analysis data for periods prior to the 1970s when satellite data first became available must be considered very uncertain, particularly in upper air fields (Tennant [2004]).

This observational problem is of great import in this thesis study for two reasons. Firstly, the regional climate simulation that drives much of the study is dependent on re-analysis fields to define its time varying boundary conditions. Secondly, validation of precipitation fields simulated by a regional climate model is dependent on intensive coverage of observed precipitation data. Beyond precipitation, the thesis deals with soil moisture and evaporation, two variables which are difficult to observe and are poorly captured globally. While some satellite based estimates of soil moisture are available (Owe et al. [2008]), observed surface evaporative flux data is extremely hard to obtain and validate.

However, valuable information is available in both the raw observational network as well as derived products such as reanalysis simulations, and the range of various precipitation datasets available for the region.

Thus, collectively observational data constraints represent an inherent limitation. Nonetheless, adequate observational data does exist to bound the problem, and enable assessment of the fundamental and first order processes, but retaining cognizance of the inherent uncertainties must be maintained in all analyses and in the discussion of the results.

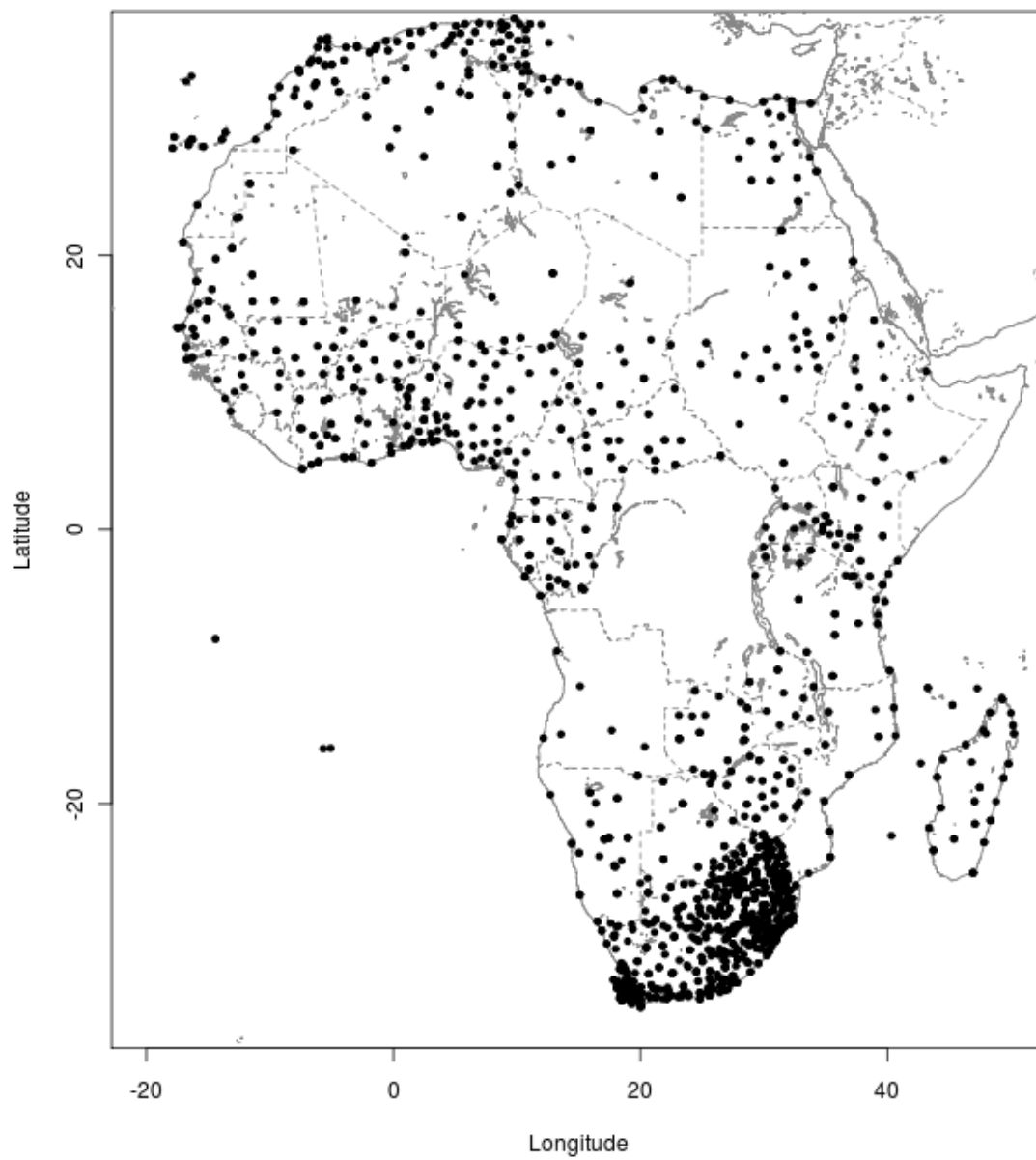


Figure 1.1: Map of weather station locations for which publicly available rainfall and temperature data is available for a least a 10 year period (Sources: GHCN, South African Weather Service, Agricultural Research Center)

### 1.1.4 Moisture Transport Analysis

As the thesis explores the regional sources of moisture it is appropriate to review existing methodologies and associated studies applicable to this objective. The current understanding of the regional climate system and moisture dynamics is the result of a great deal of research. These studies have been based on a number of different methodologies including correlation analysis, moisture flux analysis, trajectory analysis and dynamical modeling studies. The intent of this section is to provide an overview of these methods and their general strengths and weaknesses in order to develop a foundation from which to develop an alternative methodology in the form of a Lagrangian moisture source attribution model. It is acknowledged that within each general methodology are found a large spectrum of variations and implementations which are impossible to discuss and evaluate in the scope of this study. The intrinsic value and contribution of the associated work is also strongly acknowledged.

#### Correlation analysis

While not directly a method to analyze moisture transport, correlation analysis is often used as a means of associating moisture sources (evaporation) with sinks (precipitation) and hence the methodology is discussed in this section. Indeed a number of studies have used correlation analyses in order to find linkages between a forcing variable, such as sea surface temperatures (SST) in one area, and another variable, often precipitation, in either the same area or a different area (Behera and Yamagata [2001], Allan et al. [2001]). Often SST fields are reduced in dimensionality through Principle Component Analysis (PCA) prior to the correlation. Correlation analysis is very useful in that it can identify possible linkages between climate variables that are not immediately obvious from the observations. However, correlations do not provide information about the underlying physical processes and also do not identify causation. In other words, a correlation between a forcing variable and a target variable does not prove that a change in the forcing variable actually causes the change in the target variable, only that they have some degree of covariance through time. It is always possible that the variance in both parameters is caused by some other process not identified. It is also often difficult to identify or describe the physical process that could be responsible for any correlation between two variables. As such, correlations can be used either operationally in forecast systems, or as means of exploring possible physical processes. Correlation studies often form the basis for further investigation of the underlying processes, typically through a dynamic analysis method or through climate modeling.

#### Dynamic analysis

By dynamic analysis we refer to those methods that capture the dynamic nature of moisture transport and budgets as they vary across space and through time. These methods center on the atmospheric moisture flux, both directly as well as through the convergence or divergence of this flux. The underlying understanding is that given a particular three dimensional (spatial extent and vertical column) box in the atmosphere, the moisture flux passing through the box can be calculated given the wind velocity and mass of moisture at each vertical level. Typically moisture flux is calculated over the full vertical column in order to avoid issues of vertical motion. If the calculation is performed for a limited vertical layer then account must be made of vertical motion into and out of this layer which adds significantly to the complexity of the calculation as well as the interpretation. Vertical integration does have the consequence of hiding the complexities of the vertical profile of moisture and wind in the atmosphere. Certainly over South Africa a number of stable layers (D'Abreton and Tyson [1996]) associated with different transport patterns have been identified. Such structures are obscured through vertical integration of moisture fluxes.

Beyond the horizontal flux, the horizontal convergence of moisture into or divergence out of the box can also be calculated. Convergence and divergence must be calculated over the full vertical column unless explicit consideration or

accommodation of vertical motions is included. Total column convergence of moisture within a limited domain can be accounted for through two processes. Either atmospheric moisture content increases, or moisture is lost to precipitation. Likewise the divergence of moisture occurs either through the reduction in atmospheric moisture content or through evaporative gains. The relationship between atmospheric moisture convergence or divergence and precipitation or evaporation is an attractive one as it offers the possibility of examining surface moisture sources and sinks. A surface moisture source identifies itself as a long term area of moisture divergence, likewise a moisture sink is seen as an area of convergence. However, this relationship is only valid at long time scales of weeks or months. At daily time scales the variation in atmospheric moisture content is significant and impossible to disaggregate without further information in the form of precipitation and evaporation data (Trenberth [1998]). At longer time scales atmospheric moisture content variations are typically much smaller compared to moisture convergence and divergence and hence can arguably be discarded. Certainly the addition of precipitation and evaporation information adds significantly to this analysis, however, while precipitation data is relatively easy to obtain, evaporation data is generally scarce or of poor quality (Trenberth [1999a]). Some analyses attempt to capture the smaller time scale processes by splitting the analysis into a stream and eddy component with the eddy component representing the effect of short time scale processes and the stream component representing time mean processes (D'Abreton and Tyson [1995]). Such analysis does indeed provide added information though the interpretation of the results and linking to physical processes is difficult.

It is clear that a great deal of important information about the large scale transport and potential sources and sinks of moisture can be obtained through the use of moisture flux analysis. Limitations at small spatial and temporal scales are real and important and should be seriously considered in any attempt to explore regional scale moisture transport methods. Extensions of basic moisture flux analyses have also been developed that more fully capture the local scale processes through the incorporation of precipitation and evaporation data. These methods generally fall into the broad class of precipitation recycling analysis discussed in the next section.

### **Precipitation Recycling Analysis**

While in some senses a form of dynamic analysis, precipitation recycling is a distinct methodology that has been used extensively to explore regional moisture dynamics. It is worth considering this methodology separately from those above due to its applicability to the proposed thesis. Precipitation recycling is defined as the fraction of precipitation that has a local evaporative source versus that which has a remote evaporative source (Budyko [1974]). The extent of the local domain is determined by the spatial scale selected which in most studies varies from 500km through to 2000km. Various forms of the methodology have been developed as reviewed by Burde and Zangvil [2001a]. Most methodologies are based on an analysis of the vertically integrated moisture flux versus the local regional evaporative and precipitative fluxes. Assumptions are made about instant and complete mixing of evaporated moisture through the vertical column, constant atmospheric storage, and the uniformity of flow over the region. Various extensions to the methodology have been developed to address these assumptions. Burde and Zangvil [2001b] incorporated the ability to deal with non-uniform flow while Burde [2006] incorporated non-uniform vertical moisture profiles. Both extensions produce different and generally higher estimates of precipitation recycling than simpler methods. Anderson et al. [2008] developed an alternative metric substituting local atmospheric moisture convergence rather than moisture flux. This metric results in quite different results depending on the region and season but also generally produces estimates of precipitation recycling up to 30% higher than non-convergence flow methods. These results suggest that enhanced representation of regional flow complexities results in higher estimations of precipitation recycling.

Two major limitations of the methodology have emerged in the literature (Bosilovich [2002], Burde [2006], Burde et al. [2006]) and a number improvements designed to address these limitations have been developed. The first relates to the assumption that moisture is mixed uniformly throughout the atmospheric column. While this is clearly a poor assumption it does greatly simplify the formulation of the methodology. However, Bosilovich [2002], through a GCM

based tracer experiment as described above, noted that moisture available to convection is generally sourced nearer the surface where the fraction of locally evaporated moisture to remotely sourced moisture is typically higher than in the upper atmosphere. It is likely that the traditional recycling metric underestimates the recycling fraction due to the assumption of complete mixing. As already mentioned, Burde [2006], Burde et al. [2006] develop an alternative formulation to accommodate non-uniform vertical mixing resulting in higher recycling ratios in many areas.

The second limitation is that the methodology is generally applied to monthly time mean data because of the requirement of uniform flow conditions and no atmospheric storage of moisture. Daily circulation fields are generally not uniform and at the daily time scale atmospheric moisture storage is significant which breaks the assumptions of the methodology. Dominguez et al. [2006] demonstrated a recycling model that accommodated short term atmospheric moisture storage and hence is applicable at time scales on the order of days. Results showed similar spatial patterns when applied at the daily time scale but recycling fractions 12% - 33% higher than when applied at monthly time scales. If non-uniform flow is accommodated, results can also be markedly different (Burde and Zangvil [2001b]).

It is clear from the literature that conventional precipitation recycling methods depend on assumptions that produce significantly lower evaluations of recycling that if those assumptions are removed. However, in order to remove the assumptions the methodologies become much more complex and other assumptions must be made. While certainly an important and useful methodology at regional space scales and monthly or longer time scales, limitations at smaller time and space scales are significant. The methodology proposed in this thesis attempts to represent the precipitation recycling process but removes many of the constraints of the bulk recycling model and derivatives.

### **Dynamical modeling**

The third main type of methodology applied to regional climate studies is that of dynamical modeling. This takes the form of either General Circulation Models (GCM) or regional climate models. The majority of modeling studies exploring moisture source dynamics involve some kind of perturbation sensitivity experiment. In these experiments the model is forced with either an observed perturbation from the climate mean state, or with an idealized perturbation. Typically this will be a perturbation of a boundary parameter such as Sea Surface Temperatures (SSTs) or a land surface parameter. The response of the model to that perturbation is then analyzed in order to infer some real climate response to a particular forcing. Such modeling studies have proved foundational in developing our understanding of forcings such as the El Niño Southern Oscillation (ENSO) both through observed perturbation studies as well as idealised studies (Cook [2001]). While studies using observed perturbations are arguably more realistic, they are often more difficult to interpret due to the complexity of the perturbation. Idealised perturbations typically use fairly simple, spatially constrained perturbation fields and hence are easier to interpret in terms of physical processes.

While the first dynamic models were actually limited area models (Weart [2010]), much foundational climate systems analysis work has been done using GCMs. More recently sensitivity studies using RCMs have gained popularity due to the higher spatial resolution and associated ability to resolve finer scale processes and systems. In particular, the role of the land surface in southern Africa has been studied through RCM based experiments (New et al. [2003], MacKellar et al. [2007, 2009]). One challenge with RCM based studies is the lack of feedback between the RCM and forcing GCM. For small domains this problem is not significant as the impact of a small region on the global climate is generally limited. However, for larger domains, such a whole of Africa domain, the impact of a perturbation across the RCM domain is almost certain to have global feedbacks. Without feedbacks to the GCM these impacts and feedbacks are not captured in the experiment. Stretched grid based models such as C-CAM (McGregor and Dix [2008]) are configured to have a high resolution over a limited domain of interest and lower resolution over the remainder of the globe. This approach solves the feedback and other problems with RCMs but does also introduce other complexities such as scale dependent process parameterisations. Parameterisations represent processes that operate at scales smaller than the model grid scale and so cannot be resolved explicitly by the model grid scale

dynamics. Parameterisations are typically designed or tuned to particular grid scales and special attention must be paid to appropriate parameterisations in stretched grid models.

Dynamical model based methods are very powerful as they allow an investigation into the atmospheric response to a particular, controlled, perturbation. However, understanding the physical processes and complex feedbacks associated with such responses requires much more work beyond actually running a model. Studies generally rely on various forms of dynamic analysis as described above in order to unpack the atmospheric response. The associated limitations of those methods apply. A classic example of such an experiment and associated analysis challenges is found in New et al. [2003], where the regional precipitation response to a perturbation in the land surface was remarkably complex and associated with thermodynamic and circulation feedbacks which counteracted the surface flux drivers.

Model skill or accuracy is also an important concern. The complexity and accuracy of models has increased over the last several decades, partly due to improved understanding of the climate system components and partly due to increased computational capacity. However, many models still fail to capture certain climate systems and processes. The ability to accurately capture systems such as the El-Nino Southern Oscillation (ENSO) and processes such as monsoonal rainfall vary between models and the models skill must always be considered in any such experiments.

The methodology developed in this thesis is uses an RCM simulation of the regional climate and as such is dependent on the RCM produced atmospheric fields. While no perturbations are introduced in the RCM in this study the Lagrangian moisture source methodology is certainly applicable in the case of model perturbation experiments and this could form a valuable future line of exploration.

## 1.2 Southern African Regional Climate System

As the second component of this thesis considers moisture sources for the southern African region and South Africa in particular, it is important to have some understanding of the climate system in this region. The intent of this section is not to provide an overview of all aspects of the regional climate system as this would be beyond the scope and the focus of the thesis. Reason et al. [2006] provides a comprehensive overview of the current understanding of the southern African regional climate system. The intent is rather to provide enough of a description of the relevant processes and systems in order to allow for an informed analysis and discussion of the results presented in later chapters. The relevant systems and processes include the regional circulation that is responsible for the transport of moisture, the synoptic states and sequences responsible for the initiation and maintenance of precipitation processes, and the possible sources of evaporative moisture to feed the precipitation processes. Sources of inter-annual variability of these systems are also described as the region is particularly influenced by the effects of inter-annual variability. However, inter-annual variability is not a specific focus of this study as the scope of the study does not allow such an analysis.

Like any regional climate system, the southern African regional climate is a function of both global and hemispheric scale circulation features as well as local scale features such as sea surface temperatures, topography, vegetation, and soil moisture. Understanding of the impact of these local scale features on the regional climate is fairly limited for the southern African region though it is the subject of some research which will be discussed later in this chapter. The thesis, as described above, has as a central hypothesis that the local land surface is an important component of the regional climate, particularly as a source of moisture. The extent to which this thesis is supported by experimental results will become apparent in the later chapters.

It is important to note that, with regards to the regional moisture source and transport dynamics, the details described in the subsequent sections have largely been determined through the use of the existing methodologies described in

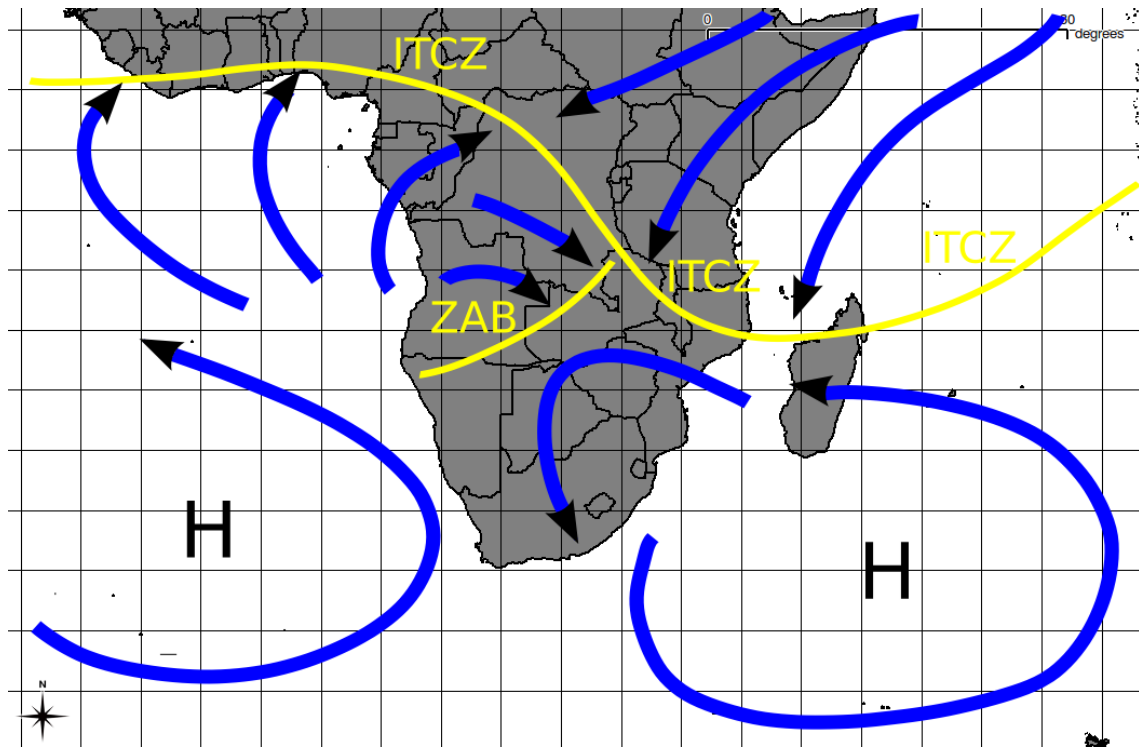


Figure 1.2: Austral summer general regional circulation. High pressure anti-cyclones are represented by H, the Inter Tropical Convergence Zone (ITCZ) and the Zaire Air Boundary (ZAB) are indicated by the yellow line. Blue arrows indicate the general lower level atmospheric circulation.

the previous section. As such, their associated strengths and weaknesses come into play. It will become clear that the complexities of the regional climate and moisture dynamics are perhaps not well captured by all of the methodologies used in the literature, and consequently the current understanding of these complexities may be limited.

However, regardless of these complexities and potential gaps in our understanding, the general regional climate gradients and seasonal shifts can readily be understood as synoptic features conditioned by global and hemispheric circulation systems. Precipitation processes can likewise generally be linked to these synoptic and large scale systems, modulated by local forcings to a greater or lesser degree, depending on the synoptic mode.

### 1.2.1 General regional circulation

The regional circulation dynamics of southern Africa are dominated by five main circulation systems as illustrated in Figure 1.2 (Summer) and Figure 1.3 (Winter). These circulation systems are common to many areas of the world that extend from the tropics through to the mid-latitudes. Southern Africa is However, unique in the extent of the land mass, the topographic features of the land mass with highest topographies on the eastern side and lower topography to the west, and the dominance of large ocean basins to the west, east and south.

#### Indian Ocean

To the east of the sub-continent the South West Indian Ocean (SWIO) high pressure system produces anti-cyclonic circulation but this results in easterly and north easterly winds along the eastern coastlines of South Africa and Mozambique. A great deal of literature identifies the tropical and south west Indian Ocean as the primary driver of southern African precipitation (Goddard and Graham [1999], Landman and Mason [1999], Mason [1995], Washington

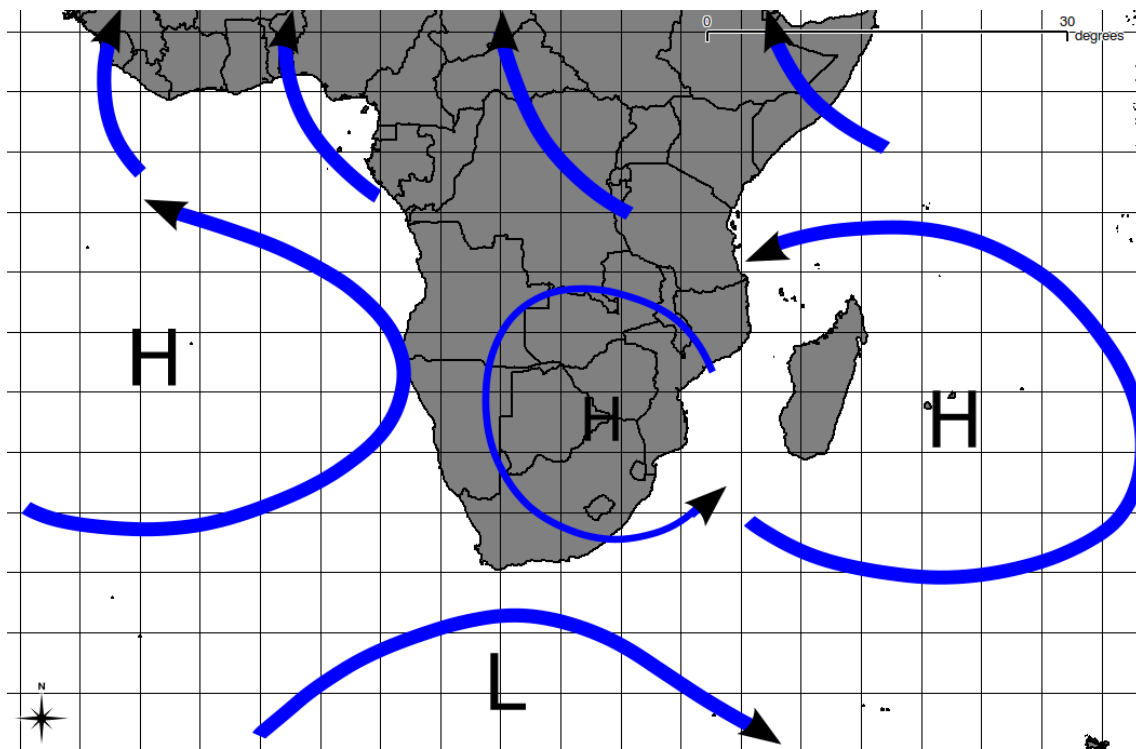


Figure 1.3: Austral winter general regional circulation. High pressure anti-cyclones are represented by H, blue arrows indicate the general lower level atmospheric circulation.

[2006], Cook [2000], Marchant et al. [2007], Reason and Mulenga [1999], Reason [2001], Todd et al. [2004]). The mechanism is twofold. Firstly, Indian Ocean SST anomalies, structures, and gradients, strongly determine the basin scale atmospheric circulation patterns, in particularly the positioning of the SWIO anti-cyclone. Secondly, Indian Ocean SST anomalies influence the availability of moisture made available for precipitation with the sub-continent. These two mechanisms can be described in more detail:

Indian Ocean SSTs strongly determine the basin scale circulation by driving the surface thermal gradients across the basin. The intensity, extent, position, and shape of the SWIO high pressure system is partly determined by SSTs and partly by global scale structures such as the Walker circulation. The structure and strength of the tropical easterly flow into the sub-continent is also strongly associated with SST structures (Reason [2001]). The positioning of the SWIO sub-tropical convergence zone also appears to be partly related to SST structures (Cook [2000]). Goddard and Graham [1999], through an idealised dynamical model experiment, isolates the Indian Ocean as the strongest driver of rainfall anomalies in southern Africa and identifies the competition between pacific SST anomalies associated with ENSO anomalies and Indian Ocean SST anomalies as an important component of regional circulation and rainfall variability.

With more direct bearing on this thesis is the important role of the Indian Ocean as a moisture source. D'Abreton and Tyson [1995, 1996] both identify the Indian Ocean as the most important moisture source regional for the sub-continent. D'Abreton and Tyson [1995] uses a vertically integrated moisture flux convergence method to identify moisture source and sink regions and in so doing identifies the Indian Ocean as far more important than any other region. D'Abreton and Tyson [1996] applies a simple backward trajectory method to trace high moisture content air over southern African back to the Indian Ocean.

The SWIO is thought to have an important role in the development of Tropical Temperate Troughs (TTTs) (Fauchereau et al. [2009]) and enhanced SSTs in this enhance the development of these troughs. However, the relationship with rainfall is probably more complex as the longitudinal positioning of TTTs seems to be associated with SST patterns. An eastward shift in warmer SSTs and the associated TTTs can produce drier conditions over the subcontinent as the associated rainfall band moves over the ocean.

To the north of Madagascar it seems possible that an interesting SST driven association is found. High SSTs in this area produce tropical disturbances and rainfall over this ocean region potentially reducing the likelihood of such disturbances over the continent and hence producing dry conditions over the continent. We shall see in later chapters how this area is potentially very important for southern African rainfall in terms of the regional moisture balance and transport.

### **Atlantic Ocean**

To the west of the sub-continent, the South Atlantic High Pressure (SAHP) system, driven by the Hadley circulation, produces anti-cyclonic circulation and drives a dominantly southerly low level wind over the south western part of the continent. This southerly wind is critical for the west coast coastal ocean upwelling systems which drive the important coastal fisheries in the area. The SAHP periodically ridges around the south of the continent producing easterly winds along the south coast and south easterly winds along the south east coast. As strong as the arguments are for the dominance of the Indian Ocean as the regional moisture source, some literature does also identify the Atlantic ocean as a moisture source for the region (Reason and Rouault [2006], Hermes and Reason [2008], Vigaud et al. [2009], Rouault et al. [2003]). The tropical western Atlantic Ocean serves as a source of moisture for tropical and sub-tropical Africa, south of the equator which in turn, through the dynamics of the Angola low pressure, the continental heat low, as well as tropical temperate trough systems, serves as a source of moisture for southern Africa. Hermes and Reason [2008] also identifies south east Atlantic SSTs as important drivers of regional circulation and moisture advection, though not as an evaporative moisture source. In addition, the reverse trajectory work of Crimp and Mason [1999] shows a possible high altitude south Atlantic moisture source for a particularly large rainfall event in the summer rainfall region of South Africa. The origin of this high level moisture source is not really ascertained though tropical South America seems a likely location and the South Atlantic Convergence Zone (SACZ) a likely mechanism. Nicholson and Entekhabi [1987] also identified warm near coastal SSTs along the south west coast of southern Africa as having a positive impact on coastal rainfall, partly through the direct impact of moisture availability, but dominantly through circulation changes and increased instability.

Thus while the tropical Atlantic serves as a source of evaporative moisture for the sub-continent, the dominant role of the SSTs in the South Atlantic region is through circulation controls such as shifting the latitude of the surface westerlies and promoting or suppressing cyclo-genesis (Tyson [1987])

### **Agulhas and Mozambique currents**

Associations with SSTs in the Agulhas and Mozambique current regions are possibly related to increased evaporation and moisture transport into the sub-continent through the tropical easterlies. This is an important moisture pathway for the region and these particular ocean moisture sources will be explored directly in later chapters. Rouault et al. [2002] in particular, show the importance of the Agulhas as a moisture source for heavy rainfall events in South Africa.

### **Tropics, mid-latitudes and connections**

Towards the equator the Inter-Tropical Convergence Zone (ITCZ) and associated tropical low pressure systems periodically extend southwards producing wide spread rainfall in the north of the sub-continent (Preston-Whyte et al. [1989]). The Zaire Air Boundary (ZAB), which originates in the South Atlantic, is another zone of convergence influencing the western part of the sub-continent and merging with the ITCZ towards the eastern side (Preston-Whyte

et al. [1989]). The southern branch of the African Easterly Jet (AEJ-S), a weaker sister to the Tropical Easterly Jet to the north, is driven by reversed temperature gradients between the tropics and the sub-tropics in the later part of the year as the ITCZ moves northwards and the land surface dries and cools. The jet has been associated with rainfall in the southern African region (Nicholson and Grist [2003]).

To the south of the continent the thermal wind driven mid-latitude jet and embedded Rossby waves drive the formation and passage of mid-latitude troughs. These troughs produce mid-latitude cyclonic systems near the surface with associated warm and cold fronts (Preston-Whyte et al. [1989]). The warm fronts generally occur too far south to impact southern Africa. Cold fronts are However, the dominant rain producing systems for the southern coast though they regularly extend as far north as Namibia and are responsible for winter snows and cold conditions in the Lesotho highlands.

Linkages between tropical low pressure features and mid-latitude troughs drive the important Tropical Temperate Troughs (TTTs), which appear to be associated with around 50% of the rainfall in South Africa (Preston-Whyte et al. [1989]) and have been described fairly extensively (Todd and Washington [1999], Todd et al. [2004], Harrison [1984]). Finally, over the continent itself, the thermal low pressure and west coast trough are driven by surface heating during the summer months. The Angola low pressure over Angola is a heat low which also plays a role in regional moisture transport (D'Abreton and Tyson [1995]). These low pressure systems drive the advection of moisture into and over the sub-continent and contribute to the vertical instability required for convective activity.

### 1.2.2 Absolutely stable layers

A further feature of the regional atmosphere that doesn't fall into the above systems is the semi-permanent stable layers identified in Freiman and Tyson [2000] (Figure 1.4). These stable layers appear to be present over continental South Africa through most the year though are typically stronger during winter. They are a result of two processes. The first is the general subsidence and adiabatic heating caused by the descending limb of the Hadley circulation. The second is the presence of clear skies and strong nocturnal radiative cooling producing a stable vertical profile with absolutely stable layers. Absolutely stable layers are layers where the environmental lapse rate is less than the adiabatic lapse rate. A coastal layer occurs at around the 850hPa level which is below the level of the escarpment. Over the interior two layers at 700hPa and 500hPa occur with the first defining the top of the interior mixing layer and the second defining the height of maximum subsidence over the continent due to the Hadley circulation. While the 500hPa layer is observed more often during summer, the 700hPa layer is found to be more common during winter. It is suggested that these circulation layers prevent significant vertical motion and so constrain the advection of air into and out of the region to particular levels. In addition the lower stable layers act to inhibit convection. In winter, the stable layers, combined with reduced surface radiative heating, produce dry conditions. In summer surface heating is sufficient to produce the instability in the lower troposphere necessary for convection to start. This heating coupled with tropical and mid-latitude disturbances allows convective precipitation.

### 1.2.3 Superposition of systems and sequencing

These systems do not operate in isolation. Many of them are involved simultaneously in any particular synoptic state on a particular day and their interaction and inter-dependence are critical in the development of the regional climate. The sequencing of synoptic events involving these systems produces the weather which aggregated over time characterises the climate of the region. As the focus of the thesis is rainfall, and the associated moisture processes, the following sections will describe in greater detail some of the more important rainfall producing systems; Tropical Temperate Troughs, convective precipitation and frontal precipitation.

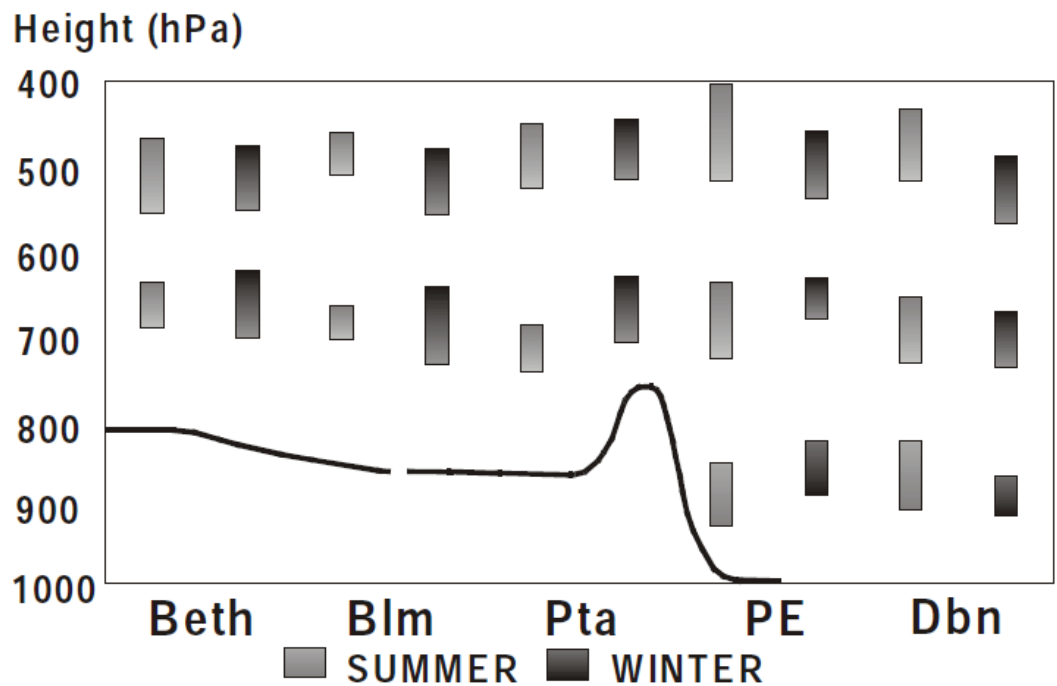


Figure 1.4: Mean heights of absolutely stable layers during summer and winter over Bethlehem (BETH), Bloemfontein (BLM), Pretoria (PTA), Port Elizabeth (PE) and Durban (DBN). Standard deviations for the base heights of the layers are illustrated by vertical lines. (Freiman and Tyson [2000])

#### 1.2.4 Tropical Temperate Troughs

Tropical Temperate Troughs (TTT) link tropical low pressure troughs with transient mid-latitude troughs as the latter migrates eastward over the southern ocean. The resultant band of rainfall and cloud extends from the tropics in a south easterly direction towards the mid-latitudes. The position of the trough in this region varies from a more westerly position where a significant portion extends over the sub-continent, to a more easterly position where the majority of the trough occurs over the SWIO. Analysis of TTT features and dynamics was largely initiated by the availability of satellite imagery that allowed the description of the structure of the systems beyond the bounds of the South African land mass which previously determined the limits of observation and analysis (Todd and Washington [1999]).

It is estimated that a large proportion of summer rainfall in South Africa is derived from TTT events (Harrison [1984]) making them significant weather systems for the region. Much work has been done to determine the dynamics and variability of TTTs as it would seem that much of the regions inter-annual variability derives from variability in the position and occurrence of TTTs (Hart et al. [2010], Fauchereau et al. [2009], Todd et al. [2004], Todd and Washington [1999], Washington and Todd [1999]). It is also significant that TTTs occur relatively infrequently compared to other summer season rain producing systems. Their significant contribution to the regions rainfall is generally as a result of the typically large scale, heavy precipitation events they produce.

The dynamics of a TTT involve a mid to upper level circulation linkage between the mid-latitudes and the tropics (Todd et al. [2004]). TTT events are characterised by a cyclonic circulation over the SWIO region and an eastward shift of both the Indian and South Atlantic high pressure systems. This produces a trough/ridge feature south of 30° with the trough to the west and the ridge to the east. The interface between the two produces strong poleward, low to mid level, moisture transport. Suggested moisture sources identified through moisture flux analysis are from both the tropical Indian Ocean and the tropical Atlantic with convergence along the Zaire air boundary at about 20°S. This moisture is then advected south around the circulation setup by the TTT. The trough induced instability produces cloud and rainfall along its length extending into the southern ocean. Significantly, it appears as if TTT dynamics,

including moisture transport and positioning, is linked to global scale circulation patterns. In particular, enhanced easterly moisture fluxes associated with reduced westerlies across the entire tropical Indian ocean and the maritime continent are strongly associated with TTT events in the region of southern Africa. Links to the Walker circulation over the Pacific and the Southern Oscillation seem to be robust (Fauchereau et al. [2009]).

The relevance to this thesis is that of moisture sources. Existing studies and understanding of TTT moisture dynamics suggest remote moisture sources (tropical Indian Ocean and tropical Atlantic) rather than any local moisture sources. Certainly the moisture flux analyses support this understanding. However, the limitations of moisture flux analysis have been discussed and it is likely that regional land surface moisture sources are not able to be represented by such analyses, leaving the degree of importance of the land surface an open question. While this study will not focus particularly on TTTs, the seasons selected for the study certainly include TTT events and hence the moisture source dynamics of these events are captured in the general analysis described in subsequent chapters.

### 1.2.5 Convective precipitation

Convection is the dominant rain producing system for the summer rainfall areas of southern Africa. Convective precipitation is complex as it typically, in the sub-tropics, occurs through relatively small convective cells or storms producing localised, intense precipitation events. While systems such as TTTs can produce very extensive, broad scale precipitation, other precipitation events are typically fairly isolated. Of course convective events will only occur during suitable synoptic conditions that produce an unstable or conditionally stable vertical profile as well as an adequate source of moisture to enable latent heat energy release.

The sporadic and isolated nature of convective rainfall adds some complexities to the analysis of the associated synoptics. While one observing station may record significant precipitation on a particular day, another station only 50km distant may record no precipitation. This adds significant noise to any associations between large scale dynamics and local precipitation. Much analysis is done using coarse resolution, time aggregated, precipitation datasets which hides much of this complexity. The observation of convective activity itself has been enhanced through the availability of satellite data which can identify the altitude of the top of convective cloud systems. However, the internal dynamics are still poorly observed.

Convective activity and associated precipitation is complex, poorly understood, and varies in character across the world (Wang and Seaman [1997]). The vertical transport of moisture is often extremely strong and yet occurs over a small spatial extent. The vertical height of systems varies greatly and altitudes of entrainment depend on the vertical profile, wind shear and many other factors. The problem of convection will be discussed in more detail in Chapters 2 and 5 in the context of regional modeling and Lagrangian trajectories. Convection is a significant problem in many climate analyses and yet for the region in question it is certainly the most important precipitation producing mechanism and hence must be engaged with.

### 1.2.6 Frontal precipitation

While much of this study is focused on the summer rainfall regions of southern Africa, it is worth discussing the role of frontal precipitation in the region. Frontal precipitation is associated with upper air driven troughs in the mid-latitudes south of 40°S. The troughs produce mid-latitude cyclones with associated warm and cold fronts (Preston-Whyte et al. [1989]). During the southern hemisphere winter months the storm tracks shift north sufficiently to impact the southern coastal areas of the region. Stronger systems with a more northerly trajectory can even extend to central and northern South Africa bringing cold and wet conditions to much of the country. The interaction of the frontal systems with the topography of southern Africa is quite complex. The southern cape mountains often block the

initial impact of cold fronts but stronger fronts rapidly migrate over these mountains bringing rain to the interior of the country. The highlands of Lesotho typically block the westerly progression of the frontal systems and snowfall in these same highlands is always the result of frontal conditions. The effect of a cold front can be felt all the way to the eastern coast of South Africa at times though often only through reduced temperatures rather than rainfall. Frontal precipitation is therefore a significant feature of the southern African region though the real rainfall impact is mostly felt in the south.

Associated with frontal precipitation are cut-off low pressure systems. These cold lows occur when a mid-latitude trough breaks off from the main mid-latitude flow and forms a closed cyclonic circulation feature in the mid to upper troposphere though in some cases this can extend to the surface. Such a circulation feature forms a strong area of low level moisture convergence and has been associated with extremely high precipitation in the south of the country. Of further interest is the formation of a so called "black south-Easter". These events occur when an elevated cut-off system migrates eastward over south of the sub-continent and the south Atlantic high pressure system ridges in near the surface, undercutting the upper air low. The result is a strong flow of moisture from the south driven by the high pressure system which then encounters unstable conditions and strong uplift driven by the upper air low pressure. The combination of moisture convergence and uplift, results in heavy rainfall events such as the Laingsburg flood of 1981. Many of the most extreme rainfall events along the southern coast of South Africa have been associated with such conditions.

The results presented in Chapters 3 and 4 show that the mid-latitude troughs certainly play an important part in the regional moisture transport dynamics, even during the summer months when frontal precipitation is minimal. Therefore, while not directly influencing regional moisture dynamics through rainfall these systems are important components of the austral summer climate system.

### 1.2.7 Seasonal variability

Intra-annual or seasonal variability is largely driven by the seasonal shifts in the South Atlantic and SWIO high pressure systems, the mid-latitude storm tracks and ITCZ. During winter the sub-continent is more dominated by the two high pressure systems with subsidence occurring over a large scale over much of region. This subsidence suppresses uplift and precipitation. Towards the south the mid-latitude disturbances move further north during winter resulting in frontal rainfall over the southern areas. During the summer months continental heating produces a heat low over the subcontinent driving moisture convergence into the region. The ITCZ and tropical moisture convergence shift further south providing a source of moisture to the north of the region. The Angola low develops during summer which is an important areas of moisture divergence (D'Abreton and Tyson [1995]) The occurrence of systems such as TTTs and other tropical disturbances drive moisture further south producing rainfall. Over the southern parts the mid-latitude systems have shifted south and very little rainfall occurs. Isolated convective events also occur due to the combination of moisture availability to drive latent heat release and surface heating producing vertical instability.

### 1.2.8 El-Nino Southern Oscillation

Probably the strongest driver of inter-annual variability for southern Africa, particularly the more tropical and easterly regions, is the El-Nino Southern Oscillation (ENSO) (Lindesay [1988], Cook [2001], Reason et al. [2000], Mason and Goddard [2001]). However, this influence is still a subject of much ongoing research. The relationship between ENSO and southern African rainfall was thought to be fairly strong and consistent with warm phase ENSO producing dry conditions in the South Africa (wetter in East Africa) and cool phase producing wet conditions (drier in East Africa). The interaction between ENSO, the Indian Ocean, and southern African rainfall has been the subject of much study (Nash and Endfield [2008], Cook [2001], Mason and Goddard [2001], Reason et al. [2000]). The relationship between

ENSO and southern African rainfall is complex and during some El-Nino periods southern Africa has not experienced the dry conditions predicted (Lyon and Mason [2007], Landman and Beraki [2012]).

There does appear to be a fairly robust physical link between ENSO and southern African rainfall related to a shift in the Walker circulation. The process, described by (Cook [2001]), involves the global shift in the positioning of the walker circulation cells. Warm phase ENSO conditions shift the walker circulation eastwards resulting in the African component of the walker cell (African cell) also shifting eastward where it is then positioned preferentially over the western Indian ocean rather than over the continent. The resultant reduction in moisture convergence, uplift and instability produces a reduction in precipitation in southern Africa. The same shift produces high rainfall in eastern Africa resulting in a dipole tropical east Africa/southern Africa rainfall response. Variations in response to the the ENSO signal seem to be at least partly a result of the varying expressions the El-Nino SST patterns in the pacific ocean. The so named El Nino Modoki pattern has been identified as a variation on the classic expression of El Nino in Pacific SSTs where the temperature anomalies occur predominantly in the central pacific rather than in the east. (Ashok et al. [2007])

Variations in latent heat flux resulting from changes in SSTs influence advection of moisture as well as the basin scale circulation patterns (Cook [2001]). However, the Indian Ocean basin is complex and the interaction between various drivers is not yet fully understood. For example, tropical Indian Ocean SSTs appear to be driven by changes in latent heat flux as a result of the advection of drier or moister air (Chiodi and Harrison [2007]). The advection of drier or moister air relates to the positioning of the South Indian high pressure system. Such complex interactions and feedbacks are difficult to disaggregate and their impact on regional climate variability is not well understood. Much work still needs to be done in this regard.

More recently, explorations of an ENSO like oscillation in the Indian Ocean, named the Indian Ocean dipole, have suggested that such a oscillation is also an important driver of Southern African rainfall (Kay and Washington [2008], Marchant et al. [2007], Reason [2001, 2002]).

### 1.2.9 Land Surface

The role of the land surface as a driver of regional climate has been a question since as far back as Charney [1975] where surface albedo was identified as possible driver of ongoing drought in the Sahel. Many other studies have explored the role of the land surface though largely through the role of surface albedo linked to vegetation changes. As the focus of this thesis is the role of the land surface as a moisture source, an exploration of the current understanding of this role, both generally and within the southern African domain very important. There is some disagreement within the literature. While some studies (Budyko [1974], McDonald [1962]) suggest that the local land surface plays a very small role in the local precipitation, this is disputed by other studies (Bounoua et al. [2000], Brubaker et al. [1993], Douville et al. [2001], Douville [2002], New et al. [2003], MacKellar et al. [2007, 2009], Koster et al. [2003, 2004b], Trenberth [1999a] ). While some of these disagreements relate more to the geographical area in question, much of the debate has also focused on methodologies.

Fennessy and Shukla [1999] performed a soil moisture perturbation experiment using a GCM and showed how precipitation responses to soil moisture perturbation are complex and relate to the interaction between changes in moisture availability and changes in moisture convergence. Koster et al. [2004a], using multi-model soil moisture perturbed GCM data from the Global Land Atmosphere Coupling Experiment (GLACE), also suggests that very arid areas and very moist areas are less sensitive to land surface moisture sources than more moderate areas. This is most likely because very dry areas are so lacking in water that even a moderate increase in available moisture through a land surface source is insufficient to initiate precipitation. In very wet areas precipitation is not limited by moisture availability but rather by sources of uplift and instability. However, in moderate areas the availability of land

surface sourced moisture can provide the extra moisture needed to initiate condensation and the latent heat needed to drive a convective system. Reale et al. [2001] and Reale and Dirmeyer [2002] performed a similar analysis with a slightly different model and produced largely identical results.

Giorgi et al. [1996] used an RCM soil moisture perturbation experiment to determine the importance of local sources of moisture for an extreme event in the United States and determined that the local land surface played very little role. In fact a negative feedback was identified whereby dry soils produce stronger surface heating and hence greater column buoyancy which enhances convective precipitation.

Methodologies such as moisture recycling (Budyko [1974]), as implemented by Trenberth [1999a], suggest that the regional precipitation recycling fraction in southern Africa varies from less than 10% in the west through to possibly as high as 22% in the east at a 1000km analysis scale. This analysis was done using relatively low resolution (2.5°) re-analysis data and monthly time mean moisture fluxes. As mentioned previously, further development of the precipitation recycling methodology suggests that incorporating transient, daily time scale synoptic events as well as non-uniform vertical mixing increases estimates of moisture recycling (Burde and Zangvil [2001a,b], Burde [2006], Burde et al. [2006]). In particular, relatively recent work also based on Lagrangian methods, suggests that the regional land surface could be an important source of moisture for regional precipitation in some areas and under certain climatic conditions. Of note is the study of moisture sources for the Sahel (Nieto et al. [2006]) and for Brazil (Drumond et al. [2008]). It is therefore important to determine if the method being used in a moisture transport analysis is effective in the region of interest given the potential complexities of the regional climate system.

Two significant regional modeling studies focused on the southern African region have highlighted the role of the land surface. The first study (New et al. [2003]) involved a number of simulations including a control simulation with modeled soil moisture, a perturbation sensitivity simulation with desiccated soil moisture, and a further sensitivity simulation with saturated soils. The results suggest an unexpected negative feedback with desiccated soils producing a slight regional increase in precipitation. The driving mechanism appears to be low level convergence caused by increased surface temperatures as a result of decreased latent heat flux at the surface. While these simulations were unrealistic in the sense that the soil moisture perturbations are not within the bounds of observations, and the simulations were not dynamically consistent with the GCM forcing fields, they are a useful indication of the type of complex feedbacks that can exist within the regional climate. Another study (MacKellar et al. [2007]) showed how realistic changes in land use can result in changes in surface temperature as well as precipitation. The climate response is shown to be quite different under different synoptic conditions. This result points to a synoptically conditioned land surface role.

These studies, focused on southern Africa, as well as other studies in other parts of the world do seem to suggest that the role of the regional land surface is not well understood. In addition, it seems likely that the use of simple analyses and low resolution data results in an incorrect estimation of this role. Additionally, given that high resolution dynamical modeling experiments seem to suggest that the land surface plays a larger role in the regional dynamics than low resolution non-dynamical analyses suggest, it seems reasonable to surmise that low resolution, non-dynamical analyses tend towards an under-estimation of the role of the land surface in the regional climate system. The remainder of this study will focus on the development of a methodology to explore regional moisture dynamics followed by the presentation and discussion of results for a two season study focused on southern Africa.

### 1.3 Conclusion

The objectives of this thesis are threefold, as described above. Firstly, to develop a Lagrangian moisture source attribution model and verify its performance. To this end, the chapter has explored the existing moisture transport analysis methods and the strengths and weaknesses were discussed. This understanding forms the basis for the

development of the Lagrangian model in Chapter 2. Given the lack or inability to directly observe moisture source/sink relationships it will clearly not be possible to validate the model against observations. However, aspects of the model can be compared to precipitation observations and other validation methods can be explored to determine the rationality of the model results.

Secondly, given the lack or inability to directly observe moisture source/sink relationships it will clearly not be possible to validate the model against observations. However, aspects of the model can be compared to precipitation observations and other validation methods can be explored to determine the rationality of the model results.

The third component of the thesis involves the application of the Lagrangian model to the southern African domain and, in particular, determining if the regional land surface plays an important role as moisture source for the region. The rationale for selecting this interesting domain has been discussed. These include the regions large climate variability, both spatially and temporally, as well as the important human dimensions of water scarcity, economic and social development and vulnerability.

In order to provide a climatic context in which to discuss the output of the Lagrangian model the southern African regional climate system was explored in some detail. Existing understanding of regional moisture transport dynamics have been described and these will form a basis for much of the discussion of the results presented in later Chapters and in the concluding discussion. In particular, the regional rainfall producing mechanisms were discussed as these are extremely pertinent to the discussion and interpretation of both the Lagrangian model performance, and the model output presented in subsequent chapters.

The following chapter will detail the development and implementation of the Lagrangian attributed moisture source model. Chapters 3 and 4 will present results from a study of two summer seasons and Chapter 5 will discuss these results and conclude the thesis

## Chapter 2

# Lagrangian Model Development

### 2.1 Introduction

The previous chapter described a number of commonly used methodologies applicable to studies of atmospheric moisture sources and transport. The chapter also discussed the importance of these studies in order to add to our understanding of the climate system and in particular the complexities of regional climate systems. Without repeating much of what was covered in the previous chapter it is important to emphasize the relevance of such studies and the limitations of existing methods before we discuss the development of a new method.

It has been noted by many studies (Ashton, 2002, Bruce, 1999, Cook et al., 2004, Handmer et al., 1999, Hendrix and Glaser, 2007, Klein and Maciver, 1999) that rainfall variability is an extremely important climatic variable because of its impact on both natural and human systems. In many areas of the world rainfall variability is one the greatest climate risks and this is particularly the case in southern Africa. As human development increasingly stretches the limits of the available water resources (Ashton [2002]) this variability has a greater impact on society. The impact of drought or flood in one area often extends to neighbouring areas (Hendrix and Glaser [2007]).

Many studies attempt to explain rainfall variability through correlating or otherwise relating sources of moisture such as sea surface temperatures (SST) to rainfall at a particular location or over a particular area (Nicholson and Entekhabi [1987], Mason [1995], Reason and Mulenga [1999], Reason and Rouault [2006], Rouault et al. [2002, 2003]). Other studies relate rainfall variability to changes in atmospheric circulation patterns or circulation indices such as ENSO (Cook [2001], Mason and Goddard [2001], Reason et al. [2000]). The role of the land surface as a non-oceanic source of moisture for rainfall as well as precipitation recycling has also been the subject of much investigation (New et al. [2003], MacKellar et al. [2007, 2009], Douville [2002], Fennessy and Shukla [1999], Ferranti and Viterbo [2006], Koster et al. [2003, 2004a], Schär et al. [1999], Zangvil et al. [2004]). However, only a few studies (D'Abreton and Tyson [1996], Dirmeyer and Brubaker [1999], James et al. [2004], Dirmeyer and Brubaker [2007], Stohl et al. [2008], Sodemann et al. [2008]) have attempted to directly and dynamically associate precipitation events with evaporative (or evapo-transpirative) sources of moisture. The method presented here falls into the last category.

Analysis of vertically integrated, time averaged, moisture flux fields, is a common means of trying to understand moisture transport within a region. However, there are many concerns with this method. The primary concern is that moisture flux fields do not provide information regarding the evaporation-precipitation cycles that occur within the atmosphere. A largely uniform moisture flux field can hide the reality that evaporation and precipitation processes are occurring along the path of the moisture transport. This is important because intermediate precipitation events break the continuity in the flow of moisture from evaporative source regions to target precipitation regions. Moisture lost in

a precipitation event can be replaced through subsequent evaporation which then becomes the dominant source of moisture for subsequent precipitation events. Time averaged, vertically integrated moisture flux fields will not be able to identify such important dynamics.

A further problem with vertically integrated moisture flux fields is the selection of the integration levels used. Some work such as Freiman and Tyson [2000] indicate that moisture transport within a region (in this case, southern Africa) can be constrained to quite narrow layers by semi-permanent absolutely stable layers in the thermodynamic vertical profile. In the southern African example two such major layers are identified at the 500hPa and 750hPa levels with independent moisture transport occurring within each layer. Vertically integrating moisture flux over 1000hPa to 300hPa as is often done would aggregate the two distinct moisture transport layers into one losing a great deal of information. While convective processes are able to move moisture through such layers this only adds to the difficulty of vertically integrated moisture fields as vertical motions are largely obscured.

Time mean analysis is also problematic as much information is lost in the time averaging process. In many locations, precipitation events do not occur during synoptic conditions that resemble the long term mean but rather during conditions that are large deviations from the long term mean. While filtered compositing and other methods can provide more information they are often difficult to interpret in terms of the particular synoptic systems and physical processes. (Meehl et al. [2001]) highlights the importance of considering multiple time scales and the bi-directional interactions between time scales. While the occurrence of short time scale features, such as individual rain events, is to some degree controlled by long time scale atmospheric modes of variability, the long time scale modes of variability are in turn a result of the composite of short time scale events. There is therefore a two way interaction between time scales that is an important component of any atmospheric analysis and highlights the need to capture multiple time scales any such analyses.

The methodology developed in this chapter is motivated by the constraints of the above methodologies. It is based on a Lagrangian framework which allows the direct tracing of moisture from source to sink at high temporal and spatial resolution given a suitable gridded wind field. High temporal resolution attributed evaporative source maps are produced which can be used to unpack both the short event scale and the longer term aggregate moisture source dynamics for a particular target domain. Lagrangian models have been used extensively for tracing atmospheric constituents, particularly in the air pollution studies because their numerous advantages over other methods. The advantages and details of Lagrangian models will be discussed in more detail in section 2.4.3 below.

The use of relatively low resolution re-analysis type data to study moisture transport dynamics is problematic as has already been discussed. These problems extend to Lagrangian models. While a Lagrangian model is able to trace atmospheric constituents at high spatial resolution, the uncertainties in the calculated trajectories introduced by the use of low resolution wind fields are extensive (Stohl et al. [1995]). Such datasets do not capture many important structures such as sharp sea surface temperature (SST) gradients and steep topography as well as smaller scale atmospheric processes such as convective systems. While these models do attempt to capture these small scale processes in the form of parameterisations, details of which will be discussed in section 2.3.1, such parameterisations have important limitations and generally only capture the aggregate effects of small scale systems over a large area rather than capturing the complexities of these systems in any detail.

Due to the importance of the spatial resolution of the driving wind fields, the Lagrangian model developed in this chapter is driven by a high resolution (RCM) that is used to provide high resolution wind and moisture fields. RCMs offer the potential to provide a higher resolution realisation of the regional climate system. However, there are caveats and concerns with such models as will be discussed in section 2.3.2. RCM fields driven by global re-analysis products are often used as a high resolution re-analysis type product. However, unless specific observational analysis is incorporated into the RCM, it cannot be considered a re-analysis product. The RCM is generally constrained to the large scale re-analysis state only at the boundaries and is free to develop its own dynamics in the interior of the domain (Christensen et al. [2001]).

However, RCMs represent a physically consistent world that, while not perfect, are credible representations of the primary dynamics of a regional system. As such they offer a valid and credible laboratory environment within which to explore fundamental questions of process, as is the objective here with examining the role of land surface in the moisture processes. Hence, the RCMs arguably provide the best possible source of high resolution gridded atmospheric fields for studies such as these and while the uncertainties introduced by the use of such models must be accommodated it is felt that the value added over low resolution datasets is significant, and a very pragmatic approach for the research question.

## 2.2 The precipitation process

It is important to note that there are two important factors that control the occurrence and magnitude of precipitation in a location. Firstly there needs to be sufficient atmospheric moisture content at suitable levels in the atmospheric column above the location. This moisture content is either locally sourced from evaporation or remotely sourced through advection into the region of interest. Advection of moisture is therefore a critical link in the precipitation process and is controlled by the larger scale circulation systems. Secondly, there needs to be a means of inducing vertical atmospheric motion in order to initiate condensation and hence precipitation. Vertical motion can be orographically or convectively induced though it is noted that orography can trigger convection so the two processes often occur simultaneously. Convective vertical motion is generally prompted by an unstable or conditionally stable vertical temperature profile and enhanced or sustained through the release of latent heat. Latent heat release driving convection links back to the requirement of sufficient atmospheric moisture. In summary, moisture availability is not sufficient for the occurrence of precipitation without a means of vertical motion, and likewise, vertical motion is not sufficient without sufficient moisture availability. In order for sufficient atmospheric moisture to be available, the moisture must either be locally sourced or remotely sourced and advected into the area. There is therefore never a direct relationship between moisture transport or availability and precipitation. Sometimes precipitation will be limited by moisture availability. At other times it will be limited by a lack of uplift or instability. A reduction or enhancement of moisture availability does not directly imply a reduction or enhancement of precipitation though the two are often related. It is specifically the analysis of this moisture transport component of the system that is the focus of the methodology presented here and the results must be viewed and interpreted in that light.

Locally sourced moisture is termed recycled moisture. Koster and Suarez [1995] showed that land surface processes contribute significantly to precipitation variability over continents. The methodology used will be critiqued later but the results obtained are still of interest and go so far as to suggest that oceanic sources can, under certain circumstances have a much smaller influence than continental sources, particularly in the mid-latitudes and in highly continental locations. Local evaporation variability and hydrological persistence is shown to be a very important factor particularly during summer convective rainfall seasons. Other estimates of precipitation recycling have shown widely ranging results Trenberth [1999a], Eltahir and Bras [1994, 1996], Burde et al. [2006]. However, it is clear that over continental regions during summer convective rainfall, local moisture recycling is a factor that cannot be discounted. The methodology presented diagnoses the contribution of the land surface sourced moisture to precipitation events.

It is also noted that evaporation from the land surface not only provides moisture to the atmosphere but also releases latent heat which in turn can impact on the regional synoptics. A regional modeling study by New et al. [2003] shows that reducing the regional soil moisture to the point of desiccation can have impacts on temperatures of the order of 2°C as well as impact regional circulation patterns. The results also showed a surprising increase in precipitation in some areas when the soil moisture was removed. Does this imply that the regional land surface is not an important source of moisture? We cannot make this conclusion for the reasons given above. If the change in instability and moisture convergence caused by increased surface heating due to a reduction in evaporation produced conditions more conducive to rainfall then even if less absolute moisture is available greater precipitation levels can occur.

MacKellar et al. [2007] explored the synoptic responses to changes in land surface characterisation in a RCM and found that under certain synoptic states changes in temperature were of the order of 1 °C while precipitation changed by up to 2mm/day. The results highlight the complexity of the regional responses and the need to understand each component of the regional climate system.

If the moisture is remotely sourced then it must be advected from its evaporative source. This advection is driven by both large scale and regional scale circulation systems. It can therefore be concluded that many processes are involved prior to the occurrence of precipitation and in order to adequately explain precipitation variability, all these processes need to be considered in combination. Climate models or model derived data sources are currently the only means of investigating all the processes in a comprehensive way. A number of possible datasets are applicable to moisture source analysis and some discussion of these datasets is appropriate at this point. Various datasets have different advantages and disadvantages and it is important to both select an appropriate dataset as well as be aware of the limitations or caveats of that selection.

## 2.3 Data Sources for moisture source analysis

Most moisture transport methodologies generally rely on some form of multi-level, gridded, representation of atmospheric moisture and winds as well as surface fluxes of moisture (evapotranspiration and precipitation). All methodologies considered here rely on gridded data products. While the accuracy of such data sources is often in question either due to the observations informing the final data or due to resolution limitations, it must be noted that for many studies the first order representation of the regional processes is the critical criteria. Such a representation can often be of a qualitative nature rather than an absolutely accurate quantitative measure if our objective is to understand the regional processes. Quantitative accuracy is more important when attempts are made to forecast or project future conditions. Almost all such gridded datasets are based on numerical or statistical models. Some datasets incorporate station observational data (both surface and upper air) as well as satellite derived data in a re-analysis type of simulation. These datasets are typically more representative of reality than purely model derived datasets. However, in data sparse areas such as Africa numerical model derived data is relied upon to provide a plausible approximation of the climate state in the absence of good observations and hence the accuracy of these datasets must be carefully considered in any interpretation.

Numerical models can be divided into Global Climate Models (GCM) and Regional Climate Models (RCM). The following sections describe GCMs and RCMs in very general terms focusing on issues relevant to this thesis which include the treatment of moisture processes and precipitation as well as boundary layer mixing and regional scale processes. More comprehensive treatments of GCMs and RCMs can be found in numerous texts including McGuffie and Henderson-Sellers [2005].

### 2.3.1 Global Climate Models

Global Climate Models (GCMs) are an extremely common tool used in the analysis of the global climate system. One of the first attempts at simulating the climate is described in Charney [1949] and building on those first attempts the complexity, accuracy, and diversity of climate models has grown rapidly in the last 60 years. Weart [2010] presents a comprehensive history of the development of climate modeling with a focus on GCMs. McGuffie and Henderson-Sellers [2005] provides a more detailed description of the underlying physics, numerics, and other details. In a Global Climate Model (GCM) the model developers attempt to represent the physics of atmospheric motion, energy radiation, moisture fluxes, phase changes, and various other processes through numerical methods. Typically GCMs represent the global atmosphere as discrete grid boxes at various discrete vertical levels. Numerical methods are used to solve

the set of partial differential equations of atmospheric motion defined on this discrete grid. Spectral models use a wave decomposition representation of the atmosphere to avoid problems with representing a regular grid on a sphere. However, the principles are the same.

GCMs have certainly formed the foundational tool in climate research throughout the last several decades. The vast majority of our understanding weather and climate including complex sources of variability such as ENSO are as a result of GCM modeling studies. Projects such as CMIP (Meehl et al. [2000]) have produced a comprehensive set of climate model studies of current and future climate states and have formed the basis of a great deal of literature much of which is summarised in the various Inter-governmental Panel on Climate Change (IPCC) reports such as IPCC [2007].

While various numerical methods are employed in order to solve the equations of motion, differences between models largely centre on the representation of other processes rather than the fundamental atmospheric motion. Processes such as evaporation, transpiration, sensible heat flux and latent heat flux are calculated at the grid box scale. Radiation physics are solved through various different methods at the grid scale and depend on the simulation of cloud coverage at different levels. More recent models include the effects of aerosols in the radiation physics as aerosols have a significant effect on the radiation balance of the atmosphere. Atmospheric processes not resolvable at the scale of the grid boxes are represented through parameterisations which attempt to represent the contribution of sub-grid-scale processes to the grid scale state. Boundary layer mixing, convective motions, precipitation and clouds are generally represented in the model through these parameterisations. Of these, convection (Arakawa [2004]), and the simulation of clouds, are the processes with the greatest climate impact due to their strong role in the moisture, heat and radiation budget of the atmosphere. However, these processes are still poorly represented in the numerical models though great progress has been made in recent years.

In many respects climate re-analyses such as NCEP/NCAR (Kanamitsu et al. [2002]) and the ECMWF ERA (Uppala et al. [2005]), which are extensively used for climate studies including moisture transport analysis, are themselves GCM datasets. Re-analyses are produced by specialised GCMs that incorporate a data assimilation component capable of ingesting various forms of observed data in order to constantly nudge or correct the model state towards the atmospheric state informed by the observations. In some senses this forms a sophisticated interpolation of the observations and as such these re-analyses form a best guess approximation of the full atmospheric state at any particular time in the past. While re-analysis data has been produced extending back to before the era of satellite observations, the earlier periods must be treated with some care as most non-satellite observations were and continue to be land based and observations in ocean areas are very sparse. Satellite based data has provided a substantial improvement and hence re-analysis data post the mid 70's is likely to be more representative of the real climate. However, the lack of observations in the southern hemisphere, particularly of the upper atmosphere means that re-analyses data must still be considered as an approximation of the historical climate state.

The parameterised processes, particularly evaporation, precipitation, and convection, are very important in the light of the proposed methodology because of the strong control they have over moisture transport and availability in the simulated atmosphere. In order for the proposed methodology to have any validity it is important that the model used at least represents the real climate moisture processes at a qualitative level. Modern GCMs are generally able to represent the large scale observed climate features and many are able to resolve and represent more complex systems such as monsoonal rainfall and inter-annual variability such as ENSO and the North Atlantic Oscillation (NAO). Validation of GCMs is however, a complex task and metrics for validation are varied and often depend on the intended end use of the model.

Of further relevance to the proposed methodology is that parameterised processes influence the grid scale state variables of the GCM output fields but often the specific role of a parameterisation is not represented in the archived model output. An example of this is convective processes. While convective parameterisations can capture significant vertical motions of air mass and moisture as well as remove moisture from multiple model levels through precipitation,

these vertical motions and moisture state changes are generally not available in output fields as they represent sub grid scale processes.

We have already determined that the methodology described in this chapter is driven by an RCM in order to obtain a higher resolution realisation of the regional wind and moisture fields. However, RCMs are always driven by GCM data of some form (which includes re-analysis data, itself a model product) and hence the limitations of GCMs must always be considered when using an RCM. In the case study presented later and the seasonal analyses presented in chapters 3 and 4 the NCEP re-analysis will be used as the driving fields for the RCM.

### 2.3.2 Regional Climate Models

In reality, while GCMs have dominated the history of climate systems analysis, the first numerical models of the atmosphere were actually regional models Charney [1949]. This was a result of the computational and observational constraints of the time. However, as computation constraints lifted, model development shifted towards GCMs. In the last 15 years or so the development of RCMs has gained momentum with modern models incorporating many of the same complexities as GCMs include vegetation based land surface schemes (Chen and Dudhia [2001a,b]), simple hydrology models, and the effects of aerosols Grell et al. [2005]. A regional model configured for a limited area of interest and forced at the boundaries by output from a GCM allows much higher grid resolutions to be integrated at much lower computation expense than running a GCM at such resolutions would require. RCMs can be integrated at grid resolutions ranging from 100km to as fine as 1km or even, under special circumstances, finer resolution. Typical grid resolutions are around 25km to 50km. Clearly, at such resolutions, much finer detail can be explicitly resolved than the 100km to 300km scale of a GCM. It must be noted that the computation expense of high resolution regional modeling is not insignificant. The nature of the numerical solution to the fluid dynamics equations typically requires a linearly decreasing integration timestep as grid resolution decreases and this shorter time step significantly increases the computation time required (Courant et al. [1928]). Additionally, as the complexity of the convective and other parameterisations increases the computational requirements.

RCMs have been used extensively for climate systems analysis over the last decade and have proved themselves to be powerful tools. Projects such as the European ENSEMBLES project (Hewitt et al. [2005]) have made great progress in developing an understanding of the strengths and weaknesses of RCMs through the coordinate comparison of a large suite of RCMs over the same domain and time periods. A similar project under way at the moment is the Coordinated Regional Climate Modeling Experiment (CORDEX) which will coordinate the comparison, analysis, and application of a similarly large suite of RCMs over a number of regions of the globe.

An interesting form of regional climate model has emerged over the last ten years. These models are so called stretched grid models. They are GCMs in that they represent that global atmospheric state just as a regular GCM does, but they incorporate a stretched horizontal grid that allows for much finer grid resolution over a particular area of interest. As such they gain many of the advantages of an RCM in resolving finer scale details while avoiding some of the problems involved in forcing an RCM at the boundaries. The C-CAM model (McGregor and Dix [2008]) is a good example of such a stretched grid model and has been applied to regional climate modeling over southern Africa (Engelbrecht et al. [2007]). Another example of a stretched grid model that has been applied over southern Africa is CAM-EULAG (Abiodun et al. [2011]).

Mention has already been made of the use of RCMs in the southern African domain (Crimp and Mason [1999], New et al. [2003], Tadross et al. [2006], MacKellar et al. [2007, 2009]). These studies have utilized the ability of RCMs to resolve the complex topography of the region. However, perhaps more importantly, many of the studies have utilized the land surface model component of the RCMs in order to perform land surface sensitivity studies. The complex gradients of soil and vegetation can readily be captured by a RCM where the low resolution of a GCM would fall significantly short.

It is important to note that the higher resolution of an RCM does not remove all problems with parameterisations. Unless the model is integrated at very high resolutions less than 10km, parameterisations of processes such as convection and boundary layer mixing are still used and can still lead to problems with the model results. As with GCMs the parameterised processes are not well represented in model output fields which leads to problems with downstream models as described later.

One particular challenge associated with the RCMs in Africa is that of validation. Typically there are few observed datasets available with which to comprehensively validate the model output. This is particularly true for upper air fields where almost no observations exist at the spatial scales involved. Validation therefore often falls back on surface fields such as precipitation. Again observational records are often sparse as discussed in section 1.1.2. However, validation is important and the available observed datasets are used with care. Figure 2.1 shows two different observational based gridded precipitation dataset representations of two seasons over the southern African domain. The University of East Anglia CRU dataset (New et al. [2000]) is shown on the left and the CMAP (Xie and Arkin [1997]) dataset is shown on the right. It is interesting to note the differences between two different attempts to capture the observed rainfall record. The CMAP dataset incorporates satellite based information with surface observations while the CRU dataset only includes surface station records. Figure 2.2 shows the output of the RCM that will be used in this thesis, the NCAR/PSU MM5 model (Grell et al. [1994]) for the same seasons. The left column shows the results using the Kain Fritsch (Kain [2004]) convection parameterisations while the right column shows results using the Betts Miller (Betts [1993]) parameterisation. We can see that there are significant differences in simulated rainfall between the two parameterizations with the Kain Fritsch method producing arguably smaller anomalies for the seasonal mean. Later, in section 2.6.1, the selection of the Betts-Miller scheme will be discussed and defended in the light of its diurnal and daily time scale characteristics which are not evidenced in figure 2.2. While it is highly likely that the RCM fields are biased, we must also be aware of the uncertainties in the observational datasets, always bearing in mind the distribution of stations informing the gridded products in the region (figure 1.1).

In light of this it is clear the inherent limitations of RCMs are a constraint on second order accuracy in the model simulation. In this thesis the concern is a high resolution physically consistent 3-dimensional and high resolution data set with which to explore the moisture processes; for this purpose the RCM is appropriately skillful.

Thus, despite the challenges of validation, the use of an RCM for moisture source and transport analysis in the southern African region is felt to be appropriate. We must bear in mind that much value is to be gained from a higher resolution representation of the wind and moisture fields, especially as they are used to drive a Lagrangian model. The RCM that will be used in this study will be described in more detail in section 2.6.1 but it has been shown to at least qualitatively represent the spatial, seasonal, and to some degree the inter-seasonal variability observed in the region.

Having examined the possible sources of data we can now examine existing methodologies that could be applied to such data in order to explore moisture transport and source dynamics.

## 2.4 Moisture Transport Methodologies

While Chapter 1 discussed some of the general methodologies applicable to moisture transport and regional climate studies, the following section will explore some of the more specific methodologies used to identify moisture source regions. These methods range from direct methods using real observations of precipitation to Eulerian and Lagrangian methods.

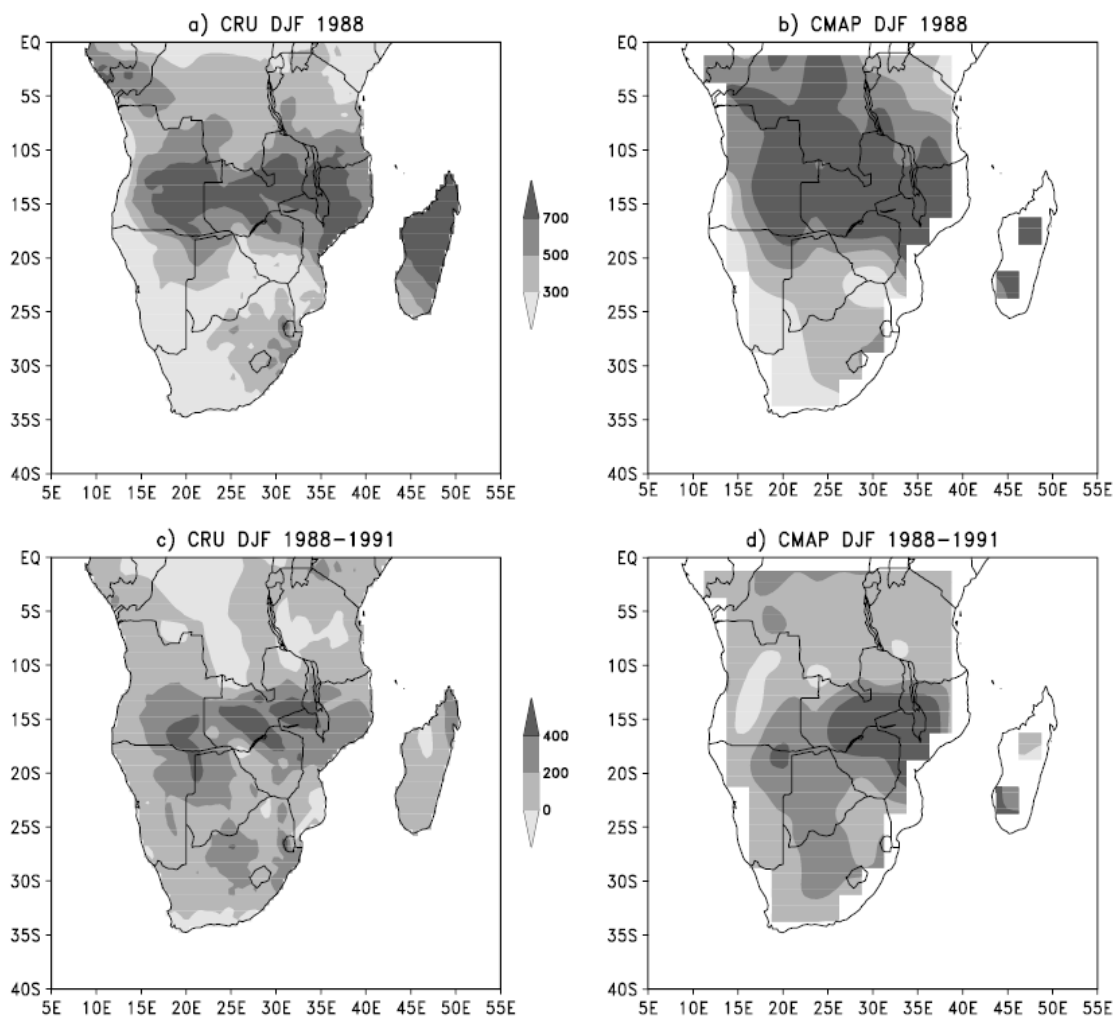


Figure 2.1: December–February (DJF) 1988=89 seasonal rainfall (mm): a) CRU, b) CMAP. DJF inter-annual (1988=89–1991=92) rainfall anomaly (mm=season): c) CRU, d) CMAP ( Tadross et al. [2006])

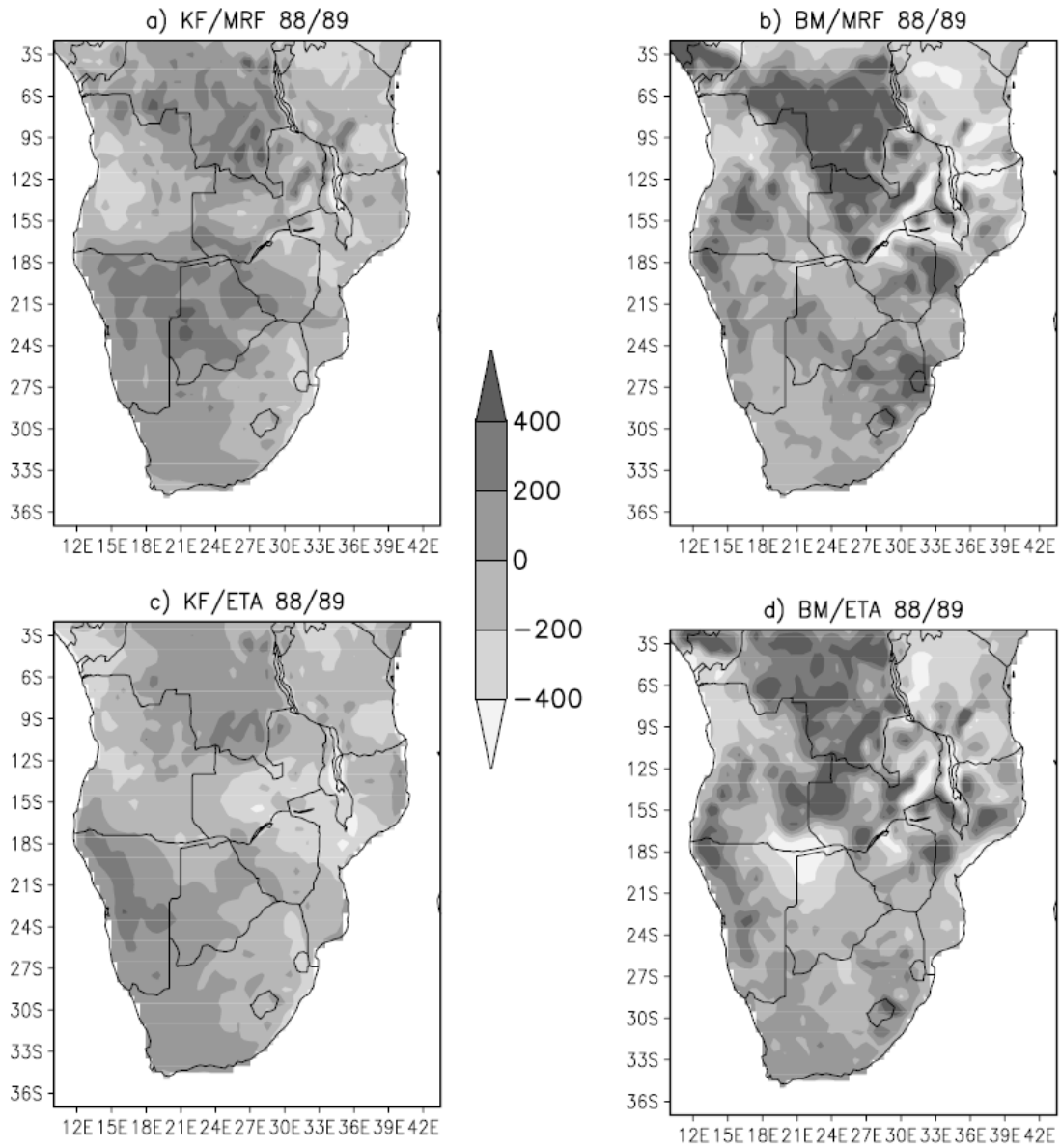


Figure 2.2: DJF MM5 rainfall anomaly (mm=season) with respect to CRU observations (MM5-CRU) for the 1988=89 season. a) KF/MRF, b) BM/MRF, c) KF/ETA and d) BM/ETA ( Tadross et al. [2006])

### 2.4.1 Direct techniques

Some studies have used direct techniques to determine the geographical source region of precipitated moisture. Gat and Carmi [1970] and Gat and Matsui [1991] are two such studies that use isotopic analysis of water to determine the ocean area source for continental precipitation. Different ocean areas can be characterised by different isotopes of water which are fairly stable through time. While a very direct measure and indeed very useful, it is limited by observational sampling of precipitated water as well as, to some extent, the very generalised source areas identified. It also only identifies the source without allowing any exploration of the transport pathways.

### 2.4.2 Eulerian techniques

One approach to moisture transport analysis is the Eulerian transport methodology. Several experiments have been performed using modified GCM codes that include a passive Water Vapor Tracer (WVT) (Bosilovich and Schubert [2002], Bosilovich and Chern [2006], Koster et al. [1986]). These WVTs are included in the model as passive prognostic variables. They are passive in that they do not influence the model evolution at all. WVTs are typically integrated in parallel to the models intrinsic, active, water vapor variable and undergo the same processes, such as advection and precipitation, as the models water vapor variable. However, the WVT only originates (evaporates) from a pre-defined region and hence represents moisture sourced from that defined region. The WVT physical tendencies are calculated in proportion to the tendencies of the model water vapor. Therefore precipitation of the WVT occurs in proportion to the relative quantities of WVT and models total water vapor content. WVT precipitation amounts can therefore indicate the relative contribution of a particular defined evaporative region to a grid cells precipitation.

In some models such as Bosilovich [2002], multiple WVTs can be defined and associated with different source regions of interest. It is then possible to map the precipitation of moisture from each of the source regions in turn as well as calculate the relative contributions from each source region to a particular target region of interest.

There are several limitations to this technique. One limitation is the number of tracers that can be traced. Each tracer requires a completely separate moisture tracer variable in the code. Bosilovich and Schubert [2002] did manage to share a single tracer for two very distinct areas but noted the complexity this adds to later analysis. They used 13 tracers and a residual tracer to account for other more distant global moisture sources.

Related to the limitation of the number of tracers is the need to predefine the source regions of interest. For a hemispheric scale experiment such as Bosilovich and Schubert [2002], or a very large scale experiment such as Koster et al. [1986], the objective is to identify the roles of various ocean basins and continental areas as moisture sources for a number of continental regions, and so identification of potential source regions is logical. However, for smaller scale experiments such as a regional analysis it is often not known in advance what the significant moisture source regions might be. Indeed a moisture source region such as a warm boundary current may be of quite a complex structure rather than a large homogeneous region such as an ocean basin.

Another limitation of the inline tracer technique is the need to run a customized GCM in order to perform a moisture source analysis. Besides the computation cost of such an experiment and associated limits in terms of integration time, it also restricts the analysis to models that have been suitably customized. With the availability of global re-analysis datasets such as the NCEP/NCAR reanalysis (Kanamitsu et al. [2002]) and the ECMWF/ERA re-analysis (Uppala et al. [2005]) it is often desirable to perform a moisture source analysis using such datasets. Additionally, the complexity of modern GCM codes means it requires a great deal of time to add a tracer sub-model component.

Model based Eulerian methods are therefore, while very powerful and useful, limited in their practicality and flexibility. However, many more recent models do include tracer components that can be flexibly configured. These tracer

components are typically used to trace chemistry components such as sulphates or aerosols but could also be applied to tracer water vapor components. A number of RCMs also now include such tracer components opening up some interesting possibilities for tracing fractional water vapor components in RCMs.

### 2.4.3 Lagrangian techniques

As alternative to model based Eulerian techniques are Lagrangian based techniques. Lagrangian techniques are based on the principle of tracing the passage of air parcels or tracers through the atmosphere. Whereas Eulerian methods describe the atmosphere through the use of fixed grid boxes, Lagrangian methods describe the atmosphere through the representation of moving parcels of air. Lagrangian techniques have long been used in tracer type experiments for two main reasons. The first is the relative numerical simplicity and accuracy of the advection process. Advection of a tracer simply involves integration of air parcel motion in the Eulerian velocity field. While the numerical accuracy of this integration is subject to issues such as source data resolution and time stepping (as will be discussed later) the complexity of Eulerian mass advection and associated diffusion issues are largely removed if the representative air parcels are sufficiently small. The second reason is the intrinsic ability to trace individual air parcels and associated tracer contents continuously through the atmosphere and hence connect a source with a sink directly via a Lagrangian trajectory pathway. Eulerian approaches produce tracer concentrations at each grid point with no intrinsic information about tracer movement though these can be deduced from related wind fields.

For this reason Lagrangian trajectories have been used extensively in air mass transport studies, pollution studies and moisture transport studies Anfossi et al. [1998], Seibert and Frank [2004], Sodemann et al. [2008], Stohl [2001], Stohl and James [2004, 2005], Stohl et al. [2008]. In most cases the methodology is very similar. A modeled air parcel is used to represent a finite mass of air or tracer. In some studies, individual tracers are used to represent large masses of air with a single trajectory representing one particular event (pollution emission, precipitation event). These methods are computationally very efficient but are very susceptible to stochastic trajectory integration errors and potentially do not capture diffusive processes relevant to large masses of air. By contrast, in ensemble particle type models, many trajectories representing very small parcels of air are integrated simultaneously in a monte-carlo type integration. The resultant analysis is often based on some form of particle aggregation rather than single trajectories. Particle methods also frequently introduce artificial stochastic noise into the velocity fields in recognition of the unresolved stochastic motion in the forcing wind fields. Individual trajectories in a particle integration therefore represent one of multiple possible pathways rather than one single accurate pathway. The resultant cloud of pathways is considered representative of the possible spread of parcel motions including both real and numerical spread.

#### 2.4.3.1 Gridded wind field accuracy

All Lagrangian models are dependent on some form of forcing wind field. This typically takes the form of a gridded product. The accuracy the gridded velocity fields is generally out of the control of a trajectory experiment. Many experiments use datasets such as the NCEP/NCAR reanalysis or ECMWF/ERA reanalysis (Stohl et al. [1998, 2001], Stohl [2001], Stohl and James [2004, 2005], James et al. [2004]. While often difficult to assess, the potential inaccuracies of the selected velocity fields should always be considered. Of particular interest and a continual challenge to trajectory integrations is vertical motion. Most model derived datasets are not of sufficient resolution to resolve convective motion. As a result the vertical motion represented in the dataset is generally only large scale vertical motion, either topographically forced or as a result of synoptic subsidence or uplift. However, in many geographic areas convective motion plays a very important role in mixing air masses between lower and upper troposphere.

Spatial and temporal resolution limitations of the source wind fields are also an important factor. Stohl et al. [1995] performed a number of sensitivity experiments to determine the relative importance of spatial and temporal resolution

on the accuracy of trajectory integration. It was determined that under most conditions a higher temporal resolution is of more importance than a higher spatial resolution. This result was confirmed by Draxler [1987]. Azadi et al. [2006] confirmed the importance of high temporal resolution forcing data. Of course, in very complex flow situations involving topography, higher spatial resolution will also play an important role. The question of temporal resolution relates to the rate of propagation of synoptic systems. As a synoptic feature propagates through the integration domain it is vital that the interpolated velocity field at the location is accurately represented. Taken to an extreme, a velocity field with a 24-hour time resolution could result in entire synoptic systems propagating past a parcel location and not reflecting in the parcels interpolated wind field.

#### 2.4.3.2 Interpolation errors

Interpolation from the gridded velocity field to the parcel location is largely an exercise in balancing computational expense and accuracy. For sufficiently high resolution gridded fields there is little to be gained in high order interpolation methods. For experiments involving single tracers more computational time can be dedicated to higher order interpolation schemes but for experiments involving many thousands of tracers as will be discussed later, the added computation cost of high order interpolation schemes does not significantly alter the results Stohl et al. [1995].

#### 2.4.3.3 Integration errors

A similar argument applies to the numerical method used to integrate the parcel position in time. The simplest method is a zero order integration that assumes a locally uniform flow field. The computation cost of higher order iterative schemes is high because of the cost of interpolation of the wind fields to the parcel position at each iteration. As with the interpolation scheme itself, for single parcel trajectories where high accuracy is required a high order integration scheme is required. However, for large ensemble type integrations, higher order schemes make little difference to the final ensemble result.

#### 2.4.3.4 Unresolved processes

The challenge of non-resolved processes is significant. While processes such as boundary layer mixing can be approximated through a turbulence parameter added to the wind field ( Anfossi et al. [1997], Stohl and Thomson [1999]) this is complex and may not be in agreement with the boundary layer mixing calculated in the source model. Boundary layer mixing is itself a complex problem and there have been many methods used to approximate observed mixing. Of fundamental importance is the calculated height of the Planetary Boundary Layer (PBL). Many models do in fact produce a PBL height field as a diagnostic variable though methods of deriving this parameter differ. Where this is not available, other methods must be used to approximate the PBL height field. Once the PBL height is known some assumptions about moisture mixing within this layer can be made as described in Sodemann et al. [2008] as well as later on in this thesis.

Model convection schemes are many and varied and the selection of an appropriate scheme depends on many factors and on the objectives of the simulation. Whichever scheme is used in the RCM or GCM, there are seldom sufficient prognostic or diagnostic variables output to fully diagnose the vertical motions calculated in the convective scheme. Vertical wind velocity output from RCMs or GCMs are generally only the large scale component of vertical velocity and do not contain a convective component. Some trajectory modeling methodologies have attempted to incorporate a full convective scheme within the trajectory model in order to calculate trajectory paths under convective conditions (Forster et al. [2007]). Not only is this very complex but the convective scheme implemented in the trajectory model

may not follow the same principles as the scheme used in the RCM or GCM. This would result in some discordance between the two models. The selection of a method for approximating convection therefore seems to be subjective and case specific. For the purposes of the method presented here no attempt to represent convective processes is included.

#### 2.4.3.5 Monte Carlo trajectory modeling

As mentioned above, one approach to trajectory modeling is to integrate relatively few trajectory parcels in the assumption that single parcels can in fact accurately represent large amounts of tracer. This is plausible under fairly stable laminar flow conditions and may be applicable to pollution studies. However, as has been discussed above, there are many uncertainties and sources of error in trajectory modeling. Representing large amounts of tracer per parcel is subject to large errors. A single parcel cannot represent the natural diffusion and bifurcation of tracer paths in the atmosphere and integration errors could be large resulting in misinterpretation of the results. Another approach that has been used is to allow each parcel to only represent a small fraction of the tracer mass and integrate many thousands of trajectories (Dexheimer and Bowman [2004]). A stochastic component can also be introduced to the velocity fields in order to represent turbulence present in the atmosphere but not represented in the model velocity fields. This will give a spread or cloud of trajectory paths which more accurately represents the observed diffusion and bifurcation of atmospheric motion. Numerical errors potentially increase the spread of the trajectories but this is preferable to a single trajectory error the magnitude of which is unknown and yet must be considered in the interpretation of results. Given the increased computational resources now available many trajectory modeling studies use this monte-carlo approach. A similar method has been implemented successfully on a global scale in Stohl and James [2004] using ECMWF GCM fields.

The addition of a stochastic component to the velocity field can be quite complex as ideally an accurate measure of both horizontal and vertical turbulent mixing needs to be calculated. While GCMs and RCMs approximate this turbulence mixing through various methods based on vertical stability and velocity shears a full boundary layer mixing scheme is beyond the scope of most trajectory models. Many models apply a nominal turbulent component to the velocity field whenever a particle is within the atmospheric planetary boundary layer (PBL). Boundary layer height is a diagnostic of many atmospheric models but can also be calculated from surface winds and temperature profiles. A common method is the bulk Richardson number but other methods can also be used. For the purposes of this study the PBL height was obtained as a regional model diagnostic output field. However, as will be discussed in the next section, the introduction of stochastic turbulence in a time reversed model is problematic and not implemented in the final version of this methodology.

#### 2.4.3.6 Time reversed Lagrangian trajectories

While intuitively it would seem to make sense to integrate parcel positions forward in time, this is not always the most computationally efficient or manageable approach. If, as in the case of precipitation moisture source mapping, the tracer source area (area of evaporation) is potentially much larger than the tracer target area (a confined precipitation region) then time forward trajectory modeling requires a large number of tracer parcels to be integrated in order to represent all possible sources. Only a relatively small number of these tracer parcels will terminate within the precipitation target domain and hence are discarded. This is computationally expensive. If time reversed modeling is used then the target region (precipitation domain) becomes the tracer source region and the source region (evaporation domain) becomes the target region. Only parcels that originate within the precipitation domain are integrated backwards and all of these parcels either terminate over a source region or exit the integration domain, both of which are informative results.

At the simplest level, reversing the Lagrangian numerics is simply a case of multiplying the time delta by -1. The kinematic integration numerics are inherently reversible. However, complexities do arise around other aspects, particularly convective and stochastic processes. If a convection model is integrated in the model this can be rather complicated to integrate backwards in time. No current time reversed trajectory model incorporates any form of convective processes and as already noted, convection will not be included in this study.

There is an added complication regarding a time reversed turbulent mixing. If a stochastic component is added to the velocity field to approximate unresolved turbulent mixing then this component of the Lagrangian integration is not time reversible. For this reason, though turbulent mixing was implemented in the model, it was turned off for the time reversed experiments.

#### 2.4.3.7 Trajectory vertical velocity

Treatment of vertical velocity is the most prominent factor distinguishing between different trajectory integration techniques. Vertical motion of the trajectory can be dealt with in a number of different ways. While it would seem logical that using observed or modeled vertical velocity fields is the most accurate, for a number of reasons this is not always the best approach. Firstly, vertical velocities are not always available. Secondly, if some vertical velocity field is available it is sometimes not appropriate given the horizontal or vertical resolution of the velocity field. Vertical velocity is not a parameter that is observed regularly or easily and hence is often not a very reliable field in many observational products. Convective vertical motion occurs at time and space scales that are typically not observable. For model derived fields similar problems exist. Vertical motion in convective systems is parameterised in the model and this is generally not represented in the prognostic vertical velocity fields. Additionally, many models do not represent topography accurately resulting in inaccurate vertical velocity fields.

The various alternatives to three-dimensional integration are isobaric, isentropic, iso-sigma and several hybrid techniques (Danielsen [1961], Merrill et al. [1986]). Isobaric and isentropic integration forces the trajectory to remain on the same pressure surface or isentropic surface respectively. Techniques such as isobaric and isentropic integration are typically useful above the turbulent planetary boundary layer (PBL) and in synoptic conditions where vertical motion is negligible in relation to horizontal motion. However, these methods all break down within the sub-grid scale mixing of the PBL. This breakdown is a result of the unresolved turbulent mixing that is not explicitly resolved by the velocity fields. In the case of the isentropic method, turbulent mixing means that potential temperature is not conserved in the boundary layer. For isobaric motion air parcels in the boundary layer readily change pressure levels resulting in a breakdown of the isobaric trajectory assumptions. However, above the PBL, where turbulent mixing is less important, these techniques can be useful. Convective systems however, remain a challenge and in the context of moisture and precipitation processes this is a significantly important problem as is described in Danielsen [1961].

It was therefore concluded that for the purposes of this study the model derived grid scale vertical velocity fields would be used as they would seem to be the most representative of real vertical motions at the spatial scale concerned and under the baroclinic conditions typical during convective precipitation processes.

## 2.5 Methodology

The above discussion lays a foundation that supports the development of a Lagrangian moisture source model. In the light of the above discussion it is important to note that the Lagrangian method does offer a great deal of advantages over Eulerian methods. While the sources of error and limitations described above are important, their potential impacts can be accommodated through appropriate implementation as well as interpretation of the results. The

implementation of the Lagrangian model is now described with particular reference to the sources of error described above. We shall return to these sources of error in Chapter 5 where the results are discussed with due consideration of possible errors or biases in the method.

Lagrangian trajectory methods have been used to track moisture associated with a precipitation event and in some cases map the upstream evaporative sources. James et al. [2004] used a large number of backward trajectories to trace air movement into an extreme precipitation event over Europe. Brimelow and Reuter [2005] implemented a similar analysis for a number of extreme events in the Mackenzie River Basin in the USA. Specific humidity changes along the trajectories were then mapped out to identify potential sources of moisture for the event. A global high resolution re-analysis product, ECMWF, was used to drive the trajectory integrations. A limitation of this method is that only one evaporation precipitation cycle can be integrated as no means of tracking the role of further precipitation events is included. Sodemann et al. [2008] implements a similar technique for attributing moisture sources to precipitation over Greenland.

The methodology developed here uses a 3-dimensional, time reversed, lagrangian trajectory integration. Parcels are initiated through the diagnosis of condensation in the atmospheric column above a precipitation event. Both precipitation losses and evaporative gains are traced along each trajectory pathway and the aggregated attributed moisture sources for each precipitation period are generated. A source attribution component accommodates the role of upstream precipitation events in decreasing the contribution of upstream evaporative sources. Details of the method are described in the following sections.

### 2.5.1 Trajectory generation

Trajectory parcels are generated at the time reversed inflow (forward time outflow) boundaries of the target precipitation region. Figure 2.3 illustrates the concept. Integrated moisture flux at a particular layer is converted into the equivalent mass of moist air represented as trajectory parcels as the boundaries of the target domain. This process is implemented through the following steps. The air mass flux is calculated at each RCM vertical layer for each boundary of this region for each time-step in the integration according to the following formula:

$$M_{flux} = \frac{\Delta p}{G} \mathbf{v} \Delta T \cdot \Delta x$$

Where  $\Delta p$  is the pressure difference through the model level,  $G$  is the gravitational constant,  $\mathbf{v}$  is the boundary normal wind magnitude,  $\Delta T$  is the integration time-step, and  $\Delta x$  is boundary length. Because  $\Delta x$  is both large and constant across the domain, it is removed and the mass flux is considered per unit distance along the boundary.  $M_{flux}$  therefore represents the total mass of moist air entering the target domain at a particular RCM model level. The inflow is calculated for each vertical layer. Wherever this flux at a particular layer is inward (into the target domain in reversed time) new trajectory parcels are generated with each parcel representing a fraction of the total moist mass flux into the region. The mass flux is then converted into a cloud of trajectory parcels representing the same mass of moist air and traveling at a velocity determined by the RCM wind fields along the target domain boundary. The number of parcels generated per time step is proportional to the inbound mass flux as described by:

$$N = \left\lceil \frac{M_{flux}}{P_{mass}} \right\rceil + 1$$

Where  $P_{mass}$  is a constant, representing a finite mass of moist air associated with the trajectory. The value of  $P_{mass}$  is determined by trial and error to be as small as possible while limiting  $N$  to a number that is computationally feasible.

It is desirable that  $P_{mass}$  is as small as feasible in order that the mass of moisture is represented by as many parcels as possible reducing the potential impacts of integration error on each parcel. This is based on the assumption that errors are stochastic and have a normal distribution. There is little to suggest that this is not the case for normal grid scale trajectory integration. For some of the more complex sources of error mentioned earlier it is likely that the distribution is not normal. This is discussed in greater detail in Chapter 5. In the example case described below on the order of 2 million trajectories were generated in a 3 month integration period. The additional remainder trajectory is used to represent the remainder of the moist mass not divisible by  $P_{mass}$ . Hence the moist mass represented by each trajectory is equal to  $P_{mass}$  except for the remainder trajectories which have a mass of:

$$M_{flux} - P_{mass}(N - 1)$$

The entire moisture flux represented by  $M_{flux}$  is therefore converted into trajectory parcels moving at the wind field velocity into the target domain (in reversed time).

Trajectory initial locations are perturbed stochastically within the spatial range of the RCM grid cell and the vertical extent of the RCM level. This stochastic spread was chosen in order to both represent that spatial extent of the RCM grid cell boundary as well as introduce a stochastic element into the trajectory integrations. This is in recognition of the stochastic component of the real climate that is not represented by the RCM wind fields. While not absolutely necessary, using stochastic trajectory starting positions ensures that a regular pattern of starting positions does not occur. Such a regular pattern of starting positions could easily produce patterns of trajectory pathways and moisture sources that are a result of the regular starting positions rather than any real transport characteristics. Given the large numbers of trajectories integrated this would seem unlikely, However, stochastic starting positions are nevertheless incorporated.

## 2.5.2 Precipitation diagnosis

The altitude at which parcel moisture is condensed to form precipitation is critical to the methodology as trajectory pathways can be very sensitive to initial altitude. This sensitivity is the result of vertical wind shear where the wind velocity and/or direction at one RCM level is significantly different to an adjacent level. If the RCM level at which precipitation is diagnosed is not correct the resultant trajectory pathways could be markedly different and likewise the attributed source areas. The RCM fields (and most other sources of data) do not provide this information directly. The surface precipitation values normally archived give no indication of the altitude of the source moisture. It is therefore necessary to develop a method of diagnosing the precipitation process at the altitude of the trajectory parcel. This will allow the calculation of the contribution of every parcel, at whatever altitude, to the grid scale precipitation. The following section describes the method of precipitation diagnosis developed for the Lagrangian model.

While they remain within the target domain the trajectories are integrated through space using the reversed RCM wind fields in order to integrate backwards in time. At each trajectory time-step the RCM derived specific humidity field is interpolated to the new parcel position and an equivalent new parcel precipitable water mass is calculated for parcel. The difference between this new mass and the value from the previous time-step is calculated. If this change in mass,  $dM$ , is positive then the parcel has lost moisture (gained moisture in reversed time) and hence could have contributed to precipitation during the integration time-step. However, due to trajectory integration errors as well as interpolation errors, small changes in parcel mass often occur when no precipitation is occurring. In order to constrain the diagnosed precipitation several additional conditions must also be met.

1. The magnitude of  $dM$  should be greater than 1% of the total precipitable mass of the parcel. This threshold was determined by trial. Higher values resulted in a very large under-estimation of precipitation, smaller values seemed to produce spurious precipitation diagnosis. This spurious diagnosis can be filtered by the other conditions described

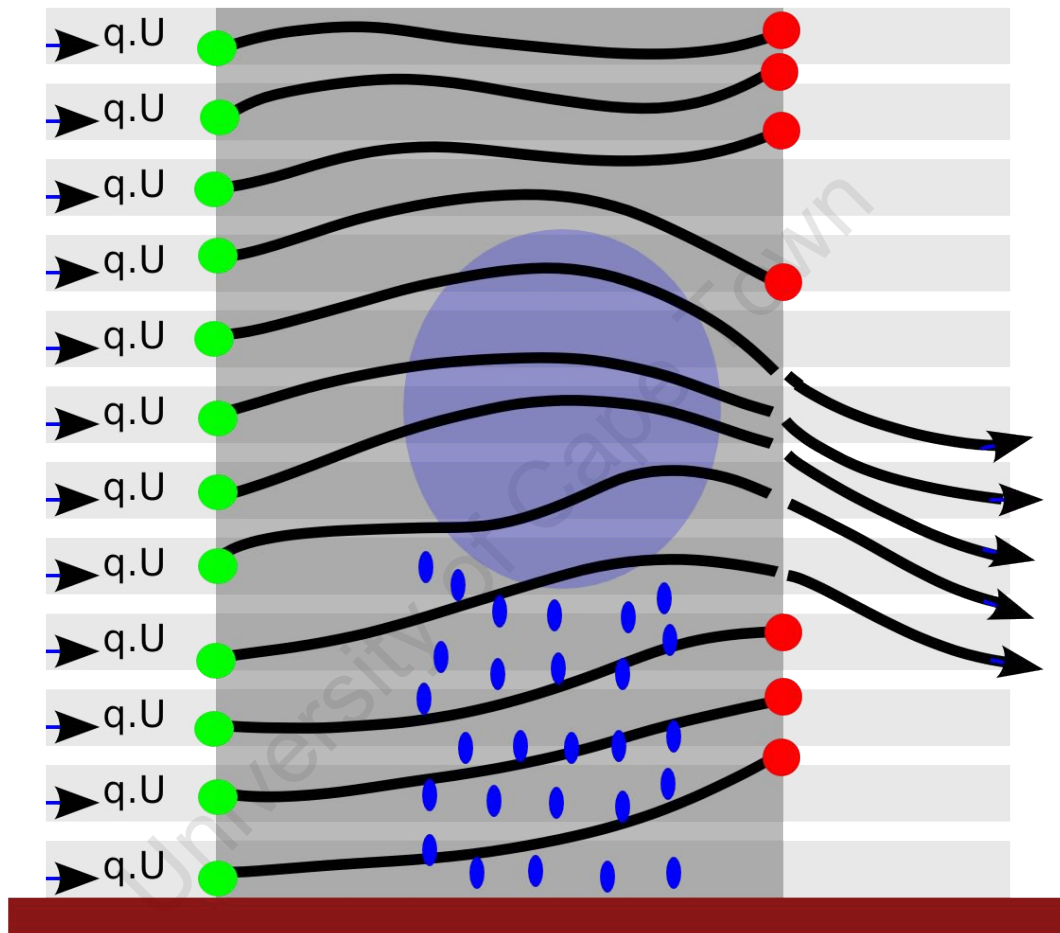


Figure 2.3: Moisture trajectory generation: Model level integration mass flux ( $qU$ ) is calculated at each level. This mass flux is converted into trajectory parcels (green circles). The trajectory parcels are then traced through the target domain. Parcels that are involved in precipitation within the domain are retained and their trajectories are continued into the remainder of the domain. Parcels not involved in precipitation within the domain are terminated (red circles).

below but the 1% threshold was found to be able to remove a great deal while still resulting in fairly good estimations of precipitation compared to the RCM surface precipitation fields.

2. The RCM grid cell must have experienced precipitation within the integration time-step. Because the trajectory integration time-step is typically much shorter than the RCM archive time period, the RCM precipitation is assumed to have fallen uniformly throughout the RCM archive period. This may not be perfectly accurate, but using an RCM archive period of 1 hour it is felt to be a reasonable assumption. Because RCMs typically produce a large amount of trace rainfall it was also required that the RCM precipitation rates exceeds 0.2mm/day so that such trace rainfall events would not be incorporated in the analysis.

3. The RCM rain liquid water field is required to be non zero. This was condition was introduced in order to constrain the height of the diagnosed precipitation. It is noted that in deep convective events, some significant changes in  $dM$  occur at altitudes above where one would expect precipitation to originate. Presumably this is a result of the convective parameterisation in the RCM. The convective parameterisation will move moisture vertically through the RCM levels faster than is represented by the vertical velocity wind fields. Moisture changes will therefore be experienced by the parcel trajectory that are not associated with precipitation processes but with the convective parameterisation's attempts to represent convective motions within the grid scale. As this methodology cannot incorporate the RCM convective processes directly it was felt that restricting diagnosed precipitation to levels where the RCM produced rain liquid water was a good way of removing the false diagnosis of precipitation due to the convective parameterisation.

The methodology makes some assumptions that are worth mentioning. Firstly, rain re-evaporation is ignored as there is no way to diagnose this process. The RCM convective parameterisation incorporates this process internally but it is not represented in any way within the RCM fields. It is therefore possible that rain liquid water is present at a level but that water never reaches the ground due to re-evaporation. The Lagrangian model would therefore diagnose more rainfall than actually reaches the ground. Rain re-evaporation can be considered as a similar process to convection in that it moves moisture vertically in the column. The effect of this on the Lagrangian model is however, impossible to determine. The risk associated with this is that the the Lagrangian model diagnoses rainfall that is not reaching the ground and so biases the moisture source attribution either towards more local sources or towards more remote sources. Which of these scenarios is more likely is extremely difficult to determine and would probably vary depending on the specific atmospheric conditions at a particular time. It must be noted that the Lagrangian model cannot diagnose rainfall unless rain is actually falling on the ground in the RCM so this does place some restriction on miss diagnosis of rainfall in the extreme case where all rain water is re-evaporating. Furthermore, the high the altitude of the diagnosed rainfall the more likely that rain re-evaporation will occur below that level. High level condensation is associated with higher level moisture sources which are typically sourced from more remote evaporative sources. It is therefore not unreasonable to suppose that the effect of miss diagnosing rain re-evaporation may not bias the results towards local sources of moisture and may even, given high level condensation processes, bias the results towards more remote moisture sources.

Secondly, it is assumed that parcel diagnosed precipitation contributes to the underlying grid cell. This may not be the case for high level parcels where the prevailing wind can advect rain water significant distances before it reaches the ground. Again, the impact of this is difficult to determine but can be considered to be relatively small. The intent of the methodology is not to provide grid scale resolution accuracy but rather to identify the first order patterns of moisture sources.

The parcel changes in  $dM$  are accumulated for each parcel while the parcel remains within the target domain. As soon as a parcel leaves the target domain it is filtered based on the accumulated diagnosed precipitation. If this precipitation amount exceeds 5% of the initial parcel precipitable water then the parcel is deemed to have contributed significantly to the precipitation within the target domain and the integration of that parcel is continued into the remainder of the domain. Diagnosis of precipitation continues within the rest of the domain as this is a factor in the derivation of the source attribution as described in the next section. Otherwise, the parcel is deemed as having not

made a significant contribution to the precipitation. The 5% threshold was selected in order to identify parcels that made a significant contribution and discard those that made very little contribution. This was partly done in order to reduce the number of parcels integrated and hence the computation time required, but it also serves the role of reducing noise in the results.

### 2.5.3 Trajectory Integration

Parcel positions in three dimensions (latitude, longitude and altitude) are integrated through space using reversed wind fields from the RCM gridded output in order to represent parcel motion in reversed time. This means that parcel positions are being traced from their end point in the target precipitation domain, backwards in time towards their origin. In this model parcels are integrated backwards all the way to the RCM boundary or until they have been integrated for a maximum of 7 days. It was found in the southern African domain that most parcels reach the RCM boundary within 3 or 4 days, particularly in the higher latitudes where the prevailing circulation systems are strongly defined.

While in many situations a simple first order numeric method of integrating the parcel position is adequate, for strongly curved or accelerating wind fields a second order or higher numerical method adds greatly to the trajectory accuracy (Stohl [1998]). Because of the potentially strong horizontal and vertical wind velocity gradients within the boundary layer and strong curvature over and around complex topography, a second order integration was used in this model. This method is described by the following formula:

$$P_{t+1} = P_t + \mathbf{v}\Delta T + \mathbf{v}'\Delta T$$

The new parcel position  $P_{t+1}$  is therefore a function of the old position  $P_t$ , a constant wind vector component  $v$ , and the rate of change of the wind vector in both space and time  $v'$ . The model time-step is represented by  $\Delta T$ . Numerically this formulation was calculated using a 3 step integration:

$$P' = P_t + \mathbf{v}(P_t)\Delta T$$

$$P'' = P' - \mathbf{v}(P')\Delta T$$

$$P_{t+1} = P_t + \mathbf{v}(P_t)\Delta T + \frac{P_t - P''}{2}$$

Comparison of this integration methodology with a simple first order integration showed that while above the boundary layer the differences are small, within the boundary layer and particularly in regions of complex topography the two methods yield notably different results after more than 12 hours of integration. It is also important that the parcel position is integrated as accurately as possible in order that the interpolated parcel moisture values are as accurate as possible. Errors in parcel position will translate into errors in parcel moisture which directly impact on precipitation diagnosis and evaporative source attribution described later.

Trajectories represent a certain defined mass of moist air with associated specific humidity which can be added to through evaporation or lost through precipitation along the trajectory path. In time reversed integration evaporation

causes moisture loss from the parcel while precipitation causes moisture to be added to the parcel. There are three phases in the lifespan of a trajectory in this methodology. These phases are; trajectory parcel generation, parcel precipitation diagnosis, and parcel evaporative attribution. Precipitation diagnosis has already been described in the trajectory generation section above, and the same method is used during the remainder of the trajectory lifespan.

In order to determine the evaporative source regions, which is the major purpose of the Lagrangian model, the evaporative moisture gains of each parcel must be determined along the parcels pathway. As for precipitation, the only information we have about evaporation is from the RCM surface fields. We therefore need a means of determining the contribution of evaporation to the parcel moisture content. The following methodology has been developed and implemented.

#### 2.5.4 Evaporation and source attribution

Evaporative contributions to the parcel moisture are diagnosed if two conditions are met.

1.  $dM$ , the change in parcel moist mass, must be negative and greater than 1% of the total parcel precipitable mass. As with the precipitation diagnosis, this is to reduce spurious diagnosis resulting from trajectory integration or grid interpolation errors. The value is largely subjective and the result of trial and error.

2. The height of the trajectory must be below the top of the PBL and below 1000m above the surface model. The extra 1000m threshold was applied because the height of the PBL can, under convective conditions, reach as high as 5000m altitude. While this is realistic in terms of vertical motions, convective vertical motion is not represented in the RCM fields and hence we have selected to ignore convective motions. Non-convective turbulent mixing is likely to only extend to around 1000m above the surface, hence the selection of the 1000m absolute threshold.

Calculation of the height of the PBL is done differently in different models but in the example used here the MRF PBL scheme is used as it is a diagnostic output of the PSU/NCAR MM5 regional model used for the test cases. It makes sense to use the model derived PBL height as this would be consistent with the other model derived fields. Evaporative entrainment of moisture into the trajectory parcel is deemed only to be possible within the turbulent vertical mixing of the PBL. Any additions of moisture above the PBL level are considered numerical error resulting from inaccurate trajectory path calculations or due to the resolution limits of the forcing fields.

Rain re-evaporation is a process that cannot be captured by the Lagrangian model because there is no direct information in the outputs of the RCM that allow the model to identify this process. Rain re-evaporation would be diagnosed as a decrease in parcel moisture (in reversed time) and hence could be identified as a local moisture source. The 1000m height limit imposed in condition 2 above will not eliminate this effect as rain re-evaporation can easily occur below this level. We must therefore consider the possibility that rain re-evaporation could indeed be biasing the moisture source results towards local moisture sources and that this would be an incorrect result as re-evaporated rainfall is not a local land surface source of moisture. One possible solution to this would be to turn off evaporation diagnosis when rainfall is occurring in the RCM. During precipitation events rainfall largely dominates evaporation in terms of magnitude (Trenberth [1999a]). However, this would require further experimentation and testing that would form the basis for further model refinement not included in this thesis.

It is important to note that the convective scheme of the RCM is also an important factor and in particular how a convective scheme determines the degree of rain re-evaporation. The Betts-Miller scheme used in this work (Betts [1993]) is a profile relaxation based scheme and so while rain re-evaporation is implicitly assumed, it is not explicitly represented in the scheme. We therefore have to conclude that rain re-evaporation could bias the resultant moisture source attribution towards local sources of moisture rather than remote sources. A case study is presented in Chapter

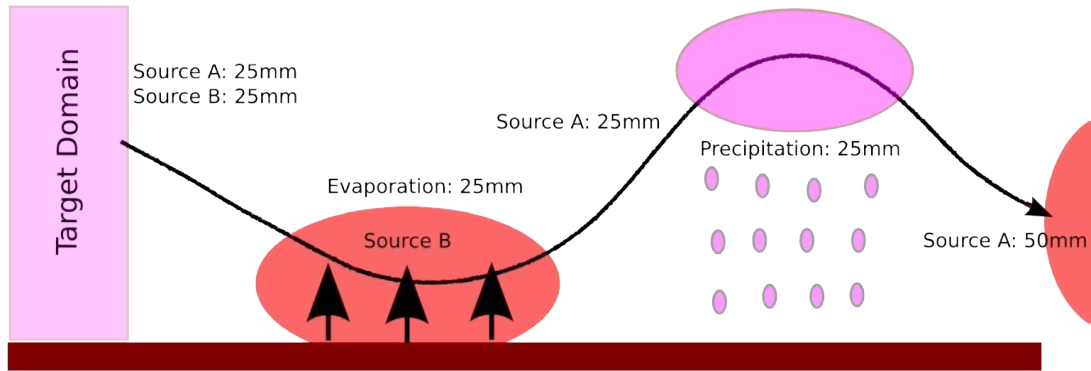


Figure 2.4: Idealised trajectory pathway with evaporative source and precipitation event. Initial parcel moisture is source from source A (50mm). 25mm is lost to the precipitation event. The evaporative source contributes 25mm to the parcel moisture. The resultant mixture of sources arriving at the target domain is 50% for source A and 50% for source B even though source B contributed twice as much moisture in absolute terms.

3 that suggests that the Lagrangian model is not grossly over-estimating local sources, however, the results presented in the following chapters should be considered with due consideration of this important issue.

The process of associating moisture sources and sinks, (ie. a source of evaporation, with a specific spatially and temporally defined precipitation event) can be described as source attribution. We wish to ascertain the absolute contribution of each grid cell to the final precipitation event in question. The fraction of moisture that a particular evaporation event contributes to the parcel moisture reduces as downstream evaporation events contribute to the total parcel moisture. However, the absolute contribution remains constant despite contributions from other evaporative sources.

With regards precipitation events, these involve an absolute loss of moisture. A precipitation event removes moisture from the trajectory parcel and hence a fraction of the moisture contributed to the parcel by upstream evaporation events is lost. The absolute attribution of upstream moisture sources is therefore reduced by a downstream precipitation event. In an extreme scenario, a large precipitation event could remove all moisture from a parcel and hence render any upstream evaporative sources null in terms of contribution to further precipitation events. While complete removal of moisture from parcel of air is impossible, this example illustrates the role of precipitation events in evaporative attribution. Figure 2.4 shows an idealised trajectory pathway where the trajectory has an initial upstream moisture source (source A). The trajectory loses moisture to an along path precipitation event. It then gains moisture from an evaporative source (source B). Even though the second source is of smaller magnitude than the original source, the resultant mix of source moisture arriving at the target domain is equal for the two sources. In time reversed analysis it is therefore necessary to maintain an attribution factor ( $A$ ) to scale the absolute attribution of each evaporative source based on intervening precipitation events. This factor is modified during diagnosed precipitation according to:

$$A = A \left( \frac{M}{M + dM} \right)$$

Where  $A$  is the attribution coefficient which varies between 0 and 1,  $M$  is the moist mass of the trajectory from the previous integration time step (after the event in non reversed time), and  $dM$  is the mass of moisture lost from the parcel to precipitation during the integration time-step. Therefore the larger the precipitation amount the smaller the resultant attribution factor. The attribution factor is initialised to 1 at the point the trajectory leaves the target domain and tends towards zero. Precipitation defines  $dM$  as positive so that  $A$  can never become negative. In the extreme

case of complete moisture removal mentioned above,  $M$  would be zero and hence the resultant attribution coefficient becomes zero. Subsequent attributed evaporation amounts would therefore also be zero.

Finally, the absolute contribution of a source is scaled by the fraction of parcel moisture that is actually removed in the target precipitation event. Even if a evaporative source has contributed a large absolute mass of moisture to the parcel, if only a small fraction of the parcels moisture contributes to the final precipitation event in the target domain then the absolute contribution of the source is correspondingly small. Hence the final attributed contribution of a moisture source to a particular trajectory parcel is:

$$S_{attrib} = \Delta M \cdot A \cdot P_{frac}$$

Where  $P_{frac}$  is the fraction of the total parcel moisture that precipitates out in the target event.

Figure 2.5 plots evaporation, precipitation, attribution and attributed evaporation parameters for an idealised trajectory as it progress backwards in time with the time axis being hours prior to the event at  $t=0$ . The idealised scenario represents an initial target precipitation event at  $t=0$ . A second upstream precipitation event occurs between  $t=-28$  and  $t=-45$ . A regular, sinusoidal cycle of evaporation occurs peaking every 24 hours.  $t = 0$  represents the moment when the trajectory departs the target domain. In this case the target precipitation event is continuing to occur after the trajectory has left the domain and hence the attribution coefficient immediately begins to reduce from it's initial value of 1. It can be seen that as the attribution coefficient is reduced towards zero by the two precipitation events, so the attributed evaporation from each evaporative event is reduced.

At each integration time-step the attributed evaporation amount is calculated for the underlying RCM grid cell. The attributed evaporation amounts from all trajectories are accumulated for each RCM grid cell for each integration time step. However, the time reference of the accumulation is not the integration time step but the trajectory origination time step. The resultant accumulated attributed evaporation map for a particular time step represents the evaporative source distribution for the target precipitation time period rather than during the evaporation time period. Using the trajectory initiation time period as the reference enables analysis of evaporative sources for specific precipitation events. If the evaporation time reference had been used instead then the maps would represent simultaneously contributed evaporation, but those evaporative sources could contributed to multiple precipitation time periods due to different pathways and velocities of the trajectories from the target domain.

### 2.5.5 Trajectory endpoints

If the trajectory reaches a boundary of the RCM domain then the attributed moist mass, as for an evaporative event, is accumulated as a moisture flux through this boundary at the particular location and vertical level. As with evaporative events the accumulation is referenced to the trajectory initiation time rather than the time the trajectory crosses the boundary. These boundary attributed moisture flux fields are also retained and serve as a further useful analysis of the contribution of moisture sources external to the RCM domain to the precipitation event in the target region.

The integration output therefore consists of maps of attributed evaporation for each time step, maps of boundary moisture fluxes for each time step, and instantaneous equivalent specific humidity fields for the RCM domain. This last output represents the equivalent specific humidity fields contributed by all the parcels at each time-step in the integration and is a useful diagnosis of the moisture pathways. It should be noted that because the equivalent specific humidity fields are time instantaneous referenced by trajectory integration time-step not trajectory initiation time-step it less easy to use these fields to analyse specific precipitation events and associated trajectory pathways. However, they are still useful for time averaged pathways and analysis of the vertical motion of moisture en-route to a precipitation domain. Due to the inherent computation and storage requirements of the methodology output had to be limited and the set of output archived is a compromise aimed at providing as much utility as possible.

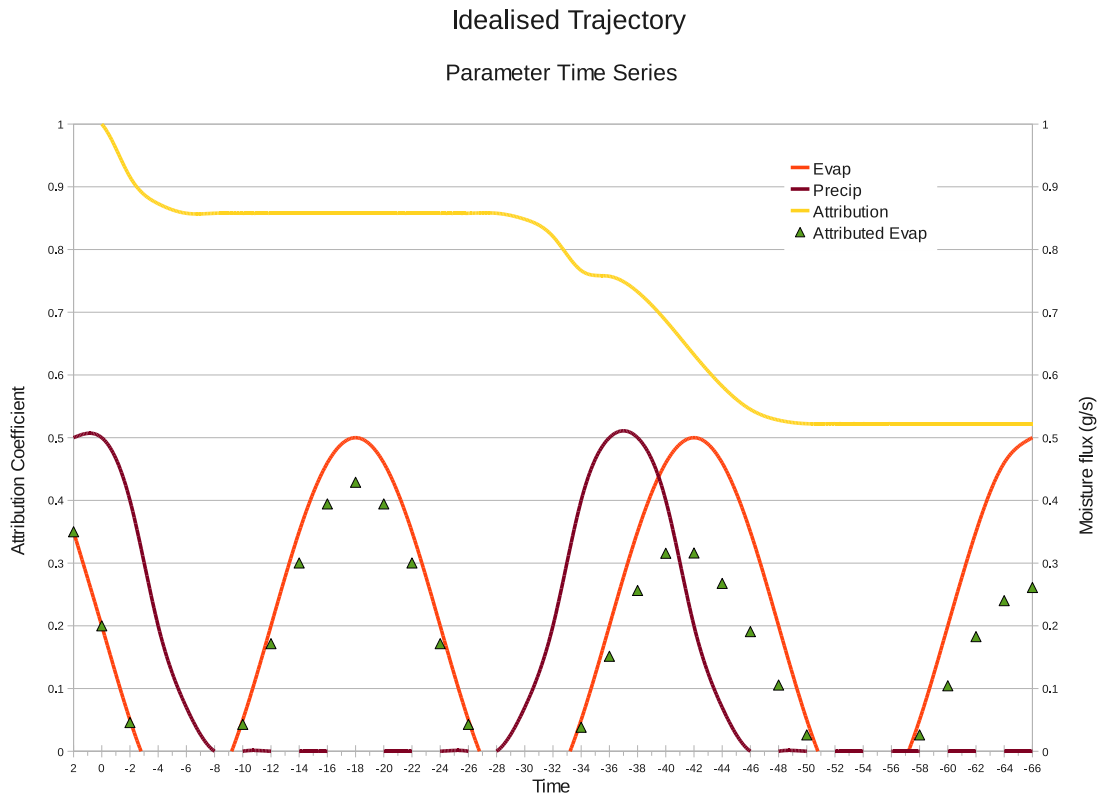


Figure 2.5: Idealised trajectory parameters varying through 66 hours of trajectory integration. The x axis represents time in hours prior to the event. Evap is the diagnosed evaporative uptake of the trajectory parcel which shows a regular idealised diurnal cycle. Precip is the diagnosed precipitation from the trajectory parcel and shows an initial event around  $t=0$  and an upstream event peaking at  $t=-38h$ . Attribution is the attribution coefficient as described in the text. Attributed evaporation is the product of the trajectory evaporative uptake and the attribution coefficient illustrating the reduced attribution of evaporation as a result of upstream precipitation events.

## 2.6 Test integration

The RCM results have been extracted from a 4 month integration of the 5th generation Pennsylvania State University-National Center for Atmospheric Research Mesoscale Model (PSU/NCAR MM5; Grell et al. [1994]) RCM forced with NCEP version 2 (Kanamitsu et al. [2002]) re-analysis fields. Re-analysis data was discussed in section 2.3.1 along with the associated strengths and weaknesses. Subsequent to this study, high resolution re-analysis such as the ECMWF/ERA interim (Simmons et al. [2007]) have become available which could possibly prove to be a more accurate driving datasets. However, the NCEP re-analysis still remains a mainstream product and has formed the basis for a generation of climate analysis.

The integration was run from October 1988 through to the end of February 1989. This period was selected as it fits within further plans for a two season moisture transport analysis within southern Africa described in Chapters 3 and 4. The MM5 model is a well established non-hydrostatic model that has been used extensively for both weather forecasting applications as well seasonal and climate scale applications. The model was configured with a 50km grid resolution over an area extending from the equator to 40°S and 5°E to 55°E as seen in figure 2.6. This domain was selected in order capture the range of climate systems that influence the region including tropical, sub-tropical and mid-latitude processes. The eastward extend was selected in order to include Madagascar that has an important role in influencing moisture transport from the Indian Ocean.

Ocean surface temperatures were prescribed by the Reynolds Optimal Interpolation (ROI) dataset (Reynolds and Smith [1994]) which provides a higher resolution surface temperature field than that generated by the NCEP2 re-analysis. While this does result in an inconsistency between the SST fields of the driving NCEP atmospheric fields and the SST field driving the RCM, the inconsistency is largely one of enhanced resolution in the RCM rather than any large scale biases. The ROI dataset is derived from satellite and buoy measurements has been used extensively as an historical record of ocean surface temperatures. The MM5 RCM uses ocean surface temperatures to determine the latent and sensible heat fluxes at the ocean surface. As latent heat flux is so important for capturing evaporation from the surface and representing the role of the ocean as a moisture source, the most accurate available ocean surface temperature was needed. In particular, the relatively narrow but warm Agulhas is an area of strong latent heat flux and is far better represented in the ROI dataset than in the NCEP2 dataset.

### 2.6.1 Model configuration

The model was configured to use the Betts-Miller (Betts [1993]) convective scheme and the MRF PBL scheme with mixed-phased large scale precipitation. The Betts-Miller scheme uses a moisture profile relaxation approach. This scheme attempts to move moisture and heat vertically through the model levels in such as way as to reduce instability and return the vertical profile to a standard observed stable profile. In this process, convective precipitation is also diagnosed. While other schemes, such as the Kain-Fritsch scheme (Kain [2004]), are more physically based, the Betts-Miller scheme was found by Tadross et al. [2006] to over-estimate rainfall intensity over the region but offer a better representation of the diurnal cycle as well as inter-annual variability than other configurations. The alternative Kain-Fritsch scheme (Kain [2004]) produces slightly better total rainfall values but the diurnal cycle produced shows convection occurring much too late in the day. In general the selected configuration simulates a too intense hydrological cycle (Tadross et al. [2006]) which must be considered in analysis of the results.

The MRF PBL scheme was found by Tadross et al. [2006] to perform the best in the southern African domain. Most precipitation within the domain is captured by the convective scheme, however, the large scale, non-convective precipitation is approximated by the mixed phase scheme of the model. Once again Tadross et al. [2006] showed this configuration to produce good results in the domain.

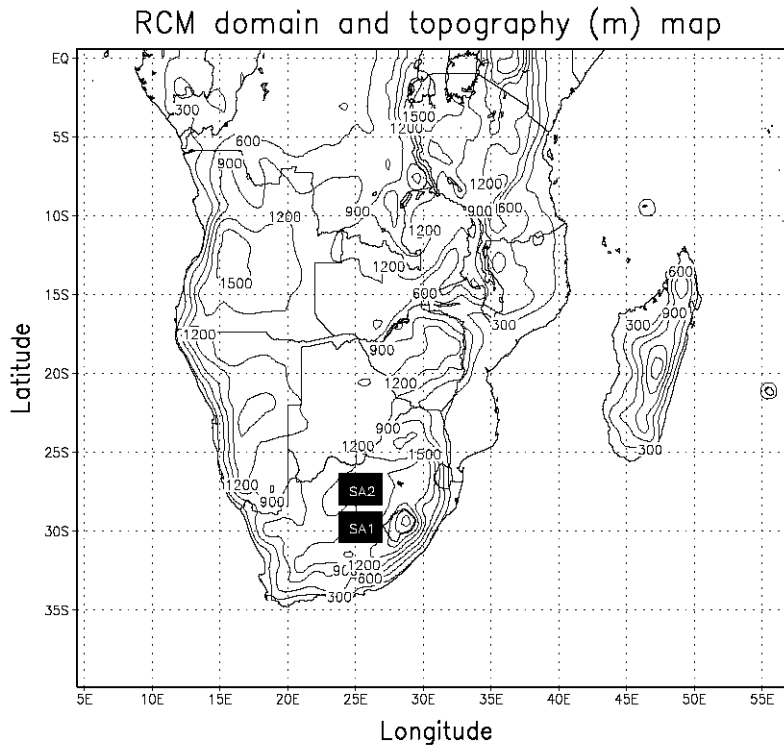


Figure 2.6: RCM geographical domain and surface altitude (meters) with analysis target regions SA2 and SA3 identified by the black rectangles

Due to the large number of parameterisation schemes available in the MM5 model it is prohibitive to determine the relative performance of each possible combination of schemes. While the studies cited have done a great deal of testing and validation of the different schemes it has not been exhaustive and it is likely that other combinations could provide as good or better results.

## 2.6.2 Land surface model

As evaporation from the land surface is integral to the source attribution model, the RCM was configured to use the NOAH land surface scheme which is the most advanced and complete land surface scheme available in the model. This scheme represents the land surface using a relatively sophisticated model (Chen and Dudhia [2001a,b]). Different vegetation types are represented by their physiological characteristics which directly influence transpiration. A multi-level soil moisture and temperature model is also incorporated in order to simulate soil moisture availability. This model configuration has been used successfully in prior work investigating the sensitivity of changes in vegetation to the southern African climate system (MacKellar et al. [2009]). An improved southern African vegetation map was also used as an enhancement over the standard simplified map provided with the model.

## 2.6.3 Model output

In order to satisfy the requirements of a high time resolution for the trajectory integration as described earlier, the model was configured to archive all required fields at a 1 hour interval. While this greatly increases the storage requirements of the simulations, testing indicated that this high resolution was important especially considering the

relatively small grid scale. 3-dimensional wind fields, moisture fields, surface precipitation and evaporative flux (evapotranspiration) are therefore available at 1 hour time interval.

The Lagrangian model was integrated at a time-step of 15 minutes with the atmospheric fields linearly interpolated to the intervening time periods. This time-step is a compromise between computational expense and integration accuracy. Even at a relatively high wind speed of 16m/s a trajectory will only cover 15km within 15 minutes. With a 50km grid size this means that several integration time-steps will be required to move across a grid box therefore avoiding many numerical errors.

#### 2.6.4 RCM and Lagrangian model validation

In order to have any confidence in the results produced by the Lagrangian model we need to validate the results. The distinction needs to be made between validation of the Lagrangian model and validation of the driving RCM. The validation discussed here is only with regards the Lagrangian model and is necessarily done with respect to the RCM driving wind, moisture, evaporation and precipitation fields. Validation of the RCM is an extensive investigation in and of itself and has been adequately covered in Tadross et al. [2006], the main result of which is that the MM5 RCM rains too often and too much in the summer rainfall regions of South Africa. While these errors will obviously influence the results of the Lagrangian model, it is however, accepted that the RCM fields at least represent a defensibly realistic climate in terms of general synoptic patterns, sequencing of events, as well as many smaller scale features involving convection and topography. However, it is further proposed that the Lagrangian model provides a useful means of evaluating and explaining some of these errors and biases in the RCM though such an exploration is beyond the scope of this study. We will therefore not compare the Lagrangian model diagnosed precipitation directly with observed precipitation as this captures too many layers of uncertainty. Lagrangian model precipitation diagnosis will only be validated relative to the RCM precipitation.

As regards validation of the parcel trajectories no rigorous means is available beyond the use of neutral density balloons (Riddle et al. [2006], Baumann and Stohl [1997]). A great deal has been written (Stohl et al. [1995], Stohl [1998], Stohl et al. [1998, 2001], Draxler [1987], Kahl [1996]) about the validation and accuracy of kinematic trajectory models and the formulation of the equations of motion used in this study are very similar to those used in many other studies. In the development of the model two different numerical methods were used, one very simple method and the more accurate method described above. Comparison of the results of both single trajectories and the complete Lagrangian model produced very small differences suggesting that the numerics are fairly robust. Visual analysis of the trajectories in comparison to RCM wind fields was done extensively. Possibly the greatest source of error in the trajectory integrations is that of vertical motion which is not fully expressed in the RCM output data as discussed earlier.

Validation of the moisture processes simulated by the Lagrangian model can possibly best be done by comparing the RCM precipitation time series for a particular domain with the diagnosed attributed moisture values for the same domain. The use of precipitation time referencing for the attributed moisture source output data allows a side by side comparison of the two time series. Figure 2.7 shows such a comparison for the target domain SA2 identified in figure 2.1 for the month of December 1988. We can see that while the attributed moisture source field does not capture the extreme values of the precipitation time series, it does represent almost all precipitation events in the series. Some small events are not captured and this is probably a result of the aggressive filtering in the precipitation diagnosis stage. As discussed above, it is felt that such aggressive filtering adds to the robustness of the results by not falsely identifying precipitation. Experiments with the level of filtering revealed that less filtering did not change the patterns of the moisture sources but did introduce spurious precipitation diagnosis and also greatly increased the integration time as the number of moisture parcels generated was much larger. The similar methodology applied in Stohl and James [2004] also failed to diagnose the full precipitation moisture amount suggesting this is an inherent limitation of the methodology.

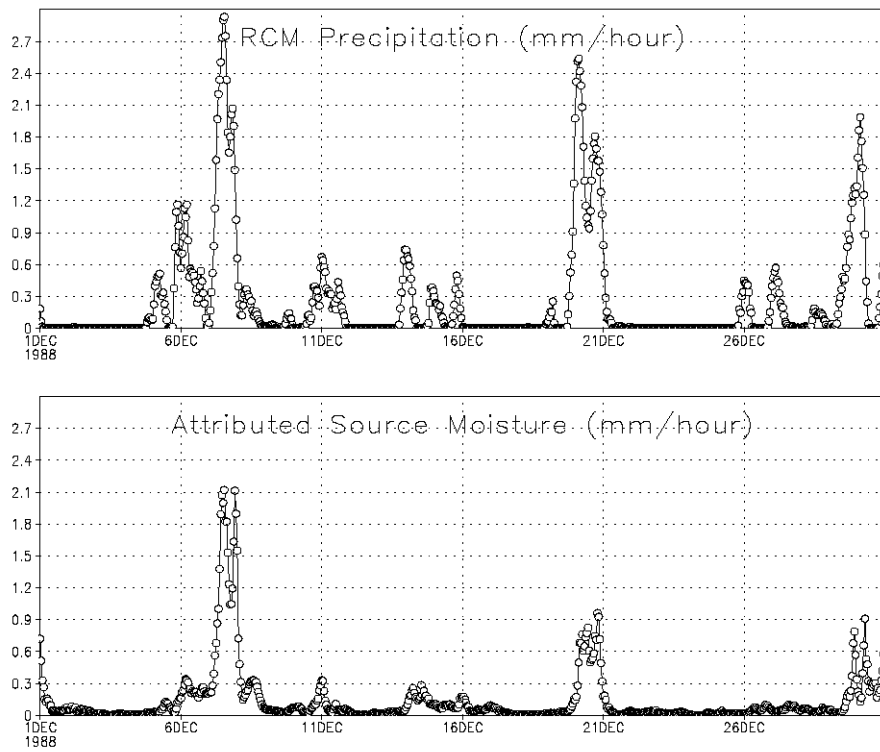


Figure 2.7: Hourly time series of RCM precipitation averaged over domain SA2 (top) and Lagrangian diagnosed precipitation (bottom) for December 1988 illustrating the ability of the Lagrangian model to reproduce the RCM precipitation field.

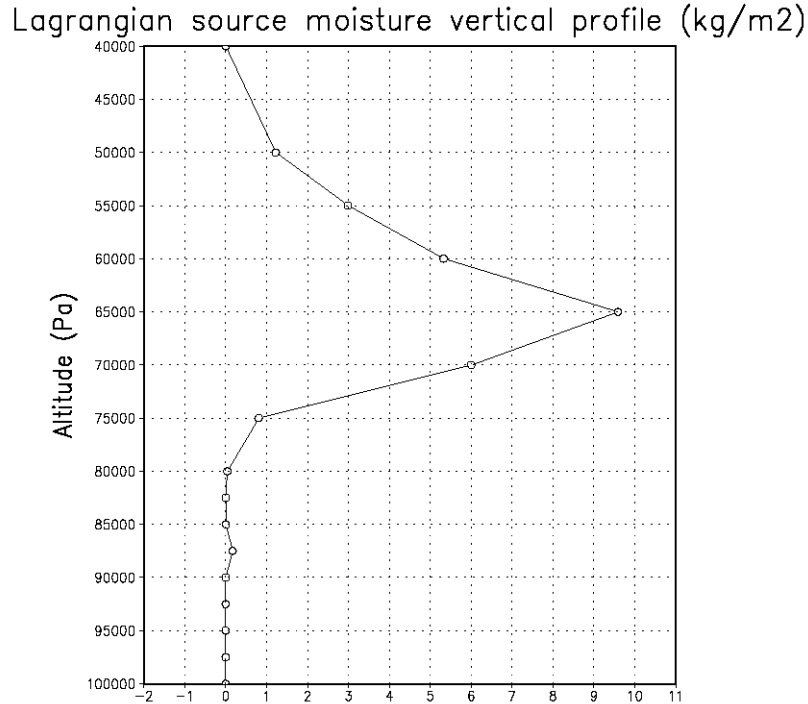


Figure 2.8: Time mean (DJF 1988/9) vertical (height in Pa) profile of Lagrangian model moisture ( $\text{kg}/\text{m}^2$ ) source arriving at boundaries of target domain SA2

While not a complete validation, it is encouraging to note that if we plot the vertical distribution of moisture arriving at the precipitation target domain (Figure 2.8) we can see that the majority of moisture is concentrated around the 700hPa level. D'Abreton and Tyson [1996] used the 750hPa level as the analysis altitude for moisture arriving in the interior of the country contributing to precipitation after the results of Freiman and Tyson [2000]. Of course the Lagrangian model produces an extensive spread of moisture through the vertical because it is free to diagnose condensation at any altitude according to the conditions described above. Analysis of particular precipitation events (not shown) suggests that there is a large degree of variation in the diagnosed vertical profile of attributed moisture which warrants further investigation.

It is clear from this analysis that the Lagrangian source attribution model does capture the significant precipitation events though it diagnoses less precipitation than the RCM produces. It is also clear that the precipitation diagnoses is able to capture the monthly precipitation totals with some acceptable level of accuracy, arguably sufficiently to investigate differences between dry months and wet months in the RCM results. Vertical distributions of contributing moisture agree with other studies. Further validation of the model is difficult due to the lack of suitable data to validate against. However, a case study of a particular precipitation event is now presented in order to illustrate the effectiveness of the methodology.

### 2.6.5 Case Study Results

The case study precipitation event falls on the 15th of February 1989 as simulated by the RCM. This event was selected as it was sufficiently large to produce a significantly large number of trajectory parcels but was also fairly isolate in time which aids the analysis as no other precipitation events in the area could confuse the results. Figure

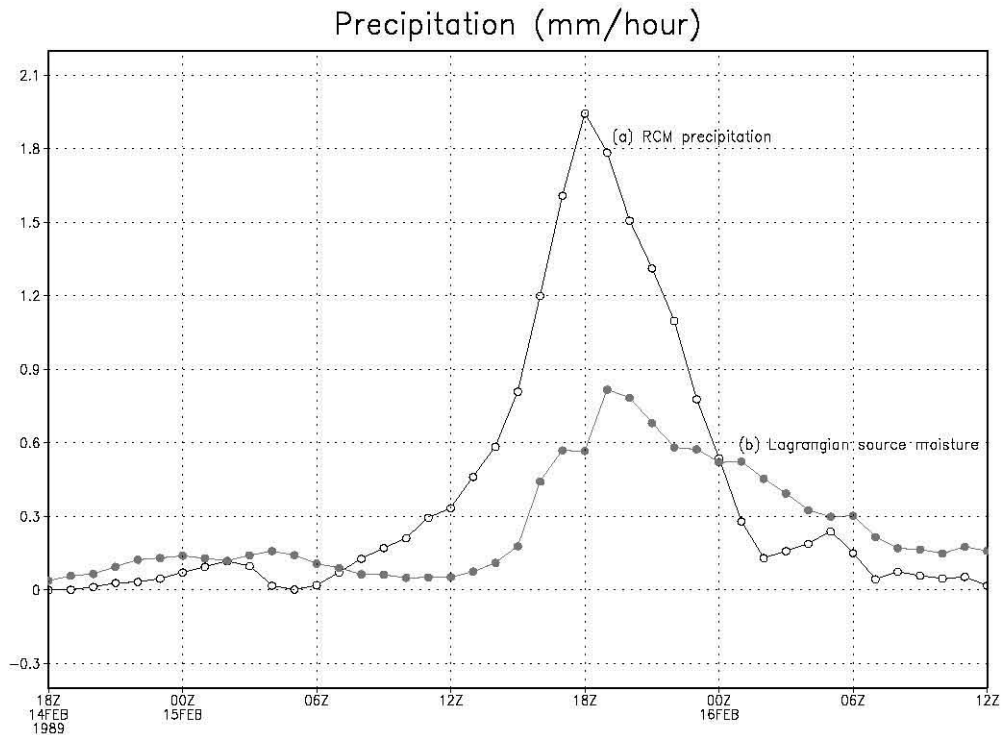


Figure 2.9: Time series of area averaged precipitation for region SA2 for the event of the 15th February 1989. (a) RCM simulated precipitation (mm/hour) and (b) Lagrangian attributed source moisture (mm/hour). The Lagrangian model captures the event but underestimates the magnitude.

2.9 shows the time series of both the RCM simulated precipitation for regions SA2 (see Figure 2.6) and the diagnosed Lagrangian attributed moisture source totals. As with the earlier validation time series we can see that the Lagrangian model captures the temporal sequence of the event well though it fails to diagnose the total moisture involved.

Figures 2.10 and 2.11 shows the progression of the regional synoptics for the event. NCEP re-analysis data are used for these plots in order to capture the synoptics on a scale larger than the RCM domain. Even though the RCM may differ slightly from the NCEP boundary forcing data, for the purposes of a synoptic analysis the use of the re-analysis fields is adequate. The sequence describes a ridging anti-cyclonic scenario. At 0600, 14 Feb, we can see that the South Atlantic High Pressure (SAHP) system has ridged almost completely around the south of the sub-continent at the surface while a very weak continental trough is located over the west of the continent. By 1800, 14 Feb, the SAHP remains present around the south and the surface continental trough has begun to deepen. This trough is a major driver of lower level moisture convergence over South Africa and is a common feature of Southern African summer synoptic conditions. Interestingly, a small low pressure system is also forming in the SWIO. By 0600 on the 15th of Feb the SAHP ridge is still in position while at 500hPa we can see a mid-latitude westerly wave forming and approaching from the south west. A mid-latitude westerly wave is characterised by upper level divergence ahead of the trough which combined with low level convergence driven by the continental low pressure trough produces unstable conditions which combined with a convergence of moisture results in precipitation. The peak of the precipitation time series occurs around 1800 on the 15th and the synoptics show an intensification of the previous state with a now extensive westerly wave.

Table 2.1 shows the breakdown of moisture contributions from each of the four boundaries of the RCM domain as well as the ocean and land surfaces for the period. Of interest is the large westerly contribution (35,94%) which is surprising considering that the dynamics suggest a convergence of moisture from the East. The land contribution

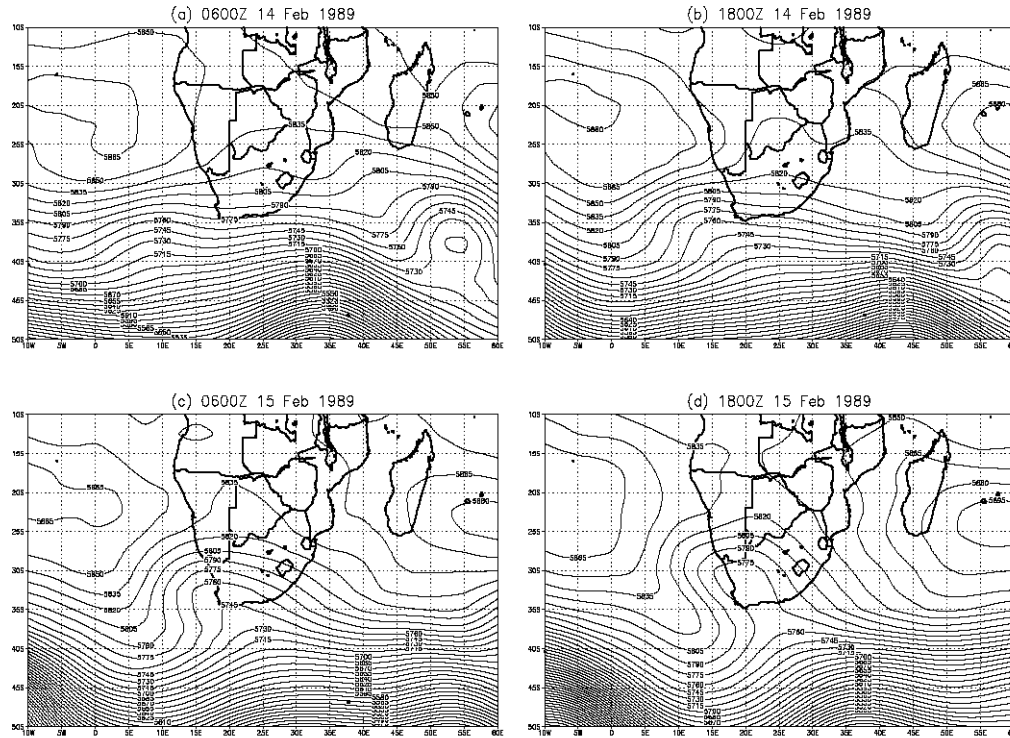


Figure 2.10: Sequence of synoptic states: (a) 0600 14 Feb, (b) 1800 14 Feb, (c) 0600 15 Feb, (d) 1800 15 Feb. Contours are 500hPa geopotential height (m). The synoptic sequence is described in detail in the text.

	Land	Ocean	North	South	West	East
Attributed Moisture ( $kg/m^2$ )	3.30	1.45	0.02	1.10	3.73	0.78
% of Total Moisture	31.78	13.92	0.23	10.63	35.94	7.50

Table 2.1: Total and fractional Lagrangian attributed moisture sources ( $kg/m^2$ ) for domain SA2 during the event of 14 - 16 Feb 1989 for Land, Ocean and RCM boundary. Land surface and ocean surface are diagnosed as the two most important moisture sources for this event.

of 31.78% is also interesting as it suggests a large local precipitation recycling component. Figure 2.12 shows the vertical profile of RCM western boundary Lagrangian attributed moisture source. The westerly moisture source consists of a very localised, intense moisture flow at the 500hPa level between 30°S and 35°S. While the 500hPa circulation field in the days prior to the precipitation event would suggest that such a moisture source could indeed terminate in the target region it would seem to be much too high an altitude to contribute, both in terms of absolute moisture as well convective moisture entrainment. However, figure 2.13 shows a vertical cross section of Lagrangian parcel moisture across the RCM domain averaged between 30°S and 35°S and figure 2.14 shows the time mean Lagrangian moisture field averaged between 700hPa and 500hPa for the 4 days prior to the event. In both figures we can clearly see a stream of moisture from the western boundary region into the interior of the domain and the vertical cross section indicates that the moisture is descending as it crosses the domain terminating at around 750hPa. While this moisture source certainly needs far more investigation it does, at least in this case, seem to be at least reasonable in terms of the RCM simulated dynamics.

The second most significant attributed moisture source is the land surface. The value of 31.78% is somewhat higher than would be expected given. Figure 2.15 shows the spatial distribution of the land surface attributed moisture source which is located within close vicinity to the target domain suggesting the local land surface acted as an important source of moisture for this event. While it is certainly possible that a single event could involve more local moisture

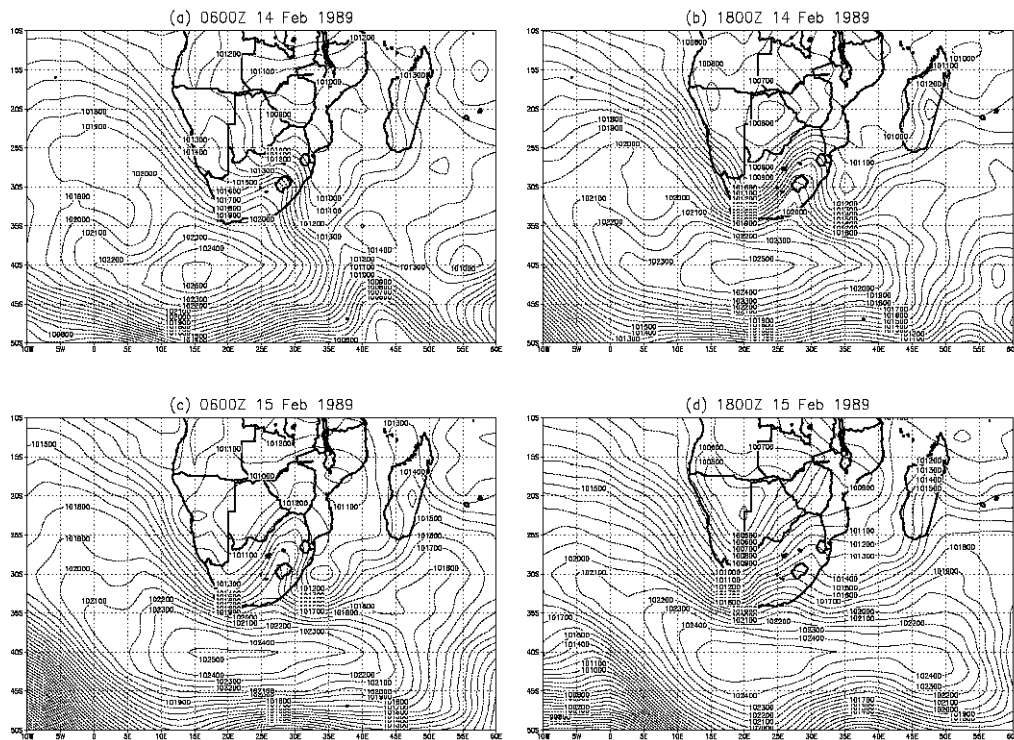


Figure 2.11: Sequence of synoptic states: (a) 0600 14 Feb, (b) 1800 14 Feb, (c) 0600 15 Feb, (d) 1800 15 Feb. Contours are Sea Level Pressure (SLP) (hPa), solid lines are sea level pressure in Pa. The synoptic sequence is described in detail in the text.

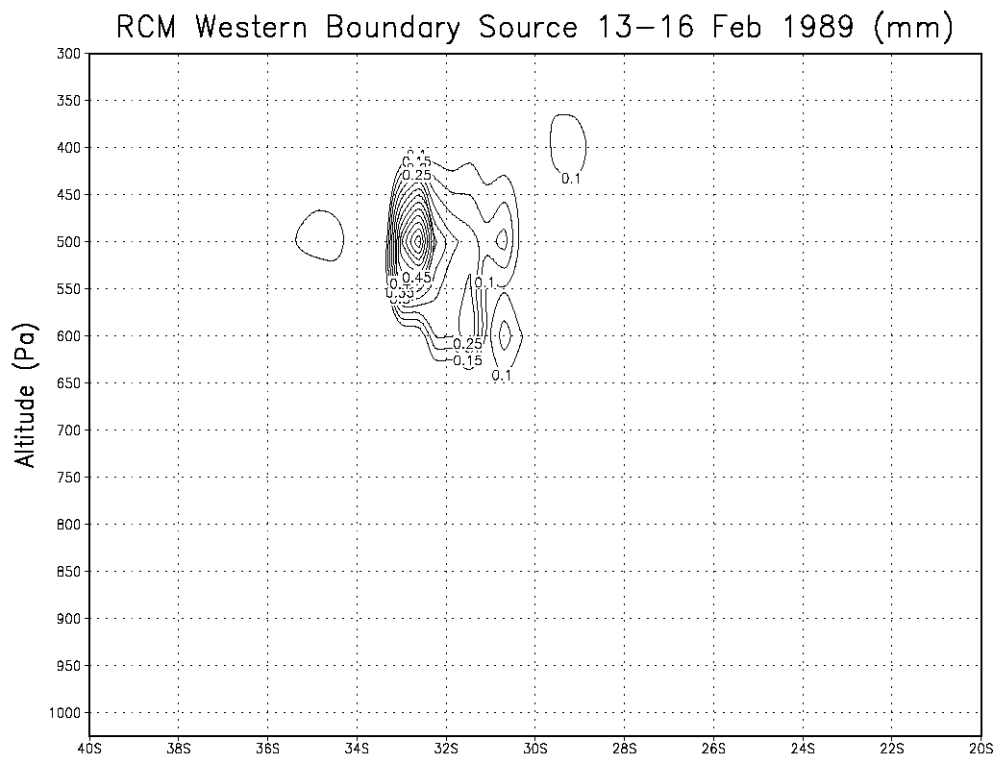


Figure 2.12: Total attributed source moisture ( $\text{kg/m}^2$ ) across the RCM western boundary (altitude in Pa) during the period of 13-16 Feb 1989 for domain SA2. This field identifies the western boundary source as being at high altitude (500hPa) and at latitude 32°S

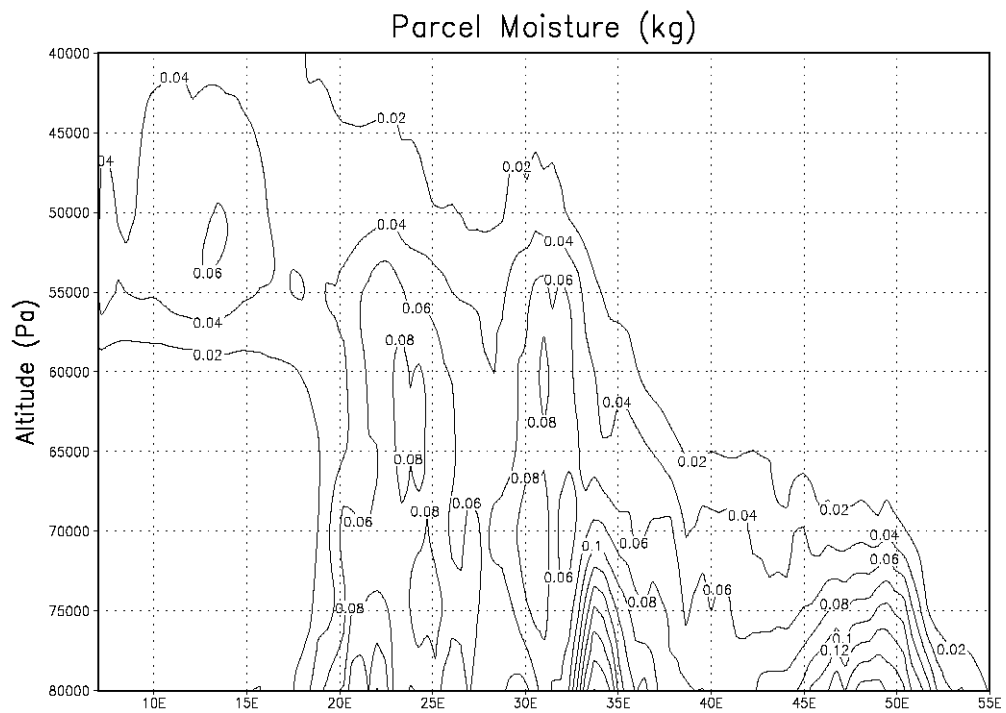


Figure 2.13: Time mean cross section (altitude in Pa) ( $35^{\circ}\text{S} - 30^{\circ}\text{S}$ ) of Lagrangian parcel moisture field ( $\text{kg}/\text{m}^2$ ) for the period 11 - 15 Feb 1989 for domain SA2. The field illustrates the progression of moisture from the western boundary source at 500hPa altitude down to lower levels nearer the target domain SA2.

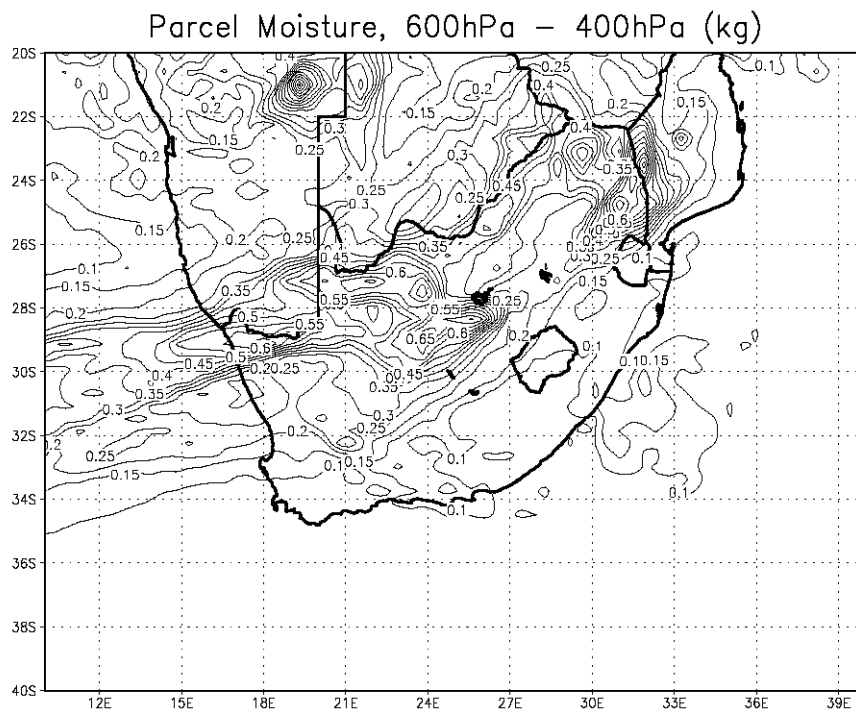


Figure 2.14: Mean Lagrangian parcel moisture field ( $kg/m^2$ ) between 600 hPa and 400 hPa altitude for the period 11-15 Feb 1989 for domain SA2. This field shows the progression of moisture from the high level western boundary source directly eastward towards the target domain.

Land based attributed moisture source (mm) (14 – 16 Feb 1989)

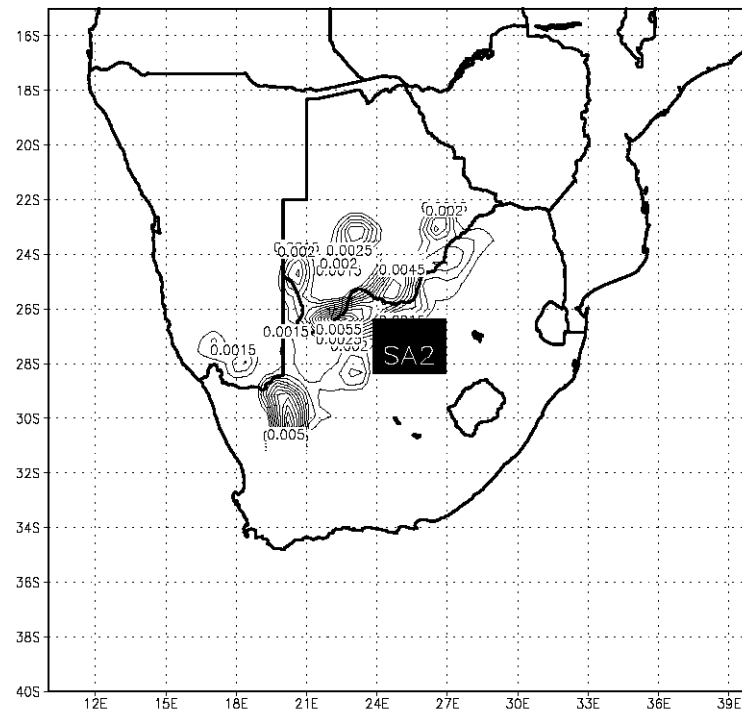


Figure 2.15: Lagrangian land surface attributed source moisture ( $kg/m^2$ ) for the period 14 - 16 Feb 1989 for domain SA2 showing significant land source regions spread both north and south west of the target domain.

sourcing than a long term seasonal average, the average land attribution fraction for the complete 1988/89 DJF season is actually between 30% and 40% so this particular event actually has a lower land surface contribution than the seasonal average.

This land surface contribution along with the related regional ocean contribution will be explored in more detail in a subsequent paper but deserves some comment here. It must again be emphasised that the diagnosis of evaporative moisture uptake in the Lagrangian model is not perfect as it is dependent on the RCM specific humidity and wind fields. If upstream convective precipitation is moving moisture upwards and these vertical motions are not captured by the RCM vertical velocity fields then spurious moisture uptake could be diagnosed at higher levels. However, under these conditions convection is indeed moving moisture upwards away from the surface into higher levels where it can then be advected into adjacent regions. The spurious uptake of moisture would therefore not be an inaccurate representation of moisture transport even if the underlying premises of the Lagrangian model are being violated. It must also be remembered that parcels cannot gain moisture below the top of the turbulent planetary boundary layer so spurious high level moisture uptake is prohibited.

However, one further caveat must be revisited. Rain re-evaporation, as discussed in sections 2.5.2 and 2.5.4, is not captured as such by the Lagrangian model. The Lagrangian model, given the constraints on evaporative diagnosis in section 2.5.4, can miss-diagnose rain re-evaporation as a local land surface moisture source as it will produce the same effect on the parcel moisture content of low level moisture parcels. It is difficult to determine the degree to which this may bias the results towards more local moisture sources and further enhancement of the method would be required to eliminate this possible bias.

## 2.7 Discussion and conclusions

The methodology presented here allows the analysis of attributed evaporative source regions associated with a particular rainfall event as simulated by a RCM. This allows for a detailed analysis of the sources of moisture feeding a particular event or of moisture sources important for an area over a longer time period depending on the length of integration of the model and style of analysis. The attributed source maps consist of the surface source maps (ocean and land) as well as the RCM boundary source maps that identify where moisture is entering the RCM boundaries. This facilitates the diagnosis of moisture sources beyond the bounds of the RCM domain. The model is forced with a high resolution RCM which provides high resolution wind, specific humidity, evaporative fluxes, and precipitation fields to drive backward trajectory moisture transport model.

The methodology is potentially powerful in that it attempts to capture the full RCM moisture dynamics rather than relying on time averaged moisture diagnostics. The use of a high resolution RCM simulation of the small scale dynamics allows a detailed analysis of the regional moisture processes including topography and land surface features. Validation of the moisture source time series shows that the method is able to represent most precipitation events though it under represents the magnitude of the moisture sources. This under representation is most likely the result of stringent filtering of the precipitation diagnosis to reduce spurious moisture sources.

An important caveat, as discussed in sections 2.5.2, 2.5.4 and in section 2.6, is that of rain re-evaporation and the possibility that miss-diagnosis of re-evaporated rainfall as a local moisture source may bias the results towards local moisture sources rather than remote sources. In section 3.4 to follow, a further analysis of a case study is performed and moisture budget analysis is done comparing the attributed moisture sources with the surface latent heat flux fields of the RCM.

The case study results presented in this section are interesting in that a significant land surface moisture source is identified in close proximity (less than 1000km distance) from the precipitation domain. Additionally a strong, high level, mid-latitude westerly moisture source was identified that dominated the more traditionally accepted easterly moisture sources. The apparent robustness of the methodology, with due consideration of the potential biases and caveats, and the results presented suggest that further exploration of the southern African moisture transport dynamics using this methodology may reveal some new and interesting information. Such an exploration is described in the following two chapters.

In summary, the results presented are encouraging as the Lagrangian model does seem able to balance its attributed moisture sources with the RCM surface latent heat fields. If the Lagrangian model were significantly over-estimating local moisture sources then the required surface latent heat fluxes produced by the RCM would not be able to provide sufficient moisture within the identified moisture source regions.

# Chapter 3

## Land and Ocean Results

### Introduction

The previous chapter described the development of a Lagrangian moisture source attribution model and presented some initial testing over the southern African domain. Initial results presented suggest that the model produces qualitatively plausible results even if there are some discrepancies between the RCM precipitation and Lagrangian precipitation magnitudes. The purpose of this initial investigation was to evaluate the performance of the Lagrangian model and hence ascertain its value as a moisture source analysis methodology. The challenge of validating such a model was discussed and will be discussed further in Chapter 5, however, it is clear that quantitative validation is almost impossible due to the lack of observations and hence the validity and applicability of the model must be based on a more qualitative analysis. Indeed, in many respects the model development stems from the inability to directly observe precipitation moisture sources and hence validation is, by definition, difficult. However, that said, results described in the previous chapter indicate that while some results are perhaps unexpected, they are supported by other evidence and can tentatively be explained through the associated atmospheric physics and surface fluxes. This gives us some confidence, beyond the rationale of the methodological construction itself, that the model is useful and can be applied more generally.

This chapter therefore continues by presenting results from a more comprehensive two austral summer season analysis. The chapter will focus on the land and ocean surface moisture sources identified by the Lagrangian model and relate these to characteristic synoptic circulation states. The subsequent chapter 4 will present the moisture sources identified along the analysis domain boundaries.

### 3.1 Description of experiment

The computational cost of the combined RCM and Lagrangian model is fairly large. In particular, because of the serial processing constraint of the Lagrangian model code (see Appendix A) the Lagrangian model could not exploit the same parallel computing environment available to the RCM. A further factor is the burden of archiving hourly 3-dimensional variables from the model. This is required in order to minimize the trajectory interpolation errors. The limited computational resources available constrained the period that could be simulated and analysed. Due in part to this constraint two summer austral summer seasons were simulated, choosing two seasons that represented markedly different seasonal modes within the range of natural variability. As discussed earlier, the focus is not to build a moisture transport climatology, but instead to gain a better insight how the land surface of the southern Africa

domain interacts with the moisture processes. For this purpose two contrasting seasons are adequate to explore this fundamental question.

In selecting which two seasons to use a number of seasons were considered. The selection is not very critical to the study, but it was considered potentially informative to explore two contrasting modes. Very dry seasons were avoided due to the small number of rain events that occur which would significantly reduce the total number of rain events simulated and hence the range of moisture source regions. Very wet seasons were also avoided as it is quite likely that such seasons are atypical of the region. Many wet seasons are wet because of one or two very strong events.

The intent was to select seasons with some variation in rainfall but that fall within the range of relatively normal years and hence the dynamics and moisture sources identified would potentially be more representative of the general regional climate. It is also critical to note that what is of interest is the RCM rainfall, not the actual observed rainfall, as it is the RCM rainfall (and other variables) that drives the Lagrangian model. The two seasons finally selected were the 1988/9 season and the 1991/2 season with the 1988/9 season being generally a moderately wet season while 1991/2 season was moderately dry in terms of the RCM simulated rainfall. RCM monthly rainfall totals for the target domains are illustrated in Figure 3.2 where the differences between the two seasons can be observed.

While the analysis period is the December through February season, the simulations were run for four months beginning in November. This is for two important reasons. The first was in order to include November as an RCM model spin up period. Model spin up refers to the period during which the interior state of the model reaches a dynamic equilibrium with the boundary forcing. While the model interior is initialised with an atmospheric state that is consistent with the boundary conditions in the GCM, this state may not be consistent within the RCM due to differences in topography as well as different representations of the atmospheric physics. Other fields such as soil moisture and temperature also take time to equilibrate with the boundary forcing fields. While atmospheric spin up for an RCM is typically only a few days, the land surface spin up is much longer due to the slow response of deep soil moisture and temperature. A single month spin up will allow the near surface simulated soil layers to reach some level of equilibrium and hence is adequate for this study.

The second reason for including November was to allow the backward trajectory tracking to continue backwards in time into November for rainfall events at the start of December.

The model configurations, both of the RCM and the Lagrangian model, are identical to the setup described in Chapter 2. Four precipitation target domains are defined and are shown in Figure 3.1. The locations of the target domains were selected in order to cover the summer rainfall area of South Africa while also covering the range of climates from the relatively dry southern central area to the relatively wet eastern area. The first three domains extend in a north-south axis through the center of South Africa in order to cover the range of moisture sources as the climate varies from more temperate to more tropical from south to north. The eastern domain (SA4) was selected in order to explore the moisture sources for an area closer to the Indian Ocean.

The RCM output fields are archived at an hourly time step, the Lagrangian model is run at a 15 minute time step with hourly archives of Lagrangian moisture fields as well as attributed source fields at both the land and ocean surfaces as well as the RCM boundary planes.

## 3.2 Presentation of results

As described in Chapter 2, the Lagrangian model produces both surface maps and RCM boundary maps of moisture sources for a given target precipitation domain. In this chapter, only the surface maps will be considered though the

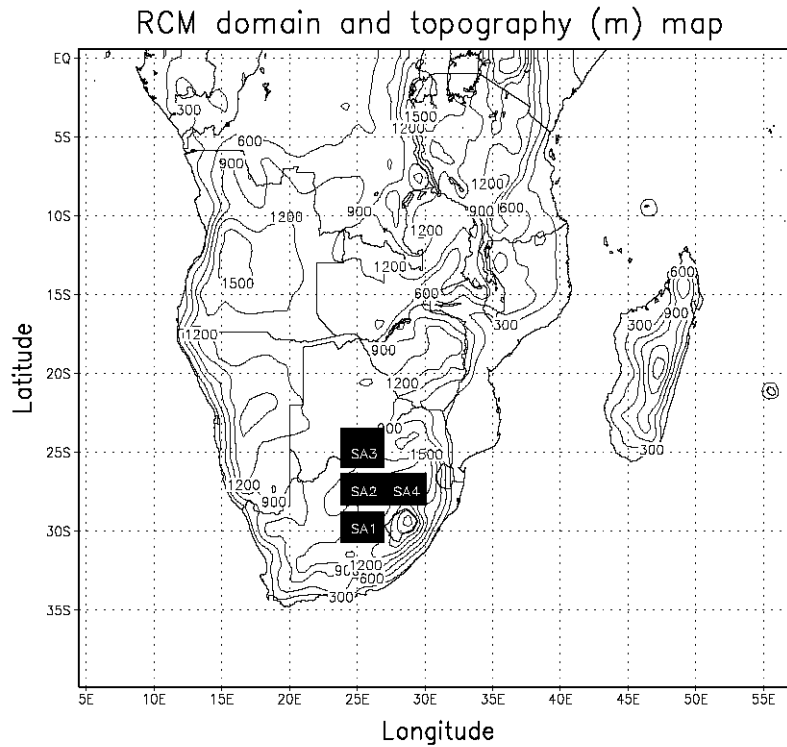


Figure 3.1: RCM domain map showing topography contours (meters) and the four analysis target domain, SA1, SA2, SA3 and SA4

magnitudes of the surface contributions are described in the context of the RCM boundary sources. The moisture source maps are archived at an hourly time step and are referenced with respect to the time of the target precipitation hour. Each map therefore represents the complete aggregated moisture source for each hour of target precipitation within the target domain. This aggregation method was selected in order to allow a detailed analysis of small time scale events. However, the compromise is that the maps do not represent a time synchronous picture of evaporation. The result is that while we can see where the moisture for an event was sourced from, we don't know exactly when it was sourced. While it would be possible to archive two sets of maps, one referenced to real time and one referenced to the target event time, at the moment the model is unable to do this due to computational memory constraints.

The moisture source maps represent that total mass of moisture contributed by an RCM grid box to the total precipitation within the target domain. In order to obtain a value in units of  $kg.m^{-2}$  we would need to divide this mass by the area of the RCM grid box which in this case is  $(5 \times 10^4 m)^2 = 25 \times 10^8 m^2$ . However, as described in Chapter 2, the total mass in  $kg$  of moisture in the Lagrangian model is already scaled by the RCM grid resolution in order to reduce the magnitude of the values for plotting and analysis. In order to convert the Lagrangian moisture mass to a value per  $m^2$  it is necessary therefore only to divide again by  $5 \times 10^4$ . Finally, we need to divide by the number of grid cells within the target domain which for the domains in question is always 20 grid cells. The resultant source field units are  $kg.m^{-2}$  which is equivalent to mm and are therefore directly comparable with the RCM precipitation fields.

### 3.3 Seasonal Synoptic Anomalies

It is helpful to first investigate the seasonal synoptic anomalies as it provides a useful context in which to interpret and understand the boundary moisture results presented in the next section. The location and strength of boundary

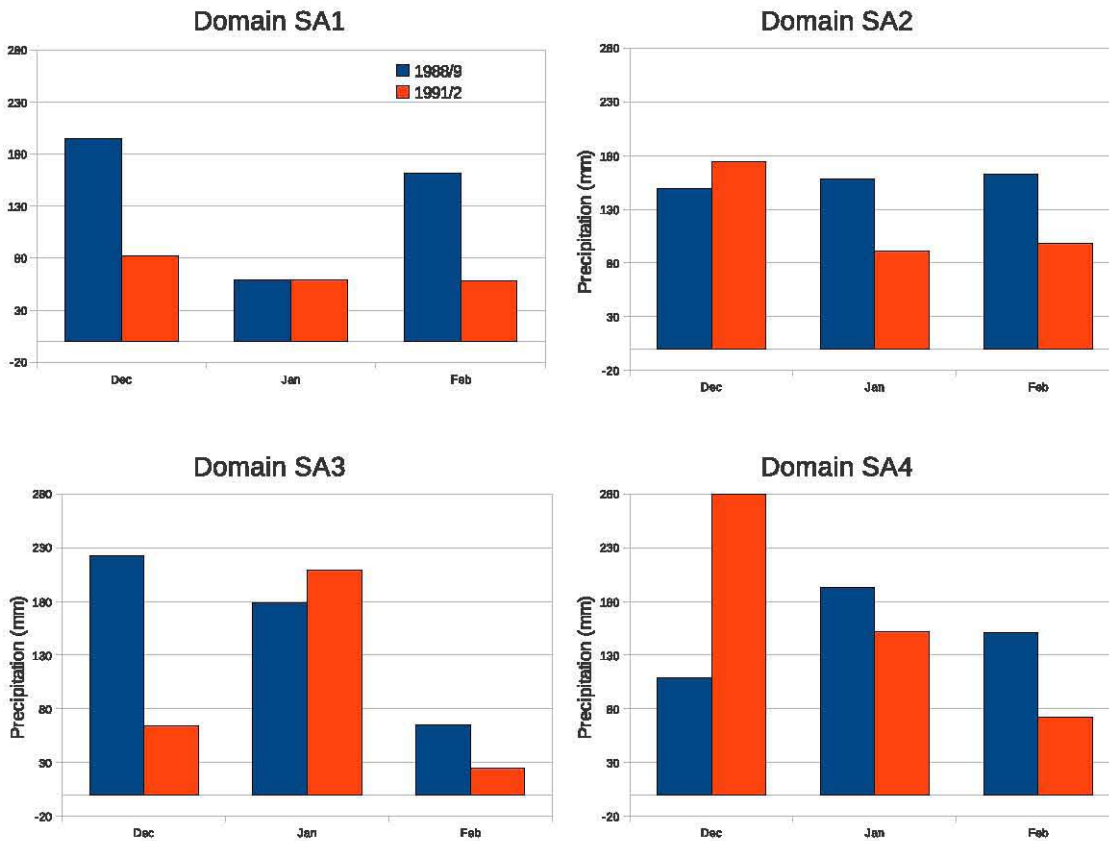


Figure 3.2: RCM simulated monthly total rainfall (mm) for each Lagrangian target domain for each season (1988/9 and 1991/2)

moisture sources will be largely controlled by the synoptic circulation fields and large scale moisture fields beyond the bounds of the RCM domain. Figure 3.2 shows the RCM simulated precipitation for December through to February (DJF) for both seasons and for each precipitation target domain. The 1991/92 season is generally drier for all target domains except for the domain SA4 which is actually slightly wetter. The dry February in 1992 which seems to be responsible for most the seasonal dryness is However, also present in domain SA4.

Figures 3.3 and 3.4 show the NCEP/NCAR re-analysis (Kalnay et al. [1996]) Sea Level Pressure (SLP) and 700hPa height anomaly fields for Dec, Jan and Feb 1988/9 and 1991/2 seasons respectively. The anomalies are calculated from the seasonal mean fields as we are interested in differences between months in the season rather than differences from the long term climatology. It is acknowledged that SLP and 700hPa height fields do not serve as a comprehensive analysis of the regional circulation and potential moisture transport. The intent of this section is to provide a general overview of the intra-seasonal circulation variations to serve as a backdrop for later results and analysis. While some attempt is made to relate circulation anomalies to precipitation anomalies this effort will of course be only partly successful. Indeed the proposed thesis is that regional precipitation is only partly dependent on the larger scale circulation and moisture transport as the regional land surface also plays an important role. Therefore, under the assumption of this thesis, any attempt to relate the larger scale circulation to the regional precipitation will only be partly successful. However, cognisance of the larger scale circulation anomalies does provide an important backdrop for later analysis.

The 1988/9 season starts off with anomalous high pressures to the south west and low pressures to the south east of the country in December. Anomalous high pressures over the southern Indian Ocean extend into the eastern sub-continent. December 1988 was fairly wet for target domains SA1, SA2 and SA3 but drier for SA4. It is possible that a northerly shift in the South Indian High Pressure (SIHP) system resulted in a more northerly flow of moisture into the sub-continent while the anomalous cyclonic pattern to the south east reduced the normal onshore flow of

moisture feeding SA4.

January 1989 shows much weaker anomalies but notably the south western high pressure anomaly and southerly eastern low anomaly have switched around. Domain SA1 is dry during this month which would agree with a reduction of ridging SAHP systems feeding moisture into the southern parts of South Africa. The other three target domains show fairly normal rainfall.

February 1989 shows a strong positive pressure anomaly to the south east and slight low pressure anomaly over the sub-continent. Interestingly, domain SA3 is the only domain showing dry conditions during this month. A low continental pressure anomaly would suggest enhanced continental convergence. However, the southerly shift in the SIHP could shift the flow of moisture from the Indian Ocean further south and so deprive the northerly SA3 domain.

The anomalies for the 1991/2 season however, show some strong variations, mostly in the region of SWIO high pressure system and to some extent in the SAHP system. In December we see a negative anomaly in both pressure systems with a slight positive anomaly over most the sub-continent and into the south Atlantic. This month is quite dry for SA1 and SA3 but normal for SA2 and actually quite wet for SA4. Clearly a simplistic relationship with circulation anomalies does not explain the rainfall magnitudes. In January the SAHP anomaly has become positive while the SWIO pressure system remains negative and in fact the anomaly moves closer to the continent. Finally, in February the SWIO pressure system has switched to a rather strong positive anomaly indicating a southerly shift in the SWIO high pressure system. Meanwhile the SAHP is weakly negative. This month is generally dry to very dry across all domains which could be related to the southern shift in the south Indian high pressure.

### 3.4 Results

Tables 3.1 and 3.2 summarise the monthly source contributions of each of the major source areas (land, ocean and RCM boundaries), for each month, for each of the two seasons respectively. RCM totals are also included for reference. The RCM precipitation values were discussed in chapter 2 where it was discussed that the RCM produces more rainfall than observations while the Lagrangian precipitation diagnosis under estimates precipitation relative to the RCM. Generally the Lagrangian precipitation variations through the season match those of the RCM though for some months there is some discrepancy. A number of possible explanations for the discrepancy were discussed in section 2.5 including miss-diagnosis of rainfall processes. One further possibility is that the Lagrangian model does not consider local precipitation recycling within the target domain. Such recycling would produce rainfall in the RCM but would not necessarily be diagnosed as rainfall by the Lagrangian model. However, given the intentionally relatively small sizes of the target domains it is not expected that significant precipitation recycling is occurring within the target domains and so this factor should be fairly small in comparison to other factors described in section 2.5.

In this chapter we will focus on the land and ocean based moisture sources which the above summary identifies as potentially significant sources of moisture for all target domains. The land surface is diagnosed to contribute between 26% and 41% of precipitated moisture depending on the location and the season, while the regional ocean surface contributes between 9% and 21%. In some months the combined regional ocean and land contribution can be as high as 70%.

Figures 3.5 and 3.6 show the corresponding spatial distribution of the land sources while Figures 3.15 and 3.16 show the corresponding spatial distribution of the ocean sources for each month of the DJF season, for each of the target domains and for each season respectively. We can see how the values in Tables 1 and 2 relate to the spatial patterns as well as the seasonal variation in source distribution for the different target domains.

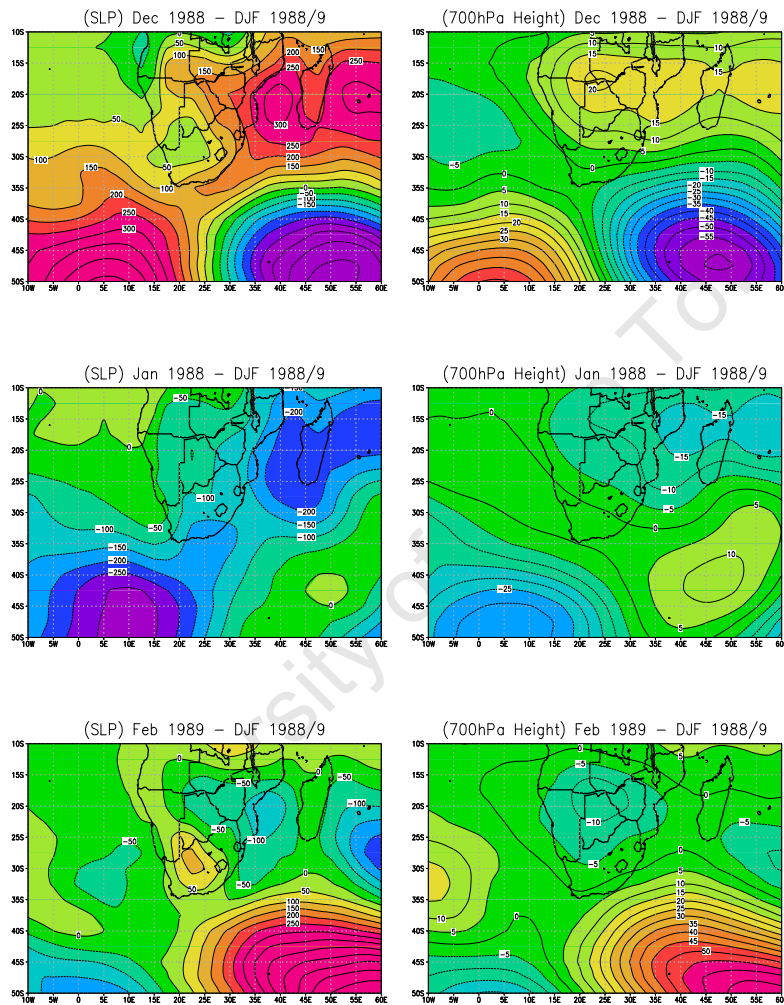


Figure 3.3: Dec, Jan and Feb SLP (Pa) and 700 hPa geopotential height (m) anomaly fields for 1988/9 season. Anomalies calculated from Dec-Feb 1988/9 seasonal mean.

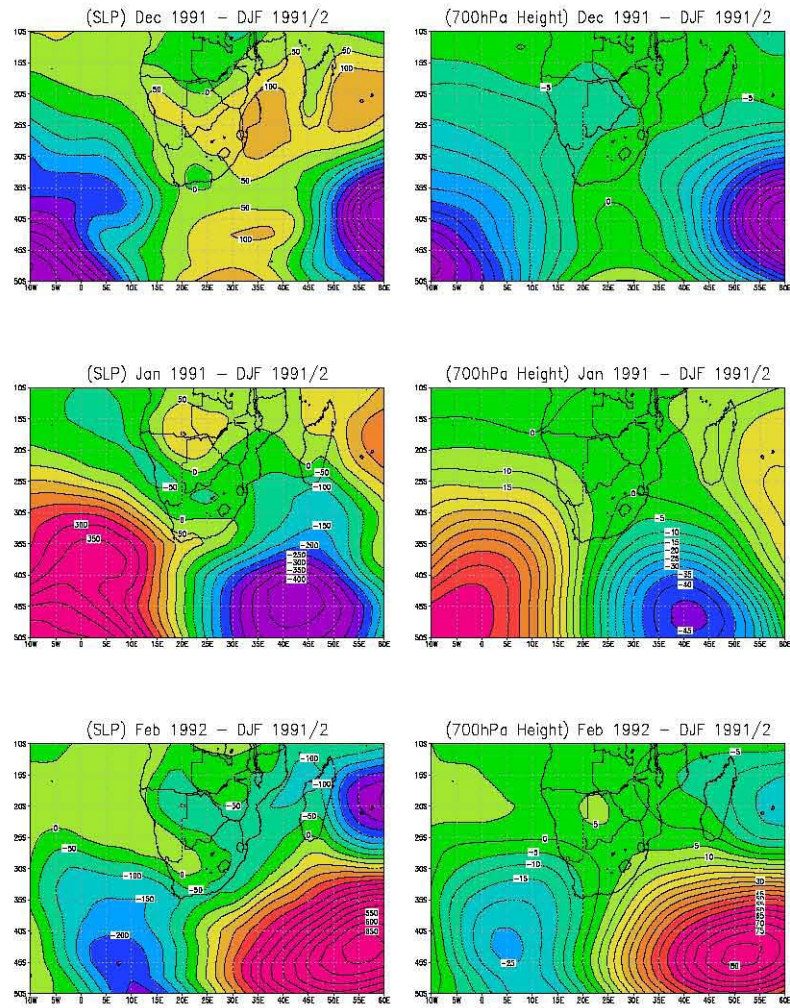


Figure 3.4: Dec, Jan and Feb SLP (Pa) and 700 hPa geopotential height (m) anomaly fields for 1991/2 season. Anomalies calculated from Dec-Feb 1991/2 seasonal mean.

SA1	Land	Ocean	North	South	West	East	Total	RCM Precip.
Dec	29 (38%)	11 (15%)	2 (3%)	11 (15%)	18 (24%)	4 (5%)	76	195
Jan	21 (40%)	7 (14%)	1 (1%)	10 (20%)	10 (20%)	3 (6%)	53	59
Feb	25 (35%)	10 (13%)	2 (2%)	14 (19%)	16 (22%)	6 (9%)	72	162
SA2	Land	Ocean	North	South	West	East	Total	RCM Precip.
Dec	29 (41%)	11 (15%)	5 (7%)	7 (9%)	13 (18%)	7 (9%)	72	149.41
Jan	25 (39%)	12 (18%)	1 (2%)	8 (13%)	9 (14%)	9 (14%)	63	157.93
Feb	21 (39%)	7 (13%)	2 (3%)	8 (14%)	10 (18%)	7 (12%)	54	162.59
SA3	Land	Ocean	North	South	West	East	Total	RCM Precip.
Dec	51 (40%)	23 (18%)	14 (11%)	11 (8%)	11 (9%)	18 (14%)	128	222.87
Jan	34 (41%)	13 (15%)	4 (5%)	8 (10%)	11 (13%)	13 (16%)	84	178.41
Feb	10 (26%)	5 (13%)	1 (4%)	4 (10%)	3 (9%)	15 (39%)	38	64.79
SA4	Land	Ocean	North	South	West	East	Total	RCM Precip.
Dec	25 (38%)	12 (18%)	3 (4%)	11 (16%)	11 (17%)	5 (8%)	67	108.93
Jan	30 (37%)	17 (21%)	1 (1%)	13 (15%)	7 (9%)	13 (16%)	81	193.18
Feb	26 (36%)	14 (19%)	2 (3%)	11 (15%)	4 (6%)	16 (22%)	73	150.99

Table 3.1: Attributed source moisture (mm) for 1988/9 DJF season for each target domain. Percentage values are the fraction of total source moisture. RCM precipitation totals (mm) are included for comparison.

SA1	Land	Ocean	North	South	West	East	Total	RCM Precip.
Dec	26 (34%)	12 (16%)	0 (0%)	10 (13%)	21 (28%)	6 (8%)	75	82
Jan	14 (29%)	6 (12%)	0 (1%)	14 (30%)	13 (26%)	1 (2%)	48	58
Feb	20 (39%)	5 (9%)	0 (0%)	3 (6%)	14 (27%)	10 (19%)	51	58
SA2	Land	Ocean	North	South	West	East	Total	RCM Precip.
Dec	26 (31%)	15 (17%)	0 (0%)	12 (14%)	24 (29%)	7 (8%)	84	174
Jan	19 (35%)	7 (12%)	1 (2%)	14 (26%)	12 (22%)	2 (3%)	54	91
Feb	12 (41%)	3 (9%)	0 (0%)	1 (5%)	6 (22%)	7 (23%)	29	97
SA3	Land	Ocean	North	South	West	East	Total	RCM Precip.
Dec	18 (33%)	10 (19%)	0 (1%)	8 (15%)	12 (23%)	5 (10%)	54	63
Jan	51 (37%)	25 (18%)	4 (3%)	29 (21%)	21 (15%)	8 (6%)	137	209
Feb	9 (36%)	2 (10%)	0 (1%)	1 (4%)	5 (21%)	7 (28%)	25	24
SA4	Land	Ocean	North	South	West	East	Total	RCM Precip.
Dec	35 (35%)	22 (21%)	0 (0%)	17 (16%)	19 (19%)	9 (9%)	102	282
Jan	24 (34%)	9 (12%)	0 (1%)	22 (31%)	15 (21%)	1 (2%)	71	151
Feb	8 (29%)	3 (13%)	0 (0%)	1 (5%)	5 (19%)	9 (35%)	27	72

Table 3.2: Attributed source moisture (mm) for 1991/2 DJF season for each target domain. Percentage values are the fraction of total source moisture. RCM precipitation totals (mm) are included for comparison.

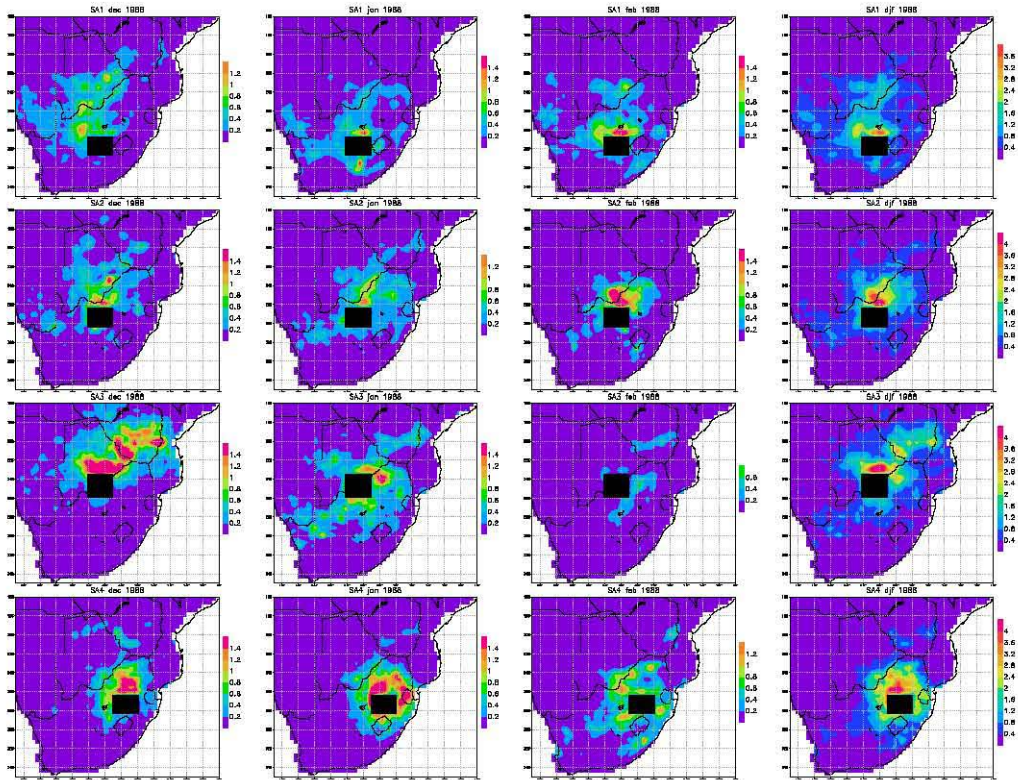


Figure 3.5: Total land surface attributed moisture source for Dec, Jan, Feb and total DJF periods for 1988/9 season, for target domains SA1, SA2, SA3 and SA4. Values are attributed moisture contribution in 10th's of a mm.

### 3.4.1 Land Surface

The land surface results presented in the previous figures show interesting intra-seasonal variations and inter-domain variations that can be at least partly related to the synoptic anomalies presented in figures 3.5 and 3.6 above. While only an initial exploration of the synoptic control of moisture sources, such an analysis does provide some first insights which are worth discussing. Each target domains monthly source maps are discussed in the following sections.

#### Target domain SA1

For target domain SA1, in December 1988, the source region is quite dominantly to the north of the domain. Through January and February this becomes less dominant. This likely relates to the shift in the latitude of the south Indian high pressure towards the south through the season. If the high pressure is further north then the strongest flow into the sub-continent will be further north possibly resulting in a more northerly track into the target domain. For the 1991/2 season the results are quite different with slightly northerly source regions in December and February and a very weak source attribution in January. The synoptic anomalies for January show a strong cyclonic anomaly to the south east of the country and an anti-cyclonic anomaly to the south west likely resulting in a the northerly flow into the target. Interestingly December and February show very similar land source regions while the synoptic anomalies are very different. This highlights the need to consider the results on an event basis rather than through time means. During a relatively dry month, the mean synoptic state will represent conditions associated with no rain and interpreting rainfall associations becomes very difficult.

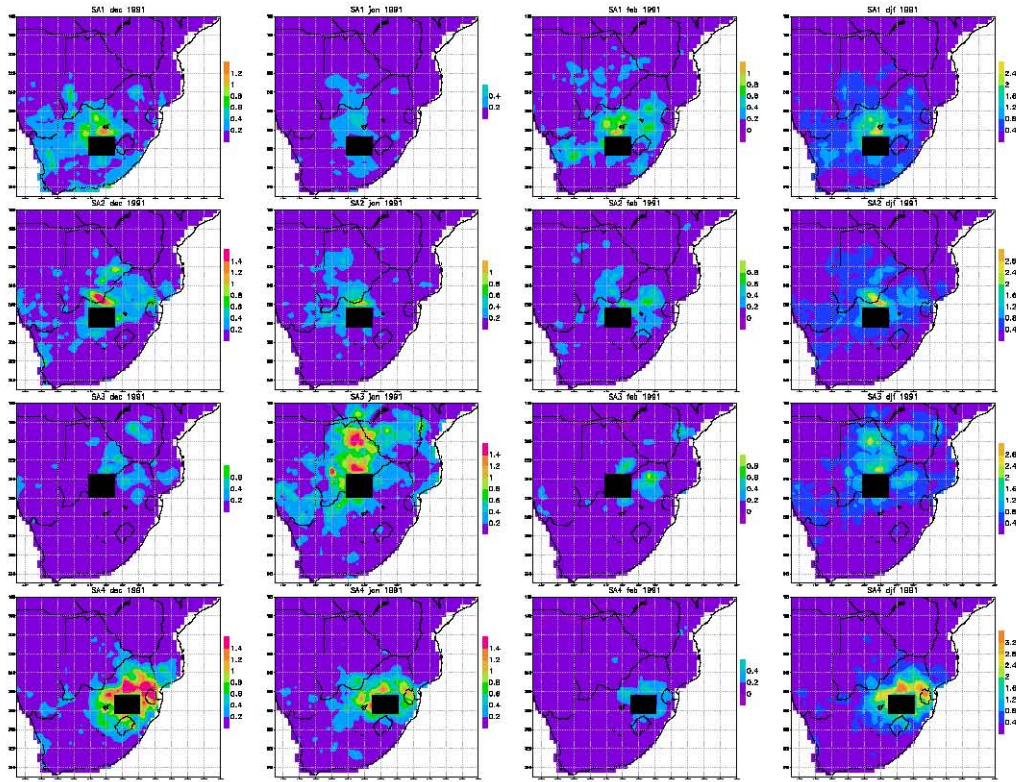


Figure 3.6: Total land surface attributed moisture source for Dec, Jan, Feb and total DJF periods for 1991/2 season, for target domains SA1, SA2, SA3 and SA4. Values are attributed moisture contribution in 10th's of a mm.

### Target domain SA2

Domain SA2 shows a predominantly northerly source region for all months in both seasons with the only real differences appearing in January and February 1992. In these two months the source attribution is much weaker and in February 1992 is more easterly. The weak absolute land surface attribution is reflected in Table 3.2. These two months are also fairly dry months in the RCM rainfall fields. Once again it is difficult to understand these results in the context of the synoptic anomalies. Generally the flow during rain events is from the north though the position and strength of the south Indian high pressure seems to determine, to some degree, the degree to which an easterly source is apparent.

### Target domain SA3

This target domain shows the greatest variation through the months, both in strength and pattern. While the source region is still dominantly northerly for most months, January 1988 shows a much more general source region and February in both seasons, as well as December 1991, show very weak source attribution. These weak source attributions can be related to low RCM rainfall during these months. However, it is important to note that the relative contribution of the land surface remains high as all other moisture sources are also weak during these months.

### Target domain SA4

This domain is interesting in that it is the only domain that is actually wetter during the 1991/2 season than the 1988/9 season in the RCM simulation. These wetter conditions can largely be attributed to December 1991 which shows the

highest monthly rainfall of any month in the two seasons. February 1992 is however, one of the driest months and this is evident in the source attribution field for that month. Generally however, the source region for this domain is northerly and easterly with some small westerly and southerly features in certain months.

### Land surface attributed source magnitude

The most interesting and striking feature of the land surface source is its relative magnitude. As discussed in Chapter 1, other estimates of precipitation recycling suggest that only at most 20% of precipitation is recycled in this region Trenberth [1999a]. The results presented here are not directly comparable to the recycling ratios as computed by Trenberth and others. However, given that the spatial scale of analysis in Trenberth's work is 1000km and the scale of the African sub-continent is on the order of 1500km, it would suggest that the land surface is not being diagnosed as a significant source of moisture in the recycling analysis.

Previous regional moisture transport analyses suggest that most moisture is sourced from outside the region (D'Abreton and Tyson [1995, 1996]) and arrive in the region at altitudes between 800hPa and 700hPa. The results presented here however, suggest that the land surface potentially plays a very significant role as a moisture source under specific synoptic modes. In order to understand this role better we need to examine the results in more detail. We shall do this by focusing on the 1988/9 season alone in order to simplify the analysis. Being a generally wetter season, the 1988/9 season offers more precipitation events from which to draw examples.

The source attribution coefficient is described in Chapter 2. It is used to decrease the contribution of upstream evaporative events due to upstream precipitation events. The attribution coefficient is output as a diagnostic variable by the Lagrangian model and can be used to explore the rate at which evaporative sources become less important as we move away from the precipitation target domain. Figure 3.7 shows the mean attribution coefficient for each of the target domains for the DJF season of 1988/9. The attribution coefficient initializes at unity at the precipitation target domain and tends towards zero as precipitation events intervene in the transport of moisture. It must be noted that the attribution fractions on the boundaries of the target domains is often less than one. This is caused by recirculation of moisture trajectories back across the domain which introduces attribution coefficients of less than one into the seasonal mean values along these borders.

We can see that for all the target domains the coefficient decreases fairly rapidly as we move away from the domain and then less rapidly further away. This is not unexpected as the likelihood of precipitation occurring immediately adjacent to the target domain is always high. Precipitation events are not spatially constrained to the target domain and in the vast majority of cases will extend beyond the boundaries of the target domain. As the Lagrangian parcel moves further away from the target domain the chance of encountering more precipitation events declines and the probability tends towards the general seasonal probability of rainfall in the greater region. We can therefore expect a more rapid decline in the attribution coefficient near the target domain.

The importance of this attribution coefficient is quite significant as not only does it modify the attributed contribution of upstream surface evaporative sources, but it also modifies the attributed contribution of the RCM boundary sources. We can see from figure 3.7 that as we approach the RCM boundaries the attribution coefficient tends to very low values. The regional boundaries may well provide a very significant amount of moisture into the region, however, a large proportion of that moisture falls as precipitation prior to reaching our specific precipitation target regions and more proximate moisture sources appear to play a larger role.

At this point we must include one particular caveat that is introduced by the MM5 RCM. Analysis of the RCM performance (Tadross et al. [2006]) in the area shows that the MM5 model tends to produce too much rainfall in the tropics. While the analysis mentioned is limited to land areas due to lack of ocean based observations, it is very likely that similar anomalies exist in the tropical Indian Ocean north of Madagascar. If this is the case then it is also quite likely

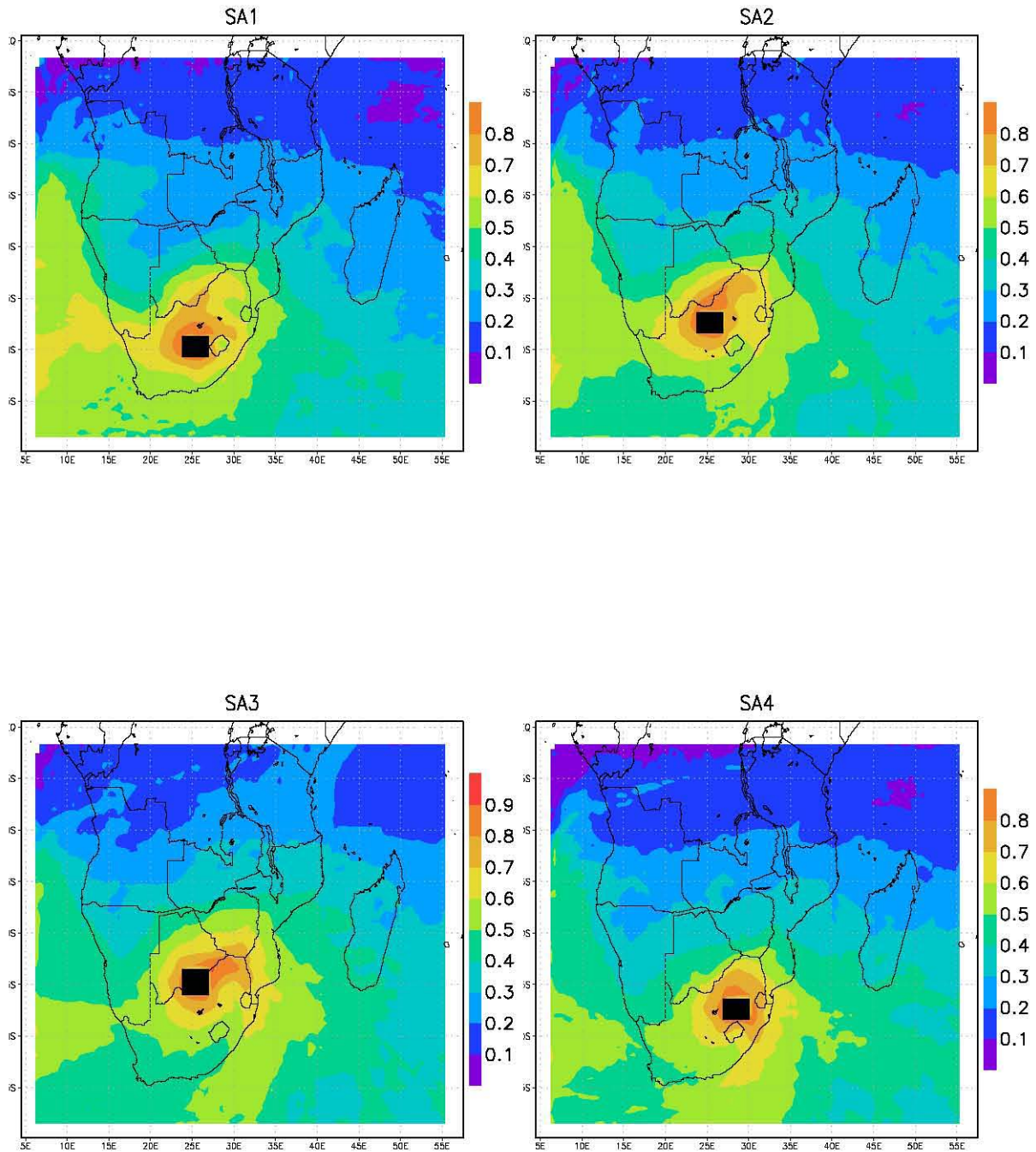


Figure 3.7: Seasonal mean attribution coefficient for all domains for 1998/9 season. Magnitudes are unitless ranging between 0 and 1.

that the Lagrangian moisture diagnostics will diagnose more precipitation than is realistic in this area and so decrease the attribution coefficient of any Lagrangian parcels traveling over this area. The result is that any moisture inflow from the RCM boundary north of Madagascar would be assigned a very low attribution. As will be seen in chapter 4, this section of the RCM boundary is indeed associated with very small amounts of source moisture. Whether the same effect is occurring in other areas is hard to determine, once again due to a lack of ocean based precipitation measurements.

As the attribution coefficient is tied to the diagnosis of precipitation in the Lagrangian model it is worth revisiting the conditions under which this occurs. The full methodology was described in Chapter 2 but some pertinent details are worth re-examining. Firstly, precipitation in the Lagrangian model is diagnosed when the parcel moisture increases (in a time reversed reference frame) by more than 1% of the total parcel moisture. Many moisture changes of less than 1% were observed during testing and are associated with spurious trajectory and interpolation errors. Secondly, precipitation can only be diagnosed if the RCM is producing precipitation in the underlying RCM grid cell at a rate greater than 0.2mm/hour. Thirdly, precipitation can only be diagnosed if the RCM grid cell rain liquid water field at the location and altitude of the parcel is non-zero. Again, this removes spurious diagnosis of precipitation. The rationale for each threshold is described in Chapter 2. It is felt that these conditions are fairly restrictive and should result in an under-diagnosis of precipitation rather than an over-diagnosis. As we are identifying moisture sources associated with precipitation events, over-estimation or false estimation of precipitation is more problematic than under-estimation. As already noted, the Lagrangian model does indeed diagnose less precipitation than the RCM.

While the restrictions imposed in the diagnosis of precipitation would seem to be sufficient to avoid miss diagnosis, another source of error must also be discussed. As was mentioned in Chapter 2, the RCM uses a parameterisation, in this case the Betts-Miller scheme (Betts [1993]), to approximate the effects of convective processes within the model grid cells. The vertical motions approximated by the parameterisations are not directly accessible to a loosely coupled model such as the Lagrangian model. It is therefore impossible for the trajectory integrations to incorporate these vertical motions. Likewise, the RCM boundary layer mixing parameterisation moves moisture within the boundary layer without reflecting such motion in the RCM wind fields. However, if we consider the scenario where moisture evaporated from the surface is mixed into the boundary layer and possibly lifted vertically through convection, the result would be to increase moisture at some layers above the surface. As long as the height of these higher layers falls below the top of the height of the top of the planetary boundary mixed layer, a Lagrangian parcel moving through these layers would experience a change in moisture content which would be diagnosed as an evaporative gain. While this assumption is not directly true, it is true that the moisture increase is associated with moisture at levels nearer the surface, some proportion of which would certainly be evaporatively sourced. The assumption being made is that Lagrangian parcel moisture increases are a result of surface evaporation, if not directly below the parcel then within a reasonably small distance of the parcel. The Lagrangian model restricts evaporative gains to below the top of the PBL as well as below 1000m above the surface, whichever condition is met first. Below 1000m it is considered likely that most significant Lagrangian moisture increases are related to evaporation. It must also be remembered that, within the limits of the trajectory numerics, in a Lagrangian framework advection of moisture is not a source of moisture changes as the trajectory parcels are moving with the advected air flow. As a result, the only means by which a parcels moisture content can be changed is either through evaporative gains, diffusion (which is slow), and unrepresented moisture transport such as mixing and convection.

We can therefore conclude that while it is impossible to verify the attribution coefficient, the Lagrangian model would seem to be fairly restrictive in its diagnosis of precipitation and hence the resultant attribution coefficient declines would seem to be reasonable. Additionally, the diagnosis of evaporation in the Lagrangian model is fairly restricted to avoid known problems with convection and boundary layer mixing. Rain re-evaporation is a concern that has been discussed in previous sections (2.5.2 and 2.5.4).

We are fairly confident that we are not over diagnosing precipitation or evaporation within the Lagrangian model. However, as this is such a critical component of the methodology and the results identify the land surface as such

Land Surface	Ocean Surface	RCM North Boundary	RCM South Boundary	RCM West Boundary	RCM East Boundary
30 (44%)	14 (20%)	3 (5%)	6 (8%)	6 (8%)	10 (14%)

Table 3.3: Relative moisture source amounts (mm) and percentages for 31st Dec through 1st Jan 1988/9

an important source, further exploration is necessary. This is done in the following section through a case study of a particular rainfall event. This allows us to examine the processes in question in great detail and calculate various moisture budgets and balances that must be satisfied if the results are to be considered plausible and, in particular, the concerns over rain re-evaporation can be limited though not fully resolved.

### Case study analysis

The purpose of the case study is to allow a detailed examination of the moisture budgets and balances for a single event and hence gain some confidence in the methodology. For this purpose the selection of a particular rainfall event is largely arbitrary though a fairly large, isolated event results in an easier and clearer analysis. We will therefore investigate the precipitation event between the 31st of December 1988 and 1st of January 1989, as simulated by the RCM. This event is one of the largest of the RCM simulated season with a well defined land surface attributed source region as determined by the Lagrangian model. We will focus on the precipitation target region SA3 as this region covers the most intense rainfall area. Figure 3.8 shows the RCM daily mean precipitation field for the period 28 Dec through to 2 Jan. Extensive rainfall can be seen across the region in a band extending from the north west through to the south east and into the SWIO region. Table 3.3 summaries the contributions from the various source (Land, Ocean and RCM boundaries) and reveals that the land surface is associated with a large 44% of all source moisture. Figure 3.9 shows the land based attributed source contributions for the 31st Dec (a) and the 1st Jan (b). On the 31st the source area extends to the north east of the target domain, almost reaching the Mozambique coastline. On the 1st the source has now also extended towards the west and north west of the target domain while still maintaining the easterly source area.

These moisture source regions corroborate with the RCM circulation fields which show a dominantly easterly flow into the target on the 31st and the transition to a westerly flow into the target on the 1st. However, the Lagrangian model informs us of not only the source direction of the moisture, which a standard moisture flux plot would do, but a detailed map of the evaporative moisture source region. Additionally we can track the movement of this moisture in 3-dimensional space through the Lagrangian parcel moisture field. This allows us to explore the vertical structure of the moisture feed. Figure 3.10(a) presents a vertical cross section of the Lagrangian parcel moisture field averaged between  $-22^{\circ}\text{S}$  and  $-25^{\circ}\text{S}$  for the 2 days prior to the event. Here we can see that the moisture approaching from the east tends towards the lower levels while that from the west approaches from higher levels. This is of course largely governed by topography. Figure 3.10(b) shows a longitudinal vertical profile averaged between longitudes  $24^{\circ}\text{E}$  to  $26^{\circ}\text{E}$  for the same period. The bulk of the Lagrangian moisture lies between the 850hPa and 700hPa levels. Previous studies (D'Abreton and Tyson [1995], Lyndsay ...) have isolate the 750hPa level as the most important moisture transport level for the sub-continent so these results do not strongly disagree with those studies.

Given the strong surface moisture source and the restrictions on the height of evaporative gains in the Lagrangian model we might have expected the Lagrangian results to describe a lower altitude moisture flow into the target region. However, clearly the surface sourced moisture is being lifted upwards before entering the target domain.

We can investigate this result further by performing a fairly crude bulk moisture budget analysis for this event. The total RCM evaporation over the diagnosed land surface source region for 3 days prior to the start of the rainfall events is integrated and a value of  $11 \times 10^6 T$  determined. The 3 day period is chosen due to the extent of the source region ( $\sim 1000\text{km}$ ) and the required transit time at the low level wind speeds of around 20km/h. This assumes no en-route losses due to upstream precipitation. To correct for this we can modify the evaporative flux values using

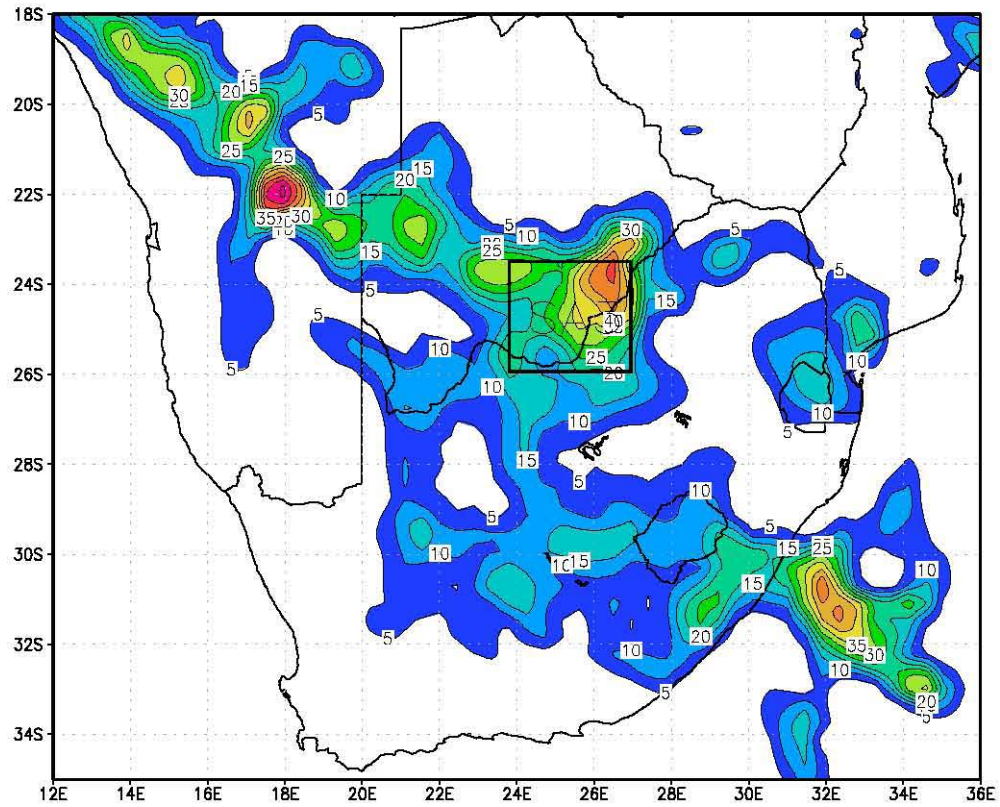


Figure 3.8: RCM Precipitation field, 28th Dec through to 2nd Jan 1988/9, (mm/day)

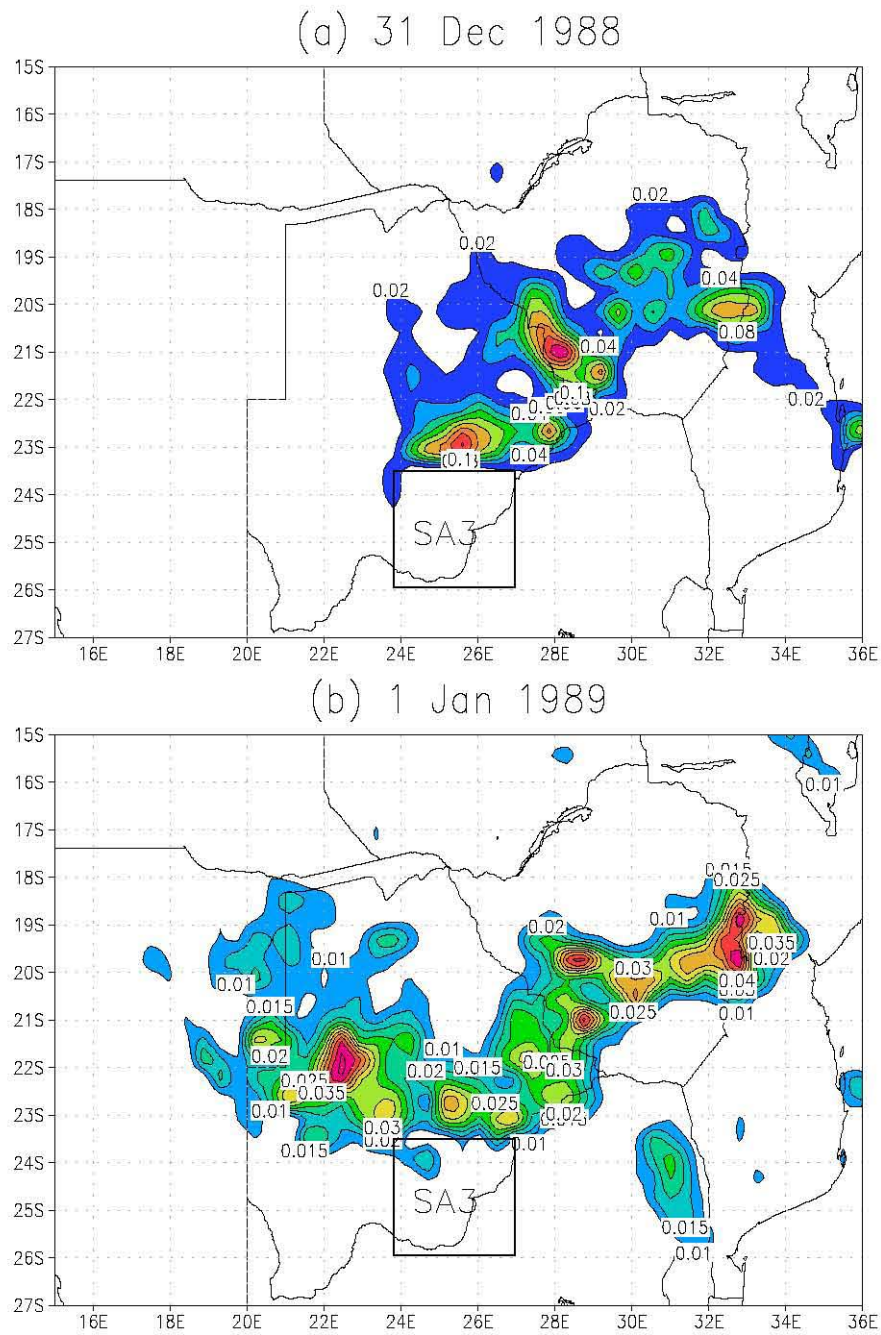


Figure 3.9: Land based source moisture (mm) for 31st Dec 1988 (a) and 1st Jan 1989 (b) feeding target domain SA3

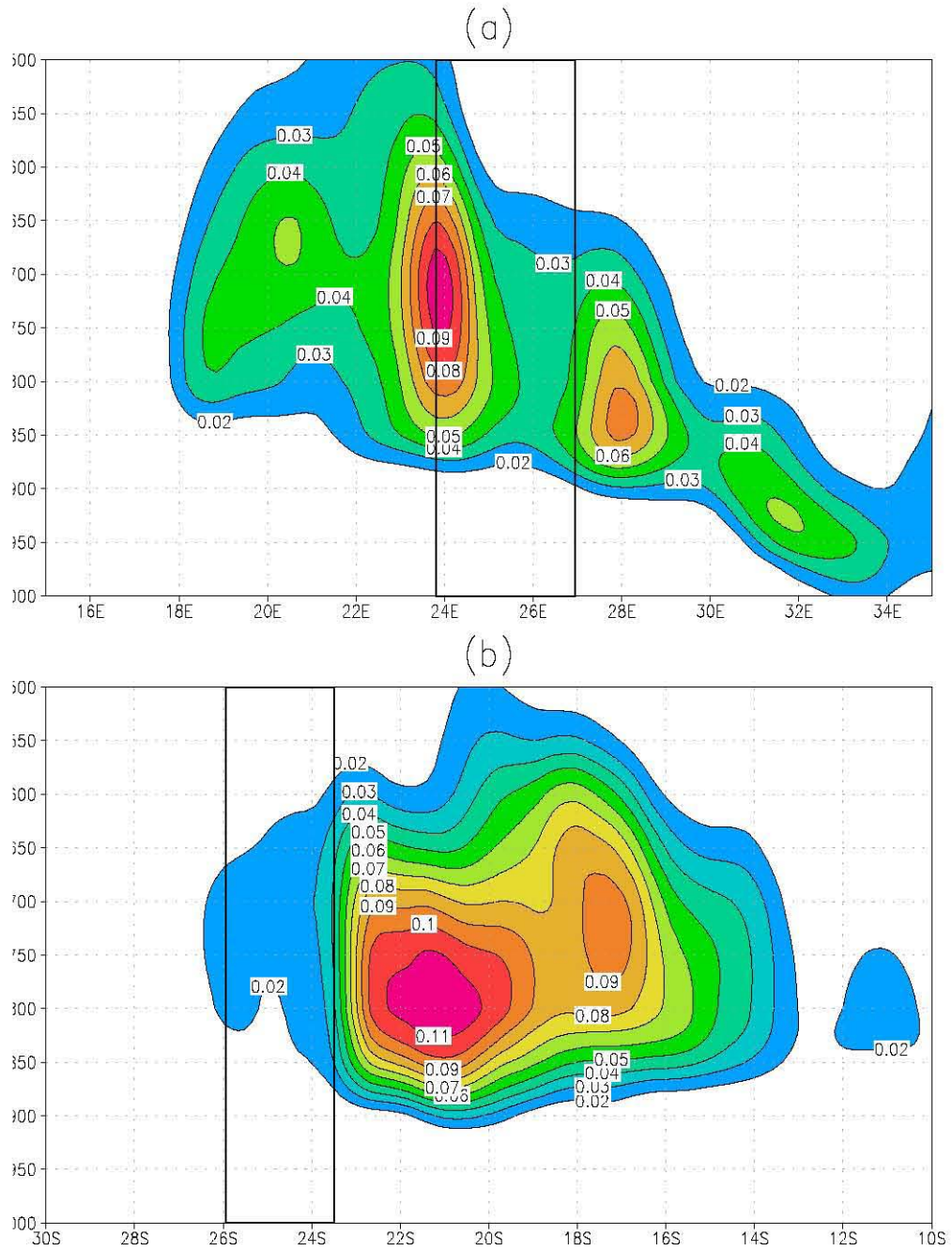


Figure 3.10: Vertical cross sections of Lagrangian parcel moisture (kg). (a) Latitudinal averaged between 25°S and 22°S, (b) Longitudinal averaged between 24°E and 26°E.

the Lagrangian model mean attribution coefficients for the same period. The attribution coefficient approximates the reduction in contribution of upstream evaporative sources due to en-route precipitation. The result is a reduced figure of  $6.7 \times 10^6 T$ . We can also use the precipitation values to calculate the total mass of moisture lost to the precipitation event over the whole target domain as  $10 \times 10^6 T$ . 44% of the total source moisture is attributed to the land surface which results in a figure of  $4.4 \times 10^6 T$  which is 65% of the diagnosed evaporative source moisture. We can conclude from this very rough estimate that the evaporative source region is certainly physically capable of providing the moisture to the precipitation it is being associated with. A more robust bulk moisture analysis would require an analysis of both the atmospheric inflow and outflow fluxes but due to the complexity of the source domain this analysis becomes extremely difficult.

### Land Source Spatial Patterns

The monthly mean land source maps presented in Figures 3.5 and 3.6 show that there is a great deal of variability in the spatial distribution of land surface moisture sources for each precipitation target domain. Hourly time scale source maps (not shown) reveal even greater variability. If we are to understand these distributions we need to consider what factors could be involved. Attributed moisture sources are identified by increases in parcel moisture as the Lagrangian parcel travels over a particular RCM surface grid box. Setting aside the caveats discussed in Chapter 2 regarding unresolved convective processes, moisture increases are assumed to be a function of evapotranspiration from the RCM grid box as well as boundary layer mixing. We can therefore assume that one of the factors governing the identification of land source regions is evapotranspiration rates. At the local scale, evaporation from the surface is a function of a number of variables. The Penman-Monteith equation is commonly used to estimate potential evapotranspiration and a similar equation is used in the PSU-NOAH LSM (Chen and Dudhia [2001a]) implemented in the MM5 RCM used in this study.

This equation requires a number of variables including specific humidity, incoming radiation, conductivity of the surface and conductivity of the air. Conductivity of the surface is a function of soil type and various vegetation parameters. Conductivity of the air is a function of boundary layer mixing which in turn is a function of wind speeds. Actual evaporation is a function of the potential evapotranspiration and soil moisture content.

A further complication is introduced by the diurnal cycle which strongly controls both evapotranspiration and convective precipitation. In most situations over the land surface, a Lagrangian parcel will only gain evapotranspired moisture during the warmer period of the day when evapotranspiration is high and boundary layer mixing is occurring. During the night existing atmospheric moisture will be advected as normal but little additional moisture will be gained. It is therefore clear that the time of day of the Lagrangian source parcel's transit of an area is an important factor in determining the source contribution of that area.

However, while evapotranspiration is clearly an important factor and the diurnal cycle needs to be considered, the distribution, if not the magnitude, of the source region is probably most strongly defined by the trajectories of the Lagrangian parcels and their proximity to the land surface at each location. The underlying land surface may be providing large amounts of evaporated moisture to the atmosphere but if the Lagrangian parcel is not close to the surface then this moisture will not contribute to the precipitation event. It is entirely possible, as we have already seen in the previous case study, that a distant land surface area could provide moisture while closer areas are not as involved.

We will therefore focus our attention not on the association between evapotranspiration and land source regions, but on regional synoptic conditions and land source regions. What are the synoptic conditions that produce particular moisture source patterns? A method is needed to associate synoptic conditions with particular moisture source patterns. However, the range and variety of moisture source patterns represented by the hourly time series is overwhelming and some means of reducing the scale of this datasets is required. Clustering allows us to do this by

generating a defined number of representative moisture source maps for which we can then generate composite circulation patterns and thereby answer the question posed. The clustering methodology is described next.

### Cluster Analysis

K-means clustering was selected as a suitable clustering methodology. The main advantage of this methodology is that it is unsupervised. This allows a large number of different clustering procedures to be performed. More complex methods such as Self Organising Maps (Kohonen [1982]) were considered, but the added features of such a method are not required in this application. K-means clustering provides an effective means of reducing the dimensionality of a dataset and it has been found that the resultant clustering solution is equivalent to the component vectors produced by a principle component analysis (Ding and He [2004]).

In order to reduce the size of the data records as well as remove some of the finer detail being passed to the clustering procedure, the resolution of the land surface source maps is reduced from 50km resolution to a 1° resolution. The full hourly time sequence of non-zero land surface based moisture source totals is generated for each precipitation target domain. Both season's data are combined at this step as we wish to define clusters that are common to both periods. This time series is then divided into subsets such that only those hours where the moisture source amount exceeds the 75th percentile value of the full series are selected. This selection is done in order to exclude smaller events that are not associated with particularly strong synoptic sequencing. The 75th percentile threshold is purely arbitrary but captures the majority of the total moisture source and produces clear clustering results.

These subsets of moisture source maps are passed through a k-means clustering procedure to produce five clusters per set of input source maps. The k-means clustering was configured to use uncentered Pearson correlation as the distance measure. Uncentered Pearson correlation is the same as regular Pearson correlation except that a value of zero is used for the sample mean. This is appropriate where the sample data vectors represent a deviation from a zero state and as such the uncentered correlation is equivalent to the cosine of the angle between the two samples. As the source distributions represent a deviation from the zero state (ie. no diagnosed source moisture), this was felt to be an appropriate distance measure. Comparisons with a regular Pearson correlation distance measure confirmed that the clustering solution is more clearly defined when using the uncentered method.

Cluster centers are found using the mean rather than the median of the surrounding vectors as this was found to produce much more distinct clusters in most cases. Source data vectors were also normalized before clustering to ensure that it is purely the spatial pattern that is being identified rather than the source magnitudes. The choice of five clusters was done after much experimentation across precipitation target domains. An algorithm was also implemented in which the optimal clustering solution was found by varying the number of clusters, however, the complexity of further analysis where each target domain has a different number of clusters did not warrant the slight advantage of more optimal clustering.

In order to produce maps representative of the final clusters, the source maps associated with each resultant cluster were averaged to produce a cluster composite source map. In this step, un-normalized source data is used rather than the normalized values used in the clustering procedure. The resultant composite maps therefore represent both pattern and mean magnitude but the cluster identification, as mentioned uses normalised values. This allows for the analysis of the clustered source maps based not only on pattern but also magnitude. It must be reiterated that the clustering and compositing procedure was performed on the combined data from both seasons. This allows the frequency of occurrence of clusters to be compared between the two seasons.

The resultant clustering allows each moisture source map to be associated with a single cluster. The mean of the source maps for each cluster represents an arch-typical moisture source map for that cluster. While the cluster maps are in themselves interesting they do not provide us with much more information about the moisture source

Name	Description
Z850	850hPa Height (m)
Z700	700hPa Height (m)
Z500	500hPa Height (m)
Q700	Specific Humidity at 700hPa (kg/kg)
U925	U-Wind component at 925hPa (m/s)
V925	V-Wind component at 925hPa (m/s)
U700	U-Wind component at 700hPa (m/s)
V700	V-Wind component at 700hPa (m/s)
SLP	Sea Level Pressure (hPa)

Table 3.4: NCEP Re-analysis variables used in synoptic sequence compositing

dynamics. The next step is therefore to associate synoptic states with each source map arch-type as represented by the clusters. This step is described next.

### Synoptic Analysis

As determined previously, the primary focus of the cluster analysis is to determine which synoptic states produce particular moisture source regions. This is done through a further compositing step where synoptic sequence patterns are composited for each cluster identified in the preceding cluster analysis. For each cluster, a subset of NCEP re-analysis variables (Table 3.4) is extracted for a number of lag time periods prior to and including the time of the target precipitation event. The variables were selected in order to represent both near surface and middle to upper tropospheric synoptics. The time lags used in this case were 0, 6, 12 and 24 hours. At the end of this step we therefore have N sets of synoptic variables for each lag time period for each cluster, where N is the number of hourly periods that map to the cluster. We can then produce a mean set of synoptic variables for each time lag period for each cluster.

Figures, 3.11, 3.12, 3.13 and 3.14 present the resultant 850hPa geopotential height synoptic sequencing for each cluster archetype. The Z850 field is used as this is most representative of circulation near the surface over the subcontinent. In the case study analysis previously described in chapter 2, we identified the 700hPa level as an important moisture transport level over the sub-continent which was noted to be in agreement with D'Abreton and Tyson [1996]. However, while the 700hPa circulation fields were produced for each cluster, as for the 850hPa, they do not add significantly to the analysis and so have not been included.

### Cluster Results

We can now integrate the cluster composites and the synoptic sequencing and gain a greater understanding of each archetype land source region identified by the clustering procedure. The time lagged composite synoptic sequences do not always show an obvious sequence that is easily interpretable. However, the sequence is presented in all cases for consistency. In many cases the synoptic sequencing provides insights into the source region that is not revealed by the zero hour synoptic state.

**Target SA1** Figure 3.11 show the clustering results for the domain SA1. The first two clusters identified for target domain SA1 are fairly similar, both showing a strong moisture source in fairly close proximity to the target domain. The first cluster shows a more westerly source than the second cluster which is dominantly to the north. The vertical profile composites both show a fairly low level source moisture feed into the target domain. However, the synoptic sequencing shows very small differences between the two sources. The SAHP system appears to be more intense

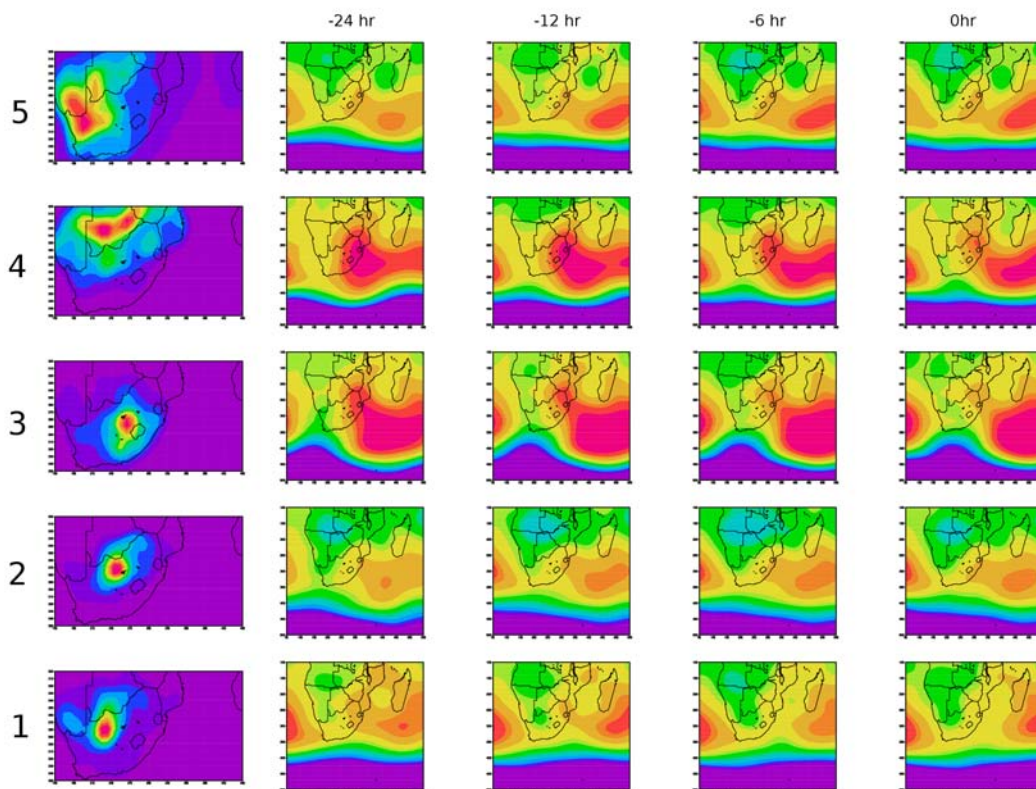


Figure 3.11: Target domain SA1 clustering results (column 1) and composite 850hPa sequences (-36 hour, -24 hours, -12 hours, 0 hours), clusters are ordered from 1 on the bottom row through to 5 on the top row.

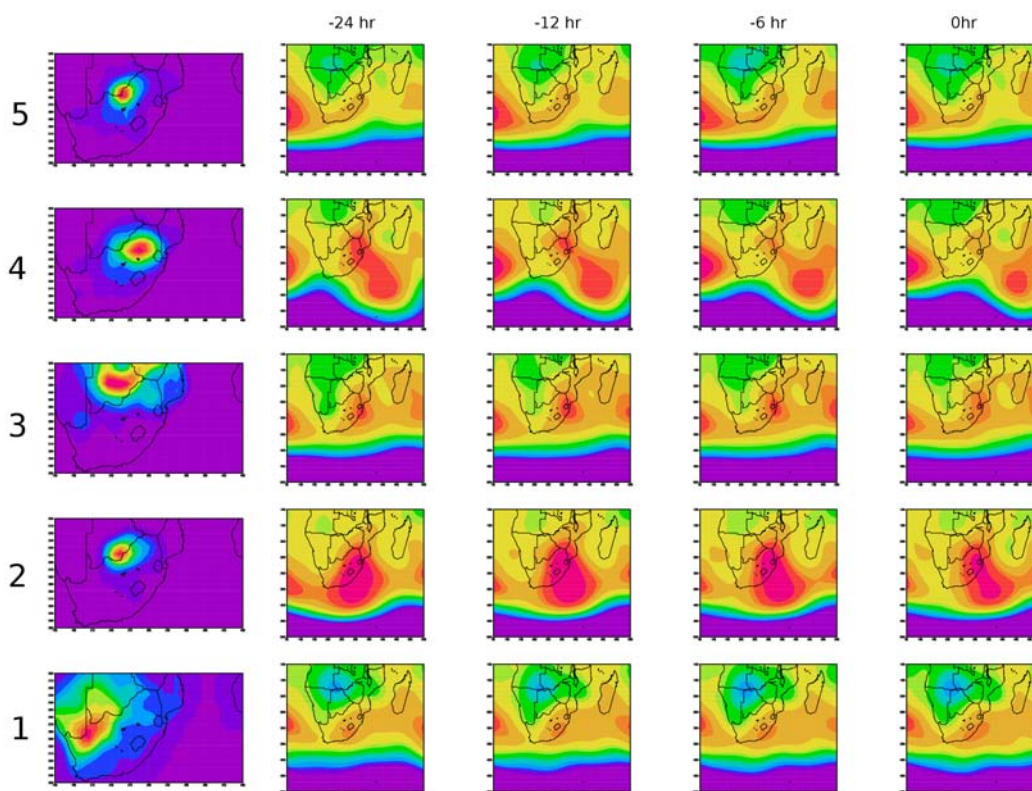


Figure 3.12: Target domain SA2 clustering results (column 1) and composite 850hPa synoptic sequences (-36 hour, -24 hours, -12 hours, 0 hours), clusters are ordered from 1 on the bottom row through to 5 on the top row.

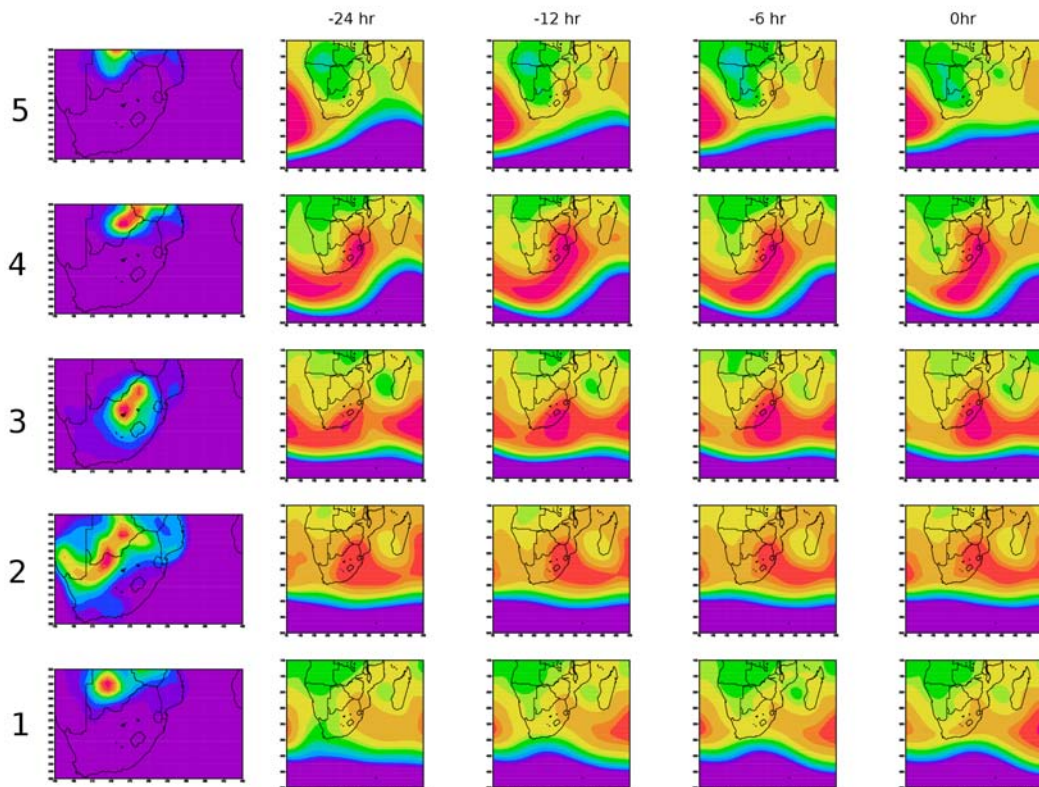


Figure 3.13: Target domain SA3 clustering results (column 1) and composite 850hPa sequences (-36 hour, -24 hours, -12 hours, 0 hours), clusters are ordered from 1 on the bottom row through to 5 on the top row.

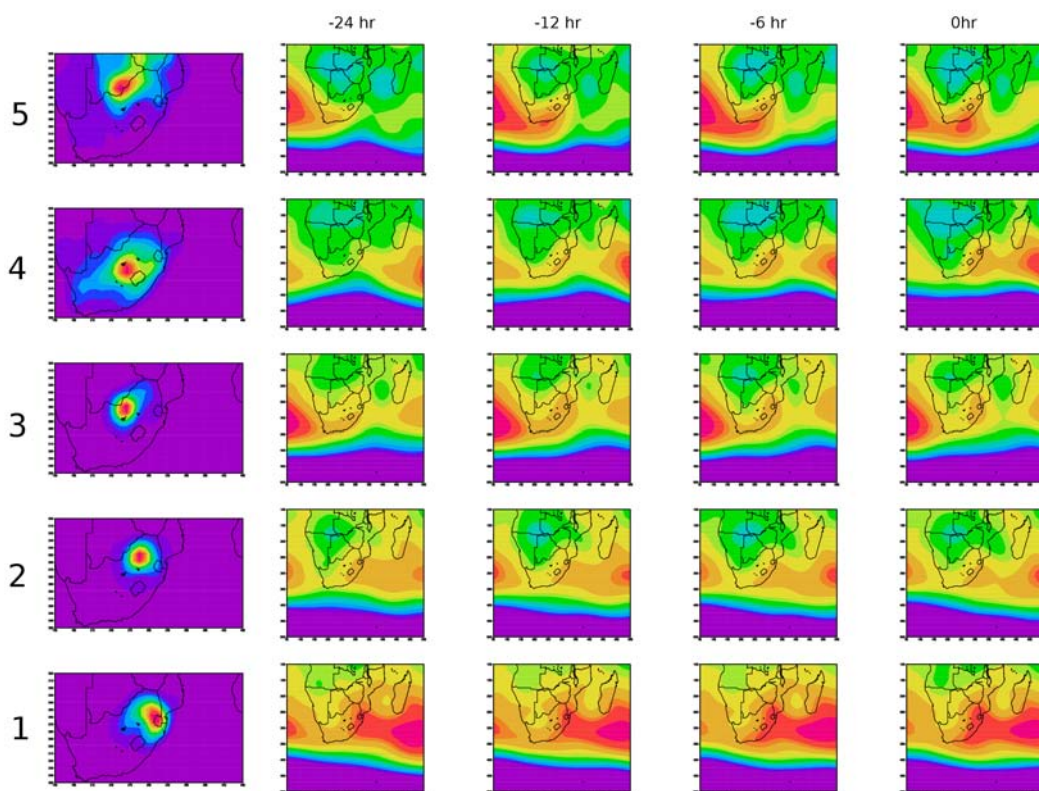


Figure 3.14: Target domain SA4 clustering results (column 1) and composite 850hPa sequences (-36 hour, -24 hours, -12 hours, 0 hours), clusters are ordered from 1 on the bottom row through to 5 on the top row.

for the first, more westerly cluster. Both synoptic sequences seem to suggest that a continental trough is driving moisture convergence over the continent. This trough appears to be deeper but more northerly in cluster two which is possibly the reason for the more northerly moisture source area.

The third cluster is located very close to the target domain. The domain box obscures the fact that a large part of the land source lies within the target domain. Within the Lagrangian model this can only occur if the moisture actually leaves the domain and then returns. Moisture sources are not attributed until the Lagrangian parcel has left the target domain. This suggests an interesting, very local, recycling of moisture and also reminds us that a source region in close proximity to the target region does not directly imply a direct flow of moisture from source to target. More detailed analysis of the actual Lagrangian trajectories, which as of writing are not retained by the Lagrangian model, would be required in order to determine the actual pathways taken between moisture source and target.

The synoptic sequencing for the third cluster shows a strong high pressure system intruding into the continent from the east and a mid-latitude trough approaching from the west at the 36 hour lag period in the 850hPa fields. Through progressively shorter lag periods the mid-latitude trough moves eastward across the south of the continent and the Indian high pressure system retreats. At the zero hour lag period, the sub-continent is largely dominated by the mid-latitude trough to the south though the SLP fields show a possible ridging of the SAHP system which could be responsible for the small amount of southerly flow and southerly moisture source observed in the cluster mean source field. Observation of such sequences in the daily moisture source fields (not reproducible in print) show that such synoptic sequences produce very complex developments of the moisture source areas as the wind direction changes very rapidly.

The last two clusters for this domain are of relatively small magnitude but are still quite interesting. Cluster number four indicates a very distant moisture source located largely over Botswana while cluster five represents a similarly distant source but located over the west of South Africa and into Namibia. The synoptic sequencing for cluster four is quite similar to that of cluster three but with a weaker mid-latitude influence. The 850hPa patterns suggest a strongly northerly flow towards the target domain with a progression from north westerly to north easterly as the high pressure system recedes. The synoptic sequence for cluster five shows very little mid-latitude influence and more tropical influence in the form of a continental trough developing through the period. As the trough develops the transport towards the target domain would progress from northerly through north-easterly and finally westerly resulting in the development of the moisture source pattern presented.

**Target SA2** Figure 3.12 shows this target domain to have quite a wide range of clustered source areas and the associated synoptic sequences are quite strongly differentiated. For cluster one, we see a similar pattern to that of cluster five of target SA1. A continental low develops through the time period resulting in a sequence of northerly, north-westerly and westerly flow into the target domain.

Cluster 2 shows a very distinct source region associated with a budding of the SAHP into the Indian Ocean. The resultant flow is clearly quite steady and strongly northerly into the target domain. The close proximity of the target domain suggests that the attribution coefficient is being degraded rapidly by adjacent rainfall events. Cluster 3 is similar but with a less intense high pressure system probably resulting in lower wind speeds and greater uplift. The source region is spatially separated from the target domain suggesting the precipitation is being drawn from a higher level and the source moisture is being lifted to this level prior to entering the target domain.

Cluster 5 is very interesting in that it shows an almost identical source region to cluster 2 and yet the synoptic sequencing is quite distinct. This suggests that the two clusters are actually quite distinct. Indeed, a time series of cluster occurrence shows that two clusters occur at quite distinct times during the period. It therefore seems that the hourly source regional maps contributing to each cluster are distinct enough to force the k-means clustering to identify them into two different clusters. The synoptic sequencing also seems to support the idea that the two clusters

represent distinct processes. Cluster 5 is being driven by a ridging SAHP system and a continental trough while cluster 2 is driven by the very distinctive budding SAHP.

**Target SA3** Cluster results for target domain SA3 show two interesting clusters in figure 3.13. Cluster two shows a small but widespread source to the south west of the target domain as well as to the north. This cluster represents the most commonly occurring source pattern across both seasons, largely occurring in January. The synoptics do represent fairly normal summer synoptics across the sub-continent with circulation largely dominated by the high pressure systems of the southern Indian and Atlantic oceans and very little mid-latitude influence. A continental trough lies across the west of the sub-continent. These synoptics in themselves do not explain the land source pattern. The large number of events that are associated with this source pattern will result in a very generalised synoptic sequencing hiding specific features that would provide clues as to the regional dynamics. It is possible that using more clusters would disaggregate this source pattern better. Further exploration of the events associated with this cluster would be required in order understand the regional dynamics involved.

Cluster five is the second interesting cluster showing a very distant source to the north but extending across an east to west band. The synoptics shows a mid-latitude trough located off the east coast of South Africa and deepening Angolan low pressure extending southwards into South Africa countering a strong SAHP to the west. Presumably the development of the Angolan low pressure results in moisture advection from the east coast initially and then southerly as the trough extends southwards.

Cluster four shows a similar pattern but located closer to the target domain. Synoptics are quite different to cluster five however, as they are dominated by an extensive ridging of the SAHP and a strong west coast trough. It is likely that the ridging SAHP would induce a more easterly flow into the target domain.

Cluster two shows a more westerly land source region and is associated with the passage of a mid-latitude trough to the south. Mid-latitude troughs seem to be generally associated with more westerly advection of moisture across the southern sub-continent.

Perhaps most interestingly for this target domain is the occurrence of what appears to “pulsing” of the moisture source. The pulsing is evident as areas of localised stronger source connected by areas of weaker source. This is most evident in cluster one, four and five. Given the large number of events that produce the mean source map it seems highly unlikely that this pulsing is a result of noise in the Lagrangian model. Rather, it points to two possibilities. The first refers back to the section on land source spatial patterns where the diurnal cycle of evapotranspiration is discussed. It is possible that, given similar rates of advection and the fact that convective rainfall typically occurs at similar times of the day, upstream sources will display a diurnal cycle signature. Given similar synoptic conditions and wind speeds, source parcels will typically pass over similar land areas during the peak of the diurnal cycle of evapotranspiration and boundary layer mixing. The result would look like the pulsing pattern that we observe in the source regions mentioned above.

The other possibility is that the high magnitude areas of the source regions actually represent areas of higher evapotranspiration. However, there seems to be little evidence of this in the latent heat flux fields of the RCM and no coherent underlying reason for the areas identified being consistently areas of higher evapotranspiration. The diurnal cycle explanation is indeed an intriguing one and should certainly be an area of further investigation. Interactions between diurnal cycles of evaporation, upstream precipitation, and target domain precipitation, must be extremely complex but could well be investigated using a model such as the one used here.

**Target SA4** Target domain SA4 lies towards the east side of South Africa. Clusters one, two and three in figure 3.14, represent easterly, northerly and westerly source regions respectively. Cluster one, associated with an easterly

source region is characterised by an intruding SWIO high pressure system which is clearly causing strong onshore flow along the north eastern coast of South Africa and the southern coast of Mozambique. This explains the easterly land surface source. Cluster two is similar except is dominated more by an Angolan low pressure system which results in more northerly flow into the domain. Cluster three shows a westerly source region and is dominated more by the South Atlantic High Pressure that ridges around the south of the continent. Again, it is difficult to explain the source region from the large scale dynamics. Clearly the RCM is simulating local scale dynamics that are producing a westerly flow. More exploration of the local scale dynamics would be required.

Clusters four and five represent the weakest magnitude source regions but interestingly are associated with quite well defined synoptics. Cluster four shows a south westerly source region and is associated with the passage of a mid-latitude system to the south of South Africa. It is assumed that the mid-latitude system produces westerly winds backing to southerly winds across the country as it passes which produce the land surface source pattern observed. Cluster five shows a spatially distant source largely located to the north west. The associated synoptics suggest the combination of a well defined ridging SAHP and easterly wave depression to the north.

### 3.4.2 Ocean Surface

The ocean surface analysis will follow a similar methodology to that of the land surface results presented above and so the methodology will not be described again. Referring again to Tables 1 and 2 we can see that the ocean surface is associated with between 8% and 21% of the total attributed source moisture across the domains and the two seasons. While not as strong a diagnosed source as the land source described above it is still a significant source in many cases. Figures 3.15 and 3.16 present the monthly mean ocean attributed source regions for each precipitation target domain for the 1988/9 and 1991/2 seasons respectively. There are a few interesting features worth noting from these results.

Referring again to Tables 1 and 2 we note that the monthly precipitation for the 1988/9 season is much more consistent than for the drier 1991/2 season. The spatial variability, expressed through the differences in target domain totals, is also smaller for the 1988/9 season. We can see the result of this in the moisture sources maps which show much higher consistency for the 1988/9 season than for the 1991/2 season.

While the precipitation target domain SA1 lies closest to the south coast of South Africa which is characterised by the warm Agulhas ocean current, this domain actually sources less moisture from the ocean than all the other domains except for domain SA4. In the 1988/9 season the dominant ocean source region for this domain is located off the southern coast of Mozambique with only a small tongue of attributed source extending down and along the south coast of South Africa. However, in the 1991/92 season the south coast of South Africa plays a much larger moisture source role with a tongue extending down the east and south coast. In particular, Dec 1988 and Dec 1991 show vastly different source regions.

Target domain SA2 is in close proximity to SA1 and so one would expect the source regions to be similar which indeed they are for most months. However, in December 1991 the source patterns are remarkably different suggesting some unique synoptic conditions which will explore in the section on synoptic sequencing.

Target domain SA3 is the furthest north and also generally has the highest diagnosed precipitation. The ocean source domain is again largely located off the southern coast of Mozambique but in the 1991/92 seasonal mean this source region extends extensively northwards up the Mozambique channel as far as 10°S. This is mostly a result of the diagnosed source region for January which is the wettest month in the season and shows an extensive coverage of the Mozambique channel towards the north.

Finally, target domain SA4, the eastern most target domain displays an attributed source region slightly further south than the other domains and with a tongue extending further into the SWIO. In the 1991/92 season the source region

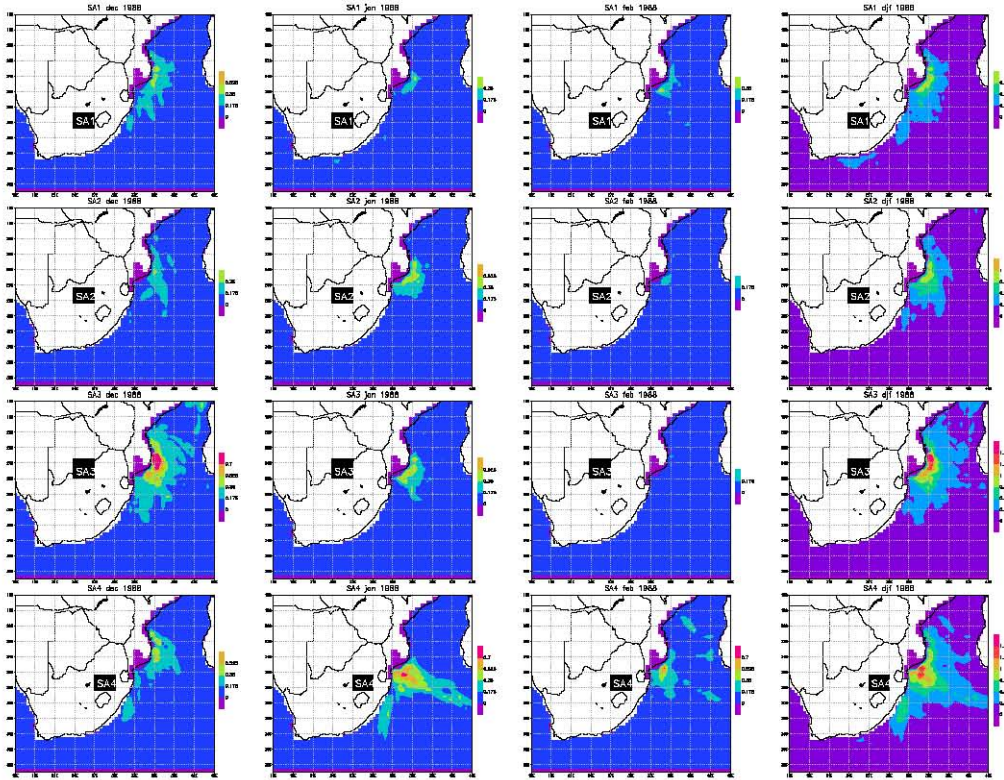


Figure 3.15: Total ocean surface attributed moisture source for Dec, Jan, Feb and total DJF periods for 1988/9 season, for target domains SA1, SA2, SA3 and SA4. Values are attributed moisture contribution in 10th's of a mm.

does also extend further down the South Africa coastline, though this occurs mainly in January. In December 1991 the source region extends quite far down the south coast of South Africa while the 1988/9 season is characterised by a strong tongue of moisture source into the SWIO.

### Cluster Analysis

The same clustering procedure as described above was applied to the ocean source regions for each precipitation target domain. Once again, a five member clustering was selected and only source magnitudes greater than the 75th percentile of all non-zero source values were included. However, longer lag periods were used for the synoptic sequence compositing. Longer lag periods of 0, 12, 24 and 36 hours were used. This is because the average time of travel from ocean sources to land precipitation targets is greater than for the land surface sources and so a longer period needs to be captured by the synoptic sequencing. Figures 3.17, 3.18, 3.19 and 3.20 present the resultant clusters along with 850hPa circulation fields. As with the land source clusters we can see that the cluster analysis has identified quite distinct clusters in most cases with only a few cases of near duplicate clusters occurring. Generally the clusters break the source region up into sections along the coastline from the south coast of South Africa up to the coast of Mozambique. There is a great deal of similarity between many of the clusters and so in the interests of space only the notably different clusters or synoptics will be discussed for each target domain.

**Target SA1** The most interesting cluster for target domain SA1 is the first cluster which shows a source region along the south coast of South Africa (figure 3.17). This is the only cluster across all domains that shows such a moisture source region. The associated synoptics show a class SAHP ridging scenario and we can assume that the moisture

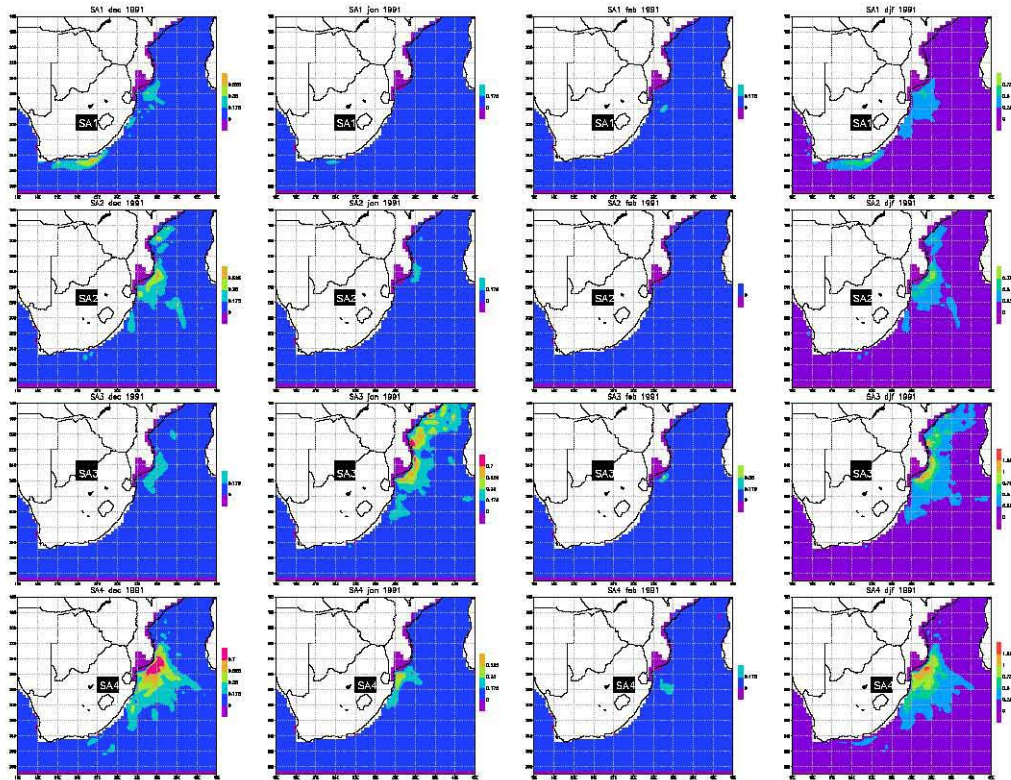


Figure 3.16: Total ocean surface attributed moisture source for Dec, Jan, Feb and total DJF periods for 1991/2 season, for target domains SA1, SA2, SA3 and SA4. Values are attributed moisture contribution in 10th's of a mm.

is largely advected directly inland as a result of the southerly winds as the high pressure ridges around. The synoptic sequence terminates with the SAHP partially ridged around the south of the country.

The remaining clusters all represent moisture source regions along the eastern coast of southern Africa with clusters two, three and four generally controlled by the positioning and intensity of the south Indian high pressure system. It seems that the further north west the high pressure intrudes the further north the Lagrangian back trajectories must travel before they reach the coast and the ocean moisture source.

**Target SA2** The most interesting cluster for this target domain is the fourth (figure 3.18). This shows an extensive arc of moisture source extending from the Mozambique coastline southwards towards the mid-latitudes. An analysis of the hourly Lagrangian parcel moisture fields shows (not reproducible in print) that this often occurs after the passage of a mid-latitude trough to the south. The wind backs from northerly to westerly and then southerly as the low pressure passes and cold dry air seems to gain moisture as it is advected northwards over the warm SWIO. It then takes quite a long time for the moisture to travel north, re-curve westward across Mozambique and then travel southwards into the target domain. The synoptic sequence lags period used here are probably not long enough to fully capture such a sequence but we can see the end of a mid-latitude low pressure passing through the eastern boundary of our synoptic domain.

**Target SA3** The most notable cluster for target domain SA3 is cluster two which shows an extremely northerly source within the Mozambique Channel (figure 3.19). This is quite distinct from many of the other clusters both in this target domain and the other target domains. The associated synoptics are also interesting in that they show a closed low pressure system over the southern Mozambique channel in the 850hPa field. It would seem as if this low

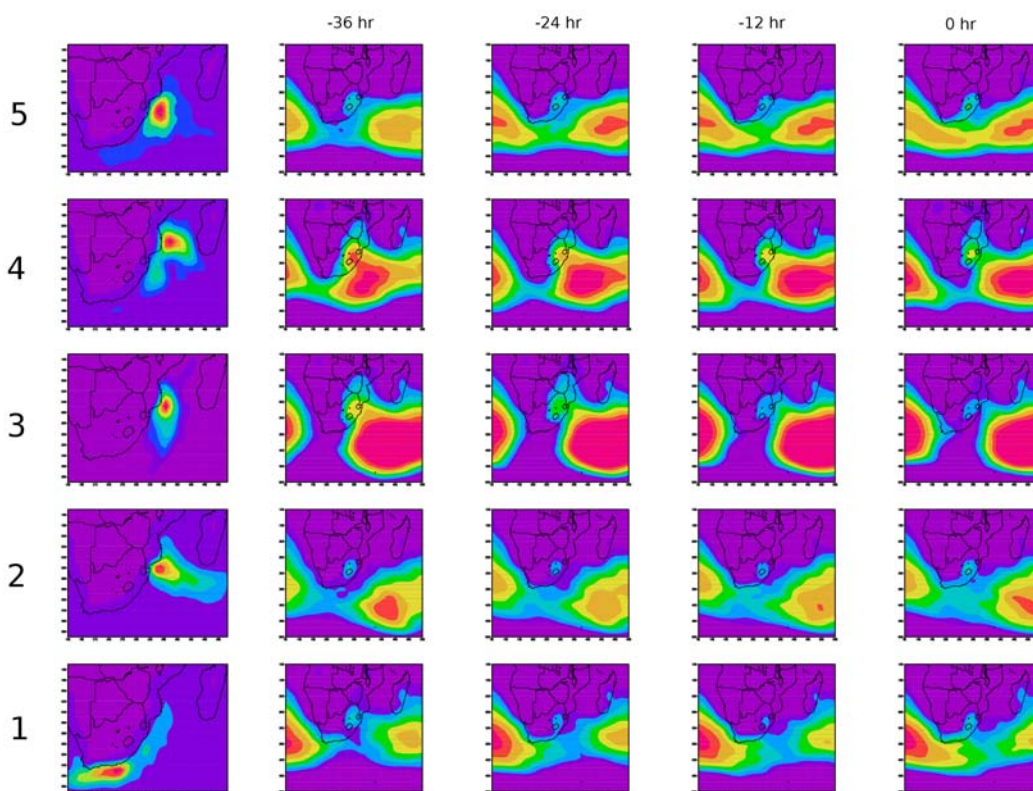


Figure 3.17: Target domain SA1 ocean source clustering results (column 1) and composite SLP sequences (-36 hour, -24 hours, -12 hours, 0 hours), clusters are ordered from 1 on the bottom row through to 5 on the top row.

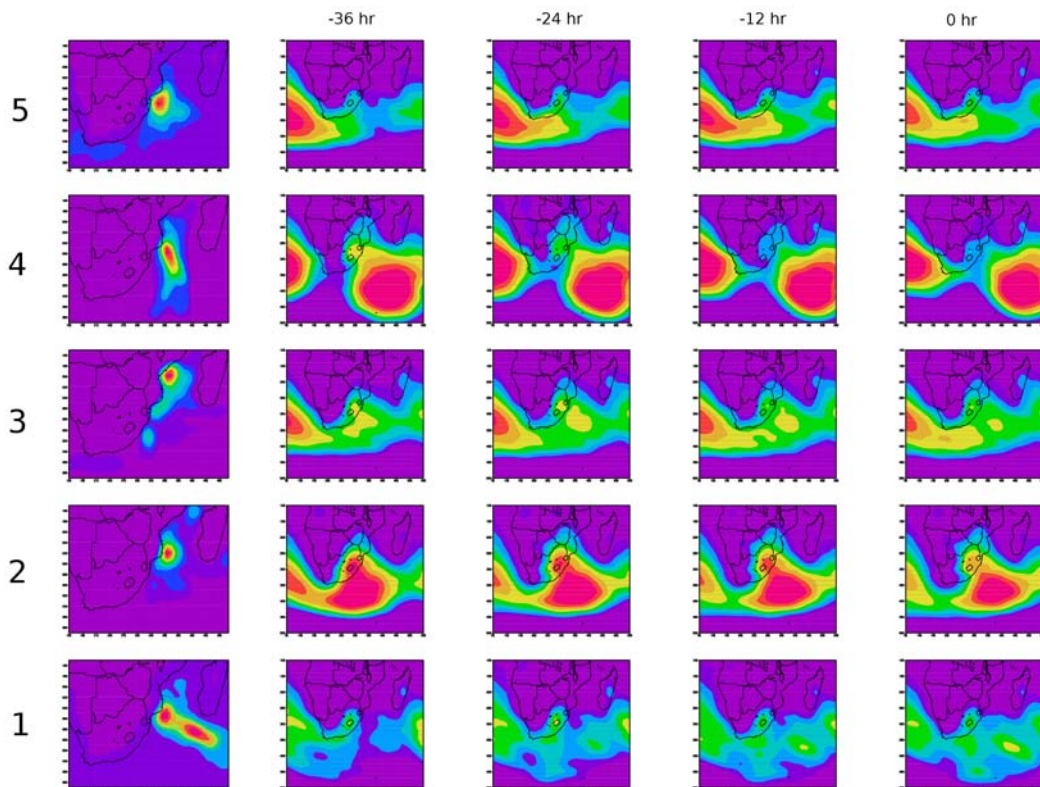


Figure 3.18: Target domain SA2 ocean source clustering results (column 1) and composite SLP sequences (-36 hour, -24 hours, -12 hours, 0 hours), clusters are ordered from 1 on the bottom row through to 5 on the top row.

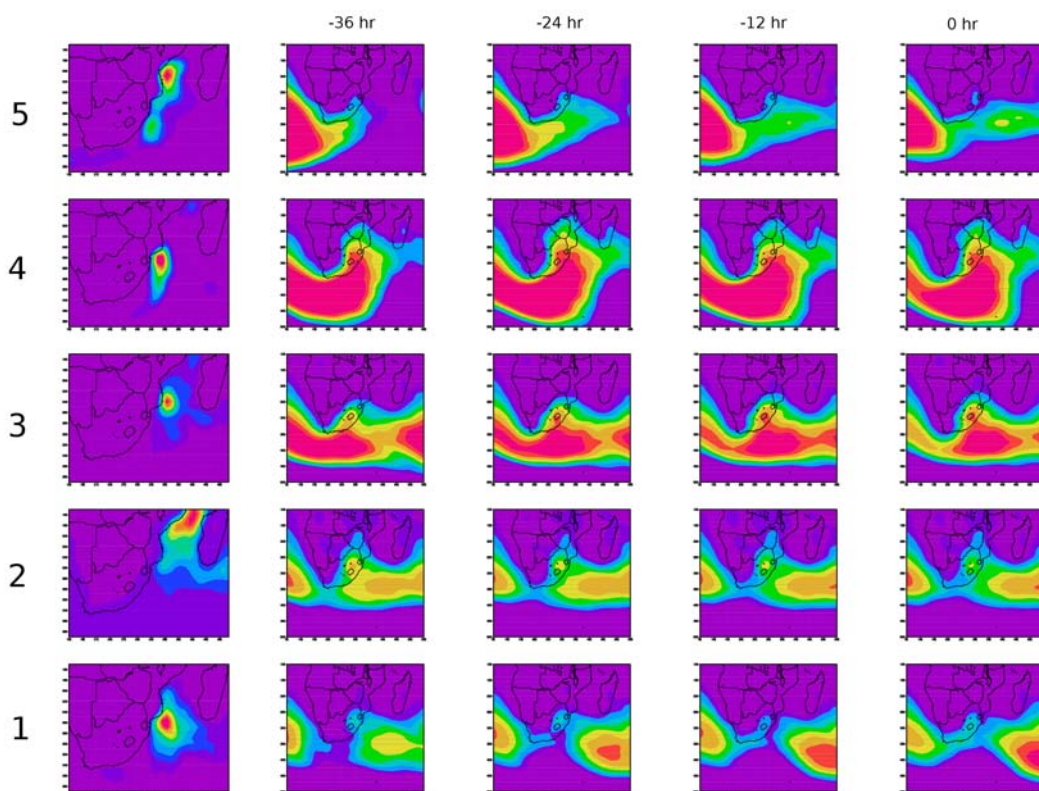


Figure 3.19: Target domain SA3 ocean source clustering results (column 1) and composite SLP sequences (-36 hour, -24 hours, -12 hours, 0 hours), clusters are ordered from 1 on the bottom row through to 5 on the top row.

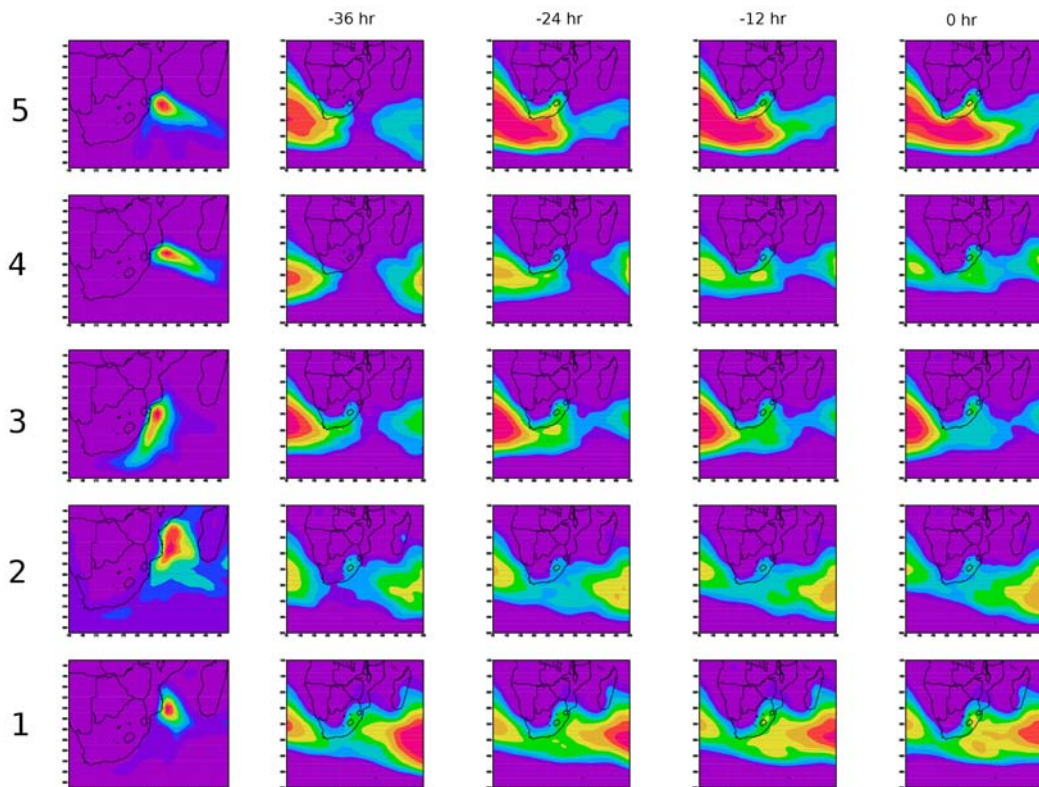


Figure 3.20: Target domain SA4 ocean source clustering results (column 1) and composite 850hPa sequences (-36 hour, -24 hours, -12 hours, 0 hours), clusters are ordered from 1 on the bottom row through to 5 on the top row.

pressure system is causing a general northward advection of moisture sourced from the east coast of Mozambique. The resultant source moisture field for the target SA3 therefore ends up significantly further north than in other clusters. Also of interest is that this is the most commonly occurring cluster for this domain accounting for more than 70% of all events. It therefore seems as if the presence of a closed low over the Mozambique Channel has a strong influence on the resultant ocean source area for this target domain. The low magnitude of this source region is most likely a result of the greater distance between the resultant source area and the target domain.

**Target SA4** This target is closer to the eastern coastline of South Africa and one would possibly expect a significant influence from the ocean. However, it sits at a fairly high altitude of between 1200m and 1500m and to some degree is quite isolated from the direct influence of the ocean. Most of the clustered source regions show the same patterns as the other target domains with the focus of the moisture source off the south coast of Mozambique. Cluster two is the most diffuse source cluster (figure 3.20) and is associated with almost no influence from the mid-latitudes and very weak high pressure systems. It appears to be largely driven by an easterly wave visible in the 850hPa height field. Cluster three is interesting in that it shows a strong coastal source extending quite far into the southern ocean. Once again, as for previous similar patterns extending to the south, it appears to be some association with the passage of a mid-latitude trough following by a ridging SAHP system.

## 3.5 Conclusions

To conclude this chapter we can distill out a number of important results and ideas. The key results are as follows:

- The Lagrangian model diagnoses significant land and ocean moisture sources for all target regions.
- Ocean source regions exhibit high variability across different synoptic modes.
- Fractional contributions of land sources are remarkably constant across synoptic modes.
- Regional synoptics are a strong driver of the spatial location of moisture sources.
- The east coast of South Africa is the dominant moisture source region for all domains.

These results will now be discussed in more detail:

The first important result is that the Lagrangian moisture transport model diagnoses very significant regional land and ocean moisture sources for all of the precipitation target regions. In most months and regions the land moisture sources contribute the majority of moisture in relation to all other diagnosed sources (ocean and RCM atmospheric boundaries). These high fractions of moisture contribution are largely a result of the attribution coefficient in the model which accounts for losses of moisture to upstream precipitation events. The result of this coefficient is that moisture sources closer to the target precipitation play a much greater role than more distant sources. The more distant sources may be greater gross moisture sources but much of that moisture is lost to en-route precipitation events and hence is lost to the final precipitation event in question.

It is possible that the combination of an overly active hydrological cycle in the RCM as well as some possible uncertainties in the diagnosis of rainfall in the Lagrangian model are also contributory to the high land and ocean source values. However, the Lagrangian model actually diagnoses precipitation amounts closer to observational values (less than the RCM) and the Lagrangian model diagnostics have several filters and checks in order to avoid spurious diagnoses of precipitation and evaporation. The case study presented in this chapter evaluated the evaporative moisture budget for the source region for a single event with the precipitation total for the same event and found the evaporation

well exceeded the precipitation. This is what one would expect as precipitation events do not remove all moisture from the air. If the RCM evaporation over the events identified source region were actually insufficient then the Lagrangian model would be drastically over-estimating evaporative gains and miss attributing source regions. While far from a validation, which is in itself very difficult given lack of observations, there does appear to be some robustness to the source patterns and magnitudes produced by the Lagrangian model.

Ocean source regions exhibit large intra-seasonal variability but also show much more diverse source regions. Much of the diversity probably results from the greater time associated with moisture transport from ocean sources. Over this greater time period it is likely that trajectory differences could cause a divergence of the moisture parcel cloud resulting in a greater spread in the source region. However, it is also likely that there is a natural convergence of moisture towards the target domain and hence the spatial area of the source regions will be greater for the more distant ocean than for the adjacent land.

Intra-seasonal variations in land source spatial distribution are large with absolute magnitudes generally related to the total precipitation amounts. However, fractional contribution of land sources remains remarkably constant through both seasons. Analysis of the synoptic conditions driving each land source region reveals that relatively subtle differences in synoptic conditions can produce large differences in moisture source areas. Of great interest for further study is the interaction between the diurnal cycles of evapotranspiration and precipitation. With both evapotranspiration and precipitation are closely time synchronized with the diurnal cycle, it seems that for some regions, with consistent and stable moisture advection, the evaporative source regions could reflect the pulsing of the diurnal cycle in their spatial patterns. The result is that certain upstream areas are more important sources of moisture due to the timing of the passage of air that passes over them.

The synoptic analysis of the moisture source patterns shows that the regional synoptic circulation fairly strongly constrains the spatial location of the moisture source region. The latitudinal position, westward extent, and intensity of the South Indian high pressure system along with the continental trough determines the pathway of air into the continent and towards the target domains. This pathway clearly largely determines the dominant land and ocean surface moisture source regions. More rapidly changing synoptic circulation fields, for example during the passage of a mid-latitude trough, produce more spatially spread source regions as the air pathways vary considerably over a short space of time.

The dominant ocean source for all target regions appears to be located off the east coast of South Africa and Mozambique and is largely driven by the South Indian High Pressure system. An analysis of the mean sequence of synoptic events producing different ocean source patterns reveals the important role of the mid-latitudes and tropical temperate connections. It appears that ocean moisture source regions are very sensitive to the unique timing and interaction between mid-latitude troughs, ridging high pressures, and continental lows. An interesting example of this is the sequence of a mid-latitude trough followed by a ridging high pressure system that produces a moisture source region extending down the east and southern coast, or south into the southern ocean, rather than the more typical SWIO source.

What is not captured in this analysis is the impact of surface moisture availability and sea surface temperatures on the distribution of the moisture source regions. Evaporation is a complex parameter, as has been discussed earlier. Surface moisture availability itself is not sufficient to ensure that a land region is a moisture source. Evaporation is dependent on temperature, relative humidity, wind speed and vertical mixing as well as soil and surface moisture availability. Changes in sea surface temperatures do impact the rate of evaporation from the ocean surface but so do wind speed, mixing, and relative humidity. This study proposed that the regional land surface plays an important role as a source of moisture for regional precipitation. The consistency of the land surface contribution over time suggests that, at least at a large scale, the land surface is not constrained in its role as a moisture source by moisture availability. If this were the case we would expect to see much larger variations in the relative contribution of the land through the months and seasons as soil moisture fluctuated. However, the impact of soil moisture and

other factors controlling evaporation do warrant further exploration. Perhaps most curiously the results of New et al. [2003] seem to suggest that in the absence of all soil moisture, the regional ocean and boundary moisture sources are able to provide sufficient moisture to maintain regional precipitation. However, such a study involves a great deal of complexity in order to disaggregate circulation impacts from moisture source impacts. This study certainly warrants further exploration of this component of the regional climate system. The Lagrangian model developed in this work would be a useful tool for this analysis and would lend itself well to unpacking the results of sensitivity type experiments of the style of (New et al. [2003])

Another very interesting avenue of further investigation is that of moisture transport through a leap frog process. The Lagrangian model as it stands is unable to trace moisture through multiple precipitation-evaporation cycles. However, the configuration of the domains and the identified source regions has produced an overlap between source regions and domains. For a number of domains the identified source region is at least partly covered by an adjacent target domain. The identified moisture source region for domain SA1 is therefore largely covered by region SA2. This means that the moisture source region for target domain SA2 also forms a secondary moisture source region for SA1. The same is true for target SA3. Target SA4 does not fit directly into this chain of source areas because it is located east of the other domains. While this study does not follow the chain to its end point which presumably would be a coastal domain with largely oceanic moisture sources, the moisture source region for SA3 does seem to suggest that such a chain might exist. If this chain does exist it would be interesting to determine the dynamics that govern it and whether this dynamic is a significant source of internal variability. A combination of RCM sensitivity studies along the lines of New et al. [2003] as well as the diagnostic application of the Lagrangian methodology described here would provide suitable tools for exploring such dynamics.

We can therefore conclude that the regional land and ocean play a surprisingly important role as sources of moisture for South African rainfall while the spatial and temporal distribution of the source areas is highly dependent on quite subtle differences in synoptic state and the temporal sequencing of those synoptic states. While the analysis cannot determine the effect of changes in these source regions on precipitation in the target region due to the complexities of such interactions, the results do highlight the importance of understanding the land/ocean atmosphere feedbacks at the regional scale and provides a useful starting point for such analysis.

It is very important to note one final caveat surrounding these results. The results presented are derived from the modeling of two distinct rainfall seasons. As described in section 3.1, these seasons were selected as El Nino and La Nina years of moderate wetness and moderate dryness as simulated by the RCM. The intent of this selection is to span to some degree the inter-annual climate variability of South Africa. The climatology of climate variability naturally cannot be captured sufficiently by only two seasons, but that is not the focus here, which instead is to explore the relative role of moisture sources using two contrasting seasonal modes.

This Chapter has dealt with the land and ocean source regions. The following chapter will examine the non-surface sources identified, namely the RCM boundary attributed source areas.

# Chapter 4

## Boundary Results

### Introduction

While the original intent behind the development of the Lagrangian source and attribution model described in chapter 2 was to explore the role of the land surface as moisture source for regional precipitation, useful information regarding the moisture sources external to the RCM domain can also be explored. Indeed the interaction between these external sources and the regional moisture sources provides useful insights into the cross scale relationships between larger scale and regional scale synoptics and moisture transport and becomes an essential component in understanding regional moisture sources.

Chapter 3 presented the results of the regional land and ocean surface moisture sources as diagnosed by the Lagrangian model and identified the land surface as an important moisture source, closely followed by the ocean surface. This chapter will present the results of the RCM boundary moisture sources. Similar analysis methods will be applied though with some variations appropriate to the boundary source analysis. The objective of the chapter is to explore the boundary moisture sources, their variation through the season, relationships to total precipitation, as well as regional synoptic circulation patterns and sequencing.

### 4.1 Monthly Results

Monthly mean boundary attributed source fields as well as seasonal mean fields are presented for each precipitation target domain and for each of the four RCM boundaries in figures 4.1, 4.2, 4.3, and 4.4 below. Due to the large number of figures that result from the permutations of target domains, years, and RCM boundaries, we will attempt to summarize only the most significant features of these results. Tables 3.1 and 3.2 describe the total and fractional contribution of each boundary source for each domain and month in each season.

#### 4.1.1 Domain SA1

This domain lies furthest south of all the domains and the RCM eastern boundary is attributed very weakly in 1988 and only slightly more in 1991. Only in February of 1991 does the eastern boundary source provide a significant mass of moisture. We can most likely relate this February increase to the SWIO high pressure positive anomaly and

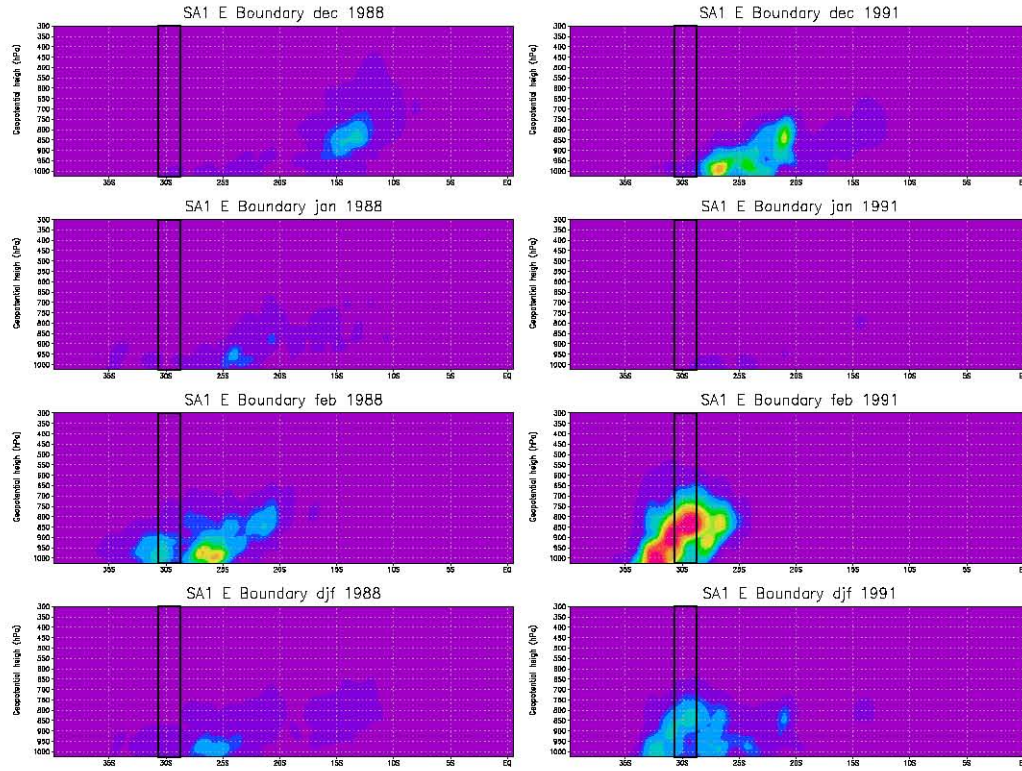


Figure 4.1: Domain SA1, Eastern boundary Dec, Jan, Feb and DJF total attributed moisture for 1988/9 and 1991/2 season.

associated easterly moisture transport from the RCM boundary into the continent (figure 3.4). The westerly moisture source plays a very important role for this domain, most likely because of its higher latitude and proximity to the mid-latitudes. The consistency is remarkable with no month in either season showing a particularly variation from the seasonal means. In both seasons January shows a significant more northerly source in conjunction with the main southerly source. This northerly component almost disappears in the later season. February 1992 does show an interesting variation in the form of a lower level (800hPa - 700hPa) source which isn't notably present in other months.

The southern boundary source also shows remarkable consistency across the months in both seasons with only February 1991 showing a significant weakening. Once again this weakening is most likely related to the SLP anomaly in figure 3.4, which would produce an anomalously northerly flow across most of the southern boundary area and would limit any flow of moisture from the south. The northern boundary plays only a very small role and that only at the start of the wetter 1988/9 season. During the drier 1991/2 season this boundary essentially provides no moisture to the target domain.

#### 4.1.2 Domain SA2

This domain shows a greater reliance on the easterly boundary for source moisture. However, the fraction of moisture obtained from this source remains low (8% - 22%) with the highest fraction occurring during February 1992. February 1992 is associated with an anomalously strong South Indian High Pressure (SIHP) pattern which would advect moist air into the domain across the eastern boundary. In January the easterly boundary sources extend as far north as 10°S. The westerly source once again plays a significant role (13% - 33%) with similar patterns to those of domain SA1. Only in February 1992 does there appear to be a weakening of this source possibly related to the opposing

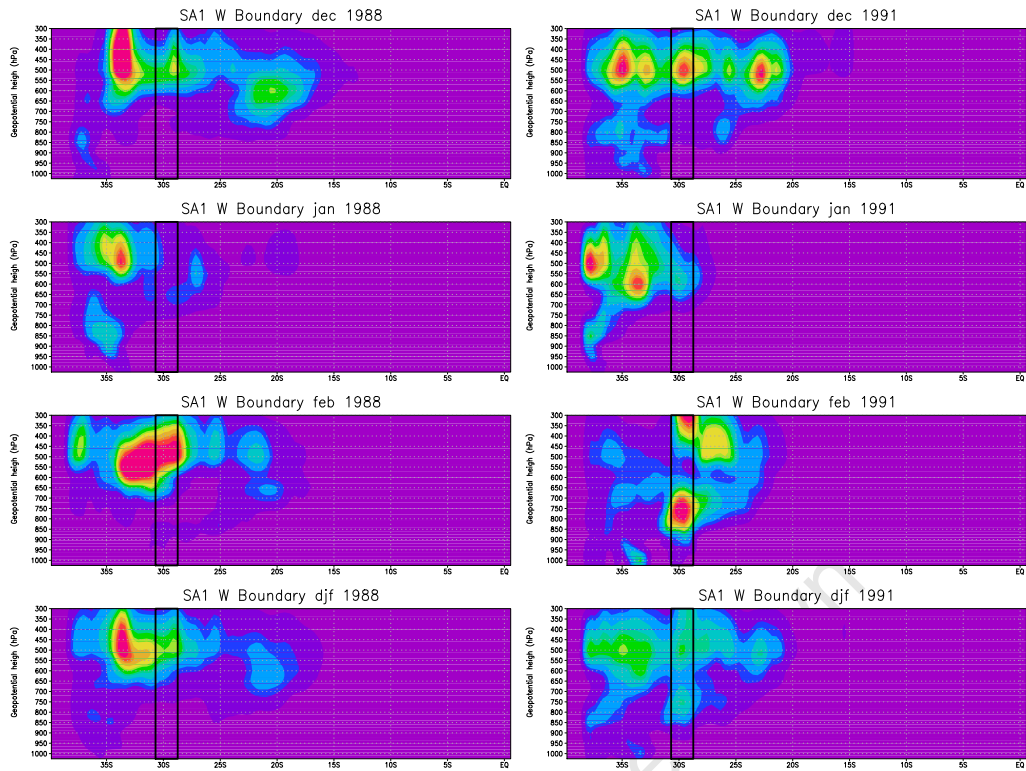


Figure 4.2: Domain SA1, Western boundary Dec, Jan, Feb and DJF total attributed moisture for 1988/9 and 1991/2 season.

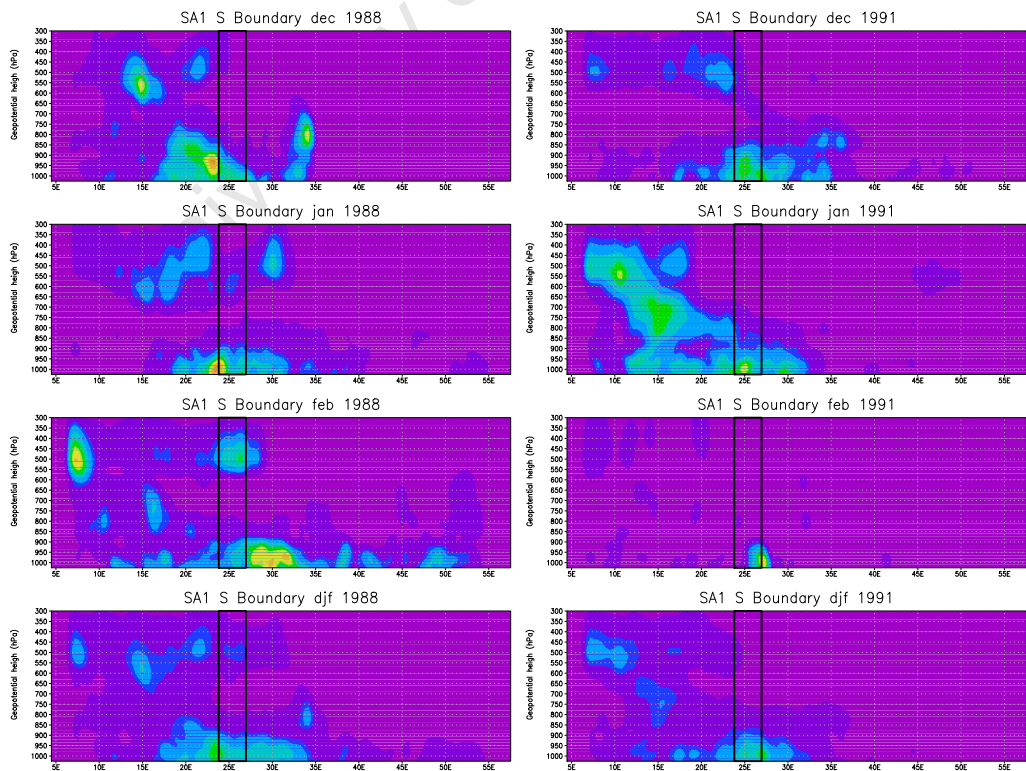


Figure 4.3: Domain SA1, Southern boundary Dec, Jan, Feb and DJF total attributed moisture for 1988/9 and 1991/2 season.

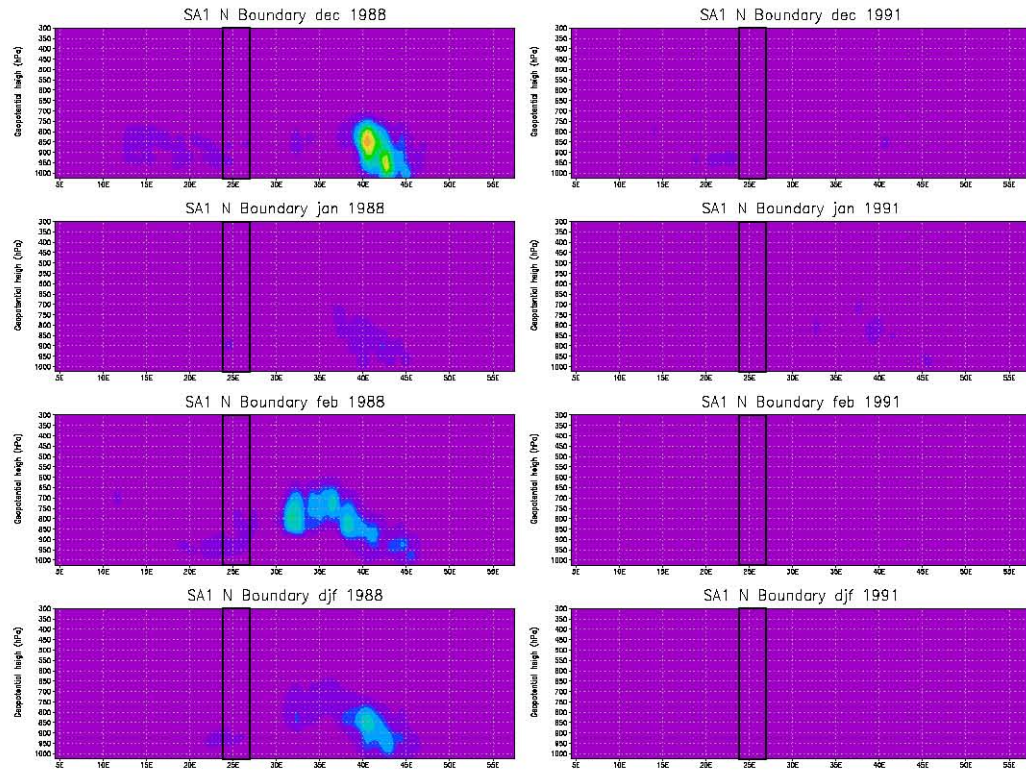


Figure 4.4: Domain SA1, Northern boundary Dec, Jan, Feb and DJF total attributed moisture for 1988/9 and 1991/2 season.

easterly source driven by the SIHP anomaly. The southern boundary is a weaker source for this domain which we expect as it lies further north than domain SA1. However, in January 1992 the southern boundary does play an important role providing as much as 26% of the total moisture. This can be related to the SAHP positive anomaly pattern which would produce a more southerly flow across the southern central part of the domain. Once again, the northern boundary plays only a very small role and this only in January 1988. In the 1991/2 season it contributes virtually none of the precipitated moisture for the domain.

### 4.1.3 Domain SA3

The northern most domain and also quite centrally placed longitudinally in the continent, this domain sources much of its moisture from the eastern boundary. During most months across both seasons the easterly source provides more moisture than the westerly source. As was seen in domain SA2, January's source region extends quite far north reaching as far as 10°S suggesting a stronger tropical moisture source during this month. Most of the moisture is sourced from quite a low level, typically below 700hPa. The western boundary does still play a role though it is weaker than for domains 1 and 2. January does show the strongest westerly source though this month is also a wet month for both seasons. The southerly source is quite different to the previous two domains in that the near surface moisture source is not present. However, in January 1992 there is a strong high level source around 500hPa altitude. This corresponds to a similar strong westerly source for the same month. The southern boundary source is most likely strongly related to the southern part of the westerly boundary source as they would both be under the influence of the mid-latitude dynamics.

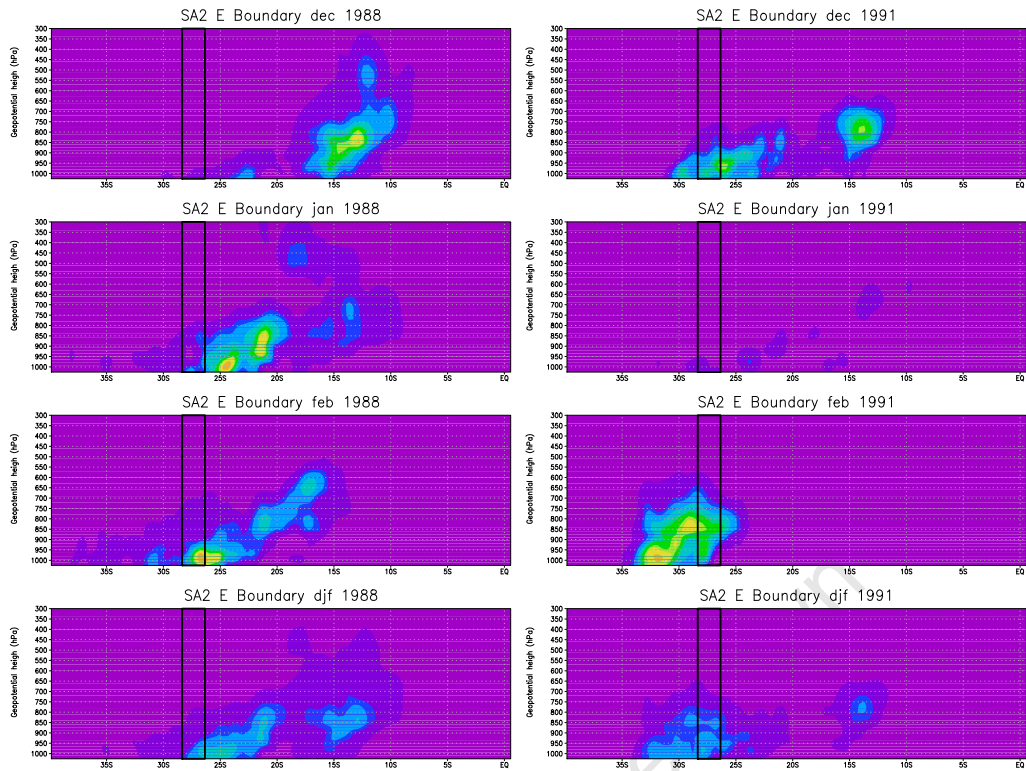


Figure 4.5: Domain SA2, eastern boundary Dec, Jan, Feb and DJF total attributed moisture for 1988/9 and 1991/2 season.

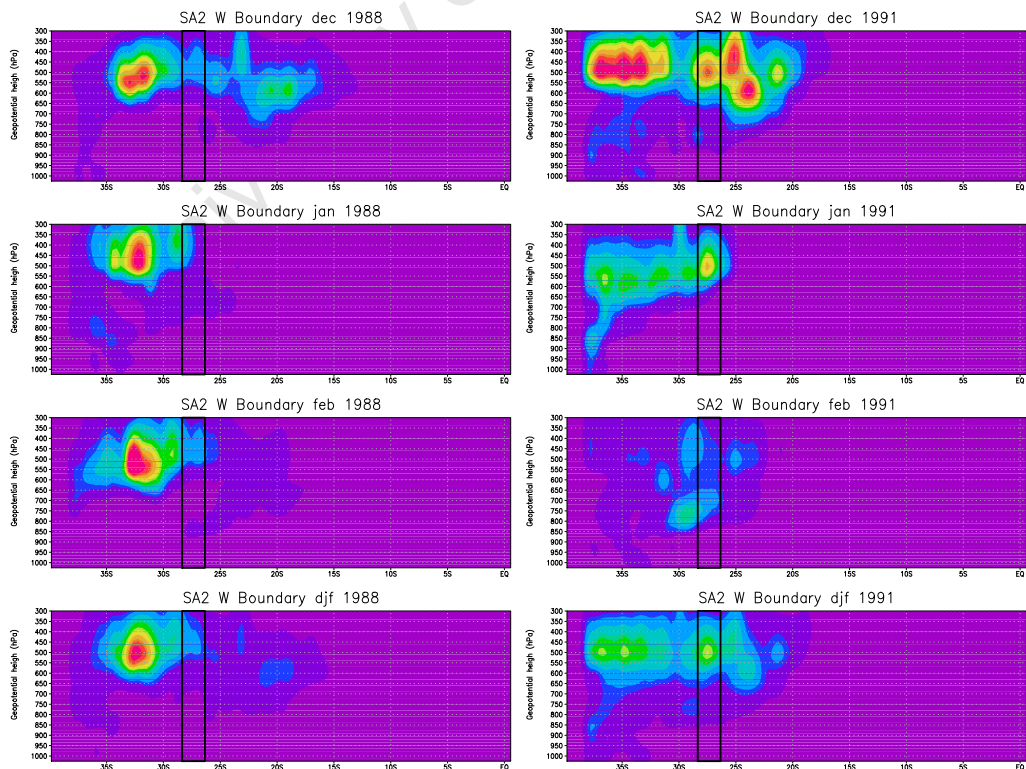


Figure 4.6: Domain SA2, western boundary Dec, Jan, Feb and DJF total attributed moisture for 1988/9 and 1991/2 season.

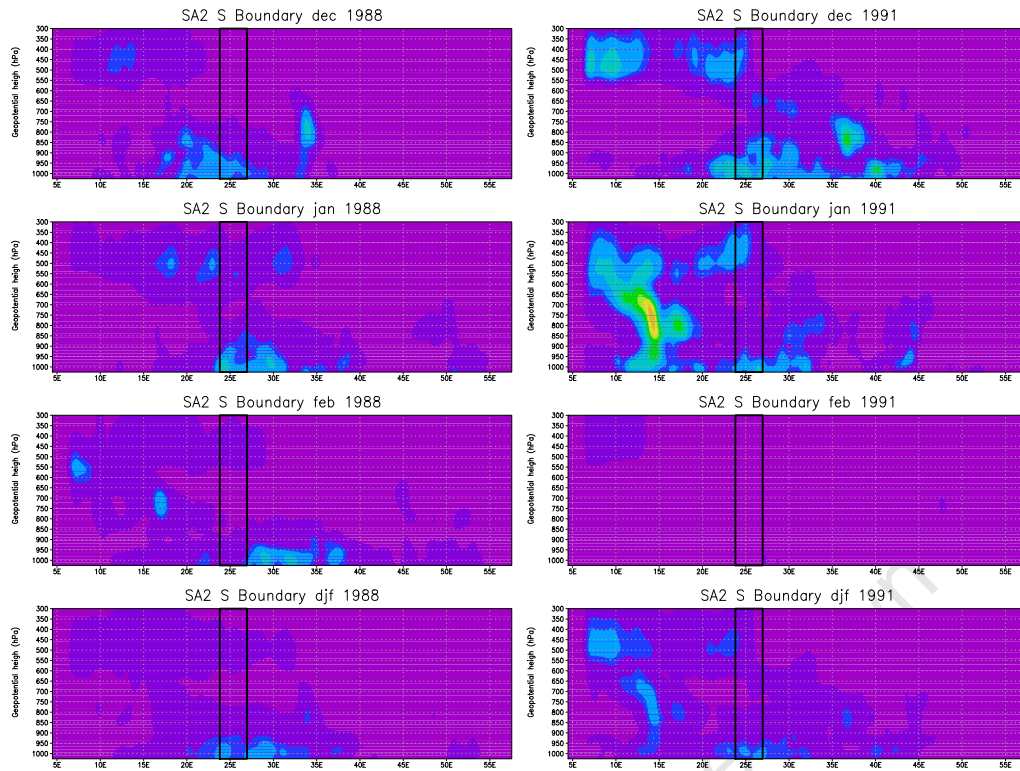


Figure 4.7: Domain SA2, southern boundary Dec, Jan, Feb and DJF total attributed moisture for 1988/9 and 1991/2 season.

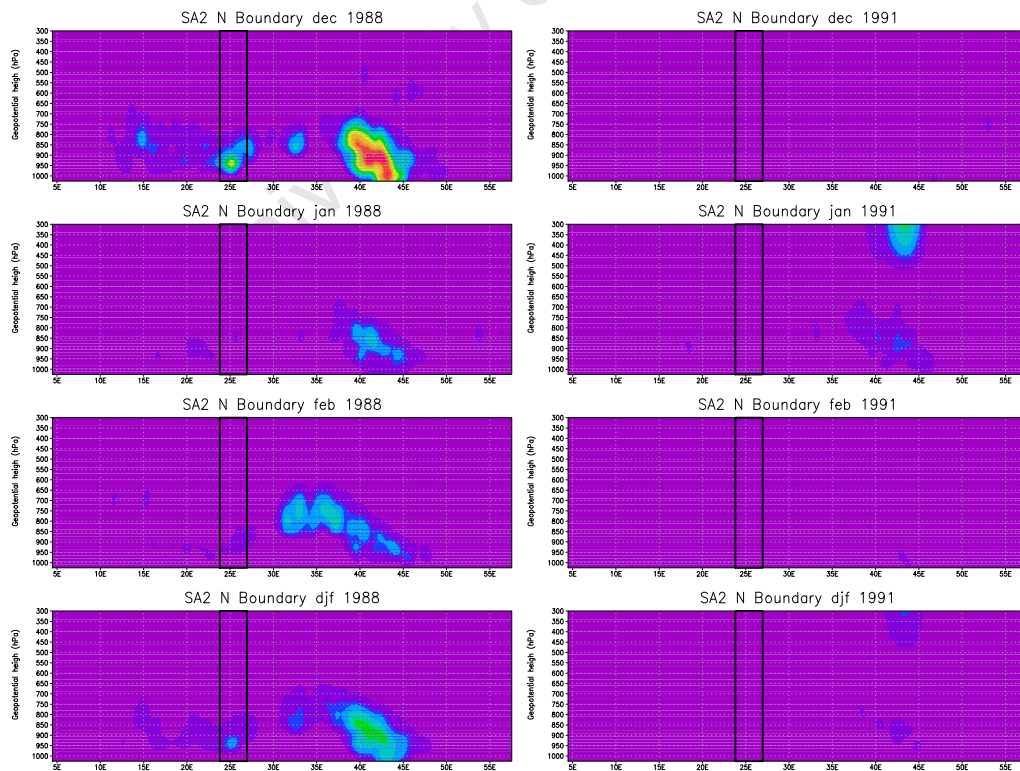


Figure 4.8: Domain SA2, northern boundary Dec, Jan, Feb and DJF total attributed moisture for 1988/9 and 1991/2 season.

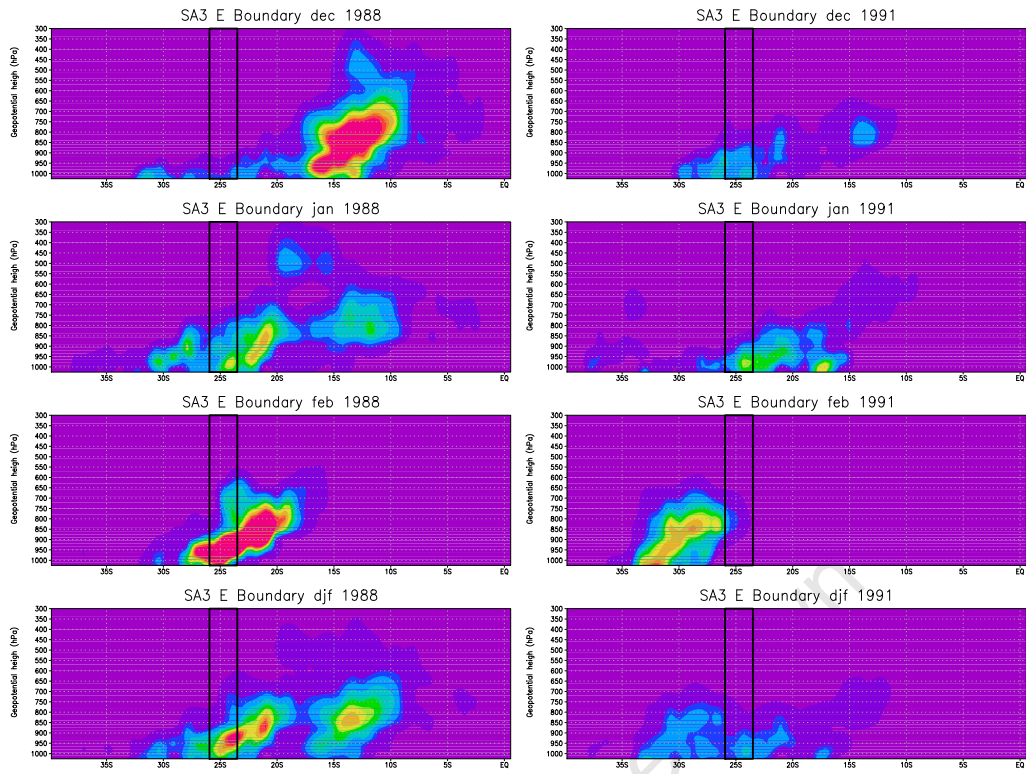


Figure 4.9: Domain SA3, eastern boundary Dec, Jan, Feb and DJF total attributed moisture for 1988/9 and 1991/2 season.

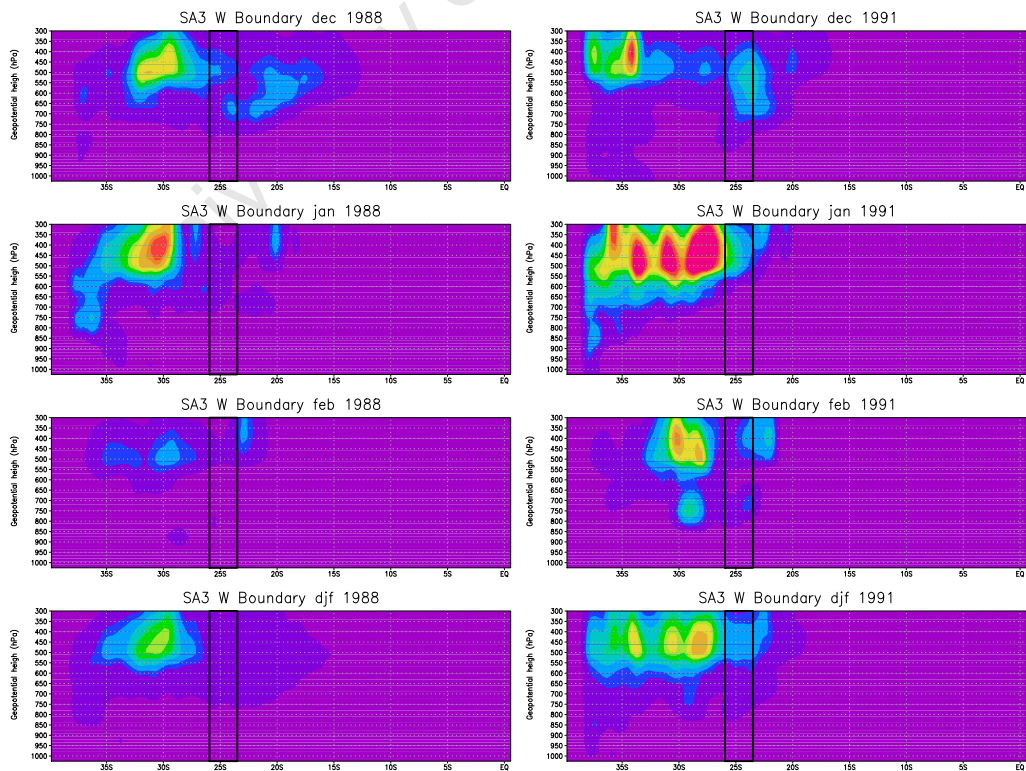


Figure 4.10: Domain SA3, western boundary Dec, Jan, Feb and DJF total attributed moisture for 1988/9 and 1991/2 season.

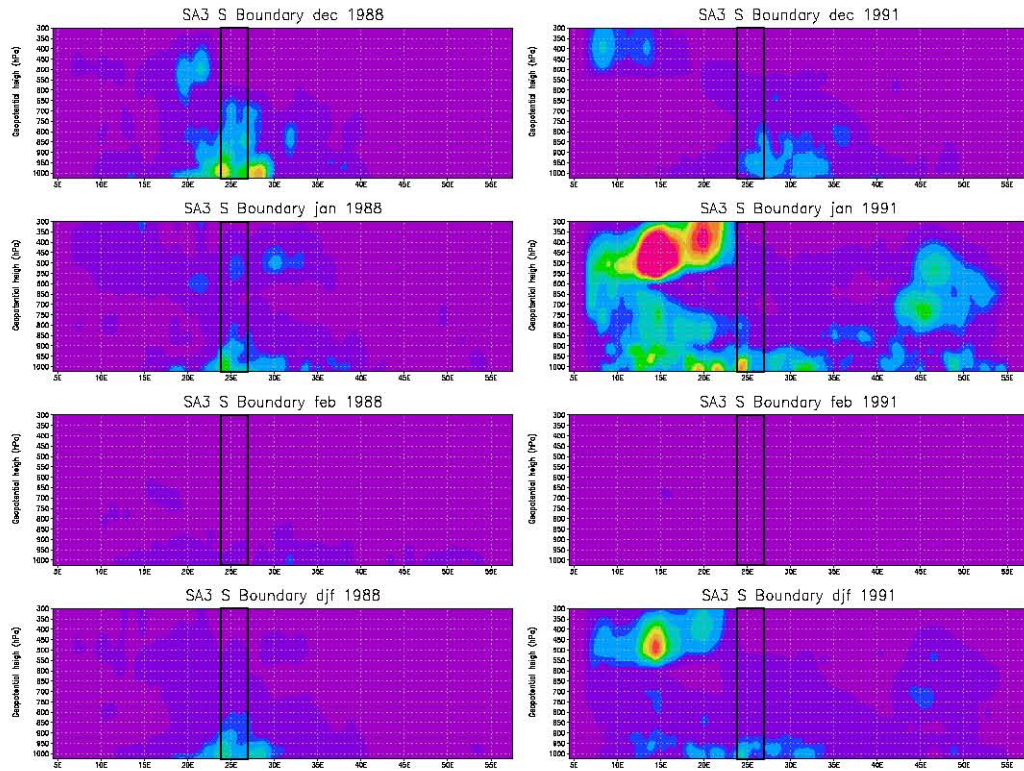


Figure 4.11: Domain SA3, southern boundary Dec, Jan, Feb and DJF total attributed moisture for 1988/9 and 1991/2 season.

#### 4.1.4 Domain SA4

This target domain is interesting in that the RCM simulated precipitation values are higher during the 1991/2 season (figure 3.2). This is the only domain that is wetter during this season which was selected for being moderately dry compared to climatology. This domain lies further east than the other domains and shows a fairly consistent eastern boundary moisture source though there are a few months where this source seems to decrease. Perhaps most notably in January 1992, which corresponds to a slightly dry month for the domain. The western boundary source shows fairly consistent patterns though it does reduce markedly during February in both seasons. Interestingly, the southern RCM boundary plays an important role, particularly during the 1991/2 season where in January it is the source of around 30% of precipitated moisture. The northern boundary plays a very small role and that only in the 1988/9 season as is common across most target domains.

## 4.2 Clustering Results

A similar clustering analysis to that used for the land and ocean surface sources in chapter 3 is applied to the RCM boundary sources and described in the following sections. The differences are that only two clusters were determined for each boundary, and the lag period used is longer. Only two clusters was determined as the boundary source patterns show fairly small spatial variations. The same NCEP re-analysis synoptic sequence compositing was performed with lag periods of 0 hours, 24 hours, 48 hours and 72 hours. Large lag periods were selected because of the greater transport time from the RCM boundaries into the precipitation target domains and hence the longer synoptic sequence involved. Each boundary source map is clustered independently. Attempts to cluster the combined

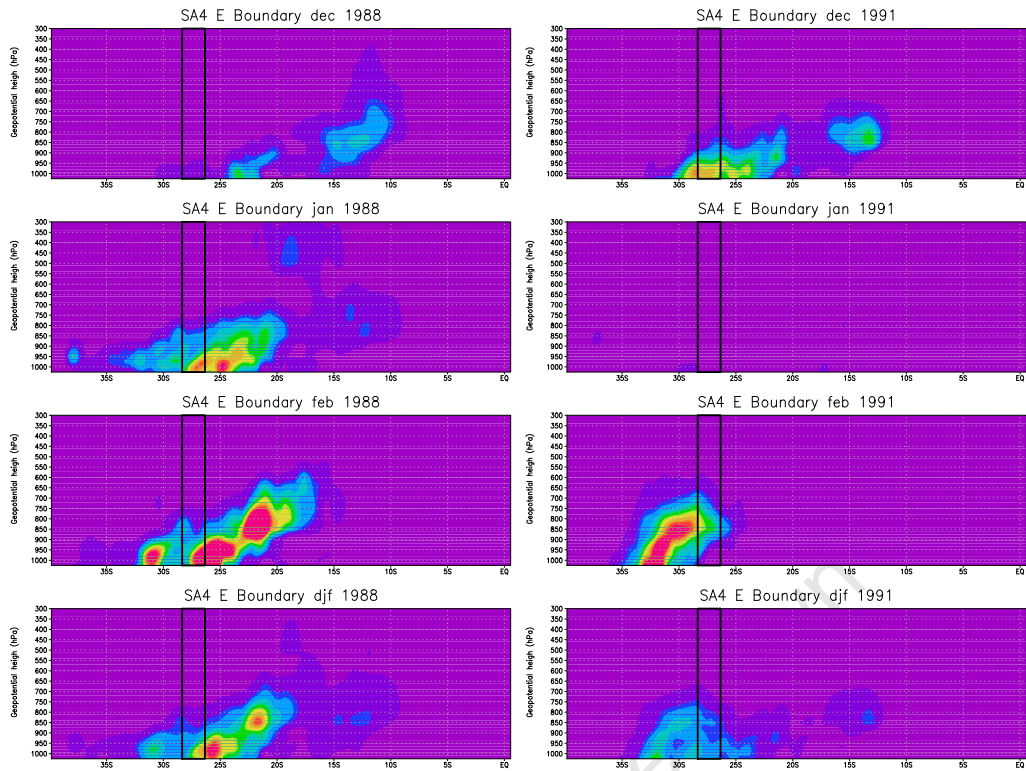


Figure 4.12: Domain SA4, eastern boundary Dec, Jan, Feb and DJF total attributed moisture for 1988/9 and 1991/2 season.

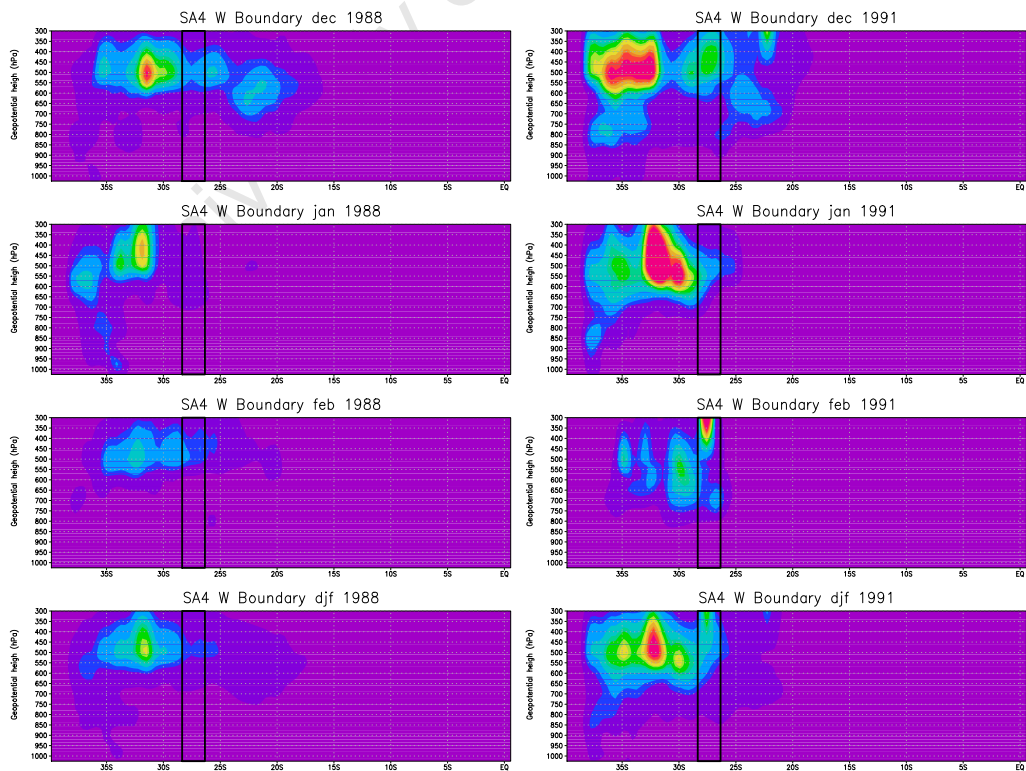


Figure 4.13: Domain SA4, western boundary Dec, Jan, Feb and DJF total attributed moisture for 1988/9 and 1991/2 season.

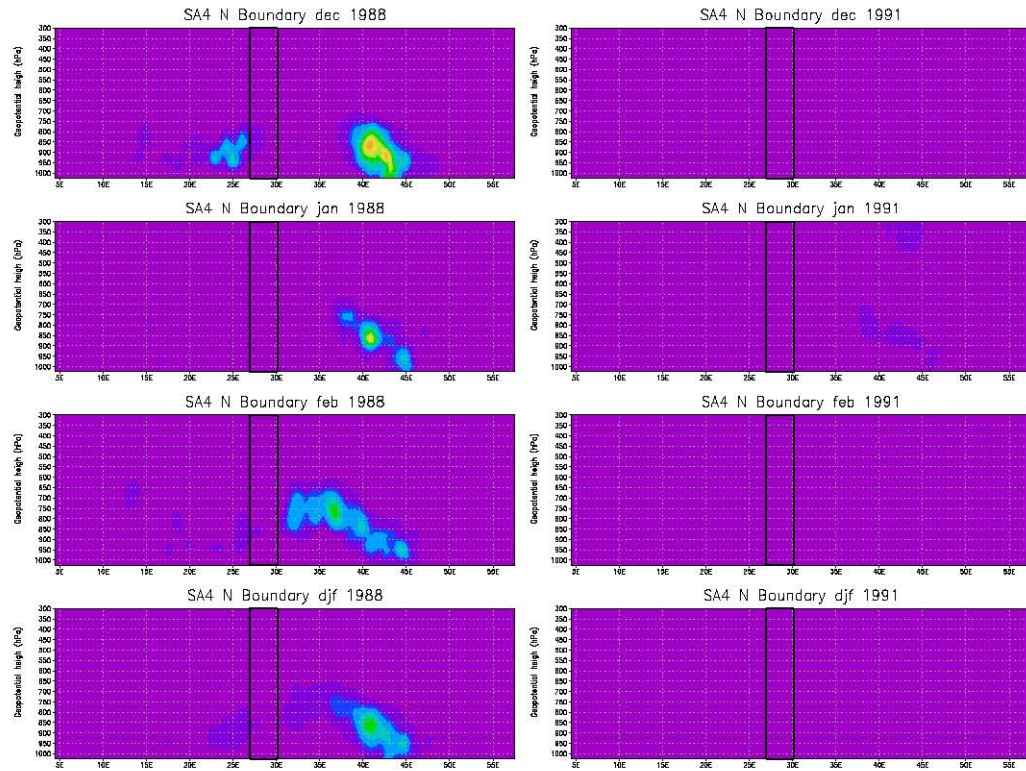


Figure 4.14: Domain SA4, northern boundary Dec, Jan, Feb and DJF total attributed moisture for 1988/9 and 1991/2 season.

boundary sources produced unsatisfactory results which is most likely a result of the size of the RCM domain. Within a large RCM domain different unrelated dynamics can occur simultaneously in different regions of the domain with the result that moisture transport across different boundaries will often not be related.

Results are presented by target domain and boundary. Only the most appropriate variables from the NCEP re-analysis composite sequences are shown for each boundary as required to explain the synoptic patterns involved. For the western boundary clusters, 500hPa fields are shown as these are most representative of the associated circulation. For the southern boundary clusters, SLP fields are shown, and for the eastern boundary, 850hPa fields are shown.

### 4.2.1 Domain SA1

The two clusters identified for the eastern boundary are seen in figure 4.15 with the associated 850hPa composite synoptic sequences. The first cluster identifies a southerly moisture source and is associated with a sequence of increasing high pressure influence from both the Atlantic and Indian ocean systems followed by a decreasing influence. Presumably the intrusion of the SWIO high into the subcontinent is responsible for the initial moisture transport while the receding of the high pressure coupled with a deepening of a continental low pressure produces the final precipitation event.

The second cluster identifies a more northerly component of the boundary source and is also associated with an intrusion of the SWIO high pressure. The more northerly location of the source is most likely a result of the more northerly extension of the high pressure into the subcontinent. The high pressure strengthens slower than for the

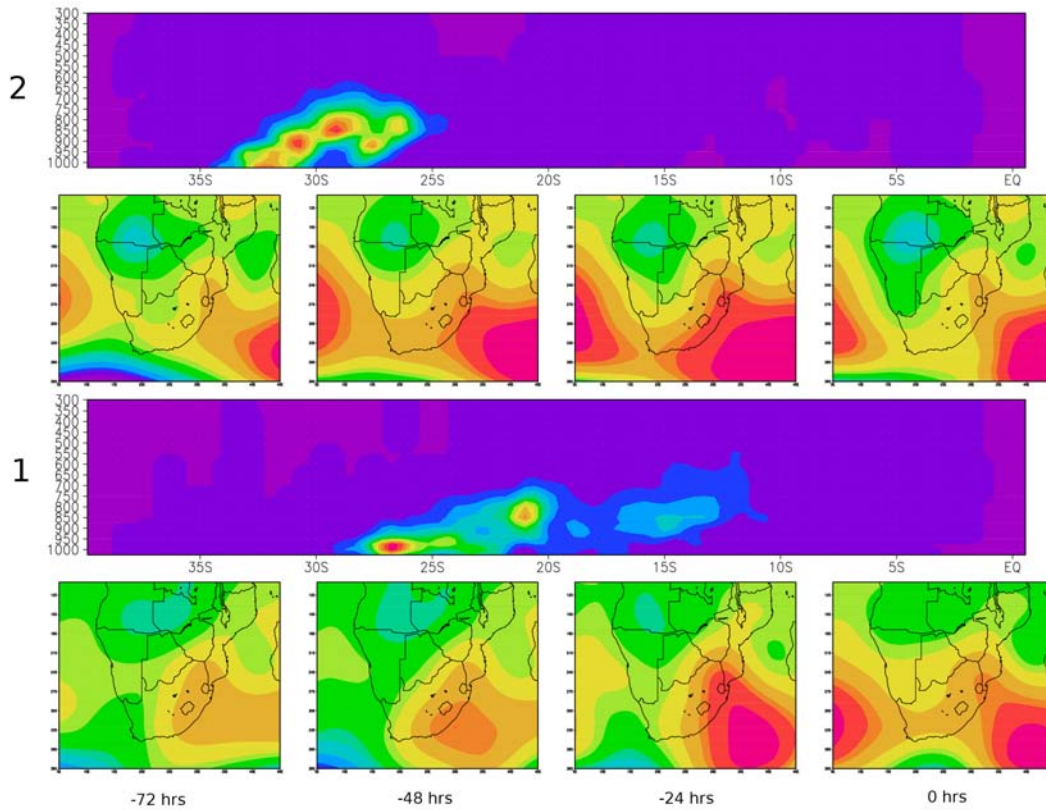


Figure 4.15: Domain SA1 eastern boundary cluster composite boundary moisture sources (column 1) and 850 hPa height synoptic sequences. Cluster 1 is on the bottom row and cluster 2 is on the top row.

previous cluster and the final precipitation event seems to be a combination of the continental trough and a mid-latitude system passing to the south.

The western boundary clusters (figure 4.16) also show a north/south divide. Due to the altitude of the cluster centers the 500hPa field is used to represent the synoptic sequencing involved. In both cases a mid-latitude wave is approaching from the south west. The first cluster sequence shows a very slow moving wave while the second cluster shows a faster moving wave. The significance of these differences is however, difficult to determine. More exploration of this westerly source is needed and will be discussed in section 4.3 below.

The southern boundary sources (figure 4.17) cluster into a western source in cluster one and an eastern source in cluster two. The SLP synoptics clearly show the two different synoptics involved. The westerly source is the result of the influence of the SAHP system which ridges around the south of the continent. As it moves around the southerly wind flow advects moisture from the south directly into the target domain. The second cluster shows a more easterly source. The dynamics suggest that this source is advected from the south under the influence of a very advanced ridging and budding of the SAHP pressure system advecting moisture from the south at a longitude of around 34°E. There is no means for this moisture to advect directly into the target domain and so it would seem as if the moisture pathway must be anti-cyclonic around the eastward moving high pressure into the sub-continent across the east coast and then advecting south into the target domain.

The northern boundary magnitudes are very low for this domain with a maximum fractional contribution of 3% and so will not be considered in this analysis.

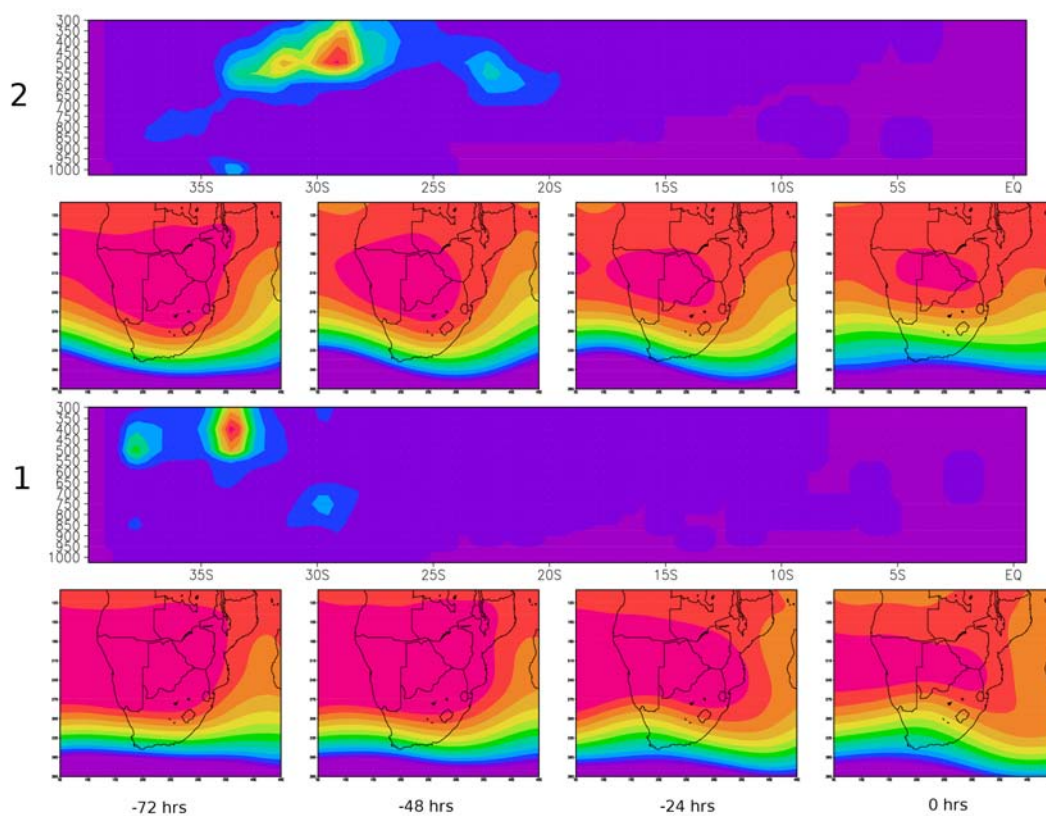


Figure 4.16: Domain SA1 western boundary cluster composite boundary moisture sources and 500 hPa height synoptic sequence. Cluster 1 is on the bottom row and cluster 2 is on the top row.

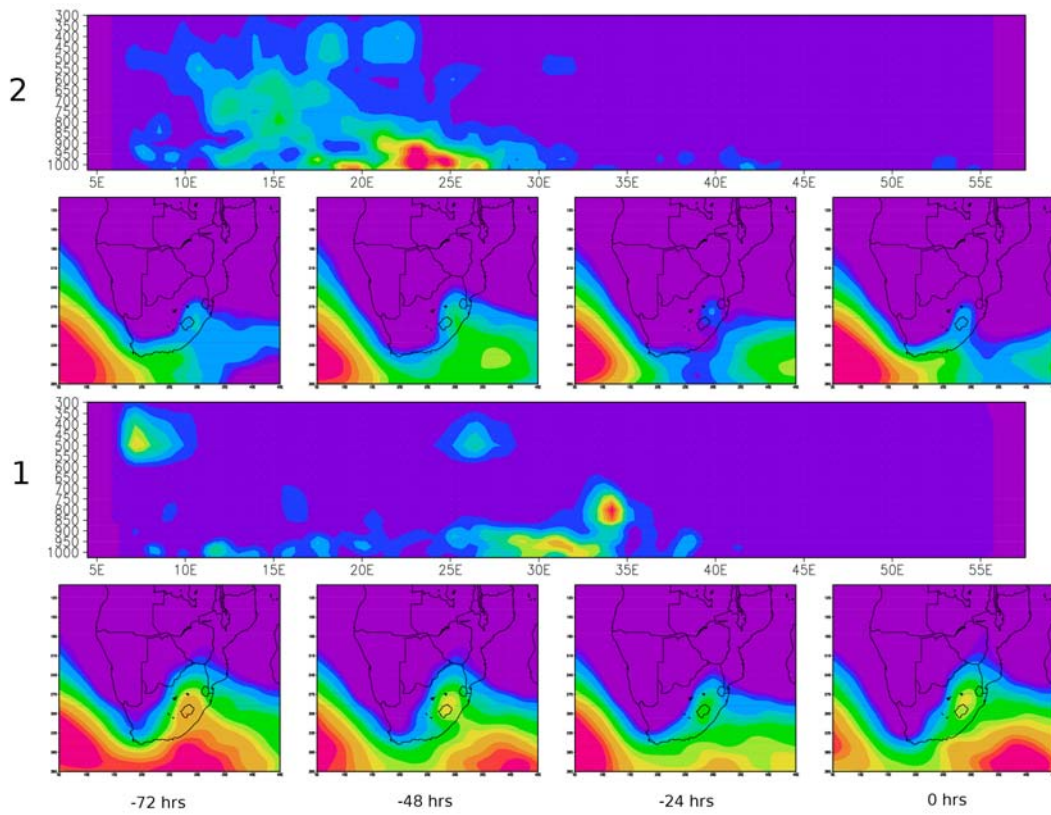


Figure 4.17: Domain SA1 southern boundary cluster composite boundary moisture sources and SLP synoptic sequence. Cluster 1 is on the bottom row and cluster 2 is on the top row.

### 4.2.2 Domain SA2

The eastern boundary source (Figure 4.18) for this domain shows a southern cluster and a northern cluster as for domain SA1. The 850hPa synoptics associated with the northern cluster show the development of a high pressure over the east coast of South Africa that extends in Mozambique and advects moisture from around 12°S into the continent and then southwards towards the target domain. The southerly source shows an almost opposite sequence with a strong SWIO high feeding moisture from around 25°S towards the continent. This high pressure weakens towards the end of the sequence as an Angolan low pressure develops to the north.

The western boundary source (Figure 4.19) also shows a northerly and southerly source region, both at around 500hPa height. The 500hPa synoptics and 700hPa synoptics both show a mid-latitude wave structure to the south of the country with the southerly source associated with a more stationary wave off the west coast and the northerly source associated with a deeper and faster moving wave.

The southern boundary clusters (Figure 4.20) are unusual in that the first cluster identifies both a high level and a low level moisture source. The high level source lies to the western side of the domain while the low level source lies to the east. It is not clear if this is the result of sub-optimal clustering or is representative of a real source pattern. The second cluster identifies a single, tightly defined, low level source towards east of the domain. The associated synoptics for the first cluster explain the low level southerly source quite easily as advection of moisture anti-cyclonically around a high pressure system located off the east coast. However, the high level source is located at around the 500hPa level and the synoptics do not suggest any meridional flow. It is likely that the variability in the synoptics associated with this cluster has produced a composite synoptic state that does not represent the dynamics involved. The large spread in the cluster source also suggests that this cluster contains a large degree of variability.

Once again, the northern boundary plays such a small role as a moisture source that results from that boundary will not be presented here.

### 4.2.3 Domain SA3

This northern most target domain (Figure 4.21) shows much more northerly eastern boundary source clusters than the domains to the south. The first cluster identifies a source north of Madagascar and the synoptics show the ridging of a high pressure around the south of the country as the driver of advection of moisture from this boundary into the country. The ridging high is not responsible for the advection across the boundary but is only responsible for the later advection of moisture down the continent and into the target domain from the north. The second more southerly source shows a more typical ridging high scenario as we have seen in previous domains. The westerly boundary source (Figure 4.22) again shows a northerly and southerly cluster, both of which seem to be associated with a mid-latitude wave visible in the 500hPa height field. The southern boundary (Figure 4.23), which for this domain accounts for, on average, around 10% of the source moisture again shows a high level source to the west which is most likely related to the high level southerly source in the western boundary clusters. The 500hPa height field does indeed show a mid-latitude wave structure passing to the south of the continent presumably advecting moisture at a high level, northwards towards the target domain.

### 4.2.4 Domain SA4

The eastern most target domain, we would expect this domain to be highly dependent on an eastern moisture source. In reality this domain sources less of its moisture from the eastern boundary than domain SA3 to its north west. The

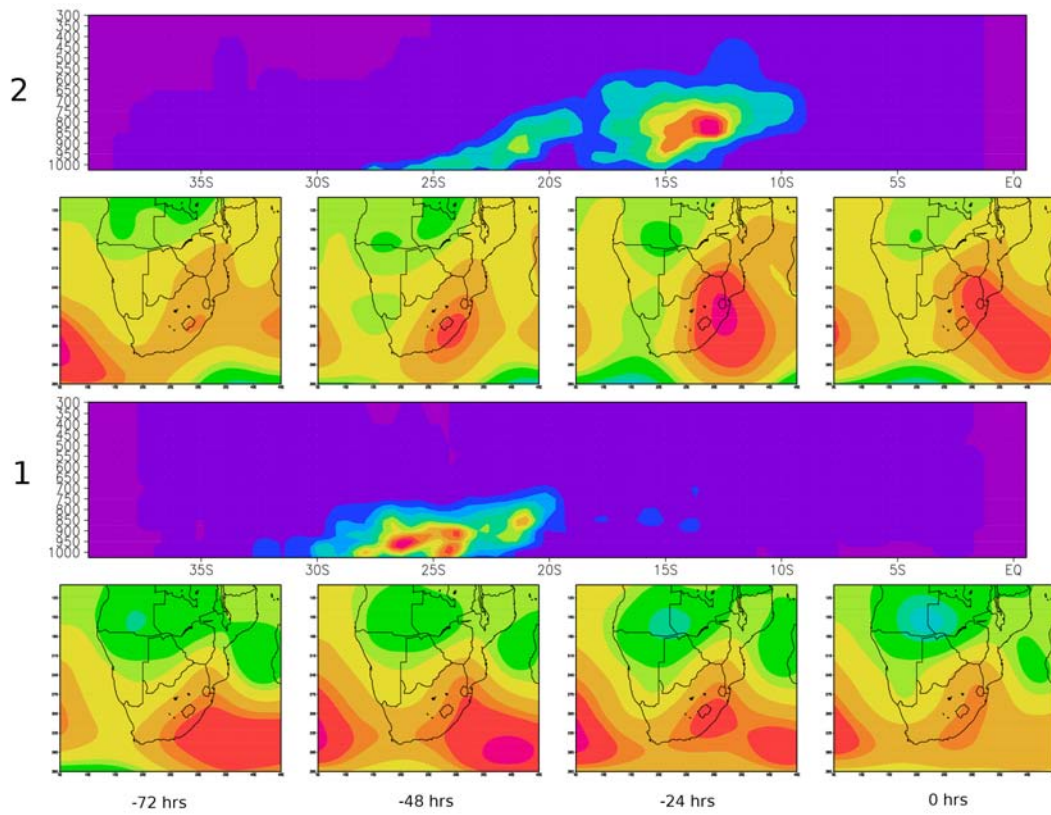


Figure 4.18: Domain SA2 eastern boundary cluster composite boundary moisture sources and 850 hPa synoptic sequence. Cluster 1 is on the bottom row and cluster 2 is on the top row.

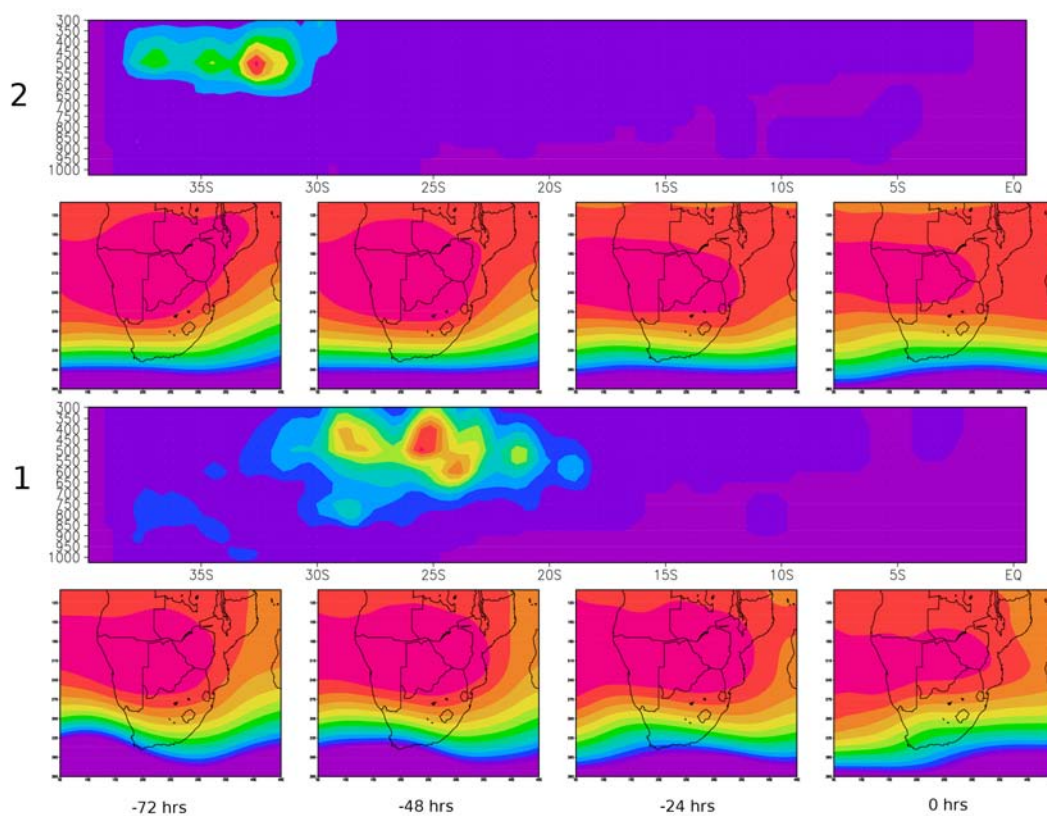


Figure 4.19: Domain SA2 western boundary cluster composite boundary moisture sources and 500 hPa synoptic sequence. Cluster 1 is on the bottom row and cluster 2 is on the top row.

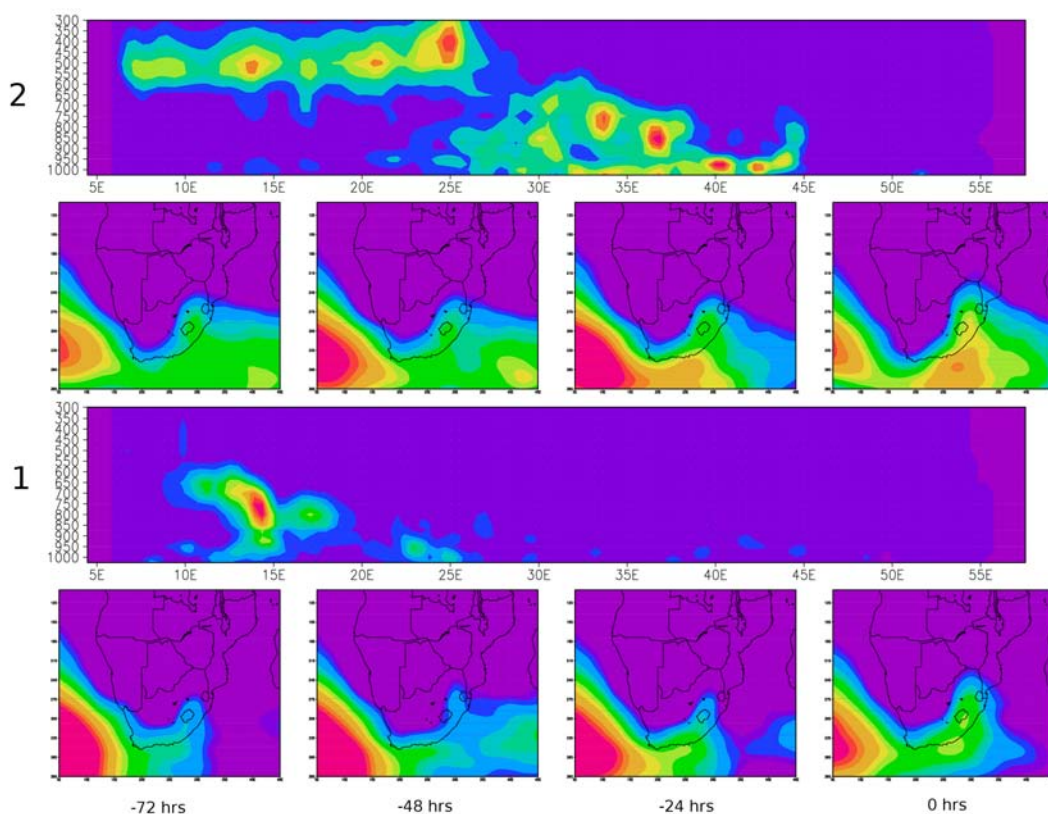


Figure 4.20: Domain SA2 southern boundary cluster composite boundary moisture sources and SLP synoptic sequence. Cluster 1 is on the bottom row and cluster 2 is on the top row.

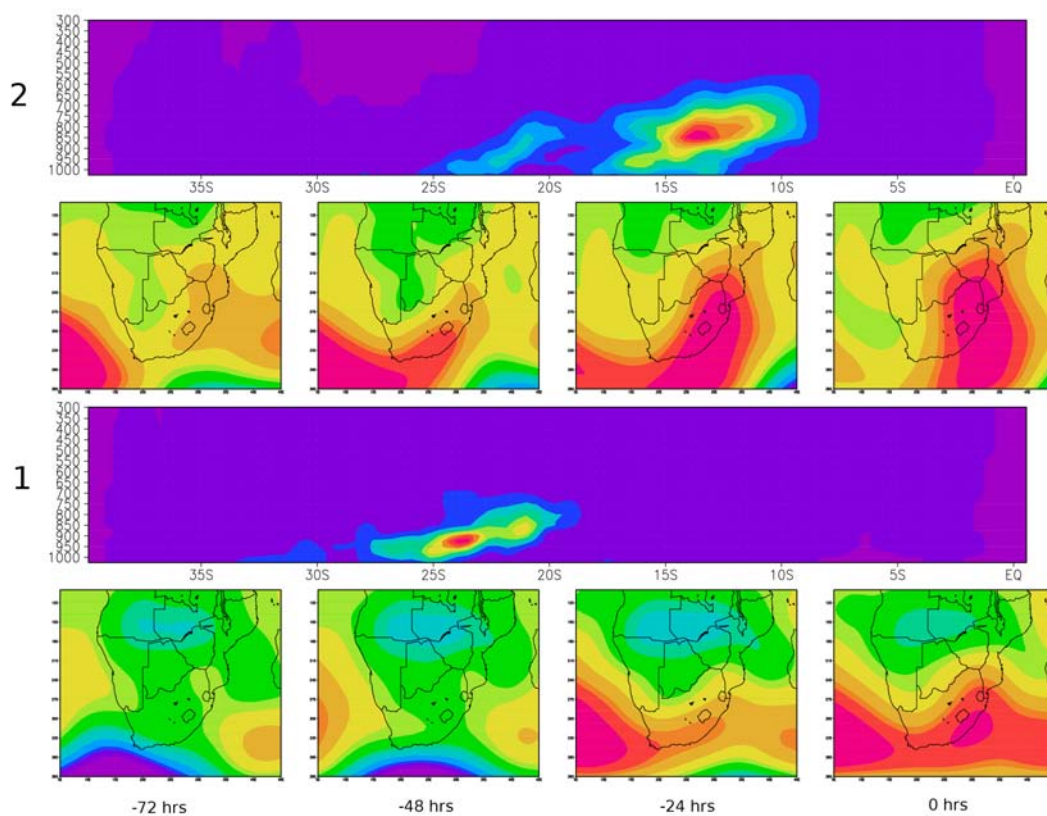


Figure 4.21: Domain SA3 eastern boundary cluster composite boundary moisture sources and 850 hPa synoptic sequence. Cluster 1 is on the bottom row and cluster 2 is on the top row.

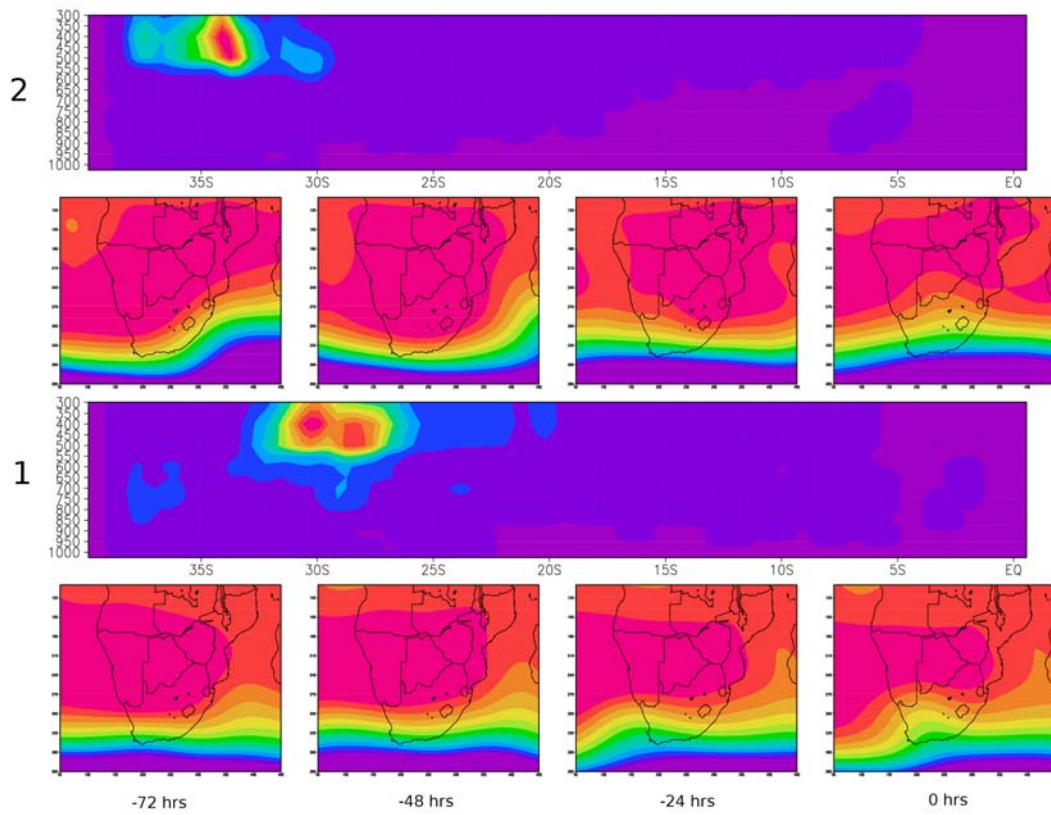


Figure 4.22: Domain SA3 western boundary cluster composite boundary moisture sources and 500 hPa synoptic sequence. Cluster 1 is on the bottom row and cluster 2 is on the top row.

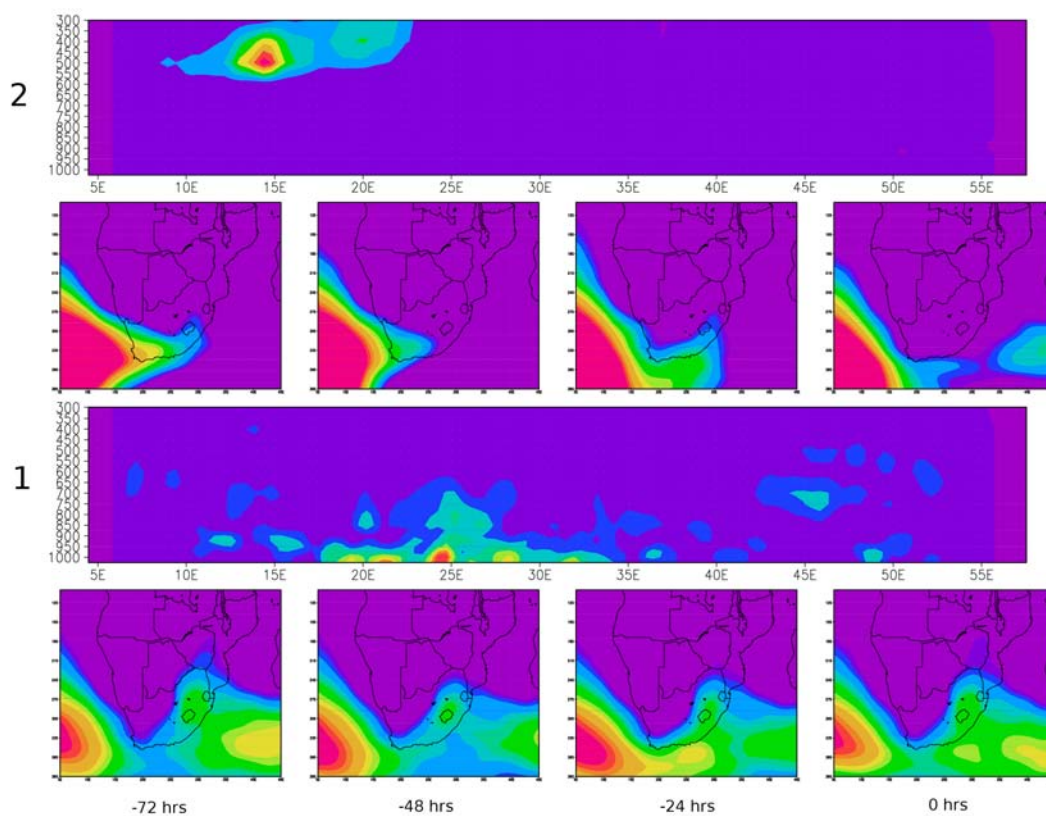


Figure 4.23: Domain SA3 southern boundary cluster composite boundary moisture sources and SLP synoptic sequence. Cluster 1 is on the bottom row and cluster 2 is on the top row.

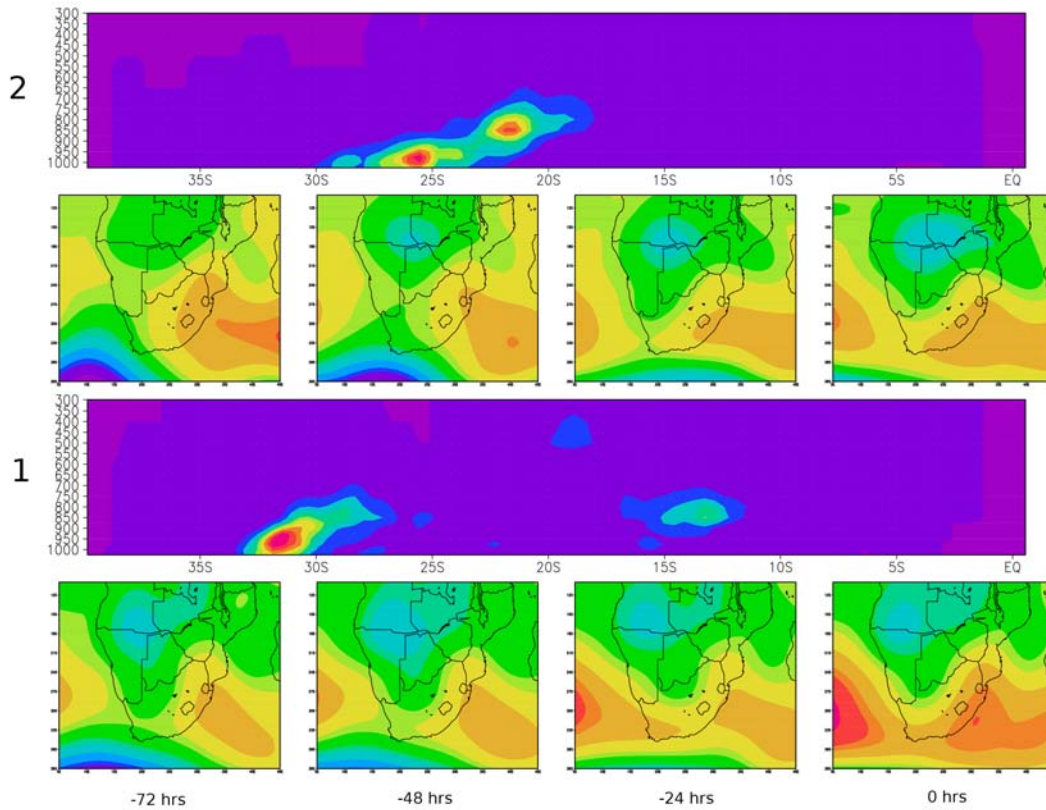


Figure 4.24: Domain SA4 eastern boundary cluster composite boundary moisture sources and 850 hPa synoptic sequence. Cluster 1 is on the bottom row and cluster 2 is on the top row.

eastern boundary clusters (Figure 4.24) show the expected northern and southern sources with the SLP and 85hPa circulation fields identifying similar dynamics. The SWIO high pressure system is responsible for the initial transport of moisture across the boundary and into the continent while a strengthening continental low pressure drives the later moisture convergence and produces the instability required for precipitation. The western boundary (Figure 4.25) shows similar dynamics to those for the previous domains with a mid-latitude wave passing to the south of the country. Clearly this westerly source needs further investigation as the synoptic sequencing is providing insufficient information in order to diagnose the dynamics involved.

The southern boundary (Figure 4.26) is actually quite an important source of moisture for this domain, most likely due to the southerly transport of moisture under the influence of ridging anti-cyclones to the south. The cluster results confirm this with longitude of the source dependent on the positioning of the ridging high pressure system.

### 4.3 Discussion

The magnitude of the western boundary source is curious as it is far higher than expected given previous studies (D'Abreton and Tyson [1995, 1996]). In fact no other study has identified such a high level moisture source at such a high latitude. The current state of the Lagrangian model does not easily allow an aggregate picture of the actual Lagrangian parcel trajectories for a whole season. While parcel trajectories can be retained from a model integration the volume of trajectories archived produces some serious visualization and even computational challenges. A short test case of a rainfall event on the 16th of February 1988 was performed and the trajectories retained. Figures 4.27 shows a vertical cross section of the trajectory pathways for all trajectories that pass through the western boundary.

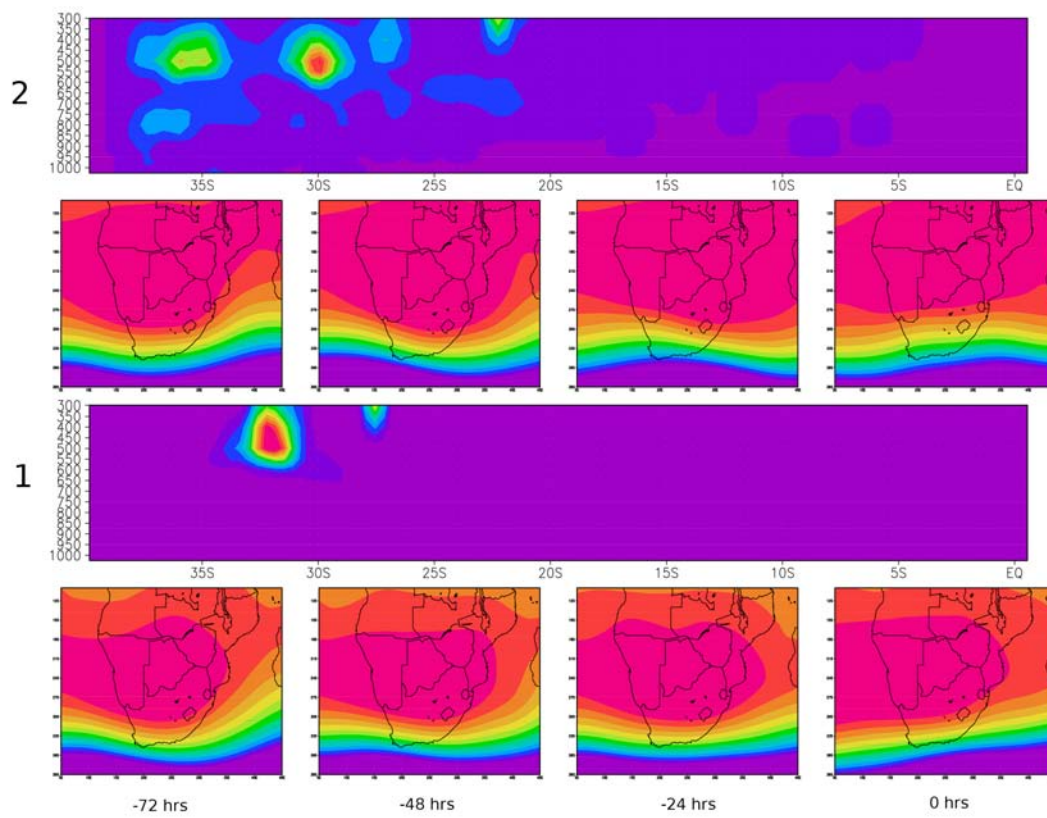


Figure 4.25: Domain SA4 western boundary cluster composite boundary moisture sources and 500 hPa synoptic sequence. Cluster 1 is on the bottom row and cluster 2 is on the top row.

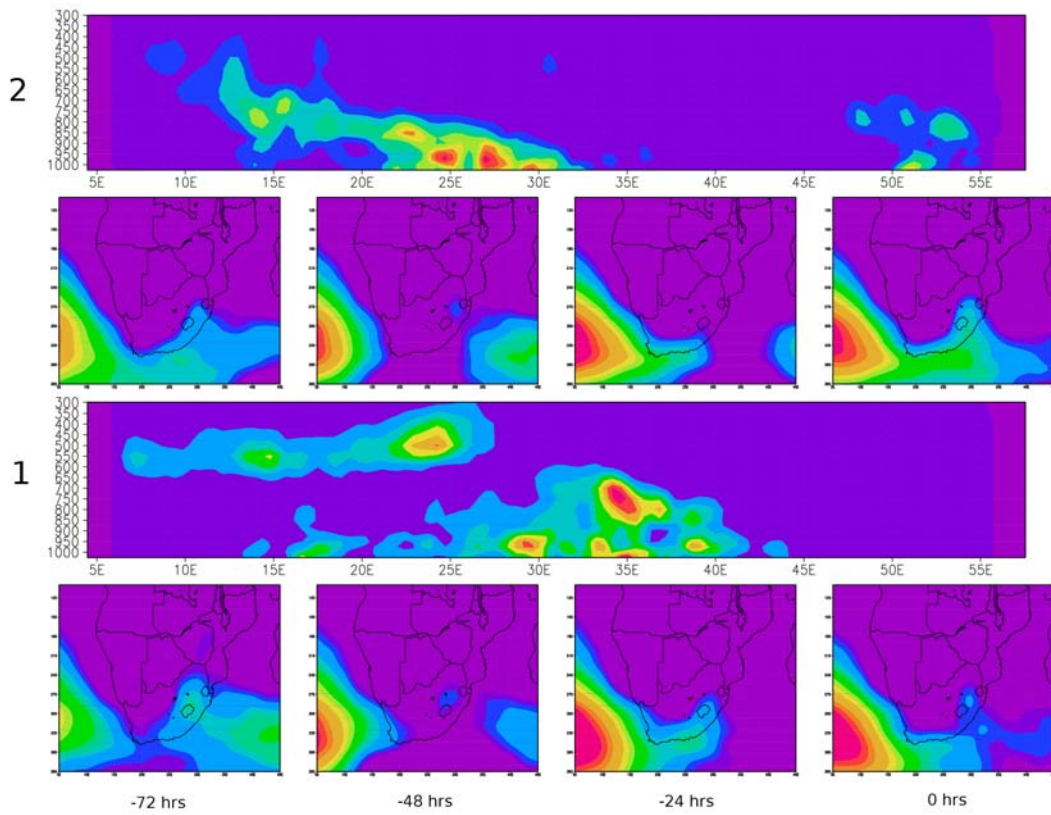


Figure 4.26: Domain SA4 southern boundary cluster composite boundary moisture sources and SLP synoptic sequence. Cluster 1 is on the bottom row and cluster 2 is on the top row.

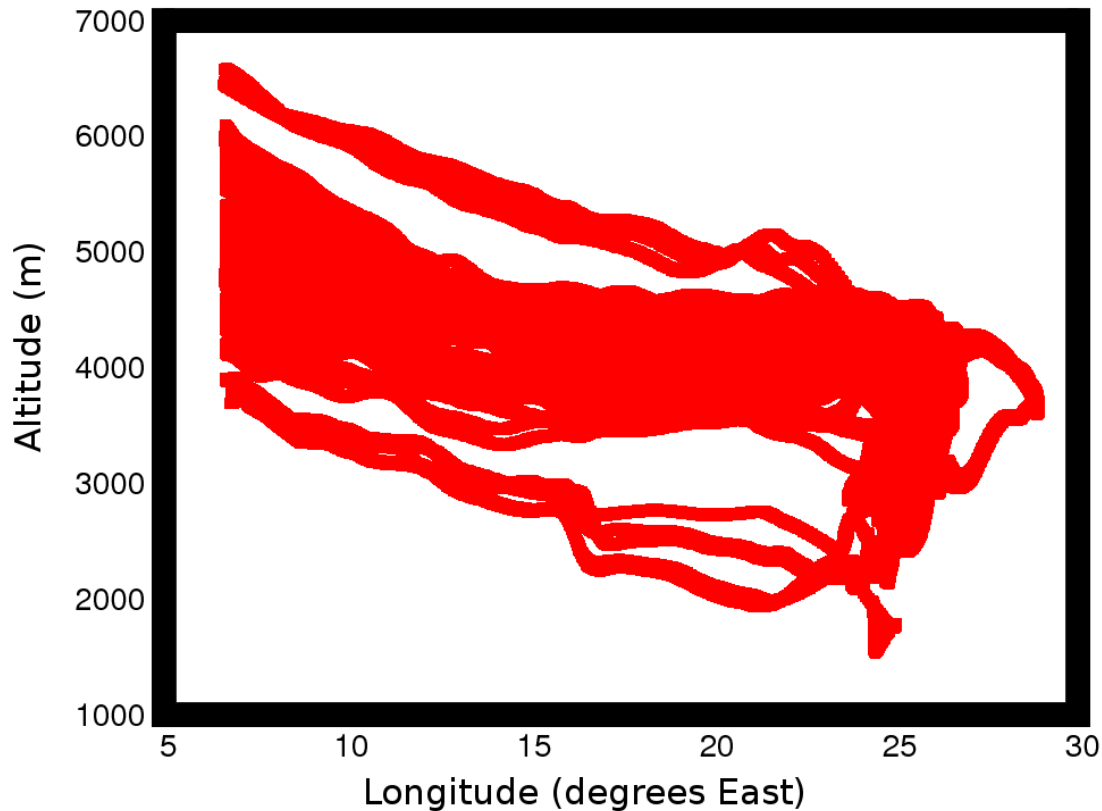


Figure 4.27: Latitudinal cross section (height (m) versus longitude) of Lagrangian parcel trajectories originating at the western boundary and arriving at target domain SA2 for event of the 16 Feb 1988

A strong subsidence of parcels can clearly be seen between the western boundary at 5°E and the precipitation target domain at around 25°E. The final apparent sharper descent is actually a result of a direction change as in this case most the parcels enter the target domain from the North.

The final altitude of the bulk of the parcels does fall within the altitude range suggested as the dominant source of moisture for precipitation over the continent (D'Abreton and Tyson [1996]). However, air parcels from such a high altitude do not contain a great deal of moisture and so it would still seem to be unusual for such a large fraction of the attributed source moisture to be sourced from such a location. If the mid-latitude jet stream is playing a role then the higher wind speeds could compensate for the lack of specific moisture content. However, the other factor to be considered is the attribution coefficient and losses to upstream precipitation events. While existing understanding and analysis does indeed suggest that the eastern boundary and ocean surface should provide the vast majority of source moisture, losses to upstream (and particularly oceanic) precipitation events are likely significant. Continental rainfall upstream of the target domains can often be extensive and it is highly likely that the Lagrangian parcels are losing a great deal of moisture before they arrive at the target domain. A similar explanation is arrived at for a study of moisture sources for the Amazon region (Drumond et al. [2008]). The western boundary source however, provides moisture from the opposite direction and passes through relatively dry areas and so it is likely that very little moisture is lost to upstream precipitation. Whether this is indeed an explanation for this moisture source would need to be confirmed through further more detailed study of the dynamics involved.

## 4.4 Conclusions

We can conclude by stating a number of observations regarding the results as well as proposing ideas for further investigation. Perhaps the most interesting general result is the relatively small contribution that the RCM boundaries play as diagnosed moisture sources. It is quite likely that this is largely a function of the attribution coefficient implemented in the Lagrangian model. A general characteristic of this attribution coefficient is that it decreases quite rapidly as the Lagrangian parcels move away from the precipitation target domain. The result is that near the RCM boundaries this coefficient is typically quite small and so the RCM boundary sources are greatly reduced as attributed moisture sources. The attribution fraction reduces more rapidly in areas with heavy precipitation. The MM5 RCM seems to overestimate rainfall over more tropical and eastern areas (Tadross et al. [2006]). This could cause decreases in the attribution coefficient in this area resulting in a reduced source attribution from the RCM boundary in that vicinity. However, while there are indeed uncertainties in the magnitudes of the attributed moisture sources, the effect of en-route precipitation events is still to reduce the amount of moisture that actually remains in the air mass between the source and the final target precipitation event. This is a factor that has not been accommodated in previous moisture transport studies in the region and is a likely one explanation for the different results presented here.

The significant diagnosed western boundary high level moisture source may be, at least partly, a function of the precipitation diagnosis methodology used in the Lagrangian model and the associated uncertainties. However, the Lagrangian trajectories themselves do confirm a subsidence of parcels from the 500hPa level at the western boundary to 750hPa level at the location of the target domain, suggesting that a flow of moisture is possible between this source and the target domain. The uncertainties around the magnitude of this source may be large, but it is certainly an area for further investigation and the role of the mid-latitude jet stream is worth considering in more detail.

The role of the southern boundary as a moisture source is also greater than expected, particularly for the more northerly domains such SA4. Much of this source is associated with the passage of ridging high pressure systems to the south of South Africa. Of particular interest is the importance of the southern boundary for the eastern most target domain. We would have expected this eastern most domain to source most of its moisture from the eastern domain boundary. The results however, indicate that the southern boundary, through the influence of ridging SAHP systems plays a more significant role as moisture source.

The commonly accepted moisture source of the Indian Ocean, both south west and tropical are well represented. Transport from the SWIO is associated with the variations in the SWIO high pressure system as well as interactions with the continental low and South Atlantic high pressure ridging events. Moisture transport is strongly coupled to the fluctuations in the location and intensity of the high pressures systems as is the case with the land and ocean surface sources.

Generally, the more southern domains draw more from the western and southern boundary sources whereas the more northern domains draw moisture from the eastern boundary. This is largely due to the relative roles of the mid-latitudes and tropical and sub-tropical circulations such as the continental heat low.

This chapter has served to present the results of the Lagrangian moisture source attribution model regarding the role of the RCM domain boundaries as moisture sources. This concludes the results section of the thesis and the remaining chapter will close the thesis with a discussion of the methodology and the results and highlight future areas of research or exploration.



# Chapter 5

## Discussion

### Introduction

The discussion to follow is intended to draw together the various components of the thesis and develop concrete conclusions and outcomes. These outcomes will mirror the initial thesis and objectives proposed in the introduction of Chapter 1.

The first component of the thesis is that a Lagrangian moisture source model is an effective method to explore regional moisture source dynamics. The second component of the thesis is that the regional land and ocean surface plays an important role as a source of moisture for precipitation in the southern African region.

We shall therefore deal with these two components in two sections in this chapter. The first section will deal with the Lagrangian model, its strengths and weaknesses, as well as possible avenues for future application and improvement. The second section will deal with the model output results presented in chapters 3 and 4 and draw some conclusions about the regional moisture source dynamics of southern African. However, to start with, it is useful to recap the major aspects of the preceding chapters.

- Chapter 1 described the thesis that the regional and ocean surface plays an important role a source of moisture for precipitation in southern Africa and specifically within sub-tropical South Africa. Existing methods used to explore regional moisture transport and dynamics were described with associated advantages and disadvantages. The limitations identified with the existing methods form a basis for the second component of the thesis which is that an alternative methodology based on Lagrangian trajectories is a suitable means of identifying regional moisture sources. Current understanding of the regional moisture transport and moisture sources were also described with more distant ocean sources being identified as the generally accepted dominant moisture source for the region.
- Chapter 2 described the development of the proposed methodology to diagnose regional moisture sources and sinks. The methodology incorporates an attribution coefficient which captures the effect of along path precipitation on the relative contribution of upstream moisture sources to a final downstream target precipitation event. An RCM is used to drive the Lagrangian moisture trajectories in a time reversed direction (moisture target towards moisture source) for computational efficiency. The resultant moisture source diagnoses are generated as spatial plots of the absolute moisture contributions of each location with the RCM domain towards the target precipitation event. The moisture source maps are generated on hourly time intervals allowing detailed analysis of individual precipitation events. Equivalent source maps are produced for each 2-dimensional plane formed by the RCM boundary surface.

- Chapters 3 and 4 presented the results generated by integrating the Lagrangian model over two austral summer seasons over southern Africa. The results are divided into two with Chapter 3 presenting the regional land and ocean source regions, and Chapter 4 presenting the boundary source maps. Significant results from Chapter 3 include the large role of the regional land surface as a moisture source for regional precipitation as well as the importance of the regional ocean, also as a moisture source, under certain synoptic conditions. Results from Chapter 4 highlighted a previously unidentified high level (500hPa) westerly moisture source around 35°S. Previous studies have associated air sourced from this region with dry conditions over the interior. Other boundary source results confirm previously identified easterly moisture sources but also identify significantly more detail and complexity than previous studies. Of particular interest is the relatively small role, in absolute terms, of the easterly boundary moisture sources.

The following section will discuss the Lagrangian model itself within the context of the original thesis and associated objectives. The intent of the section is not to repeat the discussion in Chapter 2 but rather to determine how well the original thesis is supported by the research undertaken.

## 5.1 The Lagrangian Attributed Source Model

The methodology presented in Chapter 2 combines an RCM with a Lagrangian moisture source attribution model. The test case presented in Chapter 2 demonstrated the ability of the model to identify moisture source regions for a particular precipitation event. The magnitudes and spatial patterns of the identified source regions were, in some respects unexpected given the existing literature. However, further exploration of the test case dynamics and moisture balances suggested that while indeed unexpected, the results were certainly defensible and consistent with circulation responses.

The fairly unique combination of a high resolution RCM coupled to a Lagrangian source attribution model does seem to offer an effective tool enabling us to unpack regional moisture sources and transport. The model allows analyses from small spatial scales to large regional scales as well short time scales through to longer seasonal time scales. This ability to explore a system across time and space scales is important as the climate system is composed of both short time scale events as well as longer time scale variability. Each time scale influences the other time scales and the same concept holds true for spatial scales (Meehl et al. [2001]).

Of course the challenges of validating such a model are extensive as has already been highlighted. Uncertainties exist within the Lagrangian trajectory component of this model due to a number of factors. There are distinct uncertainties in the RCM driving wind and moisture fields due to a lack of observational data, particularly at higher altitudes and under convective conditions. The RCM moisture dynamics are also a source of uncertainties though it has been identified that the RCM precipitation magnitudes are generally higher than observations. The resolution of the RCM driving fields is limited to 50km horizontally. These fields are therefore interpolated to the Lagrangian parcel location introducing another source of uncertainty. Temporal interpolation is also done as the RCM fields are archived at an hourly interval while the Lagrangian integration occurs at a 15 minute interval. Finally, the Lagrangian integration itself is a numerical approximation, all be it a fairly high order approximation, which has been shown to be suitable under similar conditions in air pollution type studies.

Nonetheless, none of these factors are likely to present a substantive modification of the conclusions that emerge from the analysis.

We shall now explore some of these sources of uncertainty in more detail. We have already determined that the model produces sensible results. The purpose of exploring the uncertainties involved is to gain a better understanding of them, which will inform our discussion of the model results in section 5.2 below.

### 5.1.1 Regional Climate Model

The ability of the PSU/NCAR MM5 RCM to produce a realistic representation of the southern African climate is well described in a number of papers (MacKellar et al. [2007, 2009], Tadross et al. [2006]) with particular emphasis on precipitation and temperatures. The model typically produces too much rainfall over much of the region particularly in the eastern and north eastern areas (figure 2.2).

An analysis of the RCM diurnal cycles of radiation and precipitation suggest that the model initiates convective precipitation too early in the day and generally is rather quick to precipitate moisture out of the atmospheric column (Tadross et al. [2006]). The Betts-Miller convective scheme does appear to produce a diurnal cycle closest to observations when compared to other variables. This was the main rationale for its selection for this experiment .

The propensity to produce rainfall is potentially problematic, however, the spatial distribution of rainfall in the region is generally well represented which suggests that the regional dynamics are being captured. Reproduction of the magnitude of specific events is not always consistent with observations, however, the challenges of comparing station observations to RCM gridded output fields does raise many problems for validation, particularly for smaller localised events. There is little that can be done to improve the performance of the RCM within the scope of this study and for the purposes of this study it has been selected as the best possible source of high resolution climate information. Certainly there is significant work still to be done in the development of RCMs.

Nonetheless, the model is clearly a least a plausible representation of the regional climate dynamics if not an exact representation of the particular events or seasons simulated. As such, it is a viable resource for exploring the nature of relative moisture sources within the region.

### 5.1.2 Lagrangian model skill

The Lagrangian model itself is grounded on classic trajectory modeling theory. The intent of the model development was not to advance trajectory modeling itself but rather to use the extensive experience of much preceding work dealing with this method and extend it for this application.

The absolute accuracy of trajectory models generally is subject to the uncertainties as discussed above. However, the challenge of validation of the trajectory modeling component is perhaps an even greater problem than that of the RCM precipitation. There are only two real methods of validation. The first is a direct validation through physical balloon tracking observations. This has been done for a trajectory model forced by 6 hourly ECMWF re-analysis wind fields at a 2° horizontal resolution (Baumann and Stohl [1997], Stohl et al. [1998]). Even with such relatively coarse spatial and temporal resolution fields the resultant trajectories strongly resembled observed balloon tracks over a period of about 3 days after which the trajectory tracks began to diverge markedly from the balloon tracks. Further work identified the temporal resolution of the driving fields as being the source of greatest error in the trajectory tracks, even above the spatial resolution. While this obviously depends on the specific circulation dynamics it does seem to be a fairly general result and motivated the selection of hourly output fields from the RCM in this study. Koffi et al. [1998] performed a similar validation, using a higher resolution RCM output field at 0.5° spatial resolution, and found very good agreement between trajectory integrations and constant volume balloons. Riddle et al. [2006] However, shows some remarkably high trajectory model errors (up to 34% after 12 hours) when compared to balloon tracks under conditions of strong synoptic systems such as a low level jet and complex flow patterns.

The second validation method is that of source receptor validation. This has been done in pollution tracking experiments which provide a unique opportunity to validate the trajectory methodology (Seibert and Frank [2004]). The method depends on observations of both a particular pollution source or event, and a spatially dispersed observations

of pollution concentrations. The trajectory model attempts to simulate the movement (as well as the diffusion and precipitation) of the particular pollutant and predict the measured concentrations at the observation sites. It is then possible to compare the predicted versus observed pollution concentrations. While such a validation is subject to its own limitations including observational errors, and is largely concerned with lower atmosphere dynamics, it does serve to confirm the viability of the method. Results indicate that the Lagrangian trajectory based pollution tracing methodology is able to generally capture the transport of pollution from source to observation site.

Recognising the difficulties involved in validating trajectory paths, Kahl [1996] attempted to develop a means of quantifying the potential trajectory error given a synoptic state. The results were not satisfactory or suitable for general application.

Trajectory modeling is a mature method and the implementation used in the Lagrangian model is robust and well documented. There is arguably little that can be done to improve the numerics used. Therefore we must consider that the trajectory modeling component of the lagrangian model is fairly robust. Uncertainties that do exist are a result of the driving data rather than the trajectory method itself. We shall therefore move on to discuss the primary source of uncertainty in the driving fields.

### 5.1.3 Unresolved convective motion

Perhaps the greatest source of uncertainty in the Lagrangian model integration, and the most relevant for this particular methodology, is that of vertical motion. As is described fully in Chapter 2, the RCM vertical motion diagnostic fields do not represent the full vertical motion captured by the model. This is because smaller scale convective motion is represented through the convective parameterisation and these motions are not reflected in the grid scale output fields. The impact of this source of error on the Lagrangian integration is difficult to determine. While convective vertical motion can be strong, it typically only occurs over small spatial scales. Even under synoptic conditions conducive to convection, the actual spatial extent of strong convective uplift is relatively small. Lagrangian trajectory models are used extensively for pollution tracking studies which, while typically focused on more stable synoptics, are also subject to convective motions. While some of these models incorporate a convective parameterisation in order to capture such motions, inconsistencies with the forcing models convective parameterisations could potentially cause problems. Therefore, many trajectory models ignore convective motions not captured by the forcing wind fields Stohl [1998].

However, we cannot thereby conclude that convective motion is not important in this methodology or in our consideration of the results produced. Within the southern African context a great deal of precipitation is convective in nature and indeed within the target domains selected for this study the vast majority would be so. We must therefore pay special attention to the possible impacts of this source of uncertainty in the model and in particular to the convective parameterisation itself.

The Betts-Miller convective parameterisation uses a moisture profile relaxation approach (Betts [1993]). This is based on the idea that convection in the atmosphere is a result of a buildup of convective potential energy as a result of surface heating. The convective potential is a function of the vertical temperature and humidity profile. The result of convection itself is always to convert an unstable or energetic vertical profile to a stable profile. The Betts-Miller method therefore attempts to move moisture and heat vertically in the atmospheric column in such a way that the vertical profile tends towards some standard observed vertical profile. It does not therefore explicitly calculate vertical velocities or updrafts and downdrafts as do other schemes such as Kain Fritsch (Kain [2004]).

With this basic understanding of the convective parameterisation in mind, we can consider the scenario of a trajectory parcel passing through an RCM grid cell where convective rainfall is being produced by the parameterisation. The parameterisation will remove moisture and heat from some lower levels and add it to some higher levels. A parcel

in the lower levels would therefore experience a loss of moisture (an increase in a time reversed integration) while a parcel in the upper levels would experience an increase (decrease in time reversed integration). The precipitation diagnosis would therefore diagnose precipitation for the lower parcel but not for the upper parcel. This is however, arguably a correct diagnosis as the source of the moisture contributing to the precipitation is actually the lower level and not the upper level. In this simplistic example it therefore seems that while vertical motions are not explicitly captured, the resultant diagnosis is possibly not problematic. Of course, in reality, convective rainfall is likely to be more complex with multiple levels of moisture involved and, more critically, a complex time evolution. It is still possible therefore that the altitude of precipitation diagnosis has a degree of uncertainty.

Convection will also influence the horizontal track of a trajectory parcel. If the altitude of parcel is incorrect due to unresolved vertical motions, then the horizontal wind field driving the parcel motion will also be incorrect and hence the track will be incorrect. This situation is impossible to resolve given the constraints of the methodology and we can only rely on the fact mentioned earlier, namely that the fraction of horizontal area actually experiencing significant convective vertical motion is relatively small. Clearly in tropical areas this is less true and could be a significant factor in the results. It is also important to note that convective motion results in both upward motions and mass compensating downward motions. We cannot therefore begin to suggest whether the parcel trajectories would be biased to a higher or lower level. The approach taken is therefore the same as many other trajectory based methods which is to ignore unresolved convective motions and acknowledge that they add to the general uncertainty of the method.

#### 5.1.4 Impacts on attribution coefficient

In the previous section the issue of unresolved vertical motions and the potential impact on precipitation diagnosis and trajectory paths was discussed. The impact of all trajectory uncertainties, including unresolved vertical motion, on precipitation diagnosis has a further effect on the attribution coefficient. The attribution coefficient is modified by the magnitudes of the along trajectory precipitation as diagnosed by the Lagrangian model. Therefore, uncertainty in the precipitation diagnosis will have an impact on the rate of decay of the coefficient, which in turn impacts the absolute attribution of all moisture source regions. We therefore need to be very aware of this relationship in observing the results.

As noted in Chapter 2, the magnitudes of the Lagrangian precipitation diagnoses are lower than the RCM generated precipitation magnitudes. Clearly the Lagrangian model is underestimating precipitation in comparison to the RCM. This is not too surprising considering the stringent conditions imposed on the precipitation diagnosis to avoid spurious diagnosis, as described in section 2.5.2. These conditions were largely determined by trial and error as well as by consideration of the precipitation process itself. The objective was to eliminate the diagnosis of precipitation in cases where the RCM was not producing precipitation. In contrast, the RCM precipitation magnitudes are significantly higher than observed magnitudes, which is a known issue with this RCM as well as other RCMs for this area. The Lagrangian model magnitudes are therefore closer in magnitude to the observed magnitudes. We cannot argue that the Lagrangian model is more realistic, just that it underestimates the magnitudes and therefore coincidentally produces magnitudes closer to the observations.

However, this is an important observation because of the interaction with the attribution coefficient. As will be discussed in a later section, a significant result highlighted in Chapter 3 is the high attribution of nearby land surface sources relative to the RCM boundary sources. If the Lagrangian precipitation magnitudes were excessively high it could be argued that this attribution result is skewed by the high precipitation diagnosis. Indeed, if the raw RCM precipitation values were used to degrade the attribution coefficient then the attribution coefficient would degrade even faster resulting in even higher attribution given to the local land surface. We will refer back to this when we discuss the results in section 5.2 below.

### 5.1.5 Evaporation diagnosis

As for the diagnosis of precipitation, evaporation diagnosis is based on the along trajectory changes in parcel moisture content as interpolated from the RCM fields. And as for precipitation, evaporation from the surface, transpiration through plants and critically, mixing with the turbulent boundary layer are represented by parameterisations in the RCM. This last component, turbulent mixing, is extremely important as it is responsible for moving moisture away from the surface. The turbulent mixing air motions are not represented in the RCM fields. The Lagrangian trajectory pathways therefore pass through this turbulent mixed layer unaffected by turbulent mixing. Lagrangian evaporative gains are based on the assumption that increases (decreases in a time reversed integration) in the along trajectory parcel moisture are a result of a combination of surface evapotranspiration and vertical mixing of that moisture. This is a reasonable assumption as few other sources of increased moisture can be envisaged beside those resulting from trajectory integration errors. A minimum moisture change threshold is imposed in order to reduce such errors as described in section 2.5.4.

The critical factor in the evaporation diagnosis is the height of the top of the turbulent mixing layer, or the maximum height above which increases in parcel moisture cannot reasonably be attributed to surface evapotranspiration. The decision was made to use the RCM planetary boundary layer (PBL) height and a 1000m height above the surface as two maximums. Whichever is the lower is used as the height of the mixed layer. PBL height is a useful diagnostic but seems to incorporate the vertical mixing resulting from deep convection as well as boundary layer mixing and so can reach very great heights (greater than 5000m above the surface) under strong convective circumstances. We have already dealt with the problem of unresolved convection and difficulty of interpreting moisture changes under convective conditions. For evaporation diagnosis we wish to ignore the scenario of evaporated moisture being carried too rapidly to great altitudes by convection. We therefore apply a maximum cap of 1000m above the surface on the evaporative gain diagnosis. The 1000m level is based on the height of the PBL produced by the RCM under non-convective conditions and seems to be a reasonable level. During the night the PBL height typically drops to very low altitudes or even to the surface. The result is an almost total limit on diagnosis of evaporative gains during the night which is considered to be realistic.

It is hard to determine if the Lagrangian evaporation diagnosis would tend to under or over estimate evaporative gains. It is likely, given the previous discussion of strong convection, that under such a scenario it would under estimate moisture gains as moisture would be moving away from the surface and above the 1000m cap faster than the Lagrangian model can capture within its 15 minute integration time step. The rough moisture budget analysis presented in section 3.4.2 suggests that the Lagrangian diagnosis of evaporative gains is significantly less than the RCM total evaporation (latent heat flux) field magnitudes. Ignoring convective motions most likely results in an underestimation of evaporative gains under strong convective conditions. Once again, despite comprehensive validation being impossible, it is reasonable to assume that the parameters of the methodology are rational and within the realms of reality.

The issue of rain re-evaporation has been discussed extensively in sections 2.5.2, 2.5.4, and in the context of the case study in section 3.4. While rain re-evaporation remains a possible source of over-estimation of evaporation and hence would bias the results towards local sources of moisture, the case study moisture budget analysis does seem to suggest that the attributed evaporative moisture source magnitudes align well with the RCM surface latent heat flux fields giving us some confidence that rain re-evaporation. How rain re-evaporation would skew the results towards more local attribution of moisture sources and should be born in mind in considering the results.

With a thought towards the later discussion of the model results, if we consider the likely scenario where the Lagrangian model underestimates the evaporative moisture gains the result would be a reduced attribution of land and ocean moisture source regions. This would result in the RCM boundary moisture sources being more highly attributed than the land and ocean surfaces. It therefore seems unlikely that the strong attribution of the regional land

surface is a result of over-estimation of evaporative moisture gains and if anything it is likely that these gains are being underestimated.

### 5.1.6 Future Developments

There are a number possible avenues for future development of the modeling system described. The first relates to the RCM component itself. The problem of unrepresented convective motions has been discussed extensively and identified as an important source of uncertainty in the Lagrangian model integration. A possible solution to this problem would be to modify the RCM to output more diagnostics relating to the convective processes. Ideally some indication of the vertical motion of air masses as determined by the convective parameterisation would be extremely valuable. However, the disadvantage of this approach, and a major reason why it was avoided, is that this modification would have to be done for each RCM and each convective scheme that one wanted to utilise. Another problem is that convective schemes such as the Betts Miller scheme are not physically based and so do not lend themselves to the production of vertical air velocities. Other schemes such as Kain-Fritsch would be better suited to such modifications.

As second possible avenue for future development relates to the Lagrangian model, and in particular the output of the model. It has become apparent through this study that greater detail about the moisture trajectories themselves would aid the analysis and interpretation of the output. An example of this would be the ability to isolate a subset of trajectory pathways associated with a particular source area. This would require archiving the full pathways of all trajectories in such a way as to allow such sub-setting to occur in a post-processing step.

A final possible avenue which is fairly ambitious, relates to some of the results presented. In particular, it would be very interesting to be able to trace moisture through multiple cycles of precipitation and evaporation in order to explore the transport of moisture across the continent through these cycles. The reason this is quite ambitious is that it would essentially require the development of a land surface scheme to determine the fate of precipitation. Not all precipitation is re-evaporated. In fact a great proportion is removed through run-off processes, both surface and subterranean. The RCM Land Surface Model simulates such processes and it might be possible to use the output of this parameterisation in order to determine the fate of precipitated moisture, however, the technicalities and practicality of such an analysis have yet to be worked out. Certainly such an analysis would allow the exploration of land/atmosphere feedbacks and systems that have yet to be explored.

### 5.1.7 Lagrangian Model Conclusions

The above discussion has highlighted a number of aspects of the Lagrangian model, its strengths and potential weaknesses as well as sources of uncertainty in the model results. Validation remains a singular problem as the lack of observational data with which to validate the RCM wind and moisture fields is critical. Validation of the resultant moisture source areas is also impossible as the methodology is motivated by the need for such information in the first place. However, model testing and variously analyses support the conclusion that the Lagrangian model is robust and the results are certainly defensible.

The discussion has highlighted the rationale of decisions made in implementing the model as well as the various sources of uncertainty. There are uncertainties that have been discussed extensively and these cannot be ignored. However, it would seem from the discussion above that the model could actually be biased towards diagnosing more remote sources of moisture rather than local sources of moisture. This is a result of its possible under-diagnosis of precipitation which impacts the attribution coefficient, and under diagnosis of evaporation which would reduce the attribution of land and ocean surfaces in favor of boundary moisture sources. This is a particularly important

consideration as we progress into a discussion of the results which have highlighted the attribution of local sources of moisture.

The problem of convection remains important and an area for further exploration and development, however, it is likely that the model as it stands still represents the majority of the moisture processes taking place despite its inability to directly diagnose convective motions. We are now in a position to move onto discussion of the model results described in chapters 3 and 4.

## 5.2 Discussion of the results

The analysis in Chapters 3 and 4 illuminates some key findings. Of particular interest is the high attribution of the regional land and ocean surfaces as well as the high level westerly moisture source. These two features of the regional climate system have not been strongly quantified in any prior work to the knowledge of the author and hence are significant results that deserve discussion. The following sections now explore these two features, initially separately and then examining the collective implications.

### 5.2.1 Land surface moisture sources

The original thesis proposed was that the regional land surface is an important component in the climate system and, specifically, that it plays an important role as a source of moisture for regional precipitation. This thesis stemmed from previous RCM based sensitivity studies (New et al. [2003], MacKellar et al. [2009]) which showed a strong climate response to perturbations in land surface characteristics such as soil moisture and vegetation cover. The thesis was deemed important as it offers a possible explanation for some component of the regional climate variability which, as it stands, is not clearly understood. If the regional land surface is an important component of the climate system and regional moisture feedbacks and dynamics affect the regional climate then this improved understanding offers opportunities for further exploration and the possibility of improving the seasonal scale forecast skill as well informing our understanding of a regional response to a changing climate.

The thesis may seem to have some contradictions with previous work such as Trenberth [1999a] which suggests that at a maximum, the regional precipitation recycling ratio is around 20% at the 1000km spatial scale (Figure 5.1). Other studies have suggested the regional land surface plays a relatively small moisture source role except in certain highly continental areas. However, the results in Chapter 3 strongly support the proposed thesis.

The results show that the regional land surface, under certain synoptic conditions and in certain areas, could be responsible for more than 50% of the moisture contributing to regional precipitation. Furthermore, the results seem to support a moisture leap frog transport processes. The evidence for this is seen in the overlap of one target domains moisture source region with the target area of the adjacent moisture target region. This means that the precipitation in one target domain is sourcing its moisture from the upstream target domain which in turn sources its moisture from its upstream target domain. The direction of this transport seems to track the dominant northerly and north-easterly low level winds generally associated with precipitation over central South Africa. Given the target domains selected for this study the moisture leap frog processes can be traced upwind towards Mozambique but no further.

The methodology was not designed to explore these multiple cycles of precipitation and evaporation that seem likely through a moisture leap-frog mechanism. It is possible that a more suitable or advanced methodology could more

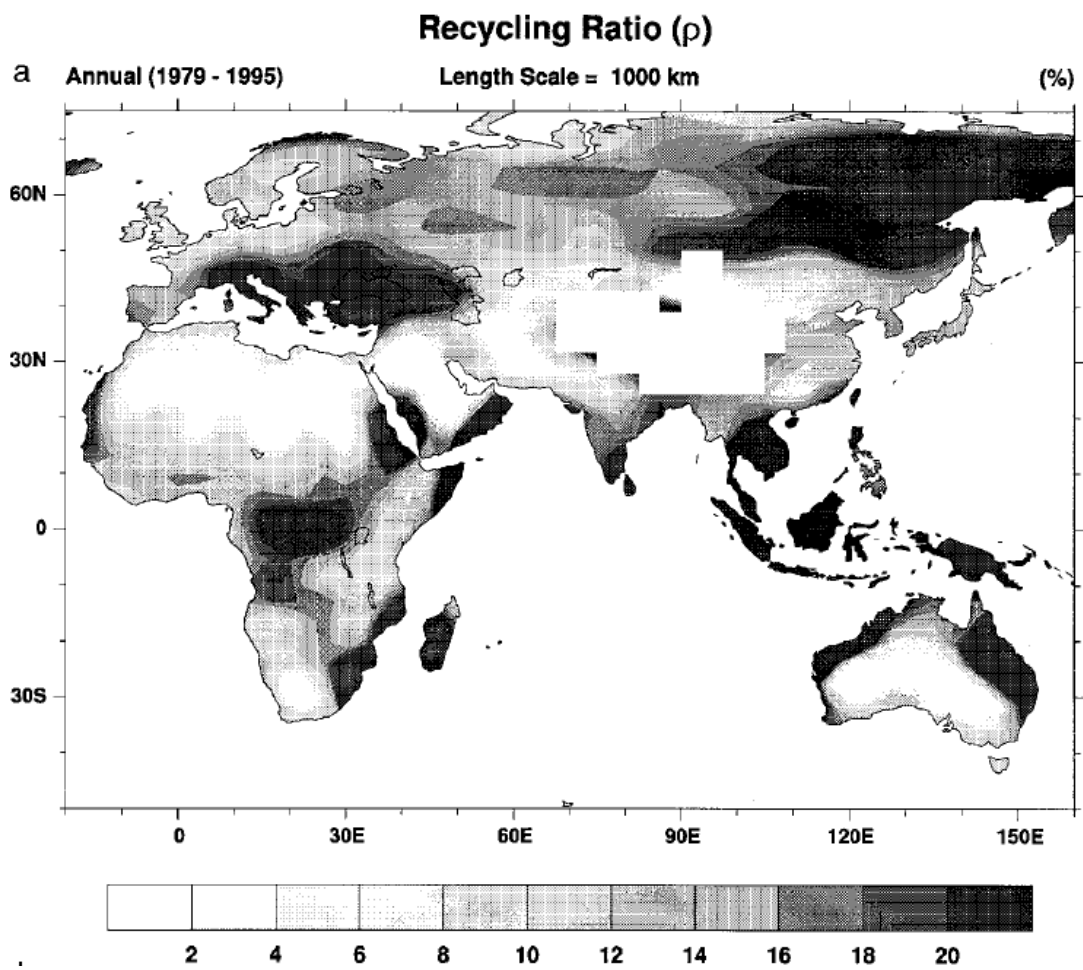


Figure 5.1: Annual mean precipitation recycling ratio (%) at 1000km spatial scale. Trenberth [1999a]

directly explore this process. A number of questions are raised which cannot be directly answered by the current analysis. The first question relates to the timing of the resultant transport. What is the residence time of moisture on or in the soil layer before it is evaporated? It would seem likely that this residence time would be a decay function of some sort with initial high soil moisture levels after a precipitation event resulting in high evapotranspiration rates and significant fraction of moisture being re-evaporated. However, as soil moisture levels return to seasonal mean values this evapotranspiration would decrease. However, the rate of re-evaporation would be dependent not just on soil moisture but also the climate conditions of cloud cover, temperature and wind speed. A more complex moisture transport model incorporating a soil moisture budget component would be required for such an analysis.

A second related question that emerges is that of the interdependence of precipitation events and the progression of events across the sub-continent. If, as the results suggest, moisture from a previous precipitation event re-evaporated from the land surface is an important source of moisture for downstream precipitation events then, by inference, a particular event could to some degree be dependent on upstream precipitation within a certain time frame prior to the event. If this is truly the case then the occurrence of precipitation events is not solely tied to the regional synoptics combined with more distant, oceanic moisture sources, but to occurrence of prior precipitation events. A number of methods could be used to explore this thesis with the most direct being a RCM sensitivity study that removes the effect of precipitation events from the regional soil moisture and instead imposes as climatological seasonal cycle of soil moisture at each grid point. Such an experiment would be more realistic than that of New et al. [2003] as not all soil moisture would be removed, only the peak values caused by particular events. A comparison of the evolution of precipitation events in such a simulation versus a standard simulation would provide some clues as to the interdependence of events.

Finally, returning to the work of MacKellar et al. [2009], the role of land surface cover and vegetation must also be mentioned. Certainly vegetation cover significantly impacts the rate of evapotranspiration as well as secondary factors such as soil moisture and water runoff. The lagrangian model could be a useful tool in determining the quantitative and dynamic impact of vegetation changes that a pure sensitivity study, as in the cited work, cannot.

### 5.2.2 Western boundary source

A previous study (Crimp and Mason [1999]), through a similar combination of RCM and trajectory analysis, notes the possible error of the tropical Indian moisture source view. That study did identify a moisture contribution from the high level westerlies for extreme rainfall over South Africa (Figure 5.3) though it was not as dominant as the results of chapter 4 identify, but nonetheless supports the credibility of the results presented here.

While a number of studies identify the tropical Atlantic as a source of moisture for central and southern Africa, the source identified is at too high a latitude and altitude to be a tropical Atlantic feature. In fact D'Abreton and Tyson [1996], through an air mass trajectory method, identify this air mass transport pathway with dry conditions over the interior of the country (Figure 5.2).

We must first consider the possibility that this result is an artifact of the methodology. There are two possible sources of error that could artificially produce such a source region. The first source of error is the diagnosis of precipitation. We have already discussed this process in the Lagrangian model, as well as the filters that limit the spurious diagnosis. In particular, requirement that the RCM grid cell be experiencing precipitation as well as the presence of rain liquid water at the level of diagnosis certainly constrain the diagnosis. However, the altitude of diagnosis does remain a possible source of error. A high level moisture source such as this suggests a high level precipitation diagnosis. The case study event in Chapter 2 that analyses a single period where this moisture source is particularly strong does seem to indicate that the actual precipitation diagnosis occurs at much lower levels, predominantly below 700hPa which agrees with D'Abreton and Tyson [1995](Figure 5.4).

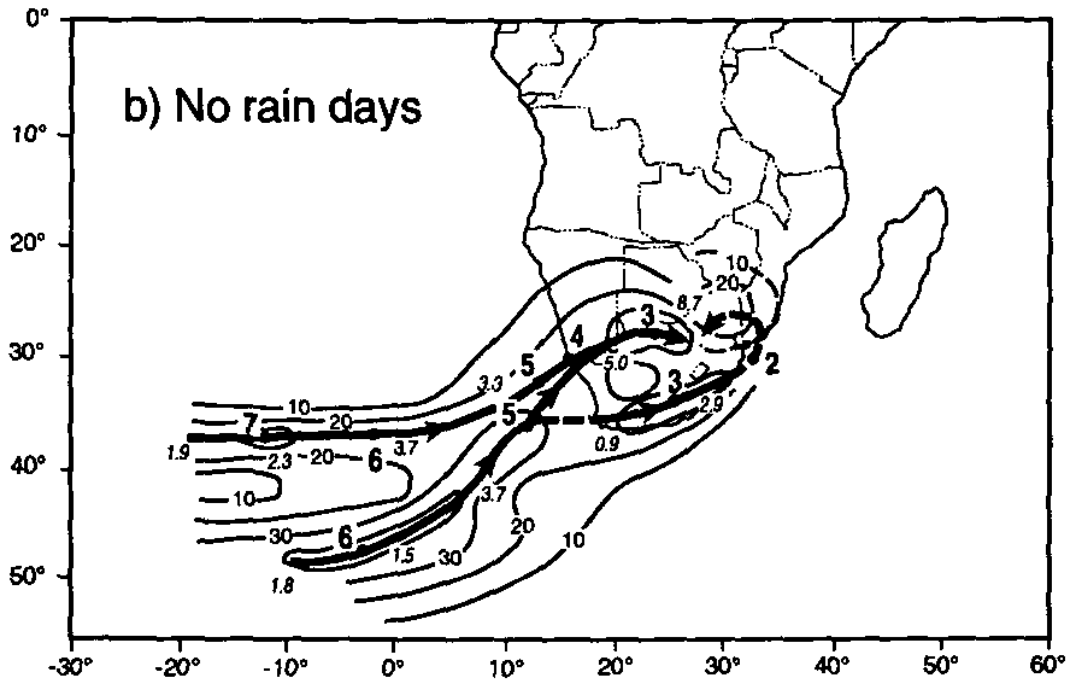


Figure 5.2: January mean backward trajectories for north west South Africa for dry days over the north eastern parts of South Africa. Contours represent percentage occurrence of trajectories. Thick lines represent the maximum frequency pathways. Large numbers indicate time of trajectory travel in days and small numbers indicate the average trajectory specific humidity ( $\text{g.kg}^{-1}$ ) (D’Abreton and Tyson [1996])

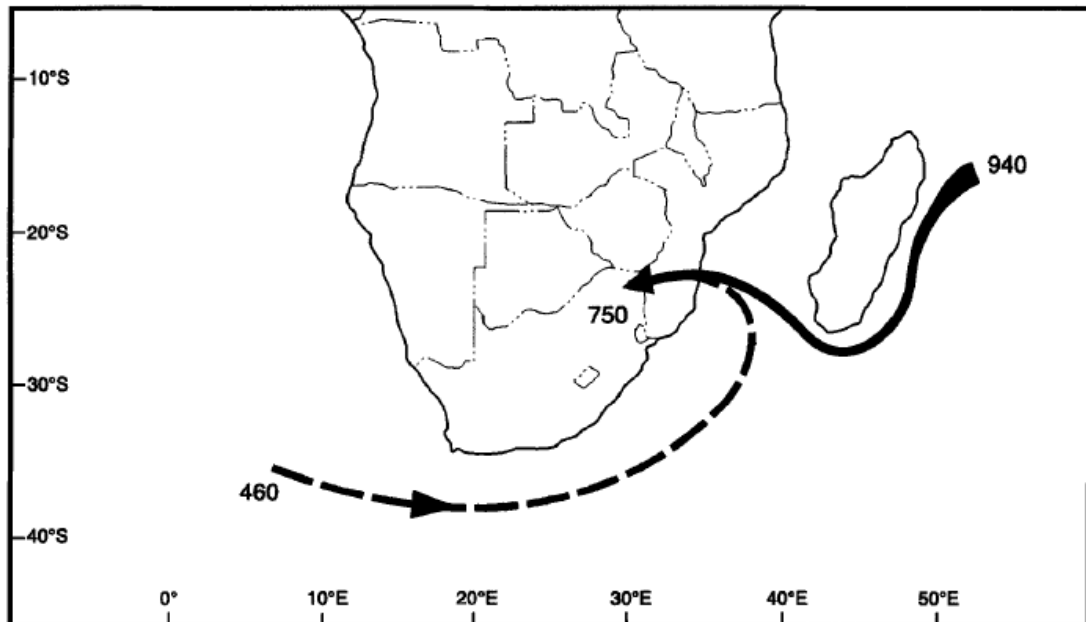


Figure 5.3: Schematic diagram showing the main (solid) and secondary (dashed) pathways of ten-day backward trajectory clusters from a point centered over the northern interior (23 S, 30 E). The trajectories were initiated at 12:00 UTC on 14 February 1996 at the 750hPa level, which is the time of a significant precipitation event. The numbers indicate the approximate starting and ending altitudes in hPa (Crimp 1996)

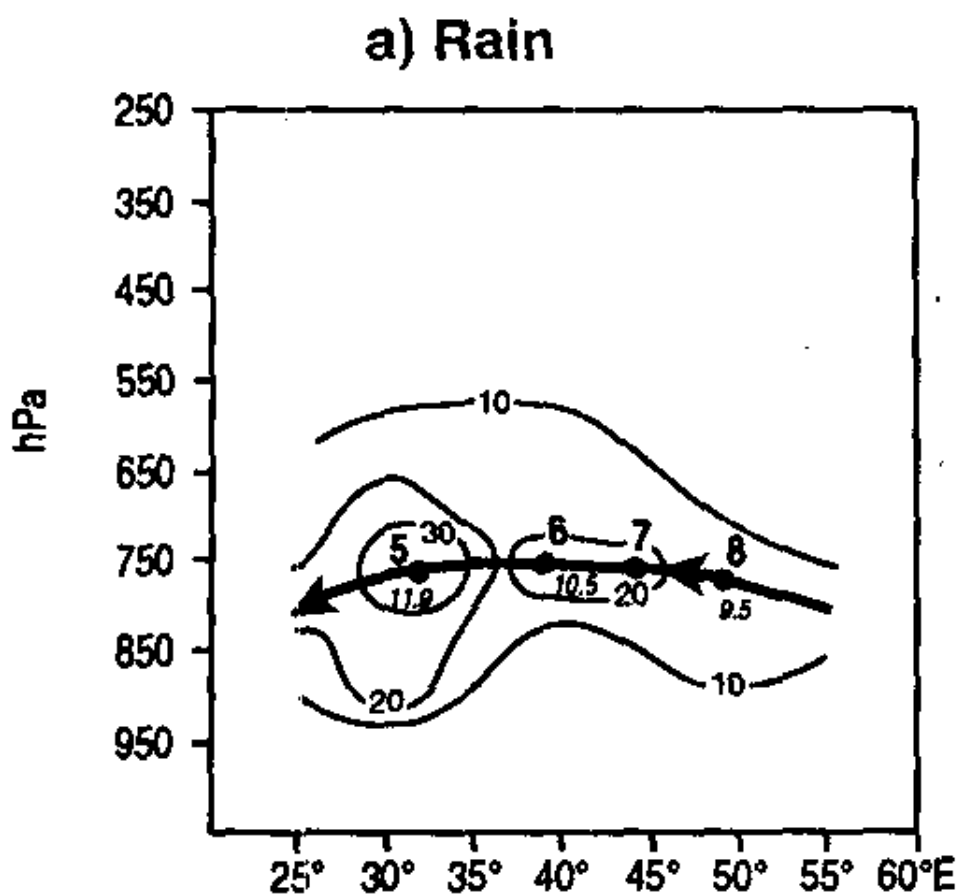


Figure 5.4: January trajectory fields for rain days for the north west of South Africa. Contours represent frequency of occurrence of trajectories. The thick line represents the highest frequency trajectory. Large numbers represent travel time in days and small numbers indicate specific humidity ( $\text{g.kg}^{-1}$ ) (D'Abreton and Tyson [1996])

The second possible source of error is the vertical velocity field driving the trajectory integration. The case study shows a fairly rapid descent of the moisture pathway from the 500hPa level at the boundary to the 700hPa level and possibly lower at the target event. Analysis of the RCM vertical velocity fields (not shown) do support such a descent over the time period and distance in question. Of course validation of the RCM vertical velocity fields is difficult with little or no observed data. The circulation dynamics at play at the time of the case study would suggest a general subsidence over the western half of the country under the influence of the South Atlantic high pressure system.

One of the challenges identified here is the disaggregation of moisture sources in the Lagrangian moisture fields. It would be useful to be able to plot the 3 dimensional atmospheric moisture field associated with a particular source region and hence analyse the moisture transport plume associated with each source field. The time reversed methodology, selected for the reasons stated in Chapter 2, makes this particularly difficult as the moisture source is only identified at the end of the trajectory integration. While the trajectory parcels are en-route and contributing to the Lagrangian moisture field the sources regions are not yet known and hence no separation of the moisture field can be done. A retrospective analysis of trajectories is possible, however, the computational demands limited such an analysis to short case studies. This is certainly an area for future improvement given increased computation resources and improved implementation.

The consistency of the western boundary moisture source through the months and across the target domains is significant. It appears that rather than being associated with one or two particular events as in the cases identified in Crimp and Mason [1999], it actually is a consistent source for most events. While much more work needs to be done to determine the dynamics of such a moisture feed and to verify the methodology, the implications for the understanding of the South African moisture transport dynamics is potentially large.

### 5.2.3 Circulation Linkages

Besides the identification of moisture sources, the results in the previous chapters also include associated regional circulation patterns. These associations are captured in two ways in the results. Firstly, the monthly regional mean circulation anomalies have been calculated by differencing each months synoptic state from the respective seasonal mean state. The monthly mean moisture source regions can then be viewed in light of these circulation anomalies. Secondly, the mean synoptic sequence associated with each moisture source region identified by the clustering analysis allows a more detailed exploration of regional synoptic sequencing and moisture sources. These associations enable us to explore the impact of regional circulation on the moisture sources for the target regions. A sufficient understanding of these linkages allows us to infer the impact of longer term circulation changes on regional moisture source dynamics. For example, changes in moisture source dynamics under circulation changes resulting from global climate change can be explored. While clearly it would be necessary to perform far more simulations and Lagrangian model integrations in order to build up statistical significance in these results, this exploration still contributes to the general understanding and helps to direct avenues of further research.

In many respects the more general results describe a regional moisture transport system that should not surprise us. The regional air transport pathways are controlled by the regional circulation which is driven by the systems described in Chapter 1, namely the two high pressure systems, the mid-latitudes and the tropical systems. Of these, for the South African domain, the two high pressure systems appear seem to have a very dominant effect on the movement of air and moisture into the target domains.

This is most evident in the boundary moisture sources identified and particularly for the eastern boundary sources. Here we can see that the latitudinal position of the south Indian high pressure strongly controls the latitude from which air converging on the target domains is sourced. As the high pressure moves south the source air mass moves further south and vice versa for a northwards shift. This high pressure also weakens and intensifies and a stronger

high pressure results in stronger flow into the sub-continent from the more distant borders whereas a weaker high pressure results in less direct flow from the borders and more attribution to regional sources. However, this is also modulated by the relative depth of the continental heat low or trough which helps to drive the convergence of moisture over the sub-continent.

These results are not particularly new as the previous analyses using different methodologies have suggested similar dynamics. However, it is both encouraging that the methodology developed here is able to identify such dynamics as well as being useful to be able to explore the dynamics in greater detail due to the nature of the methodology. In particular, the details of the synoptic sequencing and the impact of changing synoptics on the moisture source dynamics has not been described previously and offers an interesting insight into cross time scale relationships. As already mentioned, such cross scale relationships are important in climate analysis (Meehl et al. [2001]).

Perhaps of greatest interest is the role of the transient mid-latitude systems to the south and the progression air movement that they produce. The synoptic sequences identified in Chapter 3 show that specific sequences produce very distinct ocean and land surface moisture source patterns with the ocean surface patterns being easier to disaggregate due to the greater spatial scales. However, a fairly common sequence seems to involve the passage of a mid-latitude trough to the south which moves air first westward around the south of the continent, and then gradually northwards as the trough passes eastward. During this stage the air is passing over the warm Agulhas and Mozambique currents and this area becomes an important moisture source region. As the air moves north it comes under the influence of the south Indian high which begins to push it into the sub-continent aided by the continental trough over the interior. At this point it is moving westward towards the target domain and likely gaining altitude, not only due to the topographic influence but due to greater instability and buoyancy caused by surface heating over the continent. It is likely, and indeed the case studies confirm, that for a given precipitation event, multiple sources of moisture are involved ranging from the regional ocean surface to more distant sources. These moist air masses converge on the precipitation event either at different altitudes and/or at different periods of the event. As already mentioned, it would be very helpful to be able to disaggregate the Lagrangian moisture field by moisture source areas but currently the model does not allow for this. However, the combination of sources identified per event does support the argument even if the source disaggregation cannot be done in the Lagrangian moisture field.

Variations in the strength, position and structure of the SAHP system are also important and indeed often interact with the passage of mid-latitude systems to the south. Of particular interest in this regard is the occurrence of ridging high pressure extensions around the south of South Africa. These ridging events typically occur following the passage of a mid-latitude trough to the south and result in strong southerly flow into the domain. This southerly flow is often associated with strong attribution of moisture source from the southern RCM boundary into target domains SA1 and SA2 to the south and middle of South Africa. At times the ridging extends all the way to the east coast resulting in advection of southerly air mass up the coast and the attribution of the southerly boundary as a moisture source for the more northern domains.

The synoptic controls of the high level western boundary moisture feed are not well described in the results as the synoptic sequencing did not show a particularly strong picture. However, what the results do suggest is that the mid-latitudes are involved and it seems that the activity of the moisture source is associated with a mid-latitude trough to the south west of the sub-continent. This would make sense as it would suggest a northward positioning of the mid-latitude jet stream. We know that specific humidities at such high altitudes are generally low and so the only way in which a strong moisture flux can occur is if the wind speeds are high. Therefore the involvement of the jet stream or at least the northern boundary of the jet stream seems likely. Figures 2.12 and 2.13 suggest that the mechanism would be an initial strong moisture flux towards the continent as a result of the northern positioning of the jet stream. Then as the mid-latitude trough recedes or migrates eastward the moisture is captured by the general subsidence over the continent and high level westerlies continue to advect the moisture into the sub-continent. What is not clear from the analysis is the nature of the dynamics driving the target precipitation event. Clearly some other form of disturbance is involved. However, this is not evident in the synoptic analysis.

Generalised circulation linkages are difficult and the analysis presented, including the cluster based synoptic sequencing offers an initial exploration of these linkages. It is likely that a range of alternative analysis techniques would shed even more light on these linkages and particularly the combination of different synoptic drivers involved in each precipitation event. At this point it is helpful to step back and consider the precipitation process itself as described in chapter 1 and remind ourselves of the some of the fundamentals of this process. The intent is to re-contextualise the moisture source analysis within a broader picture of precipitation.

#### 5.2.4 The Precipitation Process

We know that precipitation is a result of two main factors; moisture availability, and uplift in order to initiate condensation of the moisture. Of course many other factors are involved at smaller scales but fundamentally these are the two major factors. The results presented in the previous chapters refer to the source of the moisture that is made available for precipitation. The results do not speak to the question of absolute moisture availability or sources of uplift. It is therefore important not to draw simplistic conclusions from the results. Removing a particular moisture source region, an experiment that could be performed using an RCM and explored with the lagrangian methodology, would not necessarily result in reduced rainfall in the target domain under all circumstances. Such a control would depend on the degree to which a particular moisture source provides the amount of moisture needed in order for there to be sufficient moisture for precipitation.

In chapter 1, the work of Koster et al. [2004a] was mentioned which described how in wet areas adding moisture through the land surface does not always impact precipitation because precipitation is not constrained by lack of moisture but by lack of uplift. For more marginal areas, such as South Africa, it is more likely that the addition of more moisture can raise the moisture to the threshold required to produce rainfall. However, as seen in New et al. [2003], the dynamics are quite complex. Removing moisture from the surface changes the surface heat fluxes and results in a warmer surface, and potentially stronger surface heating, which can result in convection being triggered. Shifting surface temperature gradients also influences the regional circulation with drier soils possibly resulting in stronger heat lows and greater convergence, including moisture convergence. While many of these impacts may only be important at larger scales (1000s of kilometers), similar complexities no doubt play a role at smaller scales (10s of kilometers). The Lagrangian model facilitates detailed exploration of some aspects of these complexities.

#### 5.2.5 Climate Change Implications

This section explores the possible implications of the moisture source analysis under a changing climate. While not an initial objective of the thesis and certainly not a direct outcome of the results, the understanding gained through the development of the methodology as well as discussion of the results does allow us to perform a thought experiment regarding a changing climate. While the implications of Green House Gas (GHG) induced global climate change for the southern African region are not completely clear, there is a fair amount of consensus on certain aspects. Firstly, there seems to be some consensus between models that the eastern part of the country, east of the escarpment will become wetter, while the western parts will become drier (Hewitson and Crane [2006], Engelbrecht et al. [2009]). The simplest explanation for such changes is rooted in an intensification of the Hadley circulation coupled with a moister atmosphere. This results in the strengthening of the Indian Ocean high pressure system and would result in increased moisture advection onto the east coast while associated increased subsidence over the interior reduces instability and suppresses convection. An associated shift of the mid-latitudes to the south could result in reduced rainfall along the south west and southern coastal areas though topography adds some complications in these areas.

It is necessary to limit our discussion of climate change to this fairly simplistic view, at least as regards circulation changes. Complexities and uncertainties abound within the climate change literature and data, and attempting to engage with the full complexity of the question is beyond the scope of this discussion.

However, at first impression it would seem that if the high pressure systems are intensified and larger in a warmer climate then the role of the Indian Ocean and therefore the eastern boundary moisture sources would increase. Certainly, the projections seem to indicate wetter conditions along the eastern coast of southern Africa in summer. However, what is not clear is whether this increase in moisture is largely sourced from the distant ocean basin or from more regional ocean sources as identified in this study. Under a warmer climate evaporation from the surface would potentially increase. A warmer atmosphere can support higher specific humidities and hence, in tropical and some sub-tropical regions more rainfall is potentially expected. So while the moisture transport dynamic of a stronger Indian High Pressure system suggests the more distant moisture sources would become stronger, increased rainfall means more of this distant moisture could be removed through rainfall before it reaches the sub-continent. Additionally, increased evaporation means more proximal moisture sources also increase in strength.

Whether a warmer climate would result in more dependence on local or remote sources would require performing similar experiments to the ones already presented but using a number of GCM projections of future climate to drive the RCM. This is certainly beyond the scope of this study. However, it is interesting to refer back to the work of Trenberth [1999a] where precipitation recycling is defined using the following formulation:

$$\rho = \frac{EL}{PL + 2F}$$

Where  $E$  is the evaporative flux,  $P$  is the precipitation flux,  $L$  is the length scale of the analysis domain, and  $F$  is the vertically integrated moisture flux across the domain. Precipitation recycling indicates how much moisture contributing to precipitation with the analysis domain is sourced from within the domain versus external to the domain. From this formulation, the rationale for which can be found in the referenced paper, it is clear that increase evaporation increases the recycling ratio. However, increasing precipitation actually decreases the recycling ratio. This is because the methodology assumes that the atmospheric moisture storage is constant so increasing precipitation without increasing evaporation must result in an increase in moisture flux from outside the domain to satisfy the moisture budget. This increased external flux results in a decrease recycling ratio.

However, equal increase in both  $P$  and  $E$  result in an increased recycling ratio as a greater fraction of the precipitation is sourcing local moisture rather than remotely advected moisture. The determining factor is the moisture flux component,  $F$ , which also has a strong influence on the recycling ratio. How this might change in a warmer climate will likely vary greatly spatially as circulation systems shift and change.

While this thought experiment is clearly not conclusive and only an integration of the Lagrangian model driven by future projected circulation fields would be conclusive, it does highlight, in a simple way, the likelihood that the nature of moisture sources could change in a warmer climate and just given higher evaporation and precipitation it is possible that more local moisture sources could become even more important.

## 5.3 Conclusions

The intent of this chapter was to draw together some conclusions from the previous chapters through a discussion of, firstly the Lagrangian model itself, and secondly, the attributed moisture source results produced. Having done this we are now ready to return to the initial thesis and determine if the questions posed in that thesis have been successfully answered. The initial thesis was composed of two parts. Firstly, that a Lagrangian moisture source attribution model offers a useful tool with which to explore regional moisture sources, and secondly, that the regional land surface is an important moisture source for the southern African sub-continent. These two parts were expanded into three thesis components, namely:

- Development of a Lagrangian moisture source attribution model to overcome some of the limitations and challenges of other moisture analysis methodologies.
- Evaluate the models ability to capture regional moisture sources and attempt to validate the results to the degree that is possible.
- Apply the model to the southern African domain and explore the dynamics of the moisture sources identified paying particular attention to the role of the regional land surface.

The development of the Lagrangian model was described in Chapter 2. The model development highlighted a number of important issues and challenges, many of which have been overcome or accommodated but a number of limitations remain. However, the resultant model has been shown, through various testing, to be defensible, if not verifiable, both in terms of the rationale behind its formulation as well as the nature of the results it produces.

The Lagrangian moisture source attribution model coupled to an RCM produces a series of interesting results. The most prominent result is the large moisture source role attributed to the regional land surface within 1000km of the target domains. The possibility that the regional land surface could provide up to, and in some cases more than, 50% of the moisture for a precipitation event, has not been demonstrated in previous studies of regional moisture dynamics. While the Lagrangian model does have limitations and possible sources of uncertainty, various tests and analyses suggest that the results are defensible. Validation remains a serious challenge with all such investigations both due to the lack of regular observations at the surface as well as the availability of more obscure observations that could be used to validate parcel trajectories and ocean and land surface moisture fluxes.

Two seasons are evaluated here as the focus is not on the climatology of moisture, but to understand the relative role of different sources, and as such is not specifically dependent on interannual variability of seasons. Nonetheless, the selection of the seasons was done in order to span some degree of regional variability, but the conclusions hold across both these differing seasonal modes.

Given the tested defensibility of the model and with due consideration of the uncertainties and caveats, we can conclude that the original thesis, that the regional land surface appears to play an important role as a regional moisture source, is supported by the results. In fact we can go so far as to conclude that the results show the importance of this role is surprising in its magnitude given the history of literature suggesting otherwise.

The two parts of the original thesis can therefore be concluded successfully.

Following this, a number of other interesting aspects of the regional climate system have been identified through the results. While not pertaining directly to the thesis questions they are of great interest to the subject area and are worth re-iterating here.

In particular, the important role of the land surface supports a proposed moisture transport dynamic which is that the transport of moisture across a continental region is both a result of atmospheric advection of the moisture as well as a leap frogging of moisture through a precipitation evaporation cycle. The moisture source maps produced support this both in terms of their general pattern as well as a synchronicity between the spatial patterns and the diurnal cycle of evaporation in some cases. This dynamic is also supported by the results as being the only way in which the bulk of moisture required to feed continental precipitation could actually reach the target domain. Moisture sourced from the RCM boundaries is insufficient to feed the target precipitation event.

A further interesting result worth mentioning is that, while the role of the western Indian Ocean as an important source of moisture for the continental interior is not surprising given the historical literature, the identification of a distinct, narrow coastal source region to the east and south of South Africa under certain synoptic conditions is certainly a new perspective.

Previous studies have identified this region as a possible source for extreme events in the south of South Africa. However, the analysis here supports this particular ocean region as being a significant general source of moisture for the interior through an anti-cyclonic air mass advection along the coast and into the interior from the west, possibly also linked to the passage of a mid-latitude trough to the south. The implications are that the regional SSTs are important for rainfall under certain synoptic conditions.

Finally, the identification of a high level westerly moisture source along the western boundary of the RCM has not been clearly shown before in the literature. Further work is certainly required in order to explore this dynamic in greater detail and reduce some of the associated uncertainties. However, if this moisture source can be shown to be robust through further analysis and the dynamics involved can be better described, this will significantly alter our understanding of the southern African regional moisture transport dynamics.

It is important to note the limitations of this study and the possible avenues for future work. The development of the Lagrangian model was guided by the initial thesis objectives. During the course of the study a number of new characteristics of regional moisture dynamics have been identified. These characteristics are however, not directly described by the Lagrangian model as it stands. The most important characteristic identified is the possible moisture leap frog process whereby moisture is migrated across the continent through a series of precipitation/evaporation/advection cycles. An exciting prospect is the development of a model to be able to trace such cycles, and further analysis of the regional dynamics with these cycles as the focus. The use of Lagrangian moisture source attribution models in the future offers some unique advantages and opportunities to explore the complexities of the regional climate system in greater detail.

# Appendix A

## Lagrangian Model Code Details

### A.1 Introduction

The lagrangian moisture source and attribution model used in this work was developed by the author as a significant component of the research work. The purpose of this appendix is to describe some of the details of the model code, the handling of input data, the archiving of output data, and the applicability of the code to other sources of climate data. While the code is not currently open source, the author is willing to make it available to others to support further research into moisture sources.

### A.2 Pre-existing code and rationale for development

There are existing model codes that have been developed to explore lagrangian transport in the atmosphere. Examples are FLEXPART Stohl et al. [1998] and the earlier FLEXTRA. These codes are mature and have been used extensively, including in work cited in this thesis. The various existing code options were explored at the onset of this research activity. However, it was decided that the exploratory nature of the methodology being developed required much greater code flexibility than would be possible with existing codes. It was therefore determined that a new code base be developed which could be evolved and rapidly modified in order to explore different variations of the proposed methodology.

### A.3 Code details

The code is written predominantly in C though some pre-processing and post-processing stages utilise Python and Bash scripting. The C language was chosen because it was familiar to the author but also because it allows for the development of faster code than many interpreted languages such as Python or R.

While an initial attempt was made to develop a distributed memory, parallel execution version of the code, and some success was achieved in this regard, this proved to be too much of a development burden given the rapidly evolving state of the code. Unfortunately this has placed some significant limitations on the length of integrations as the code can only execute on a single processing core. The driving RCM, MM5, is able to utilise parallel execution environments and for this work a small cluster was used to perform the RCM integrations. It would certainly seem to be a worthwhile investment, now that the code is relatively stable and mature, to develop a parallel version of the code and so allow for much longer integration experiments.

### A.3.1 Treatment of input data and configuration

All input data is input on the RCM native grid, both horizontally and vertically. The RCM native vertical grid, in the case of MM5, is defined on a pure sigma coordinate system. The integration of the lagrangian model also all occurs within the context of the RCM grid structure. Interpolation is done at each time step in order to determine state variable values at the trajectory location. Interpolation in the vertical is done directly from the model sigma levels to the geometric height of the parcel. The rationale for using the RCM grid was that it avoided any further steps of interpolation, particularly in the vertical where strong moisture and wind gradients can occur which may be lost with successive interpolation steps.

Each integration of the model targets a defined precipitation target region which is currently defined in a C header file along with a number of other configuration settings including the file system paths to the input data and the various filtering and trajectory time step parameters. This requires that the model code is compiled afresh for each integration but it does simplify the processes of ingesting configuration parameters. A possible future enhancement would be to read in parameters from a configuration file on program startup which would avoid the recompilation requirement

Other configuration parameters specify integration time stepping, start time and end time, and the moist mass carried by each trajectory parcel.

### A.3.2 Output data and archiving

While the model tracks the position of each parcel at each time step, this information is not archived as the size and complexity of such an archive is significant. It must be remembered that on average the model is integrating on the order of millions of parcel trajectories each consisting of hundreds of parcel locations through time. Rather, at each archive time step (configured as a multiple of the integration time steps), a number of analysis fields are archived. These are the following:

- 3-Dimensional parcel density on the RCM horizontal and vertical grid
- 3-Dimensional lagrangian model specific humidity fields on the RCM grid
- 2-Dimensional accumulated attributed moisture source map on the RCM horizontal grid
- 2-Dimensional attribution coefficient map on the RCM horizontal grid

These fields are archived into separate flat binary files that can be ingested easily into visualization packages such as GrADS or Ferret or, as was largely the case in this work, ingested by post-processing code written in Python. The fields allow for detailed analysis of a great deal of the lagrangian model processes as is evidenced by the results presented in the thesis. While archiving individual trajectory histories would potentially allow even more sophisticated analysis, some means of dealing with the complexity of such an archive or analysis would first be needed. Individual trajectory histories were extracted as samples during the testing and validation phases of the code development to ensure that the individual trajectory pathways were stable and performing as expected given the driving synoptic processes. Section 2.5 details some of the validation and testing issues.

# Bibliography

- B.J. Abiodun, W.J. Gutowski, A.A. Abatan, and J.M. Prusa. Cam-eulag: A non-hydrostatic atmospheric climate model with grid stretching. *Acta Geophysica*, pages 1–10, 2011.
- R. Allan, D. Chambers, W. Drosowsky, H. Hendon, M. Latif, N. Nicholls, I. Smith, R. Stone, and Y. Turre. Is there an indian ocean dipole and is it independent of the el niño-southern oscillation. *CLIVAR Exchanges*, 21:18–22, 2001.
- B.T. Anderson, G. Salvucci, A.C. Ruane, J.O. Roads, and M. Kanamitsu. A New Metric for Estimating the Influence of Evaporation on Seasonal Precipitation Rates. *Journal of Hydrometeorology*, 9(3):576–588, 2008.
- D. Anfossi, E. Ferrero, G. Tinarelli, and S. Alessandrini. A simplified version of the correct boundary conditions for skewed turbulence in Lagrangian particle models. *Atmospheric Environment*, 31(2):301–308, 1997.
- D. Anfossi, F. Desiato, G. Tinarelli, G. Brusasca, E. Ferrero, and D. Sacchetti. "TRANSALP 1989 experimental campaign II. Simulation of a tracer experiment with Lagrangian particle models". *Atmospheric Environment*, 32(7): 1157–1166, 1998.
- A. Arakawa. The Cumulus Parameterization Problem: Past, Present, and Future. *Journal of Climate*, 17(13):2493–2525, 2004.
- K. Ashok, S.K. Behera, S.A. Rao, H. Weng, and T. Yamagata. El Niño Modoki and its possible teleconnection. *J. Geophys. Res*, 112:C11007, 2007.
- P.J. Ashton. Avoiding Conflicts over Africa's Water Resources. *AMBIO: A Journal of the Human Environment*, 31(3): 236–242, 2002.
- M. Azadi, UC Mohanty, and M. Mandal. A study on kinematic trajectory calculations with different schemes using wind field of varying temporal frequency. *Journal of Computational Methods in Science and Engineering*, 6(1): 7–17, 2006.
- K. Baumann and A. Stohl. Validation of a Long-Range Trajectory Model Using Gas Balloon Tracks from the Gordon Bennett Cup 95. *Journal of Applied Meteorology*, 36(6):711–720, 1997.
- S.K. Behera and T. Yamagata. Subtropical sst dipole events in the southern indian ocean. *Geophysical Research Letters*, 28(2):327–330, 2001.
- A.K. Betts. The Betts–Miller scheme. *The Representation of Cumulus Convection in Numerical Models, Meteor. Monogr*, pages 107–121, 1993.
- M. Boko, I. Niang, A. Nyong, C. Vogel, A. Githeko, M. Medany, B. Osman-Elasha, R. Tabo, and P. Yanda. *Africa. Climate Change 2007: Impacts, Adaptation and Vulnerability. Contribution of Working Group II to the Fourth Assessment Report of the Intergovernmental Panel on Climate Change*. Cambridge University Press, Cambridge UK, 2007.
- M.G. Bosilovich. On the vertical distribution of local and remote sources of water for precipitation. *Meteorology and Atmospheric Physics*, 80(1):31–41, 2002.

- M.G. Bosilovich and J.D. Chern. Simulation of Water Sources and Precipitation Recycling for the MacKenzie, Mississippi, and Amazon River Basins. *Journal of Hydrometeorology*, 7(3):312–329, 2006.
- M.G. Bosilovich and S.D. Schubert. Water Vapor Tracers as Diagnostics of the Regional Hydrologic Cycle. *Journal of Hydrometeorology*, 3(2):149–165, 2002.
- L. Bounoua, GJ Collatz, SO Los, PJ Sellers, DA Dazlich, CJ Tucker, and DA Randall. Sensitivity of Climate to Changes in NDVI. *Journal of Climate*, 13(13):2277–2292, 2000.
- J.C. Brimelow and G.W. Reuter. Transport of Atmospheric Moisture during Three Extreme Rainfall Events over the Mackenzie River Basin. *Journal of Hydrometeorology*, 6(4):423–440, 2005.
- K.L. Brubaker, D. Entekhabi, and PS Eagleson. Estimation of Continental Precipitation Recycling. *Journal of Climate*, 6(6):1077–1089, 1993.
- JP Bruce. Disaster Loss Mitigation as an Adaptation to Climate Variability and Change. *Mitigation and Adaptation Strategies for Global Change*, 4(3):295–306, 1999.
- M.I. Budyko. *Climate and life*. Academic Press, 1974.
- G.I. Burde. Bulk Recycling Models with Incomplete Vertical Mixing. Part I: Conceptual Framework and Models. *Journal of Climate*, 19(8):1461–1472, 2006.
- GI Burde and A. Zangvil. The Estimation of Regional Precipitation Recycling. Part I: Review of Recycling Models. *Journal of Climate*, 14(12):2497–2508, 2001a.
- GI Burde and A. Zangvil. The Estimation of Regional Precipitation Recycling. Part II: A New Recycling Model. *Journal of Climate*, 14(12):2509–2527, 2001b.
- G.I. Burde, C. Gandush, and Y. Bayarjargal. Bulk Recycling Models with Incomplete Vertical Mixing. Part II: Precipitation Recycling in the Amazon Basin. *Journal of Climate*, 19(8):1473–1489, 2006.
- JG Charney. On a physical basis for numerical prediction of large-scale motions in the atmosphere. *Journal of Meteorology*, 6(6):372–385, 1949. ISSN 0095-9634.
- J.G. Charney. Dynamics of deserts and drought in the sahel. *Quarterly Journal of the Royal Meteorological Society*, 101(428):193–202, 1975.
- F. Chen and J. Dudhia. Coupling an Advanced Land Surface–Hydrology Model with the Penn State–NCAR MM5 Modeling System. Part I: Model Implementation and Sensitivity. *Monthly Weather Review*, 129(4):569–585, 2001a.
- F. Chen and J. Dudhia. Coupling an Advanced Land Surface–Hydrology Model with the Penn State–NCAR MM5 Modeling System. Part II: Preliminary Model Validation. *Monthly Weather Review*, 129(4):587–604, 2001b.
- AM Chiodi and DE Harrison. Mechanisms of Summertime Subtropical Southern Indian Ocean Sea Surface Temperature Variability: On the Importance of Humidity Anomalies and the Meridional Advection of Water Vapor. *Journal of Climate*, 20(19):4835–4852, 2007.
- J.H. Christensen, B. Hewitson, A. Busuioc, A. Chen, X. Gao, I. Held, R. Jones, R.K. Kolli, W.T. Kwon, R. Laprise, V. Magana Rueda, L. Mearns, C.G. Menendez, and others. *Regional Climate Projections. In: Climate Change 2007: The Physical Science Basis. Contribution of Working Group I to the Fourth Assessment Report of the Intergovernmental Panel on Climate Change*. Cambridge University Press, Cambridge UK and New York, NY, USA, 2007.
- OB Christensen, MA Gaertner, JA Prego, and J. Polcher. Internal variability of regional climate models. *Climate Dynamics*, 17(11):875–887, 2001.

- C. Cook, C.J.C. Reason, and B.C. Hewitson. Wet and dry spells within particularly wet and dry summers in the South African summer rainfall region. *Climate Research*, 26(1):17–31, 2004.
- K.H. Cook. The South Indian Convergence Zone and Interannual Rainfall Variability over Southern Africa. *Journal of Climate*, 13(21):3789–3804, 2000.
- K.H. Cook. A Southern Hemisphere Wave Response to ENSO with Implications for Southern Africa Precipitation. *Journal of the Atmospheric Sciences*, 58(15):2146–2162, 2001.
- R. Courant, K. Friedrichs, and H. Lewy.  
"Über die partiellen Differenzgleichungen der mathematischen Physik. *Mathematische Annalen*, 100(1):32–74, 1928. ISSN 0025-5831.
- SJ Crimp and SJ Mason. The extreme precipitation event of 11 to 16 February 1996 over South Africa. *Meteorology and Atmospheric Physics*, 70(1):29–42, 1999. ISSN 0177-7971.
- PC D'Abreton and PD Tyson. Divergent and non-divergent water vapour transport over southern Africa during wet and dry conditions. *Meteorology and Atmospheric Physics*, 55(1):47–59, 1995.
- PC D'Abreton and PD Tyson. Three-dimensional kinematic trajectory modelling of water vapour transport over southern Africa. *Water SA*, 22(4):297–306, 1996.
- E.F. Danielsen. TRAJECTORIES: ISOBARIC, ISENTROPIC AND ACTUAL. *Journal of the Atmospheric Sciences*, 18(4):479–486, 1961.
- D.N. Dexheimer and K.P. Bowman. Lagrangian Methods for Climatological Analysis of Regional Atmospheric Transport. *Journal of Applied Meteorology*, 43(4):623–630, 2004.
- C. Ding and X. He. K-means clustering via principal component analysis. In *Proceedings of the twenty-first international conference on Machine learning*, page 29. ACM, 2004.
- P.A. Dirmeyer and K.L. Brubaker. Contrasting evaporative moisture sources during the drought of 1988 and the flood of 1993: GEWEX continental-scale international project(GCIP), Part 2. *Journal of geophysical research*, 104(D16):19383–19397, 1999.
- P.A. Dirmeyer and K.L. Brubaker. Characterization of the Global Hydrologic Cycle from a Back-Trajectory Analysis of Atmospheric Water Vapor. *Journal of Hydrometeorology*, 8(1):20–37, 2007.
- F. Dominguez, P. Kumar, X.Z. Liang, and M. Ting. Impact of Atmospheric Moisture Storage on Precipitation Recycling. *Journal of Climate*, 19(8):1513–1530, 2006.
- H. Douville. Influence of Soil Moisture on the Asian and African Monsoons. Part II: Interannual Variability. *Journal of Climate*, 15(7):701–720, 2002.
- H. Douville, F. Chauvin, and H. Broqua. Influence of Soil Moisture on the Asian and African Monsoons. Part I: Mean Monsoon and Daily Precipitation. *Journal of Climate*, 14(11):2381–2403, 2001.
- R.R. Draxler. Sensitivity of a Trajectory Model to the Spatial and Temporal Resolution of the Meteorological Data during CAPTEX. *Journal of Applied Meteorology*, 26(11):1577–1588, 1987.
- A. Drumond, R. Nieto, L. Gimeno, and T. Ambrizzi. A lagrangian identification of major sources of moisture over central brazil and la plata basin. *Journal of Geophysical Research*, 113(D14128), 2008.
- E.A.B. Eltahir and R.L. Bras. Precipitation recycling in the Amazon basin. *Quart. J. Roy. Meteor. Soc.*, 120:861–880, 1994.
- E.A.B. Eltahir and R.L. Bras. Precipitation recycling. *Reviews of Geophysics*, 34(3):367–378, 1996.

- FA Engelbrecht, JL McGregor, and C.J. Rautenbach. On the development of a new nonhydrostatic atmospheric model in south africa. *South African Journal of Science*, 103(3/4):127, 2007.
- FA Engelbrecht, JL McGregor, and CJ Engelbrecht. Dynamics of the conformal-cubic atmospheric model projected climate-change signal over southern africa. *International Journal of Climatology*, 29(7):1013–1033, 2009.
- N. Fauchereau, B. Pohl, C.J.C. Reason, M. Rouault, and Y. Richard. Recurrent daily OLR patterns in the Southern Africa/Southwest Indian Ocean region, implications for South African rainfall and teleconnections. *Climate Dynamics*, 32(4):575–591, 2009. ISSN 0930-7575.
- MJ Fennessy and J. Shukla. Impact of Initial Soil Wetness on Seasonal Atmospheric Prediction. *Journal of Climate*, 12(11):3167–3180, 1999.
- L. Ferranti and P. Viterbo. The European Summer of 2003: Sensitivity to Soil Water Initial Conditions. *Journal of Climate*, 19(15):3659–3680, 2006.
- C.B. Field, V. Barros, T.F. Stocker, D. Qin, DJ Dokken, KL Ebi, MD Mastrandrea, KJ Mach, GK Plattner, SK Allen, et al. Managing the risks of extreme events and disasters to advance climate change adaptation. *A Special Report of Working Groups I and II of the Intergovernmental Panel on Climate Change Cambridge University Press, Cambridge, UK, and New York, NY, USA*, 2012.
- C. Forster, A. Stohl, and P. Seibert. Parameterization of Convective Transport in a Lagrangian Particle Dispersion Model and Its Evaluation. *Journal of Applied Meteorology and Climatology*, 46(4):403–422, 2007.
- MT Freiman and PD Tyson. The thermodynamic structure of the atmosphere over South Africa: Implications for water vapour transport. *Water S. A.*, 26(2):153–158, 2000.
- JR Gat and I. Carmi. Evolution of the isotopic composition of atmospheric waters in the Mediterranean Sea area. *J. Geophys. Res*, 75(15):3039–3048, 1970.
- JR Gat and E. Matsui. Atmospheric water balance in the Amazon basin: an isotopic evapotranspiration model. *JGR. Journal of geophysical research. Part D, Atmospheres*, 96(7):13–13, 1991.
- A. Giannini, M. Biasutti, I.M. Held, and A.H. Sobel. A global perspective on African climate. *Climatic Change*, 90(4): 359–383, 2008.
- F. Giorgi, L.O. Mearns, C. Shields, and L. Mayer. A Regional Model Study of the Importance of Local versus Remote Controls of the 1988 Drought and the 1993 Flood over the Central United States. *Journal of Climate*, 9(5):1150–1162, 1996.
- L. Goddard and NE Graham. Importance of the Indian Ocean for simulating rainfall anomalies over eastern and southern Africa. *Journal of geophysical research*, 104(D 16):19099–19116, 1999.
- G.A. Grell, J. Dudhia, D.R. Stauffer, National Center for Atmospheric Research. Mesoscale, and Microscale Meteorology Division. A description of the fifth-generation Penn State/NCAR Mesoscale Model (MM5). 1994.
- G.A Grell, S.E Peckham, R. Schmitz, S. McKeen, G. Frost, W.C. Skamarock, and B. Eder. Fully coupled online chemistry within the wrf model. *Atmospheric Environment*, 39(37):6957 – 6975, 2005.
- JW Handmer, S. Dovers, and TE Downing. Societal Vulnerability to Climate Change and Variability. *Mitigation and Adaptation Strategies for Global Change*, 4(3):267–281, 1999.
- MSJ Harrison. A generalized classification of South African summer rain-bearing synoptic systems. *International Journal of Climatology*, 4(5):547–560, 1984. ISSN 1097-0088.
- NCG Hart, CJC Reason, and N. Fauchereau. Tropical-Extratropical Interactions Over Southern Africa: Three Cases of Heavy Summer Season Rainfall. *Monthly Weather Review*, 2010. ISSN 1520-0493.

- C.S. Hendrix and S.M. Glaser. Trends and triggers: Climate, climate change and civil conflict in Sub-Saharan Africa. *Political Geography*, 26(6):695–715, 2007.
- JC Hermes and CJC Reason. Variability in sea-surface temperature and winds in the tropical south-east Atlantic Ocean and regional rainfall relationships. *International Journal of Climatology*, 29(1):11–21, 2008.
- BC Hewitson and RG Crane. Consensus between GCM climate change projections with empirical downscaling: precipitation downscaling over South Africa. *INTERNATIONAL JOURNAL OF CLIMATOLOGY*, 26(10):1315, 2006.
- CD Hewitt, G. Amanatidis, and E. EC. ENSEMBLES—providing ensemble-based predictions of climate changes and their impacts. *Parliament Magazine*, 11, 2005.
- Y. Hu, Q. Fu, et al. Observed poleward expansion of the hadley circulation since 1979. *Atmospheric Chemistry and Physics*, 7(19):5229–5236, 2007.
- T.G. Huntington. Evidence for intensification of the global water cycle: Review and synthesis. *Journal of Hydrology*, 319(1):83–95, 2006.
- IPCC. The Physical Science Basis. Contribution of Working Group I to the Fourth Assessment Report of the Intergovernmental Panel on Climate Change. *Cambridge University Press, Cambridge, United Kingdom and New York, NY, USA*, 996, 2007.
- P. James, A. Stohl, N. Spichtinger, S. Eckhardt, and C. Forster. Climatological aspects of the extreme European rainfall of August 2002 and a trajectory method for estimating the associated evaporative source regions. *Natural Hazards and Earth System Sciences*, 4(5):733–746, 2004.
- PA Johnston, ERM Archer, CH Vogel, CN Bezuidenhout, WJ Tennant, and R. Kuschke. Review of seasonal forecasting in South Africa: producer to end-user. *Climate Research*, 28:67–82, 2004.
- J.D.W. Kahl. On the prediction of trajectory model error. *Atmospheric Environment*, 30(17):2945–2957, 1996.
- J.S. Kain. The Kain–Fritsch Convective Parameterization: An Update. *Journal of Applied Meteorology*, 43(1):170–181, 2004.
- E.C. Kalnay, M. Kanamitsu, R. Kistler, W. Collins, D. Deaven, L. Gandin, M. Iredell, S. Saha, G. White, J. Woollen, et al. The NCEP/NCAR 40-year reanalysis project. *Bulletin of the American Meteorological Society*, 77(3):437–471, 1996. ISSN 1520-0477.
- M. Kanamitsu, W. Ebisuzaki, J. Woollen, S.K. Yang, JJ Hnilo, M. Fiorino, and GL Potter. Ncep-doe amip-ii reanalysis (r-2). *Bulletin of the American Meteorological Society*, 83(11):1631–1643, 2002. ISSN 1520-0477.
- G. Kay and R. Washington. Future southern African summer rainfall variability related to a southwest Indian Ocean dipole in HadCM3. *Geophysical Research Letters*, 35(12), 2008.
- R.J.T. Klein and D.C. Maciver. Adaptation to Climate Variability and Change: Methodological Issues. *Mitigation and Adaptation Strategies for Global Change*, 4(3):189–198, 1999.
- E.N. Koffi, K. Nodop, and B. Benech. Comparison of constant volume balloons, model trajectories and tracer transport during ETEX. *Atmospheric Environment*, 32(24):4139–4149, 1998.
- T. Kohonen. Self-organized formation of topologically correct feature maps. *Biological cybernetics*, 43(1):59–69, 1982. ISSN 0340-1200.
- R.D. Koster and M.J. Suarez. Relative contributions of land and ocean processes to precipitation variability. *Journal of Geophysical Research. D. Atmospheres*, 100:13, 1995.
- R.D. Koster, J. Jouzel, R. Suozzo, G. Russel, W. Broecker, D. Rind, and P. Eagleson. Global Source of Local Precipitation as Determined by the NASA/GISS GCM. *Geophysical Research Letters*, 13(1):121–124, 1986.

- R.D. Koster, P.A. Dirmeyer, A.N. Hahmann, R. Ijpelaar, L. Tyahla, P. Cox, and M.J. Suarez. Comparing the Degree of Land–Atmosphere Interaction in Four Atmospheric General Circulation Models. *Journal of Hydrometeorology*, 3(3):363–375, 2002.
- R.D. Koster, M.J. Suarez, R.W. Higgins, and HG Dool. Observational evidence that soil moisture variations affect precipitation. *Geophysical Research Letters*, 30(5):1241, 2003.
- R.D. Koster, P.A. Dirmeyer, Z. Guo, G. Bonan, E. Chan, P. Cox, CT Gordon, S. Kanae, E. Kowalczyk, D. Lawrence, et al. Regions of Strong Coupling Between Soil Moisture and Precipitation, 2004a.
- R.D. Koster, M.J. Suarez, P. Liu, U. Jambor, A. Berg, M. Kistler, R. Reichle, M. Rodell, and J. Famiglietti. Realistic Initialization of Land Surface States: Impacts on Subseasonal Forecast Skill. *Journal of Hydrometeorology*, 5(6):1049–1063, 2004b.
- W.A. Landman and A. Beraki. Multi-model forecast skill for mid-summer rainfall over southern africa. *International Journal of Climatology*, 32(2):303–314, 2012.
- WA Landman and SJ Mason. Change in the association between Indian Ocean sea-surface temperatures and South African summer rainfall. *International Journal of Climatology*, 19:1477–1492, 1999.
- JA Lindesay. South African rainfall, the Southern Oscillation and a Southern Hemisphere semi-annual cycle. *International Journal of Climatology*, 8(1):17–30, 1988. ISSN 1097-0088.
- J. Lu, G.A. Vecchi, and T. Reichler. Expansion of the hadley cell under global warming. *Geophysical Research Letters*, 34(6):L06805, 2007.
- B. Lyon and S.J. Mason. The 1997–98 Summer Rainfall Season in Southern Africa. Part I: Observations. *Journal of Climate*, 20(20):5134–5148, 2007.
- N. MacKellar, M. Tadross, and B. Hewitson. Synoptic-based evaluation of climatic response to vegetation change over southern Africa. *International Journal of Climatology*, 2007.
- N.C. MacKellar, M.A. Tadross, and B.C. Hewitson. Effects of vegetation map change in MM5 simulations of southern Africa's summer climate. *International Journal of Climatology*, 29(6):885–898, 2009.
- R. Marchant, C. Mumbi, S. Behera, and T. Yamagata. The Indian Ocean dipole-the unsung driver of climatic variability in East Africa. *African Journal of Ecology*, 45(1):4–16, 2007.
- SJ Mason. Sea-surface temperature– South African rainfall associations, 1910-1989. *International Journal of Climatology*, 15(2):119–135, 1995.
- S.J. Mason and L. Goddard. Probabilistic precipitation anomalies associated with ENSO. *Bulletin of the American Meteorological Society*, 82(4):619–638, 2001.
- JE McDonald. The evaporation precipitation fallacy. *Weather*, 17(5):169, 1962.
- J.L. McGregor and M.R. Dix. An updated description of the conformal-cubic atmospheric model. *High Resolution Numerical Modelling of the Atmosphere and Ocean*, pages 51–75, 2008.
- K. McGuffie and A. Henderson-Sellers. *A climate modelling primer*. Wiley, 2005. ISBN 0470857501.
- G.A. Meehl, G.J. Boer, C. Covey, M. Latif, and R.J. Stouffer. The coupled model intercomparison project (CMIP). *Bulletin of the American Meteorological Society*, 81(2):313–318, 2000. ISSN 1520-0477.
- GA Meehl, R. Lukas, GN Kiladis, KM Weickmann, AJ Matthews, and M. Wheeler. A conceptual framework for time and space scale interactions in the climate system. *Climate Dynamics*, 17(10):753–775, 2001. ISSN 0930-7575.

- J.T. Merrill, R. Bleck, and D. Boudra. Techniques of Lagrangian Trajectory Analysis in Isentropic Coordinates. *Monthly Weather Review*, 114(3):571–581, 1986.
- D.J. Nash and G.H. Endfield. Splendid rains have fallen: links between El Niño and rainfall variability in the Kalahari, 1840–1900. *Climatic Change*, 86(3):257–290, 2008.
- M. New, M. Hulme, and P. Jones. Representing twentieth-century space-time climate variability. Part II: Development of 1901–96 monthly grids of terrestrial surface climate. *Journal of Climate*, 13(13):2217–2238, 2000. ISSN 1520-0442.
- M. New, R. Washington, C. Jack, B. Hewitson, and UK Oxford. Sensitivity of southern African climate to soil-moisture. *CLIVAR Exchanges*, 8:45–47, 2003.
- S.E. Nicholson and D. Entekhabi. Rainfall Variability in Equatorial and Southern Africa: Relationships with Sea Surface Temperatures along the Southwestern Coast of Africa. *Journal of Applied Meteorology*, 26(5):561–578, 1987.
- S.E. Nicholson and J.P. Grist. The seasonal evolution of the atmospheric circulation over West Africa and equatorial Africa. *Journal of Climate*, 16(7):1013–1030, 2003. ISSN 1520-0442.
- R. Nieto, L. Gimeno, and R.M. Trigo. A lagrangian identification of major sources of sahel moisture. *Geophysical research letters*, 33(18):L18707, 2006.
- M. Owe, R. de Jeu, and T. Holmes. Multisensor historical climatology of satellite-derived global land surface moisture. *Journal of Geophysical Research*, 113(F1):F01002, 2008. ISSN 0148-0227.
- RA Preston-Whyte, P.D. Tyson, and RA Preston. *The atmosphere and weather of Southern Africa*. Oxford University Press Cape Town, 1989. ISBN 0195704967.
- O. Reale and P. Dirmeyer. Modeling the Effect of Land Surface Evaporation Variability on Precipitation Variability. Part I: General Response. *Journal of Hydrometeorology*, 3(4):433–450, 2002.
- O. Reale, L. Feudale, and B. Turato. Evaporative moisture sources during a sequence of floods in the Mediterranean region. *Geophysical Research Letters*, 28(10):2085–2088, 2001.
- CJC Reason. Subtropical Indian Ocean SST dipole events and southern African rainfall. *Geophys. Res. Lett*, 28(11): 2225–2227, 2001.
- CJC Reason. Sensitivity of the southern African circulation to dipole sea-surface temperature patterns in the south Indian Ocean. *International Journal of Climatology*, 22(4):377–393, 2002.
- CJC Reason and H. Mulenga. Relationships between South African rainfall and SST anomalies in the Southwest Indian Ocean. *International Journal of Climatology*, 19(15):1651–1673, 1999.
- CJC Reason and M. Rouault. Sea surface temperature variability in the tropical southeast Atlantic Ocean and West African rainfall. *Geophys. Res. Lett*, 33, 2006.
- CJC Reason, RJ Allan, JA Lindesay, and TJ Ansell. ENSO and climatic signals across the Indian Ocean Basin in the global context: part I, interannual composite patterns. *International Journal of Climatology*, 20(11):1285–1327, 2000.
- CJC Reason, F. Engelbrecht, WA Landman, JRE Lutjeharms, S. Piketh, CJ de WRautenbach, and BC Hewitson. A review of South African research in atmospheric science and physical oceanography during 2000–2005. *South African Journal of Science*, 102(1-2):35–45, 2006. ISSN 0038-2353.
- R.W. Reynolds and T.M. Smith. Improved global sea surface temperature analyses using optimum interpolation. *Journal of Climate*, 7(6):929–948, 1994. ISSN 0894-8755.

- EE Riddle, PB Voss, A. Stohl, D. Holcomb, D. Maczka, K. Washburn, and RW Talbot. Trajectory model validation using newly developed altitude-controlled balloons during the International Consortium for Atmospheric Research on Transport and Transformations 2004 campaign (DOI 10.1029/2006JD007456). *JOURNAL OF GEOPHYSICAL RESEARCH-ALL SERIES-*, 111(D23):23, 2006.
- M. Rouault and Y. Richard. Intensity and spatial extent of droughts in southern Africa (DOI 10.1029/2005GL022436). *GEOPHYSICAL RESEARCH LETTERS*, 32(15):15702, 2005.
- M. Rouault, I. Jobard, SA White, and JRE Lutjeharms. Studying rainfall events over South Africa and adjacent oceans using the TRMM satellite. *South African journal of science*, 97(11-12):455–460, 2001. ISSN 0038-2353.
- M. Rouault, SA White, CJC Reason, JRE Lutjeharms, and I. Jobard. Ocean–Atmosphere Interaction in the Agulhas Current Region and a South African Extreme Weather Event. *Weather and Forecasting*, 17(4):655–669, 2002.
- M. Rouault, P. Florenchie, N. Fauchereau, and C.J.C. Reason. South East tropical Atlantic warm events and southern African rainfall. *Geophysical research letters*, 30(5):9–9, 2003.
- C. Schär, D. Lüthi, U. Beyerle, and E. Heise. The soil–precipitation feedback: A process study with a regional climate model. *Journal of Climate*, 12(3):722–741, 1999.
- P. Seibert and A. Frank. Source-receptor matrix calculation with a Lagrangian particle dispersion model in backward mode. *Atmos. Chem. Phys*, 4:51–63, 2004.
- A. Simmons, S. Uppala, D. Dee, and S. Kobayashi. ERA-Interim: New ECMWF reanalysis products from 1989 onwards. *ECMWF Newsletter*, 110:25–35, 2007.
- H. Sodemann, C. Schwierz, and H. Wernli. Interannual variability of Greenland winter precipitation sources: Lagrangian moisture diagnostic and North Atlantic Oscillation influence. *J. Geophys. Res*, 113, 2008.
- A. Stohl. Computation, accuracy and applications of trajectories: A review and bibliography. *Atmospheric Environment*, 32(6):947–966, 1998.
- A. Stohl. A 1-year Lagrangian "climatology" of airstreams in the Northern Hemisphere troposphere and lowermost stratosphere (Paper 2000JD900570). *JOURNAL OF GEOPHYSICAL RESEARCH-ALL SERIES-*, 106(7; SECT 4):7263–7280, 2001.
- A. Stohl and P. James. A Lagrangian Analysis of the Atmospheric Branch of the Global Water Cycle. Part I: Method Description, Validation, and Demonstration for the August 2002 Flooding in Central Europe. *Journal of Hydrometeorology*, 5(4):656–678, 2004.
- A. Stohl and P. James. A Lagrangian Analysis of the Atmospheric Branch of the Global Water Cycle. Part II: Moisture Transports between Earth's Ocean Basins and River Catchments. *Journal of Hydrometeorology*, 6(6):961–984, 2005.
- A. Stohl and D.J. Thomson. A Density Correction for Lagrangian Particle Dispersion Models. *Boundary-Layer Meteorology*, 90(1):155–167, 1999.
- A. Stohl, G. Wotawa, P. Seibert, and H. Kromp-Kolb. Interpolation Errors in Wind Fields as a Function of Spatial and Temporal Resolution and Their Impact on Different Types of Kinematic Trajectories. *Journal of Applied Meteorology*, 34(10):2149–2165, 1995.
- A. Stohl, M. Hittenberger, and G. Wotawa. Validation of the lagrangian particle dispersion model FLEXPART against large-scale tracer experiment data. *Atmospheric Environment*, 32(24):4245–4264, 1998.
- A. Stohl, L. Haimberger, MP Scheele, and H. Wernli. An intercomparison of results from three trajectory models. *Meteorological Applications*, 8(02):127–135, 2001.

- A. Stohl, C. Forster, and H. Sodemann. Remote sources of water vapor forming precipitation on the Norwegian west coast at 60° N—a tale of hurricanes and an atmospheric river. *Journal of Geophysical Research-Atmospheres*, 113(D5):D05102, 2008.
- MA Tadross, WJ Gutowski, BC Hewitson, C. Jack, and M. New. MM5 simulations of interannual change and the diurnal cycle of southern African regional climate. *Theoretical and Applied Climatology*, 86(1):63–80, 2006.
- W. Tennant. Considerations when using pre-1979 NCEP/NCAR reanalyses in the southern hemisphere. *Geophysical Research Letters*, 31(11):L11112, 2004. ISSN 0094-8276.
- M. Todd and R. Washington. Circulation anomalies associated with tropical-temperate troughs in southern Africa and the south west Indian Ocean. *Climate Dynamics*, 15(12):937–951, 1999.
- M.C. Todd, R. Washington, and P.I. Palmer. Water vapour transport associated with tropical–temperate trough systems over southern Africa and the southwest Indian Ocean. *International Journal of Climatology*, 24(5):555–568, 2004.
- K.E. Trenberth. Atmospheric Moisture Residence Times and Cycling: Implications for Rainfall Rates and Climate Change. *Climatic Change*, 39(4):667–694, 1998.
- K.E. Trenberth. Atmospheric Moisture Recycling: Role of Advection and Local Evaporation. *Journal of Climate*, 12(5):1368–1381, 1999a.
- K.E. Trenberth. Conceptual framework for changes of extremes of the hydrological cycle with climate change. *Climatic Change*, 42(1):327–339, 1999b.
- P.D. Tyson. *Climatic change and variability in southern Africa*. Oxford University Press Cape Town, 1987. ISBN 0195704304.
- S.M. Uppala, PW Kållberg, AJ Simmons, U. Andrae, V.D.C. Bechtold, M. Fiorino, JK Gibson, J. Haseler, A. Hernandez, GA Kelly, et al. The ERA-40 re-analysis. *Quarterly Journal of the Royal Meteorological Society*, 131(612): 2961–3012, 2005. ISSN 1477-870X.
- N. Vigaud, Y. Richard, M. Rouault, and N. Fauchereau. Moisture transport between the South Atlantic Ocean and southern Africa: relationships with summer rainfall and associated dynamics. *Climate Dynamics*, 32(1):113–123, 2009.
- C. Vogel. Seven fat years and seven lean years? climate change and agriculture in africa. *IDS Bulletin*, 36(2):30–35, 2005.
- W. Wang and N.L. Seaman. A Comparison Study of Convective Parameterization Schemes in a Mesoscale Model. *Monthly Weather Review*, 125(2):252–278, 1997.
- R. Washington and M. Todd. Tropical-temperate links in southern African and southwest Indian Ocean satellite-derived daily rainfall. *International Journal of Climatology*, 19(14):1601–1616, 1999. ISSN 1097-0088.
- R.P.A. Washington. Climate and Dynamics-D15104-Extreme wet years over southern Africa: Role of Indian Ocean sea surface temperatures (DOI 10.1029/2005JD006724). *Journal of Geophysical Research-Part D-Atmospheres*, 111(15), 2006.
- S. Weart. The development of general circulation models of climate. *Studies In History and Philosophy of Science Part B: Studies In History and Philosophy of Modern Physics*, 2010. ISSN 1355-2198.
- P. Xie and P.A. Arkin. Global Precipitation: A 17-Year Monthly Analysis Based on Gauge Observations, Satellite Estimates, and Numerical Model Outputs. *Bulletin of the American Meteorological Society*, 78(11):2539–2558, 1997.

- A. Zangvil, D.H. Portis, and P.J. Lamb. Investigation of the large-scale atmospheric moisture field over the midwestern United States in relation to summer precipitation. Part II: Recycling of local evapotranspiration and association with soil moisture and crop yields. *Journal of climate*, 17(17):3283–3301, 2004.